AD-A241 424

US Army Corps of Engineers

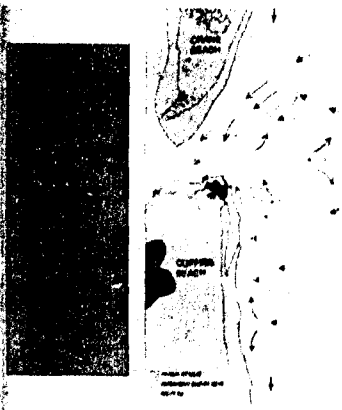

COASTAL ENGINEERING RESEARCH CENTER

TECHNICAL REPORT CERC-91-11

(2)

MORPHODYNAMICS AND STRATIGRAPHY OF ESSEX RIVER EBB-TIDAL DELTA: MASSACHUSETTS

by

J. Bailey Smith

Coastal Engineering Research Center

DEPARTMENT OF THE ARMY
Waterways Experiment Station, Corps of Engineers
3909 Halls Ferry Road, Vicksburg, Mississippi 39180-6199

DTIC
ELECTE
OCT 0 8 1991
S D
D

U.S. ARMY ENGINEER WATERWAYS EXPERIMENT STATION

August 1991
Final Report

Approved For Public Release; Distribution Is Unlimited

91-12724

Prepared for DEPARTMENT OF THE ARMY
US Army Corps of Engineers
Washington, DC 20314-1000

Under Work Unit 32538

Destroy this report when no longer needed. Do not return it to the originator.

The findings in this report are not to be construed as an official Department of the Army position unless so designated by other authorized documents.

The contents of this report are not to be used for advertising, publication, or promotional purposes. Citation of trade names does not constitute an official endorsement or approval of the use of such commercial products.

REPORT DOCUMENTATION PAGE

Form Approved
OMB No. 0704-0188

Public reporting burden for this collection of information is estimated to average 1 hour per response, including the time for reviewing instructions, searching existing data sources, gathering and maintaining the data needed, and completing and reviewing the collection of information. Send comments regarding this burden estimate or any other aspect of this collection of information, including suggestions for reducing this burden to Washington Headquarters Services, Directorate for Information Operations and Reports, 1215 Jefferson Davis Highway, Suite 1204, Arlington, VA 22202-4302, and to the Office of Management and Budget, Paperwork Reduction Project (0704-0188), Washington, DC 20503

1. AGENCY USE ONLY *(Leave blank)*	2. REPORT DATE	3. REPORT TYPE AND DATES COVERED
	August 1991	Final report

4. TITLE AND SUBTITLE
Morphodynamics and Stratigraphy of Essex River Ebb-Tidal Delta: Massachusetts

5. FUNDING NUMBERS
WU 32538

6. AUTHOR(S)
J. Bailey Smith

7. PERFORMING ORGANIZATION NAME(S) AND ADDRESS(ES)
USAE Waterways Experiment Station
Coastal Engineering Research Center
3909 Halls Ferry Road, Vicksburg, MS 39180-6199

8. PERFORMING ORGANIZATION REPORT NUMBER
Technical Report
CERC-91-11

9. SPONSORING/MONITORING AGENCY NAME(S) AND ADDRESS(ES)
US Army Corps of Engineers
Washington, DC 20314-1000

10. SPONSORING/MONITORING AGENCY REPORT NUMBER

11. SUPPLEMENTARY NOTES
Available from National Technical Information Service, 5285 Port Royal Road, Springfield, VA 22161.

12a. DISTRIBUTION/AVAILABILITY STATEMENT
Approved for public release; distribution is unlimited

12b. DISTRIBUTION CODE

13. ABSTRACT *(Maximum 200 words)*

The Essex River Inlet ebb-tidal delta system is one of several well-formed deltas along a barrier island chain in the Merrimack Embayment. Sediments comprising this barrier island chain have been supplied primarily from reworking and onshore transport of the Early Holocene Merrimack River Delta. Southerly longshore currents have resulted in a fining grain-size trend to the south along the barrier chain as well as an increase in spacing of the offshore contours.

The Essex River Inlet is anchored next to bedrock, and its ebb-tidal delta exhibits classic delta morphology whose environments respond to storms, tidal currents, wave processes, and sand transport. Measurements of tidal currents and channel bottom and intertidal bedforms indicate an ebb-dominated inlet throat and main ebb channel and flood-dominated marginal flood channels. Distal portions of the delta including swash bars and terminal lobe are dominated by southerly and landward directed wave-generated currents. Wave refraction around the delta results in a transport

(Continued)

14. SUBJECT TERMS
Ebb-tidal delta
Essex River
Morphodynamics
Stratigraphy

15. NUMBER OF PAGES
251

16. PRICE CODE

17. SECURITY CLASSIFICATION OF REPORT	18 SECURITY CLASSIFICATION OF THIS PAGE	19. SECURITY CLASSIFICATION OF ABSTRACT	20. LIMITATION OF ABSTRACT
UNCLASSIFIED	UNCLASSIFIED	UNCLASSIFIED	

13. (Continued).

reversal approximately 1.2 km south of the main ebb channel. Intertidal sand bodies are dominated by landward-oriented currents with the exception of the distal channel margin linear bars.

Sediment transport trends are dominated by gyres that involve sediment input from longshore currents into the updrift marginal flood channel, seaward sandwave migration through the main ebb channel, and onshore reworking of sediment through wave activity and swash bar migration. A study of historical aerial photographs (1943-1985) indicates a 5- to 7-year cycle of swash bar formation, migration, and attachment to the landward beach. Another process documented at the inlet is the downdrift deflection of the distal portion of the main ebb channel produced by the southerly directed longshore transport of sediment and sediment accumulation on the updrift portion of the ebb-tidal delta.

A facies model for the Essex River ebb-tidal delta envisions three stratigraphic sequences whose deposits are primarily a result of main ebb channel cut and fill, marginal flood channel accretion, and swash bar migration. The updrift ebb-tidal delta sequence is dominated by main ebb channel accretionary fill that is overlain by channel margin linear bar and thin swash bar migration deposits. The downdrift sequence is dominated by thick swash bar migration deposits that overlie abandoned marginal flood channel deposits. The distal ebb-tidal delta sequence is dominated by active and abandoned main ebb channel deposits overlain by channel margin linear bar and swash bar migration deposits.

Accesion For	
NTIS CRA&I	✓
DTIC TAB	☐
Unannounced	☐
Justification	
By	
Distribution/	
Availability Codes	
Dist	Avail and/or Special
A-1	

PREFACE

The investigation described in this report was authorized as a part of the Coastal Geology and Geotechnical Program by Headquarters, US Army Corps of Engineers (HQUSACE). Work was performed under Work Unit 32538, "Survey of Technologies in Coastal Geology," at the Coastal Engineering Research Center (CERC), US Army Engineer Waterways Experiment Station (WES). Mr. John Sanda was HQUSACE Technical Monitor. Dr. C. Linwood Vincent was CERC Program Manager.

The study was conducted from September 1988 through June 1991 by Mr. J. Bailey Smith and submitted as a thesis to the Boston University Department of Geology in partial fulfillment of the requirements for an M.A. degree in coastal geology. Dr. Duncan M. FitzGerald, Thesis Advisor, and Dr. Kenneth Finkelstein reviewed the document and are gratefully acknowledged. Additional guidance and support from Dr. Chris Baldwin and Dr. Dabney Caldwell are also appreciated. Assistance during the field investigation was provided by Messrs. Paul Betz, William Bobrowsky, Mark Brown, Steve Goodbred, Mike Gitten, J. A. Hutchins, Jeremy Leeds, Paul Losquadero, Mark Minotti, Todd Montello, Ken Parolski, Kevin Trainer and Sytze van Heteren, and Mses. Trudi Green and Anne Smith. Additional support was contributed by the Trustees of Reservations, the Sigma Xi Chapter of Boston University, and Mr. Tim Bryan.

This report was prepared by Mr. Smith, Coastal Geology Unit, Coastal Structures and Evaluation Branch (CSEB), Engineering Development Division (EED), under the general supervision of Mr. Thomas W. Richardson, Chief, EDD, and Ms. Joan Pope, Chief, CSEB. Chief of CERC was Dr. James R. Houston and Assistant Chief was Mr. Charles C. Calhoun, Jr.

Commander and Director of WES during publication of this report was COL Larry B. Fulton, EN. Technical Director was Dr. Robert W. Whalin.

TABLE OF CONTENTS

MORPHODYNAMICS AND STRATIGRAPHY OF ESSEX RIVER EBB-TIDAL DELTA: MASSACHUSETTS

PAGE

PREFACE i

LIST OF TABLES v

LIST OF FIGURES vii

INTRODUCTION 1

INTRODUCTION 1

PHYSICAL SETTING 3
Location and Physiography 3
Coastal Processes 3
Tides 3
Wind Regime 6
Wave Regime 6
Longshore Sediment Transport 6
Geologic History 10
Bedrock 10
Late Pleistocene Glacial History 12
Late Pleistocene Sea-Level Curves 16
Barrier Island Formation 16

METHODS 21
General 21
Field Investigations 21
Bathymetric Survey 21
Beach Profiles 21
Sediment Samples 24
Mapping and Determination of Migration of Intertidal Sand Bodies 24

Bedform Measurements 24
Trenches 28
Hydrographies 28
Aerial Reconnaissance Surveys 32
Vibra-Cores 32
Laboratory Analyses 32
Vibra-Core Analysis 32
Grain Size Analysis 34
Historical Shoreline and Ebb-Tidal Delta Morphologic Change 36

EBB-TIDAL DELTA CHARACTERISTICS 37

Introduction 37
Discussion 37

HYDRODYNAMICS 46

HYDRODYNAMIC REGIME 46
Results 46
Discussion 67

EBB-TIDAL DELTA MORPHODYNAMICS 77

SEDIMENT CHARACTERISTICS 77

SEDIMENT TRANSPORT PATTERNS 79
Introduction 79
Tidal and Wave-Generated Currents 79
Inlet Sediment Bypassing 79
Swash Processes 80
Longshore Sediment Transport Processes 87
Morphological Changes to Beaches and Intertidal Offshore Sand Bodies 92
Beaches 92
Intertidal Offshore Sand Bodies 95

STRATIGRAPHY 104

INTRODUCTION 104

GENERAL 105
Stratigraphy 105

Near Surface Stratigraphy..... 106

SEDIMENTARY FACIES..... 114
Spit Platform..... 114
Main Ebb Channel..... 116
Marginal Flood Channel..... 119
Swash Platform Channel..... 126
Swash Bar..... 128
Channel Margin Linear Bar..... 134

DISCUSSION..... 146

SEDIMENT TRANSPORT..... 146
Processes and Pathways..... 146
Potential Transport Rates..... 148
Volumetric Changes..... 151

STRATIGRAPHY..... 165

CONCLUSIONS..... 173

REFERENCES..... 177

APPENDICES..... 185

Appendix A: Beach profile data..... 185
Appendix B: Grain size analysis of grab samples and cores..... 200
Appendix C: Core descriptions..... 207

LIST OF TABLES

TABLE	TITLE	PAGE
1.	Bedding classification schemes utilized	29
2.	Wentworth grain size scale	35
3.	Summary of maximum currents for inlet throat stations 1-5	54
4.	Summary of mean currents for inlet throat stations 1-5	54
5.	Summary of hydrographic data for the channel thalweg (Station 3)	55
6.	Summary of maximum currents for longitudinal inlet throat stations 3, 5, 6, 7	55
7.	Summary of mean currents for longitudinal inlet throat stations 3, 5, 6, 7	55
8.	Summary of maximum currents for updrift and downdrift marginal flood channel and swash platform channel stations 1, 9, 10, 11, 12, 19	64
9.	Summary of mean currents for updrift and downdrift marginal flood channel and swash platform channel stations 1, 9, 10, 11, 12, 19	64
10.	Migration of updrift and downdrift swash bars as determined by measuring changes in distance between permanent stake and slipface	82
11.	Summary of hydrographic data for hydrography stations associated with the swash process study (stations 15-18)	86
12.	Summary of hydrographic data for hydrography stations associated with the longshore current/downdrift sediment transport reversal hydrography (stations 8-9, 11-14)	91
13.	Amounts of profile accretion and erosion at Crane and Coffins Beach as determined by change in volume over time	96

14. Change in surface area over time of updrift and downdrift channel margin linear bar and downdrift swash bar..... 100

15. Bedform measurements at specific environments..... 107

16. Changes in sediment volume for Crane and Coffins Beaches and in area for intertidal offshore sand bodies..... 154

17. Historical morphological changes to Essex River ebb-tidal delta and surrounding environments..... 158

LIST OF FIGURES

FIGURE	TITLE	PAGE
1.	Location map of Essex River Inlet	4
2.	Typical ebb-tidal delta morphology	5
3.	Wind rose diagrams	7
4.	Wave window and wave rose diagram for Essex River ebb-tidal delta	8
5.	Plot of mean tidal range versus deep water mean wave height depicting the hydrographic regime of northeastern Massachusetts	9
6.	Bedrock geologic map of eastern Massachusetts and vicinity	11
7.	Surficial geologic map of the Essex area	13
8.	Map of upper Wisconsinan moraines, moraine segments and meltwater deposits of eastern Massachusetts	14
9.	Map of Late Wisconsinan glacial lobes, retreatal positions and inferred late glacial ice-flow direction for southeast New England	15
10.	Map of location and thickness of submerged Merrimack River delta	17
11.	Sea-level curves for northeastern Massachusetts	18
12.	Sequential maps showing formation of barrier islands of the southern Merrimack Embayment	19
13.	Location map of fathometer profiles	22
14.	Location map of profile stations and profile transects	23
15.	Location of sediment samples	25
16.	Location map of stakes utilized to measure migration of sand bodies	26

FIGURE	TITLE	PAGE
17.	Monthly relative sea level for the ten year periods 1981-1990, and January, 1989 to June, 1990	27
18.	Location map of trenches	30
19.	Location map of hydrography stations	31
20.	Location map of cores	33
21.	Variations in ebb-tidal delta morphology with respect to relative magnitudes of offshore, onshore and longshore currents	38
22.	Tidal prism-ebb-tidal delta storage relationship for moderately exposed coasts	40
23.	Fathometer profile I-I' of the cross section of the main ebb channel	41
24.	Fathometer profile A-A" of the main ebb channel performed longitudinally	42
25.	Fathometer profile G-G' of the downdrift marginal flood channel and H-H' of the updrift marginal flood channel	44
26.	Location map of inlet throat hydrography stations 1-5	47
27.	Cross section of inlet throat channel with location of hydrography stations 1-4	48
28.	Velocity-time series and tide curve for inlet throat hydrography stations 1-4 on 26 July, 1989	49
29.	Velocity-time series and tide curve for inlet throat hydrography stations 1-4 on 10 August, 1989	50
30.	Velocity-time series and tide curve for inlet throat hydrography stations 1-4 on 17 August, 1989	51
31.	Velocity time-series and tide curve for longitudinal main ebb channel hydrography stations 3 and 5 on 05 August, 1990	52

FIGURE	TITLE	PAGE
32.	Velocity-time series and tide curve for inlet throat and longitudinal main ebb channel hydrography stations 1, 3 and 5 on 12 September, 1990	53
33.	Regression curves for maximum and mean currents velocity versus tidal range at the inlet throat channel thalweg (station 3)	56
34.	Fathometer profiles A-A', A-A" of the main ebb channel performed longitudinally	57
35.	Velocity-time series and tide curve for longitudinal main ebb channel hydrography stations 6 and 7 on 12 June, 1990	59
36.	Fathometer profiles B-B', B-C' and C' to B" of the main ebb channel performed longitudinally	60
37.	Oblique aerial photograph showing well-developed ebb-oriented sandwaves in the main ebb channel and well-developed flood-oriented sandwaves in the marginal flood channel	61
38.	Velocity-time series and tide curve for updrift and downdrift marginal flood channel hydrography stations 9, 11, 12	62
39.	Velocity-time series and tide curve for downdrift marginal flood channel and swash platform channel hydrography stations 10,11, 12, 19	63
40.	Plotted points for maximum and mean current velocity versus tidal range for updrift marginal flood channel hydrography stations 1 and 9 for flood and ebb tidal cycles	65
41.	Plotted points for maximum and mean current velocity versus tidal range for downdrift marginal flood channel stations 10, 11, 12 for flood and ebb tidal cycles	66
42.	Fathometer profiles F-F" and F'-F"' of the updrift marginal flood channel	68
43.	Fathometer profiles D-D' and E-E' of the downdrift marginal flood channel	69

FIGURE	TITLE	PAGE
44.	Fathometer profiles D'-D" of the downdrift marginal flood channel and E-E' of the downdrift swash platform channel....	70
45.	Net direction and magnitude of maximum currents as determined from hydrographic data.....	71
46.	Segregation of flow of the ebb-tidal delta and effect on ebb-tidal delta morphology.....	73
47.	Idealized inlet flow patterns for flood and ebb tidal stages.....	74
48.	Typical tidal current velocity-time series for a mesotidal ebb-tidal delta and for the main ebb channel, and updrift and downdrift marginal flood channels of the Essex River ebb-tidal delta.....	75
49.	Plot of tidal prism versus minimum inlet cross sectional area. The Essex River Inlet fits well within the 95% confidence limits.....	76
50.	Ground view of the slipface of the downdrift swash bar.....	81
51.	Landward migration of downdrift and updrift swash bars as determined from mapping on three different dates.....	83
52.	Oblique aerial photograph showing the landward migration of the downdrift swash bar.....	84
53.	Velocity-time series and tide curve for stations 15-18 associated with the swash process study.....	85
54.	Velocity-time series and tide curve for hydrography stations 8-9, 11-14 on 17 July, 1990 utilized to determine longshore sediment transport currents and sediment transport reversal.....	88
55.	Velocity-time series and tide curve for downdrift marginal flood channel hydrography stations 11 and 12 on 5 August, 1990 to determine the presence of a downdrift transport reversal.....	89
56.	Velocity-time series and tide curve for downdrift marginal flood channel hydrography stations 13 and 14 on 12 September, 1990 to determine the presence of a downdrift transport	

FIGURE	TITLE	PAGE
	reversal	90
57.	Wave refraction diagram of the ebb-tidal delta	93
58.	Sediment transport directions as determined from residual current measurements from hydrographies, swash bar slipface orientation and the wave swash process study	94
59.	Changes in volume over time for profiles on Crane Beach from June, 1989 to August, 1990	97
60.	Changes in volume over time for profiles on Coffins Beach from June, 1989 to August, 1990	98
61.	Location and size of intertidal sand bodies at 0.30 m below MLW	101
62.	Oblique aerial photographs on (A) 27 May, 1989 and (B) 3 March, 1990 demonstrating the migration of the outer main ebb channel	102
63.	Ebb-oriented scour megaripples on the distal portion of the downdrift channel margin linear bar	103
64.	Bedform measurements following extreme tidal conditions (ebb-tidal range of 4.0 m)	111
65.	Bedform measurements following four days of strong northeast winds	112
66.	Sediment transport directions as determined from bedform measurements and dip angle and direction of bedding in trenches	113
67.	Location of sedimentary environments of the Essex River ebb-tidal delta	115
68.	Trench # 2 cut through migrating ridge and runnel system on Crane Beach	117
69.	Cut and fill accretionary beds associated with main ebb channel migration	118
70.	Peel 1 of Core 12 (1.04 m-1.56 m) showing internal stratification	

FIGURE TITLE PAGE

characteristic of the main ebb channel environment..... 120

71. Peel 2 of Core 8 (1.90 m-2.25 m) showing internal stratification characteristic of the marginal flood channel environment..... 122

72. Peel 3 of Core 11 (1.82 m-2.24 m) showing internal stratification characteristic of the marginal flood channel environment..... 123

73. Peel 4 of Core 11 (2.50 m-2.95 m) showing internal stratification characteristic of the marginal flood channel environment..... 124

74. Peel 5 of Core 15 (2.50 m-2.78 m) showing internal stratification characteristic of the swash platform channel environment.... 127

75. Trench # 6 cut through migrating bar on the downdrift swash bar..... 130

76. Peel 6 of Core 3 (2.60 m-2.81 m) showing internal stratification characteristic of a migrating slipface of the swash bar environment..... 132

77. Peel 7 of Core 19 (2.44 m-2.87 m) showing internal stratification characteristic of the swash bar environment..... 133

78. Trench # 1 cut through slipface on the northwest side of the updrift channel margin linear bar..... 135

79. Ebb-oriented sandwaves on the proximal portion of the updrift channel margin linear bar..... 136

80. Flood-oriented sandwaves on the proximal portion of the updrift channel margin linear bar..... 137

81. Trench #3 cut through flood-oriented bedform on the proximal portion of the updrift channel margin linear bar..... 139

82. Trench #4 cut through ebb-oriented bedform on the proximal portion of the updrift channel margin linear bar..... 140

83. Trench # 5 cut through the main ebb channel scour slipface on the northwest side of the proximal downdrift channel margin linear bar..... 141

FIGURE	TITLE	PAGE
84.	Peel 8 of Core 6 (1.80 m-2.24 m) showing internal stratification characteristic of the distal channel margin linear bar environment	143
85.	Peel 9 of Core 17 (1.07 m-1.50 m) showing internal stratification characteristic of the distal channel margin linear bar environment	144
86.	Sediment transport gyres for both updrift and downdrift portions of the Essex River ebb-tidal delta	147
87.	Potential net sediment transport directions for the Essex River ebb-tidal delta as determined from Maddock's equation (1969)	149
88.	Model of onshore migration of bar complexes and attachment to Crane and Coffins Beaches	152
89.	Morphologic changes to the Essex River ebb-tidal delta as determined form vertical aerial photographs	155
90.	Historic shoreline changes of Crane Beach and Coffins Beach as determined from four different coastal charts	162
91.	Overall ebb-tidal delta stratigraphic sequence model	166
92.	Stratigraphic sequence model for the updrift portion of the Essex River ebb-tidal delta	169
93.	Stratigraphic sequence model for the downdrift portion of the Essex River ebb-tidal delta	170
94.	Stratigraphic sequence model for the distal portion of the Essex River ebb-tidal delta	172

INTRODUCTION

The focus of this study is a well-developed mixed energy tide-dominated ebb-tidal delta at Essex River Inlet, Massachusetts. This sand body, which extends seaward of the inlet for 1.4 km, formed and is modified from the interaction of waves and tidal currents (Hayes, 1975).

The Essex River Inlet was the basis of Hayes' (1975) morphological ebb-tidal delta model and has characteristic features including an ebb-dominated main ebb channel, two flood-dominated marginal flood channels, a wave-dominated swash platform and a terminal lobe. Intertidal sand bodies include several swash bars and two channel margin linear bars.

Although ebb-tidal delta processes and morphology have been studied previously at other deltas (Hayes, 1975, 1980; Finley, 1975, 1978; Hine, 1975; Hubbard, 1975, 1977; Oertel, 1975; FitzGerald, 1976, 1982, 1984; FitzGerald, Nummedal and Kana, 1976; FitzGerald and Nummedal, 1983; Humphries, 1979; and Sha, 1990), sediment transport pathways at New England mixed-energy ebb-tidal deltas have not been verified. Most sediment transport at the Essex River ebb-tidal delta occurs within sediment gyres which circulate sediment through the system. These gyres as well as transport of sediment around the terminal lobe have a direct relation to changes in beach volume and intertidal sand body area. A comparison between these present day processes and historical aerial photographs have indicated that the Essex River ebb-tidal delta undergoes a 5-7 year cycle of volume change and attachment of swash bars to landward beaches (cf. FitzGerald, 1984).

Sediment characteristics as related to stratigraphy of ebb-tidal deltas have been documented by few authors (Nelligan, 1983; Imperato, 1988; and Sha, 1989). Several hypothetical stratigraphic models of deltas have been proposed, but these are based mainly on surficial sedimentological processes and near-surface sedimentary structures (Moslow, 1977; Barwis and Hayes, 1978; and Hubbard, Oertel and Nummedal, 1979).

Kumar and Sanders (1974), and FitzGerald and Nummedal (1977) have documented large-scale ebb-tidal delta stratigraphy through subsurface seismic profiling.

The purpose of this study is to descibe the morphological changes that occur at the Essex River ebb-tidal delta, and to demonstrate how these changes are preserved in the subsurface. Thus, a large-scale stratigraphic framework for the Essex River ebb-tidal delta can be determined. Models of ebb-tidal delta stratigraphy are presented which rely upon differential sediment transport processes and patterns due to sediment input, channel migrations and swash bar migration.

PHYSICAL SETTING

LOCATION AND PHYSIOGRAPHY

The Essex River Inlet and ebb-tidal delta system are located in the Merrimack Embayment on the northeastern Massachusetts-southeastern New Hampshire coast (Figure 1). The Merrimack Embayment is backed by a 35 km long barrier island chain which stretches from the bedrock promontories of Great Boars Head, New Hampshire south to Cape Ann, Massachusetts. The Essex River Inlet is located in the southern portion of this chain and is 2.5 km to the west of Cape Ann. The Inlet is 40 km northeast of Boston, Massachusetts.

Essex River Inlet is situated between the Crane Beach (Castle Neck) and Coffins Beach barriers. Both of these barriers are backed by extensive marsh and tidal creek systems with minimal fresh water input from the Castle Neck and Essex Rivers. The backbarrier is approximately 4.1 km^2 in area, of which 56% is salt marsh, 35% tidal channel (subtidal) and 9% glacial material in the form of islands (Som, 1990).

The primary focus of this study is the well-developed ebb-tidal delta which extends 1.4 km seaward of the mouth of the Essex River Inlet. This inlet was the example that Hayes (1975) used to present his ebb-tidal delta model (Figure 2). Characteristic features of an ebb-tidal delta include an ebb-dominated main ebb channel, two marginal flood channels dominated by landward flow, a wave-dominated swash platform and a terminal lobe. Intertidal sand bodies include several swash bars, and two channel margin linear bars (Hayes, 1975).

COASTAL PROCESSES

Tides

The tides for this area are semi-diurnal and have an inequality. The mean tidal range is 2.60 m with a spring tidal range of 3.20 m, thus classifying the coast as mesotidal (Davies, 1964).

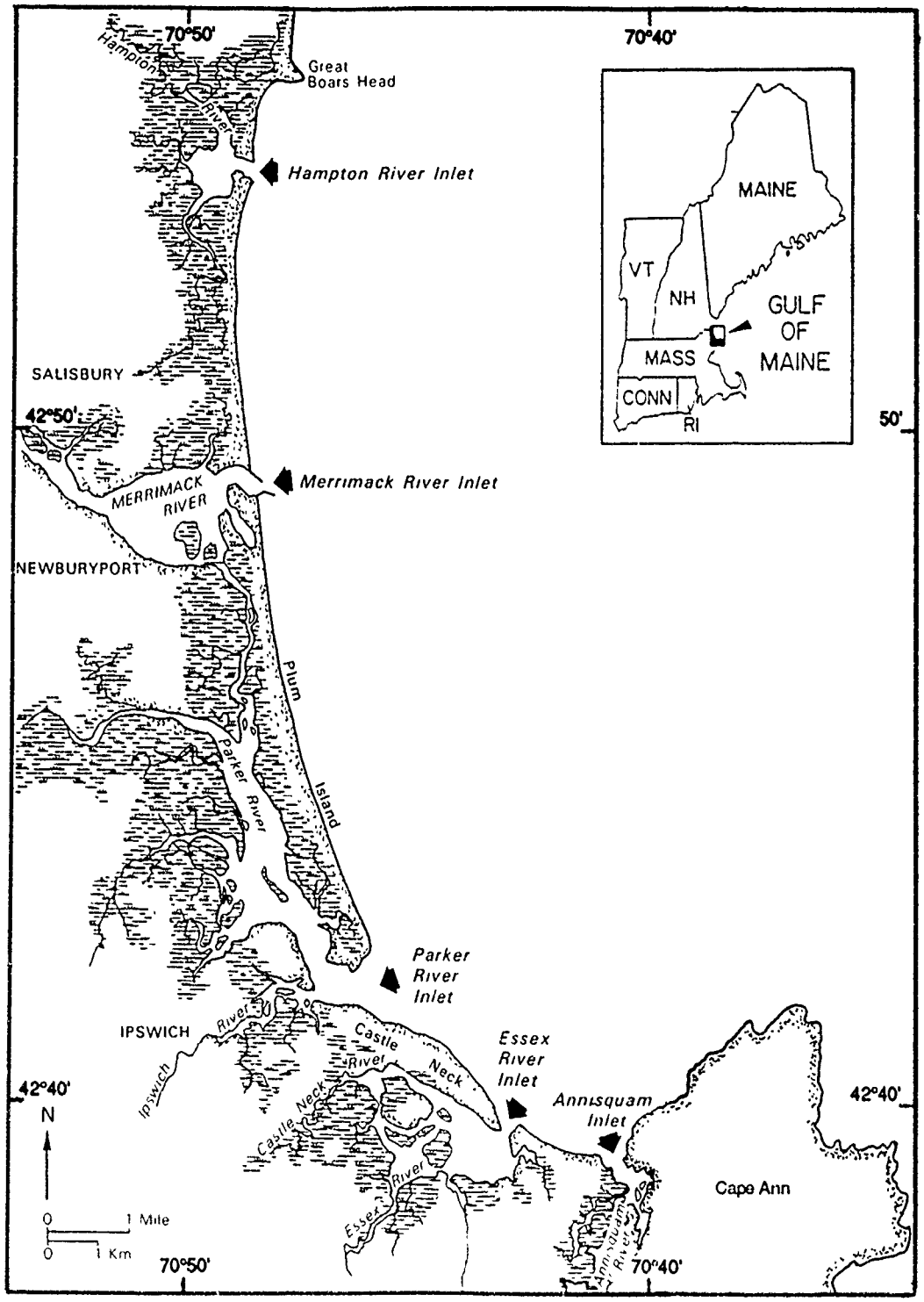

Figure 1. Location map of Essex River Inlet with respect to other inlets of the Merrimack Embayment.

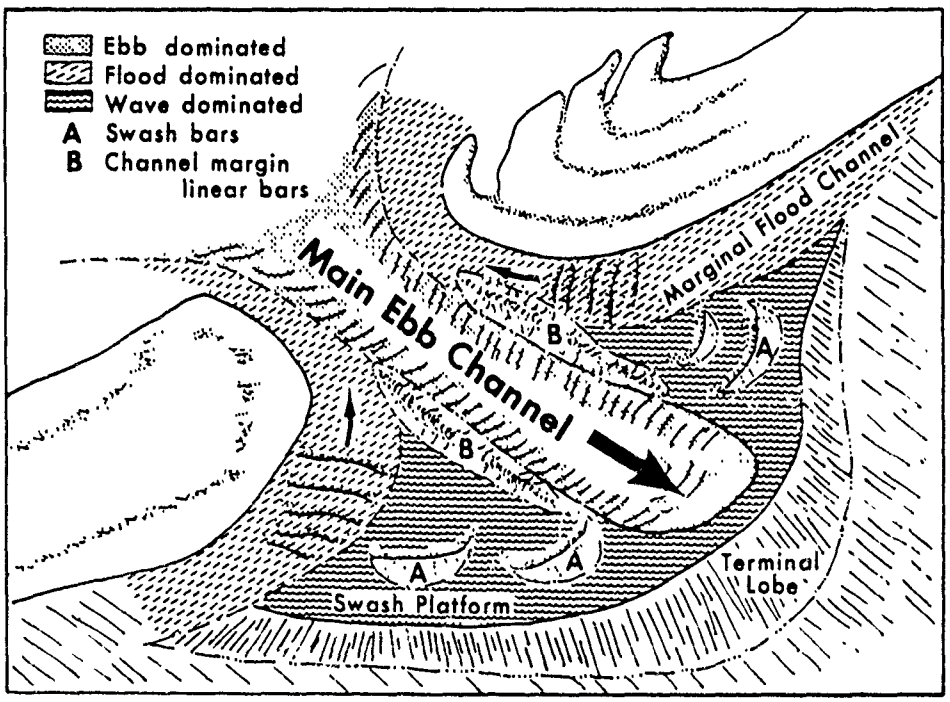

Figure 2. Typical ebb-tidal delta morphology. Note the deep central trough in the main ebb channel which is flanked by channel margin linear bars and swash platforms. Marginal flood channels separate the channel margin linear bars from the adjacent beaches. The terminal lobe is the most distal part of the ebb-tidal delta. Different patterns indicate which areas are dominated by ebb currents, flood currents or waves (from FitzGerald et al., 1976; after Hayes, 1975).

Wind Regime

The winds for this region are known from data collected over a ten year period (October, 1949 to September, 1959) at Logan Airport (Hayes et al., 1973) (Figure 3'A') and a four and one half year period (August, 1984 to November, 1988) from the NOAA Buoy 44013 located approximately 15 km east of the Boston Harbor entrance (Sverdrup, 1990)(Figure 3'B'). These two data bases show that prevailing winds are from the southwest during spring and summer months and are from the northwest during the fall and winter months. The predominant winds are from the northeast and are associated with extratropical storms.

Wave Regin

The constriction of the study area by land masses creates a limited fetch window of 15° to 65° azimuth (Figure 4'A'). Thus, the prevailing and predominant wave direction is from the east-northeast (Figure Ph 4'B').

The deepwater mean wave height for this region is 1.20 m as determined for a region approximately 30 km southeast of Kennebunkport, Maine (Station 8 of Corson et al., 1982)(Abele, 1977). This deepwater wave height coupled with the mean tidal range of 2.60 m classifies this coast as a mixed energy, tide-dominated hydrographic regime setting (Figure 5)(Hayes, 1979; Nummedal and Fischer, 1978).

The mean significant wave height for Plum Island is 0.52 m (Abele, 1977). The maximum significant wave height determined during a twenty year hindcast study is 3.93 m (Jensen, 1983).

Longshore Sediment Transport

Longshore currents in the study area are southerly directed and are mainly a result of wind and wave energy. This current and sediment transport direction are reflected by the growth of recurved spits on the southern downdrift ends of Crane Beach and Plum Island (Farrell, 1969) and increase of spacing of offshore contours to the south along the Merrimack Embayment barrier island chain. This increase in spacing of contours denotes a more gradual slope of the sea floor bottom and

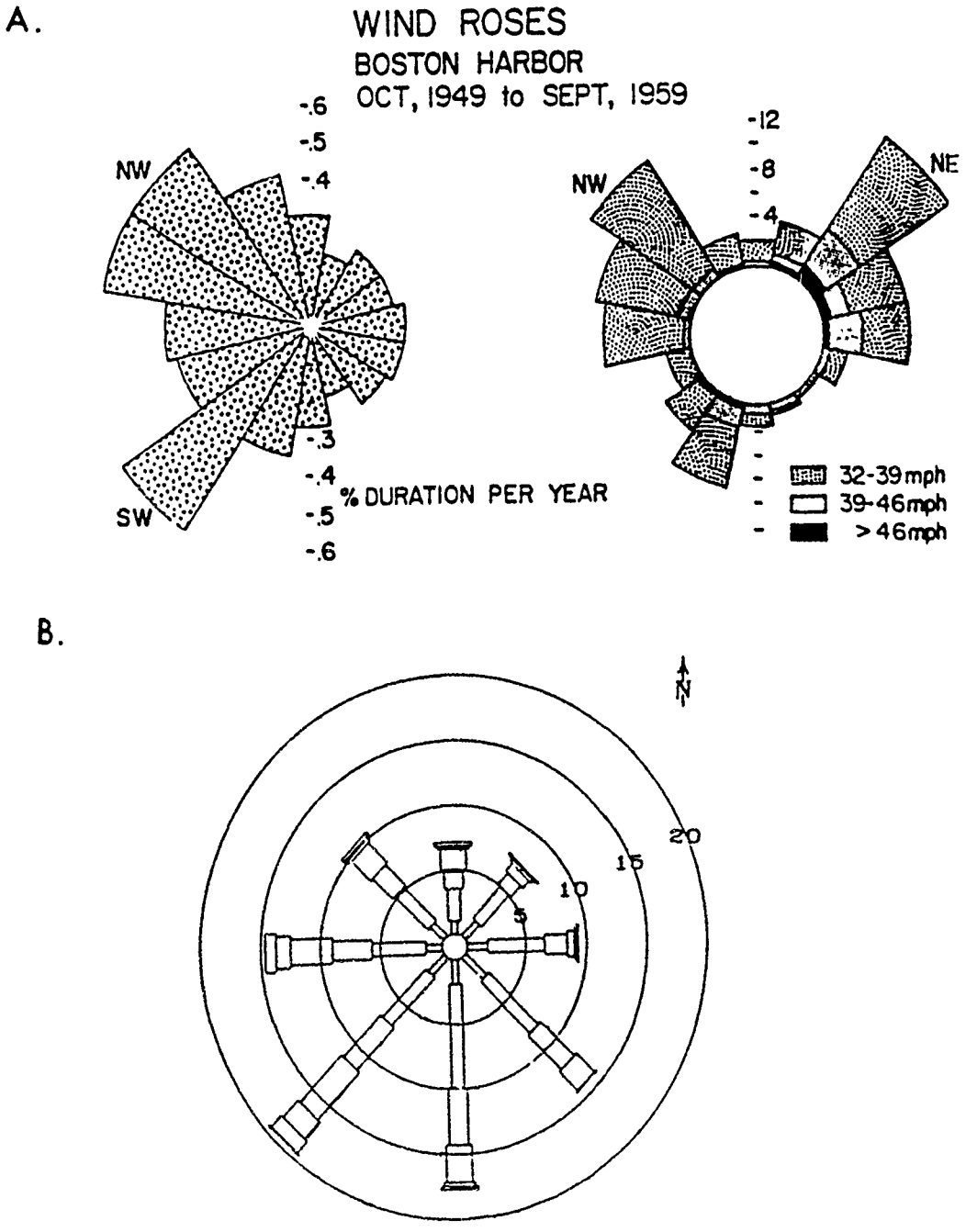

Figure 3 . Wind rose diagrams. A) Wind roses for Boston Harbor for the period 1949 to 1959. These roses show that the prevailing winds are from the southwest during summer and spring seasons and northwest during winter and fall seasons. The predominant winds are from the northeast (Hayes et al., 1973). B) Wind rose for Boston Harbor for the period 1985 to 1990. This rose shows that the prevailing winds on an annual basis are from the southwest. Each successive increase in width denotes a new 5-knot wind category (Sverdrup, 1990).

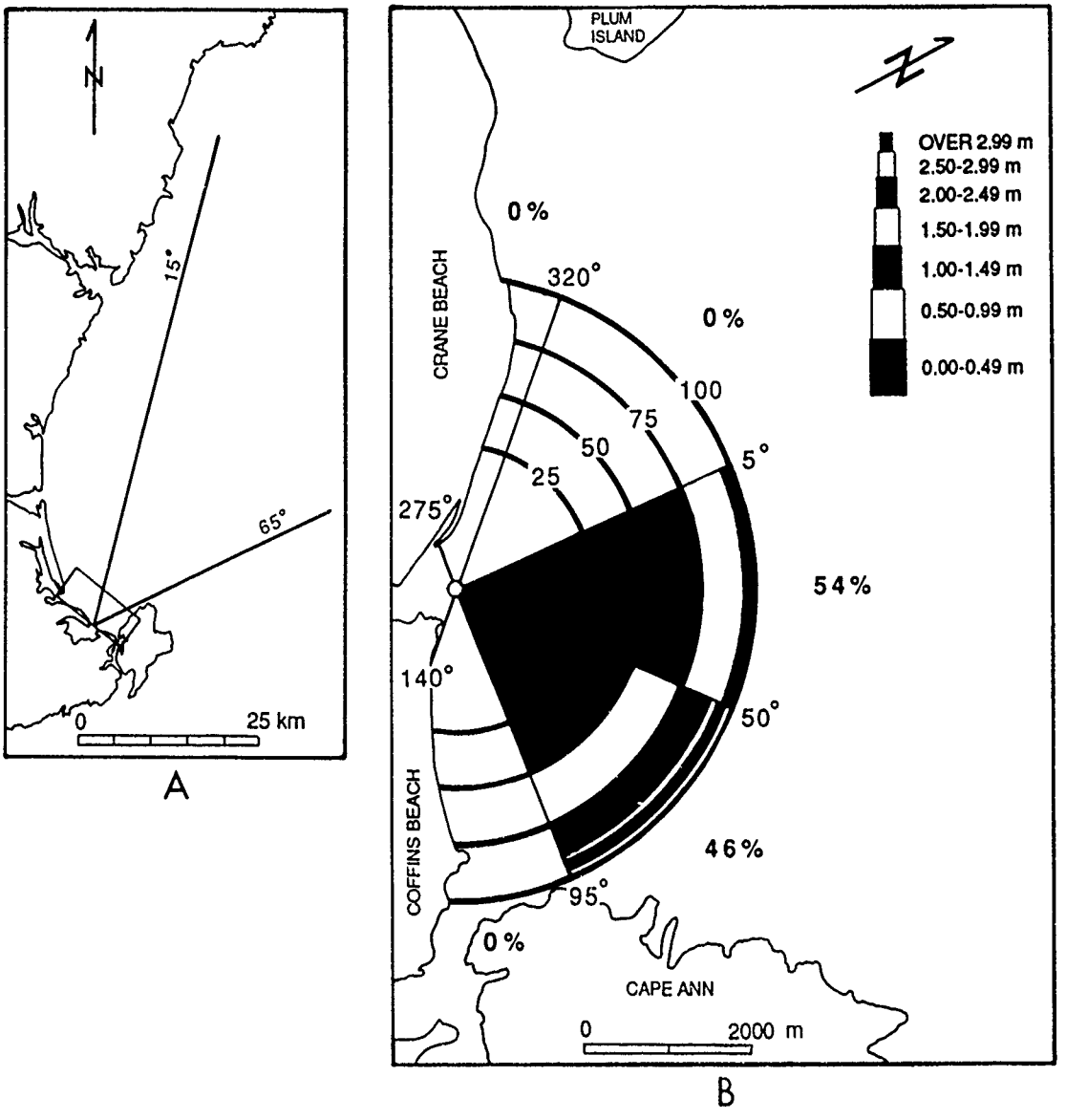

Figure 4 . A) Wave window showing limited range of wave propogation of 15° to 65° azimuth. This window is confined by the Kennebunk Peninsula to the north and Cape Ann Promontory to the east. B) Wave rose diagram showing percent occurrence and and direction of wave propogation for 20 years hindcast. The width of each bar segment indicated the significant wave height (H_S) range and the length of the bar segment indicates the percent occurrence of waves from the specified direction. For example for the 20 year hindcast, 54% of the waves were propogating from 5° to 50° azimuth. Of the 54%, approximately 75% were less than 0.5 m., approximately 20% were between 0.5 m. to 1.0 m. and approximately 5% were between 1.0 m. and 1.5 m. All directions in degrees azimuth (Jensen, 1983).

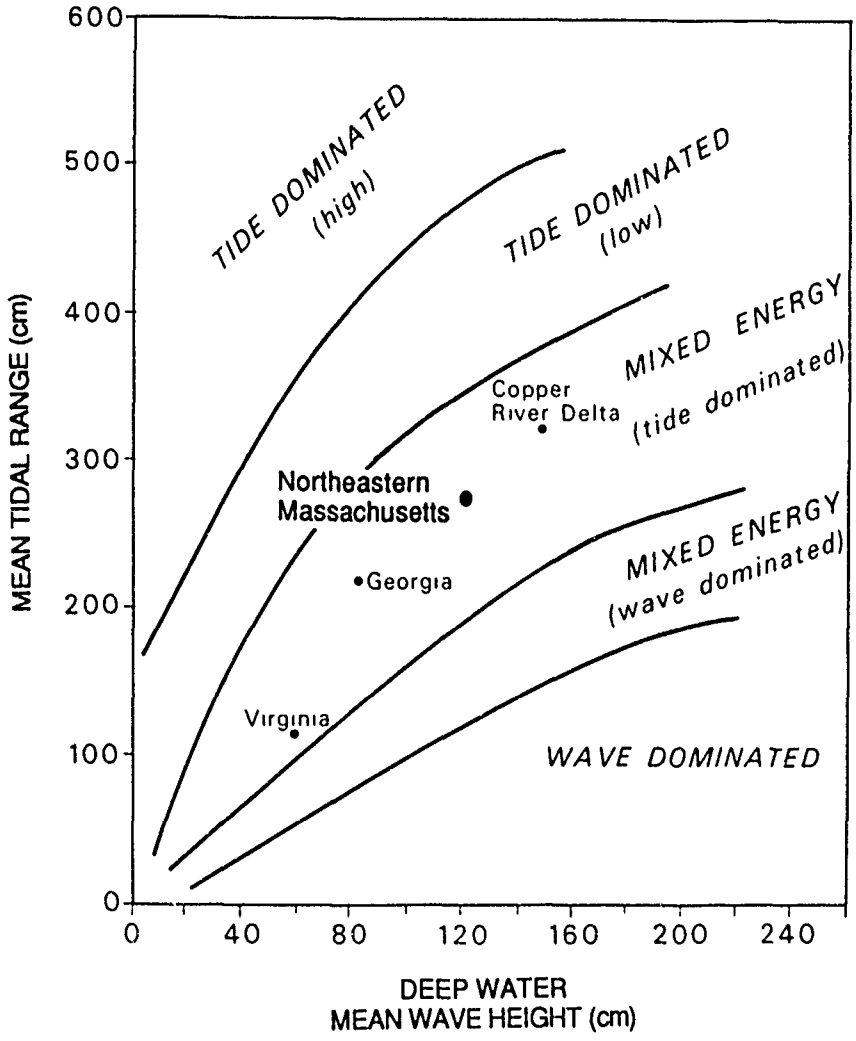

Figure 5 . Hydrographic regime of northeastern Massachusetts. This coastline is classified as mixed energy (tide-dominated). Other examples of mixed energy (tide-dominated) coastlines are Virginia, Georgia and Copper River Delta, Alaska (Hayes, 1979).

therefore an increase of sediment at southern portions of the bay. This suggests that southern portions of the Merrimack Embayment are a sink for sediment transported by longshore currents (Hubbard, 1976).

A maximum longshore sediment transport rate of 150,000 m^3/year has been calculated for Plum Island by applying data from Abele (1977), including a significant wave breaker height of 0.52 m and mean breaker angle of 4°, to Figure 4-38 of the 1984 Shore Protection Manual. The longshore sediment transport rate for Crane Beach would be significantly less than than 150,000 m^3/year due to a smaller breaker angle which results from its more perpendicular orientation to the dominant wave approach, and smaller wave heights due to increased spacing of offshore contours. A hypothesized breaker angle for Crane Beach of 1° coupled with a mean breaker height of 0.52 m would indicate a maximum longshore sediment transport rate of 38,000 m^3/year (U.S. Army Corps of Engineers, 1984).

A change in shoreline orientation and decreasing oblique wave approach throughout the Merrimack Embayment results in a decrease in longshore sediment transport rate and a fining of grain size to the south (Shalk, 1936; Goodbred and Montello, 1989).

GEOLOGIC HISTORY

Bedrock

The structural geology of northeastern Massachusetts is dominated by the Precambrian aged Nashoba Thrust Belt which represents a westward-dipping subduction zone between the Southeast New England Platform to the southeast, a fragment of the former Paleo-African plate, and the Sturbridge Geocline to the northwest, a foreland basin of the North American Plate (Barosh, 1979). Southwest-northeast trending thrust faults are associated with this late Precambrian event which include the Clinton Newbury Fault, Assabet River Fault, Bloody Bluff Fault and the Mystic Fault, which trends north of the study area by about 10 km (Cameron and Naylor, 1976) (Figure 6).

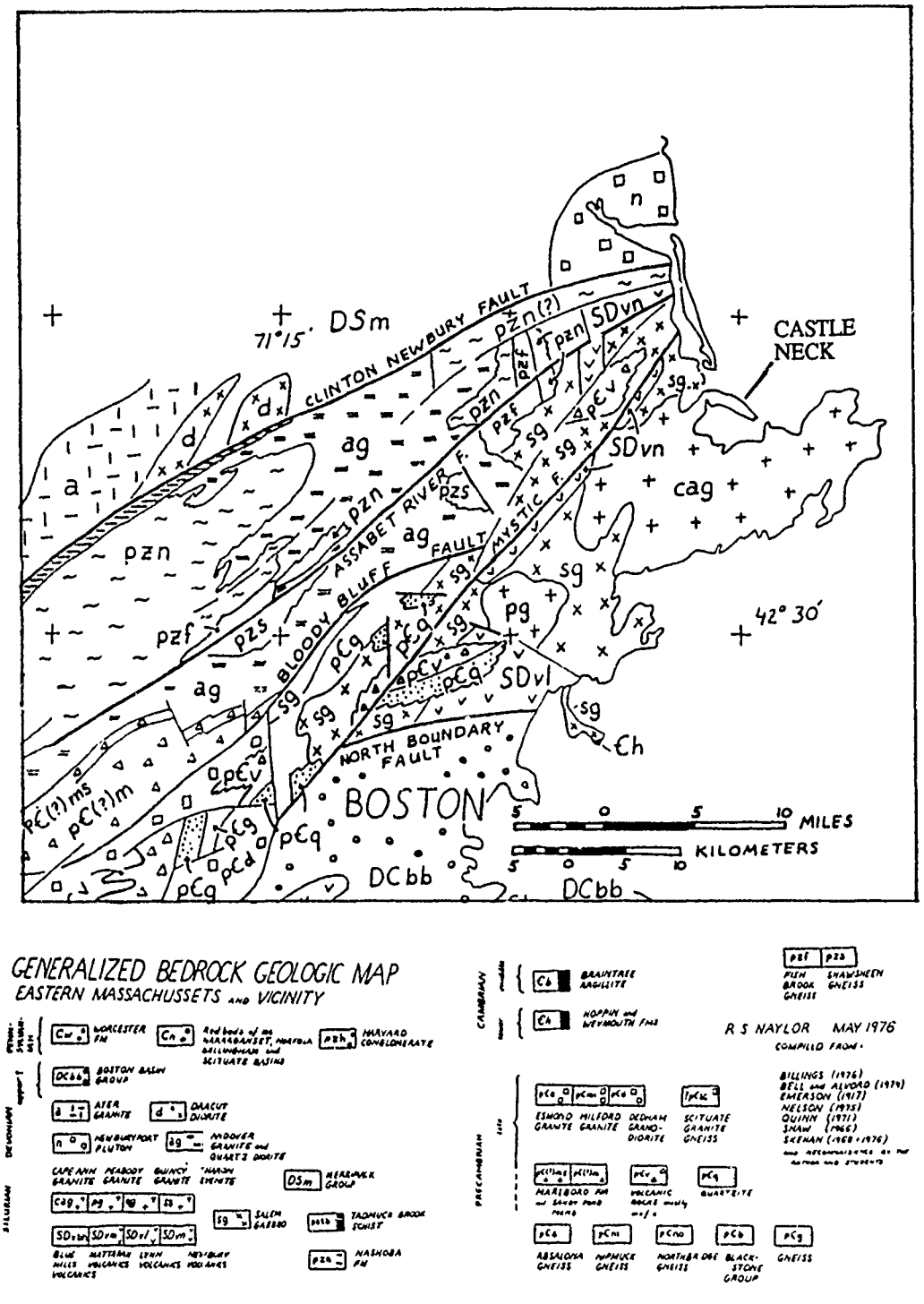

Figure 6 . Bedrock geologic map of eastern Massachusetts and vicinity. Cape Ann Granite (cag) is found in the vicinity of Castle Neck (Cameron and Naylor, 1976)

The study area is located southeast of the Nashoba thrust belt and is therefore considered to be part of the Southeast New England Platform, a geologic terrain which consists of a late Precambrian batholithic complex and associated metasedimentary and metavolcanic rocks (Barosh, 1984).

During the Taconic Orogeny of the late Ordovician-early Silurian Periods northeast Massachusetts was intruded by volcanics such as the Cape Ann Granite and Salem Gabbro-Diorite forming the resistant headland of Cape Ann (Barosh, 1984).

Local bedrock exposures in the study area are represented by the symbols 'c' and 's' in Figure 7 including Twopenny Loaf on the northwesternmost point of Coffins Beach.

Late Pleistocene Glacial History

Paleozoic bedrock is unconformably overlain by deposits associated with numerous Pleistocene glaciations, the most important and recent of which is the Wisconsinan glacial stage (Shafer and Hartshoorn, 1965). Regionally, northeastern Massachusetts is dominated by glaciomarine deposits (Figure 8). Within the study area, glacial deposits are mostly till and include ground moraine and drumlins (Figure 7). Orientations of drumlins indicate that the direction of ice movement was to the southeast (Stone and Peper, 1982)(Figure 9).

The maximum limit of glaciation into the Gulf of Maine extended roughly from the southern shore of Cape Cod to the Nova Scotian Shelf and has been dated as approximately 21,500 yrs. BP (Pratt and Schlee, 1969).

As the glacier retreated, terminal moraines were deposited on the south shore of Long Island, Martha's Vineyard and Nantucket Island. A readvance of the ice margin at approximately 15,300 yrs. BP formed the Buzzards Bay and Cape Cod lobes (Kaye, 1964)(Figure 9). The terminus of the ice margin was near the present day Merrimack Embayment coast approximately 13,200 yrs. BP (Stuiver and Borns, 1975). During this time, the glaciers depressed the land beneath sea level, resulting in a marine transgression and the deposition of glaciomarine sediments. Subsequently, isostatic rebound of the coast occurred at a rate of at least

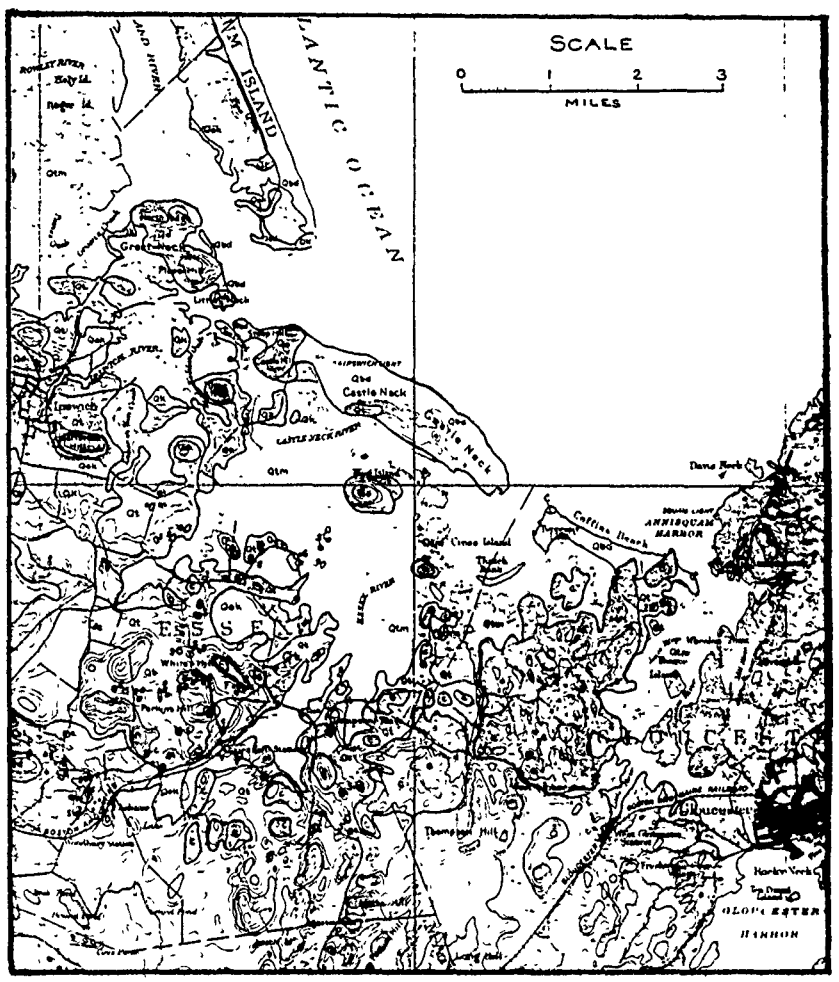

SYMBOLS

UNCONSOLIDATED FORMATIONS

Era: CENOZOIC — Period: QUATERNARY — RECENT / PLEISTOCENE

- Qbd — Beaches and sand dunes
- Qtm — Tidal marshes
- Qc — Marine clays

WATER LAID GLACIAL DEPOSITS

- Qok — Outwash plains and kame terraces
- Qk — Kames

TILL DEPOSITS

- Qt — Ground Moraine
- Qd — Drumlins and drumloidal hills

Outcrops mapped by Chute; includes some thin drift

Outcrops taken from Sears' geologic map of Essex County, Massachusetts

Figure 7 . Surficial geologic map of Essex area including Plum Island, Castle Neck, Crane Beach and Coffins Beach. Drumlins (Qd) and bedrock outcrops (c) are present at Castle Neck-Coffins Beach area (Chute, 1940).

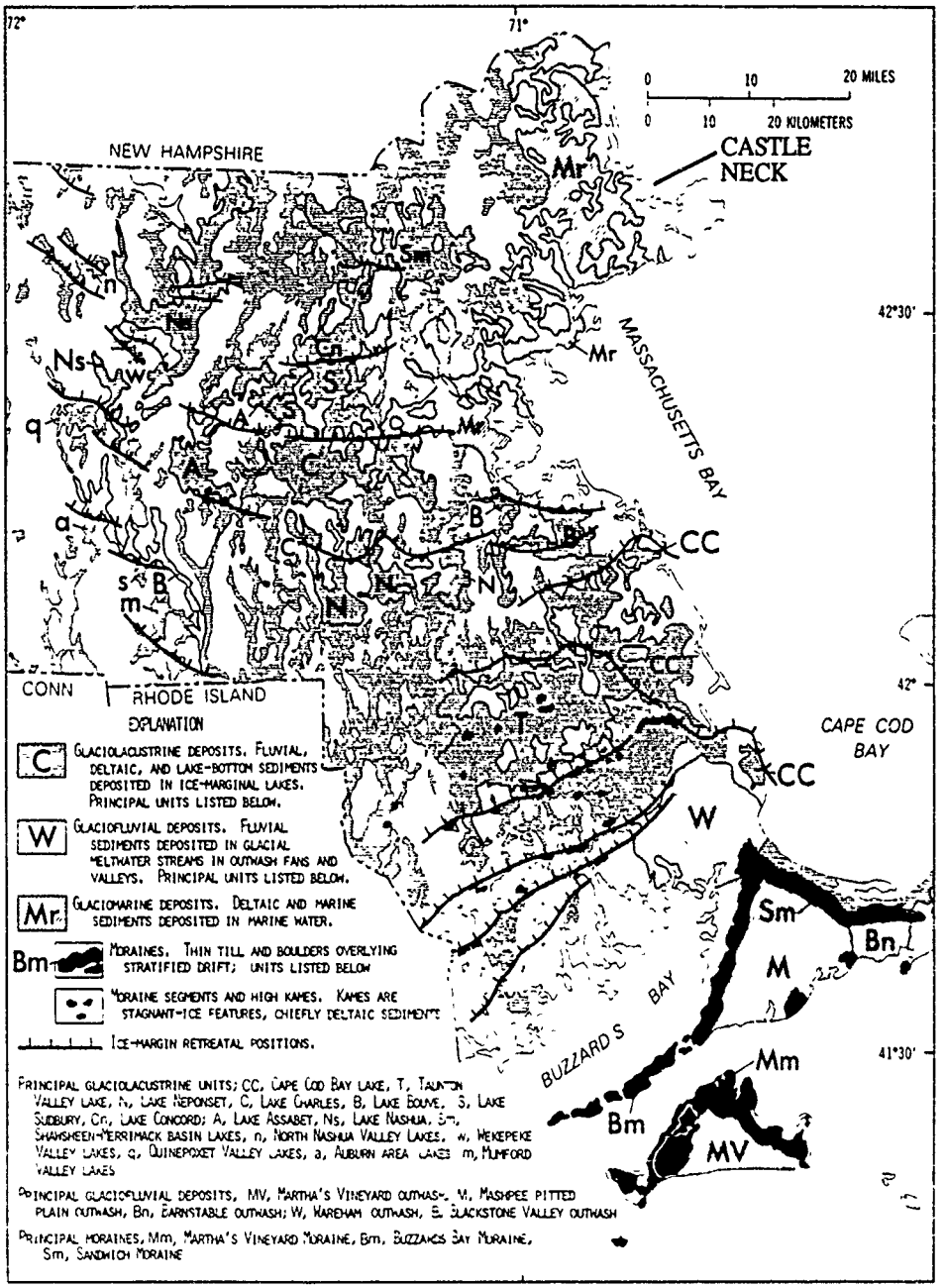

Figure 8 . Upper Wisconsinan moraines, moraine segments and meltwater deposits of eastern Massachusetts. Glaciomarine (Mr) deposits exist in the vicinity of Castle Neck (Stone and Peper, 1982). Note location of Castle Neck in top right of figure.

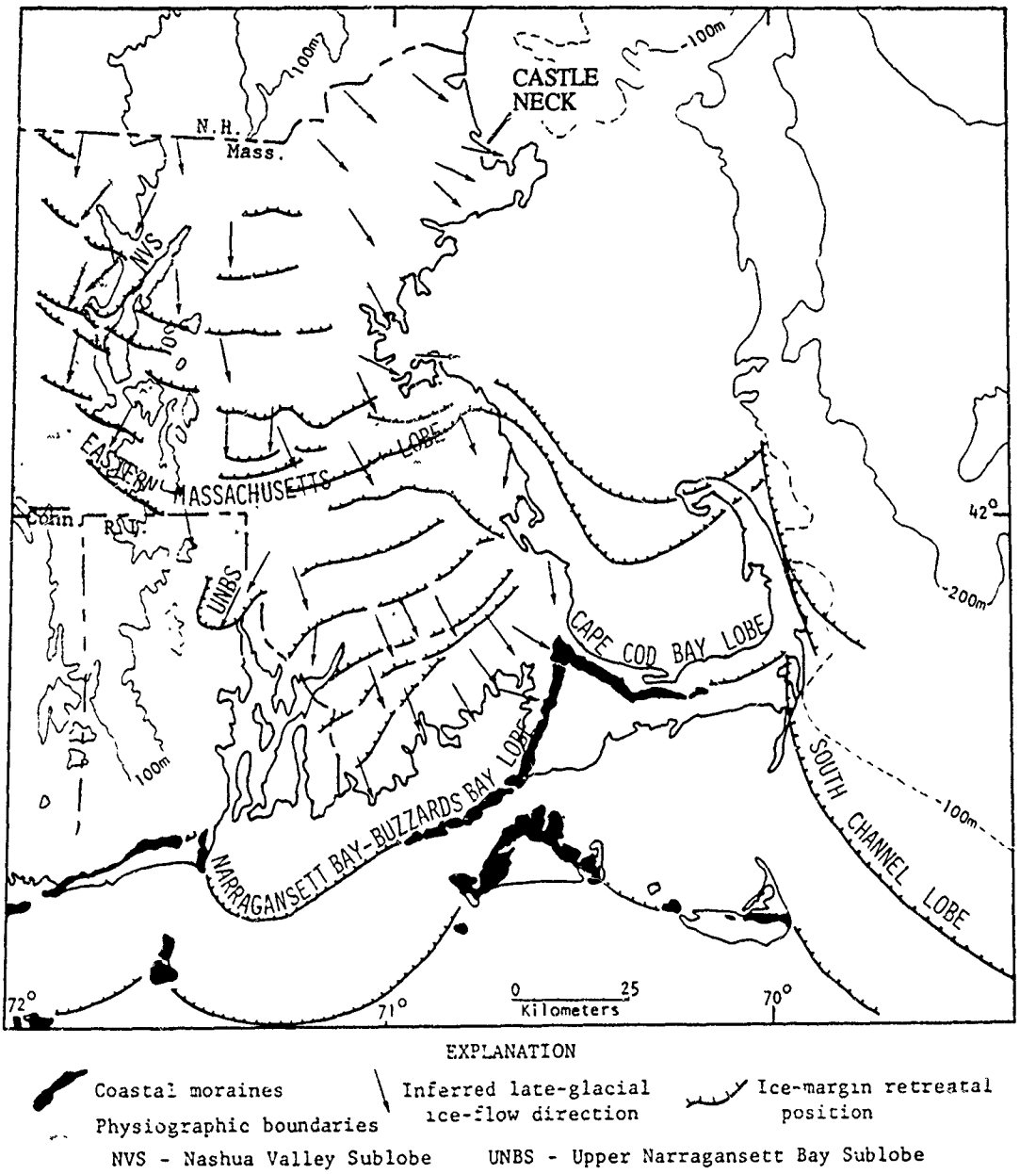

Figure 9 . Late Wisconsinan glacial lobes, retreatal positions and inferred late glacial ice-flow direction for southeast New England. In the vicinity of Castle Neck, the predominant glacial movement is from the west-northwest (Stone and Peper, 1982). Note location of Castle Neck on top of figure.

5m/1000 yrs. as the ice margin retreated northward (Oldale et al., 1983). Maximum emergence of the coastal region took place at approximately 8,500 yrs. BP (Schnitker, 1984). During this deglaciation, the Merrimack River Delta formed in the Gulf of Maine well seaward of the present day coast (Oldale et al., 1983)(Figure 10).

Late Pleistocene Sea Level Curves

Relative sea level lowering and the resulting seaward migration of the shoreline occurred during the Late Wisconsinan glacial stage. A relative sea level curve for northeastern Massachusetts and southeastern New Hampshire is presented in Figure 11'A'. Sea level changes before 10,500 yrs. BP are not clearly understood. However, two guidelines of the curve before 10,500 yrs. BP include the relative sea level highstand of +32 m at 13,500 yrs. BP and a relative sea level lowstand of -47 m at 10,500 yrs. BP (Oldale et al., 1983). The curve from 10, 500 yrs. BP to the present is more detailed and better understood as it is based upon several radiocarbon dates of Plum Island peats (McIntyre et al., 1963 and Newman et al., 1980). The curve indicates a rapid relative sea level rise of 14 m/1000 yrs. from 10,500 to 8,500 yrs. BP. As can be seen in Figure 11'A' and 11'B', the relative sea level rise from 8,500 to 4,000 yrs. BP occurred at a rate of 3 m/1000 yrs. and was followed by a slower relative sea level rise of approximately 0.75 m/1000 yrs. from 4,000 yrs. BP to the present (Oldale, 1985).

Barrier Island Formation

The formation of barrier islands within the Merrimack Embayment has been a result of relative sea level rise and associated transgression of reworked Merrimack River delta sediments (Figure 12). Rapid relative sea level rise from 8,500 to 4,000 yrs. BP resulted in the flooding of coastal features and transportation of sediments onshore in the form of transgressive barrier islands through shoreface retreat (cf. Swift, 1975). (Figure 12'B').

From approximately 4,000 to 3,000 yrs. BP, the rate of sea level rise decreased (Oldale, 1985) and it is hypothesized that the transgressive

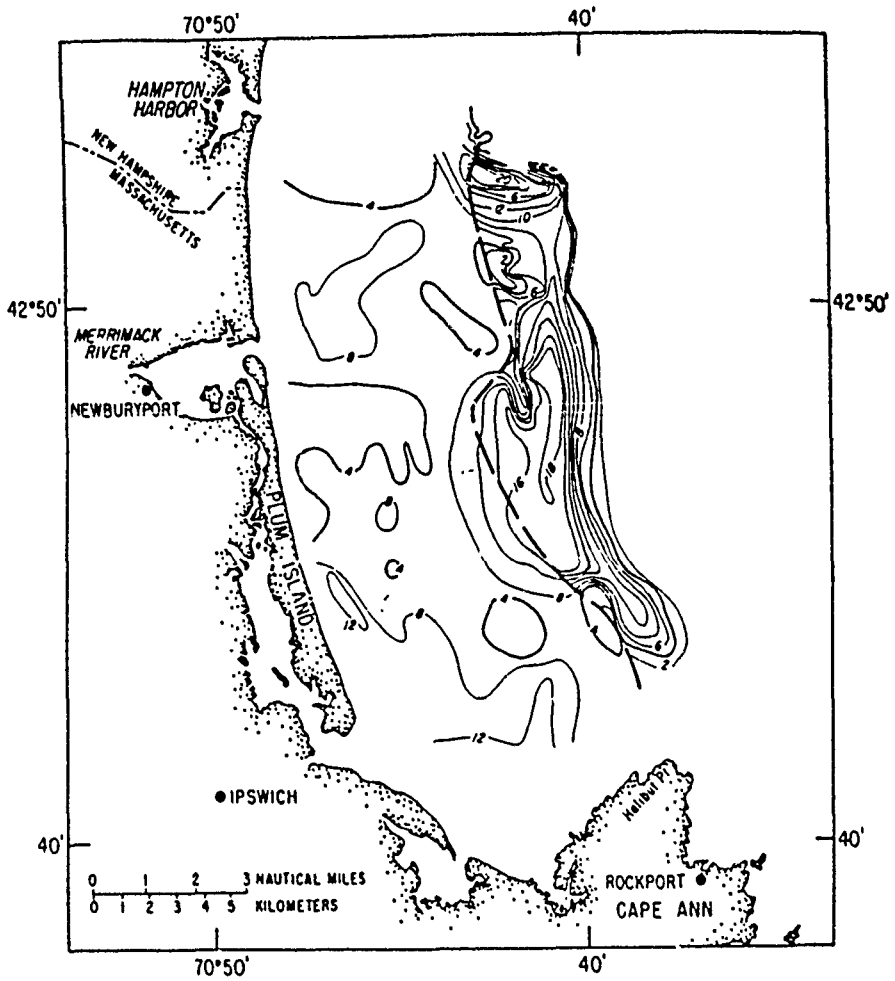

Figure 10. Location and thickness of submerged Merrimack River delta. Contour interval = 2 m. Maximum thickness of delta is 18 m. Dashed line indicates landward limit of foreset beds. (Oldale et al., 1983).

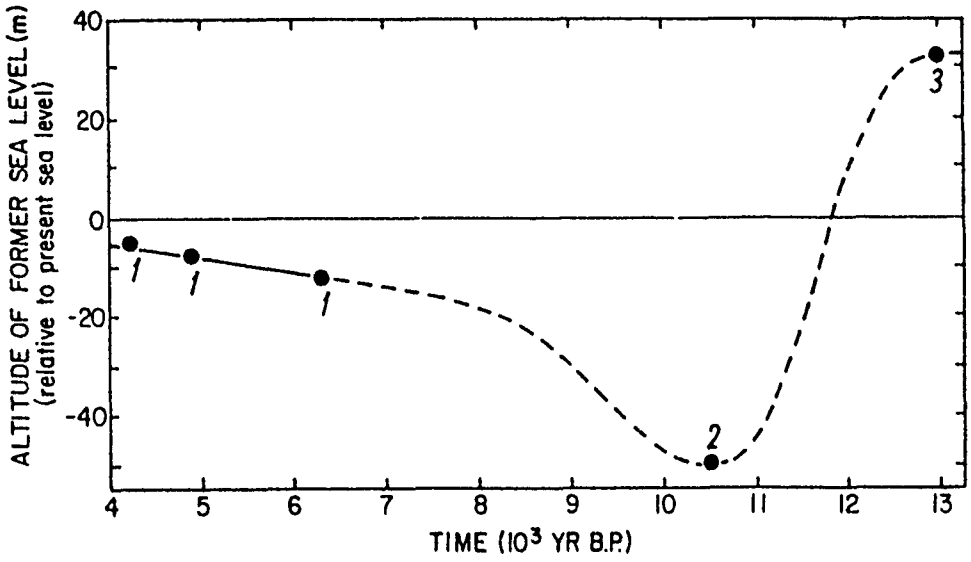

A

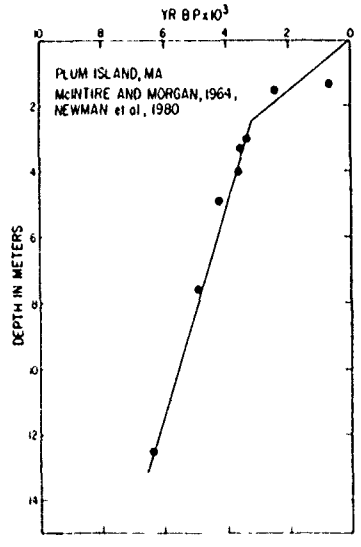

B

Figure 11. Sea-level curves for northeastern Massachusetts. A) Curve showing the inferred relative sea-level change for northeastern Massachusetts and southeastern New Hampshire coasts. Control points are from 1) Plum Island radiocarbon dates; 2) The altitude and age of the post-glacial lowstand inferred from the submerged Merrimack River delta and; 3) The late Wisconsinan highstand in the Merrimack Valley (Oldale et al., 1983). B) Curve showing middle to late Holocene sea-level rise at Plum Island, Massachusetts (Oldale, 1985 after McIntyre et al., 1963 and Newman et al., 1980).

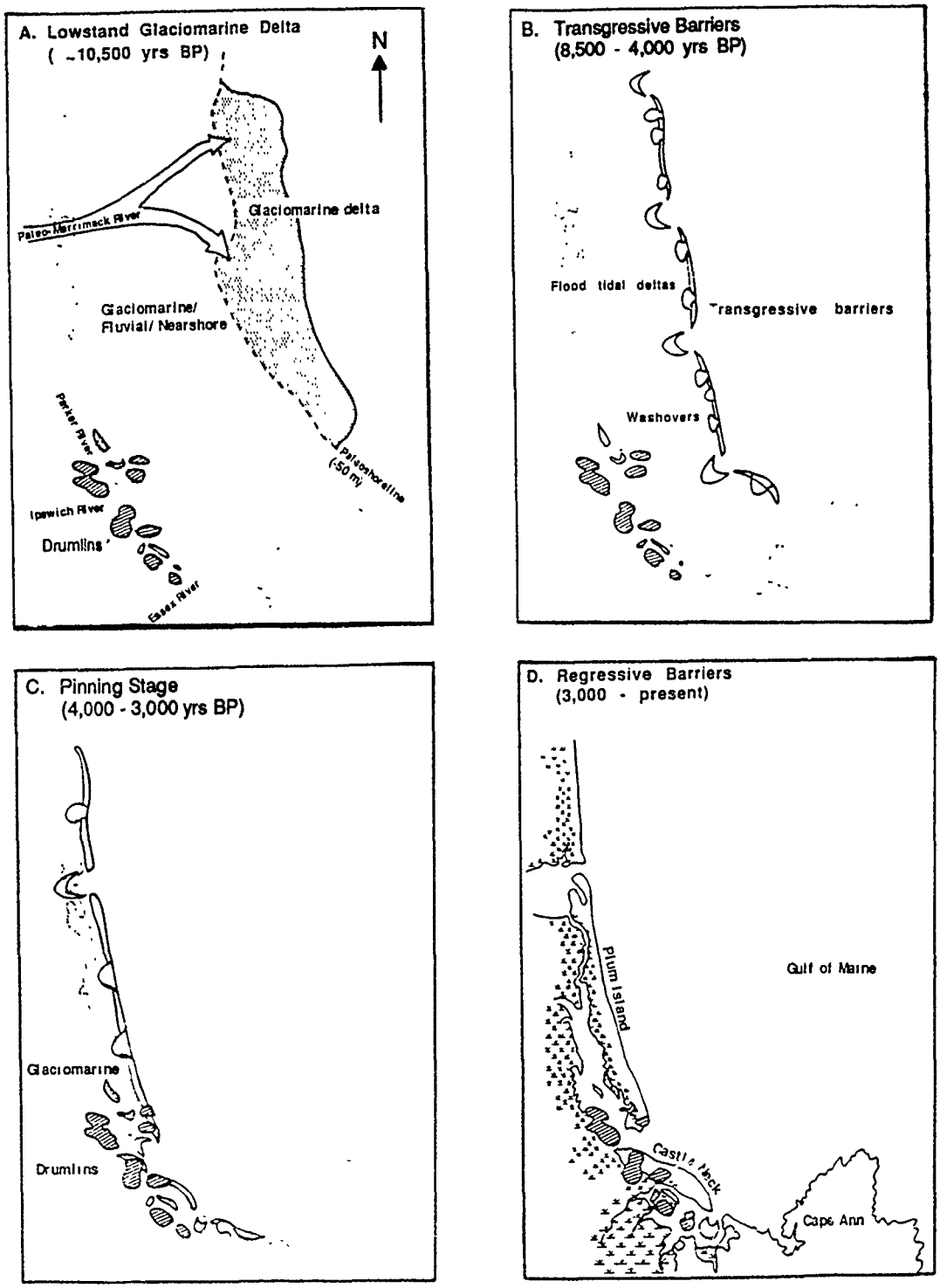

Figure 12. Formation of barrier islands of the southern Merrimack Embayment. The submerged Merrimack River delta is the major sediment source for present day Plum Island and Crane Beach (Som, 1990).

barriers encountered and subsequently were pinned to bedrock and drumlin topographic highs (Som, 1990)(Figure 12'C'). During this sediment maximum inlets, such as the Essex River Inlet, were established from breaks in between dunes, drumlins and bedrock headlands.

From 3,000 yrs. BP to the present, the rate of sediment supply from the inner shelf and nearshore environments has been greater than the rate of sea level rise (cf. Johnson, 1925). As a result, barriers have built seaward (cf. Hine et al., 1979; cf. Boyd et al., 1987) (Figure 12'D').

METHODS

GENERAL

Field investigations commenced in May, 1989 and ended October, 1990 with an intensive field data gathering period during the summer months of 1989 and 1990. Laboratory analyses began July, 1989 and were completed in May, 1991.

FIELD INVESTIGATIONS

Bathymetric Survey

Approximately 7.5 km of fathometer profiles were run at the study area utilizing a Raytheon Model DE-719B Fathometer Chart Recorder (Figure 13). This information helped to determine channel morphology and bedform orientations. Channel cross-sections were adjusted to mean sea level (MSL).

Beach Profiles

Thirteen permanent profile stations positioned with rebar stakes behind the dune scarp (seven on Crane Beach and six on Coffins Beach) were established on 14 June 1989 (Figure 14). Stations were located approximately using several compass bearings to known locations which appear on maps and coastal charts. The distance between stations on Crane Beach varied between 75 and 200 m and along Coffins Beach the distance was 150 m. All profiles were traversed roughly perpendicular to the beach strike from the stations out to or near mean low water (MLW).

The profiles were surveyed five times during the study period: June 1989, August 1989, November-December 1989, February-March 1990 and August 1990. Profiles 1A, 1-4 were not surveyed in June, 1989 due to the presence of a tern nesting area along profile transect. Appendix A shows the profile cross sections.

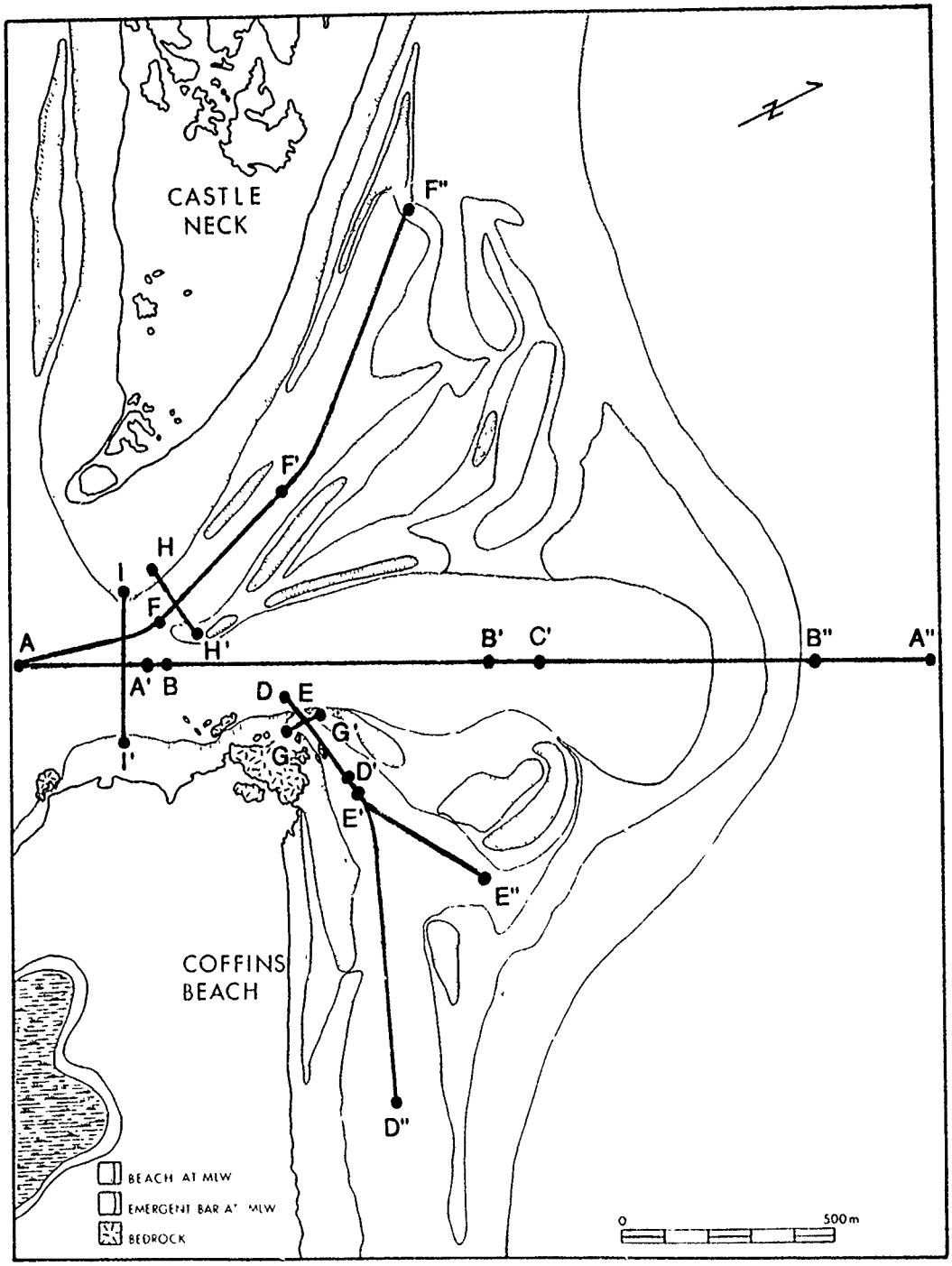

Figure 13 . Location of fathometer profiles.

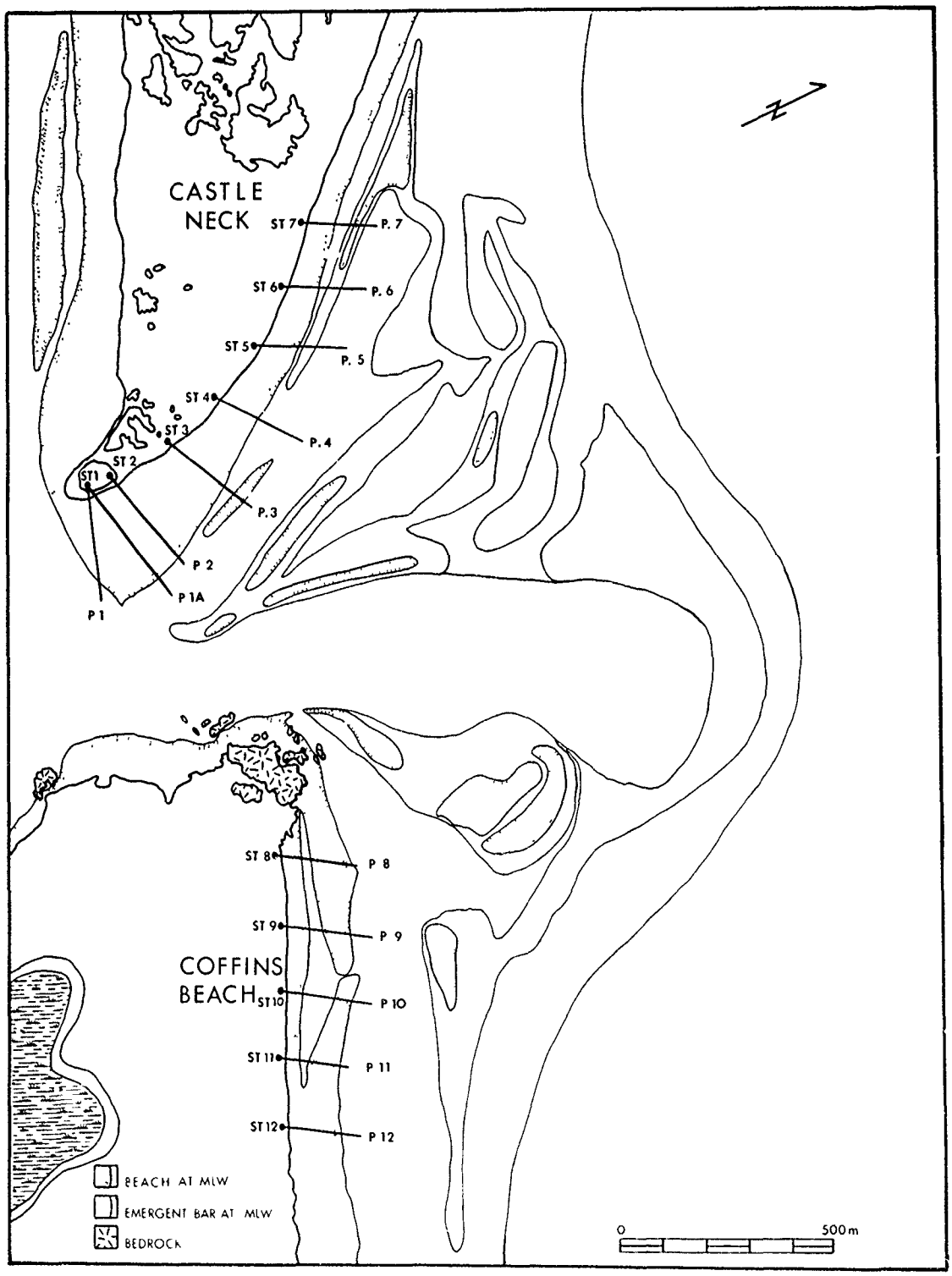

Figure 14. Location of profile stations and profiles.

Sediment Samples

The locations of the sediment samples were determined from nautical charts and aerial photographs (Figure 15). During the course of study 211 sediment samples (approximate mass of 200 grams) were collected. One hundred and seventy-seven samples were retrieved at offshore locations using a Van Veen grab sampler (Van Veen, 1936) along transect lines that connected to beach profiles. This was achieved by using two brightly colored ranges located at the profile stations. The distance along the offshore profiles was determined using sextant readings to known locations. Thirty-four samples were collected onshore during beach profile surveys.

Mapping and Determination of Migration of Intertidal Sand Bodies

Intertidal bars on the ebb-tidal delta were mapped by pace and Brunton technique. Mapping was performed on 27 June, 1989, 28 April, 1990 and 21 August, 1990 during low water. Tide levels with respect to MLW for these dates were +0.09m, -0.46 m and -0.21 m, respectively.

The boundaries of bars included 0.5 m-2.0 m high slipfaces on the landward side, abrupt change in slope along the main ebb channel, and in areas without abrupt slope change a water depth of 0.50 m was used depending on the tide. Permanent stakes were placed on all bars to use as reference points (Figure 16). Landward migration of sand bodies were determined by monitoring the distance between the permanent stake and landward slipface.

Errors in determining the areal extent of bars during surveys was due to: 1) different tidal heights and lack of defined slipface/slope and; 2) seasonal changes in sea level related to steric effects (Figure 17). However, these steric effects are minimal as monthly local relative sea level averaged over a ten year period shows only a 3.0 cm change in relative sea level over the mapping period (regard numerals 1-3 along plots of Figure 17'A' and 17'B' for three mapping dates).

Bedform Measurements

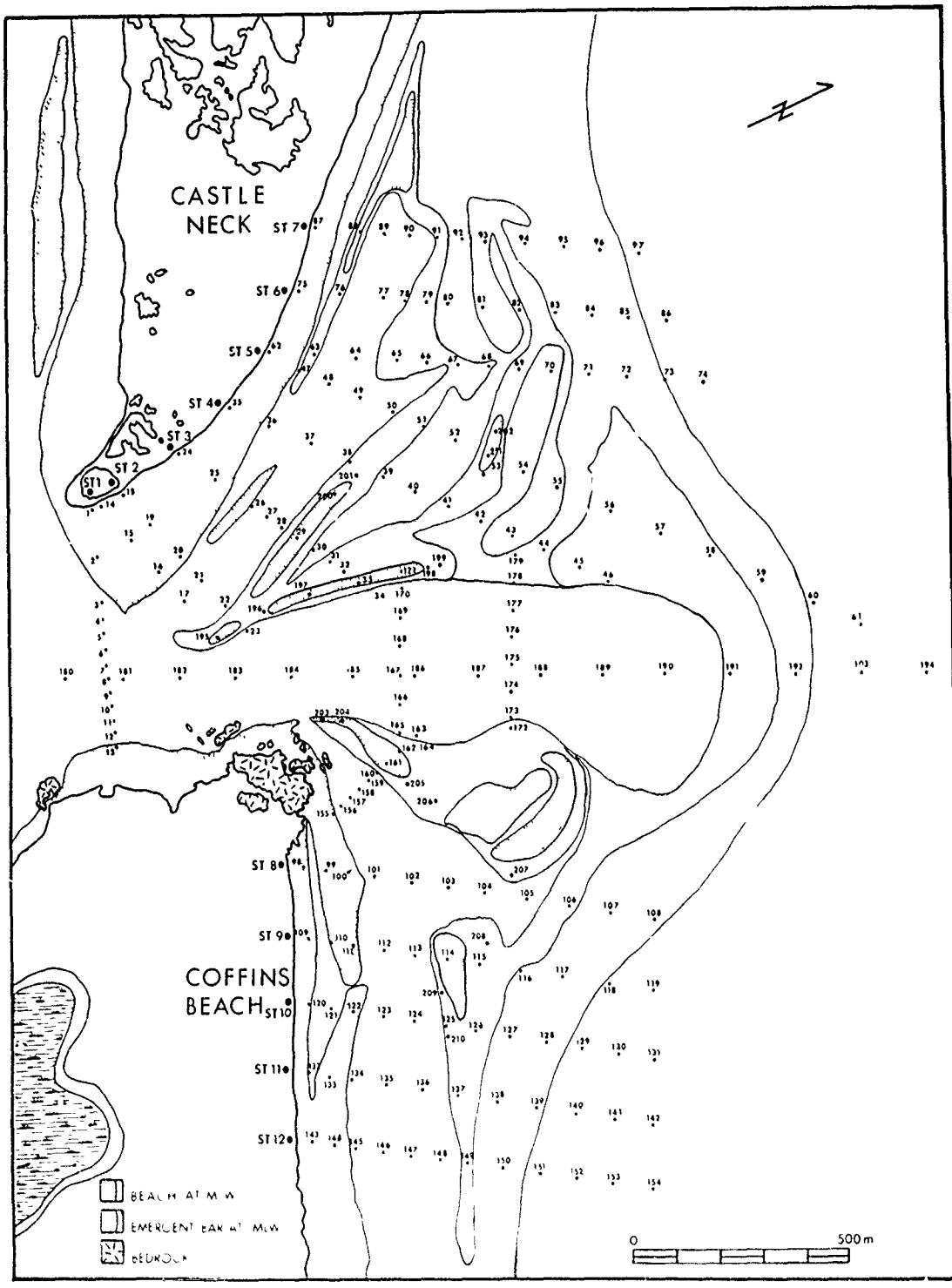

Figure 15. Location of sediment samples.

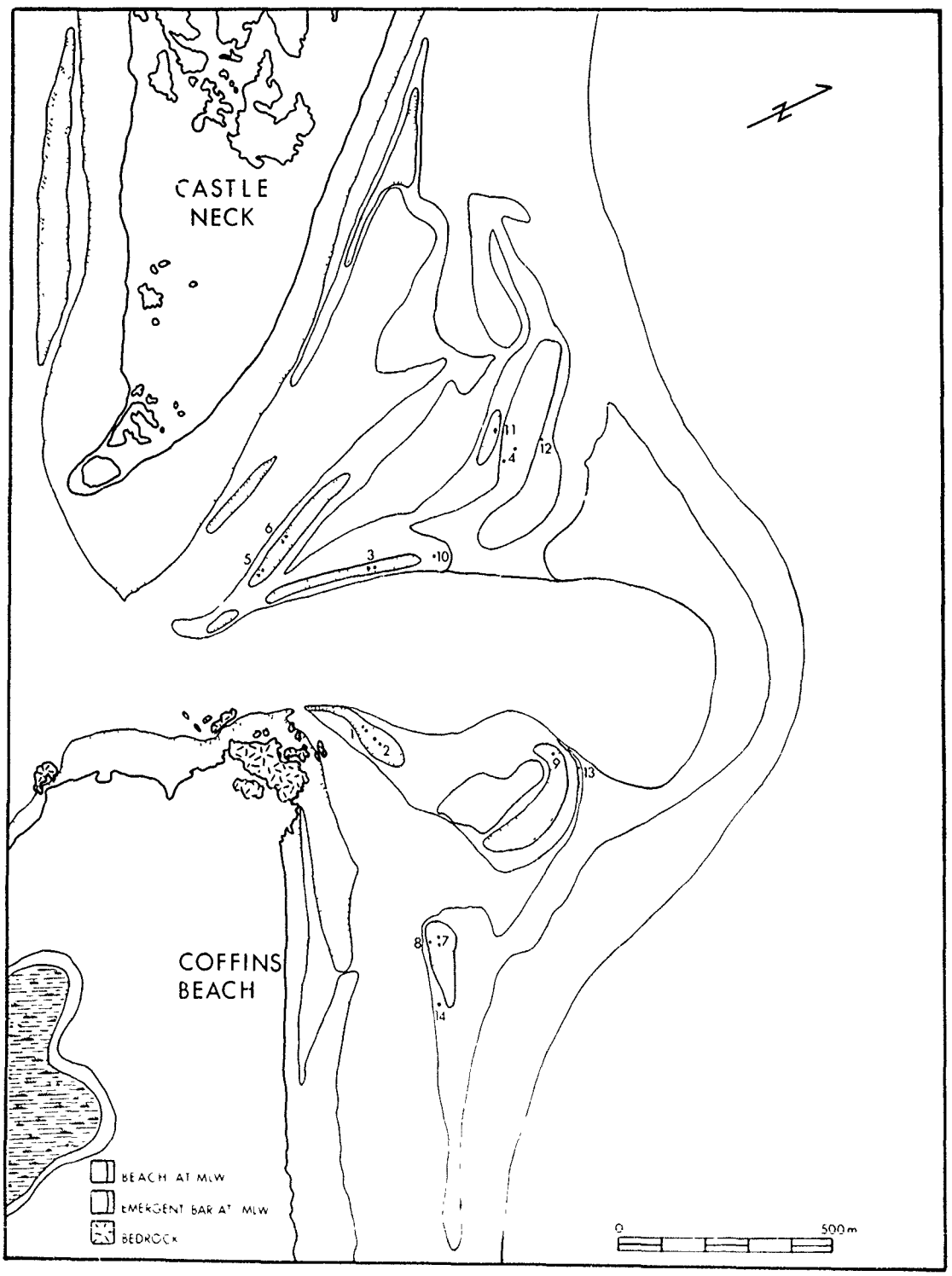

Figure 16. Location of stakes utilized to measure migration of sand bodies.

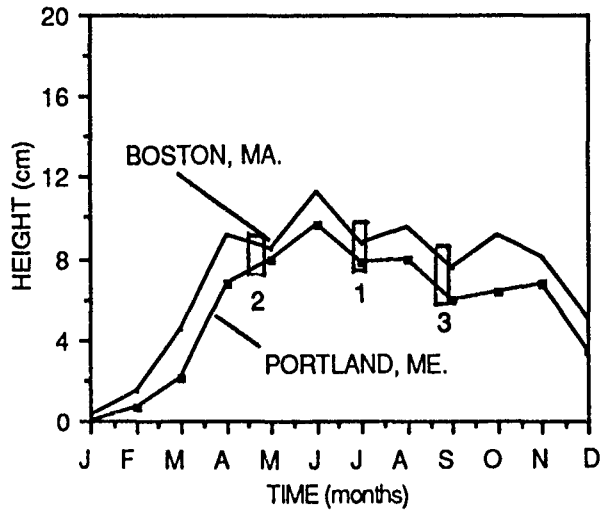

A

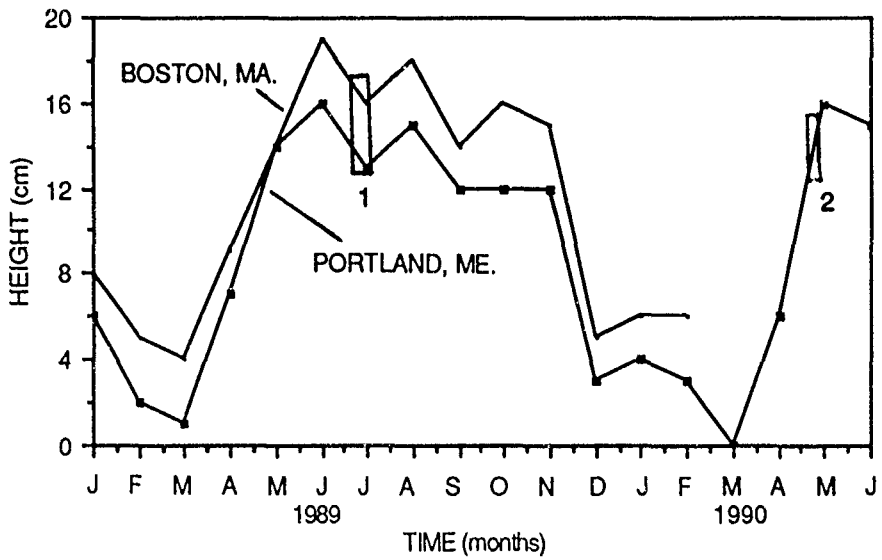

B

Figure 17 . A) Monthly relative sea level averaged for the ten year period 1981-1990 for Boston, Massachusetts and Portland, Maine. B) Monthly relative sea level for the period January, 1989 - June, 1990 for Boston, MA. and Portland, ME. Sea level heights measured with respect to local datum. Note placement of numbers with appropriate boxes to indicate dates of mapping of offshore intertidal sand bodies.

Bedform type, orientation, spacing (wavelength) and height on the ebb-tidal delta were measured on several occasions. Orientations were measured using a Brunton compass while spacing and height measurements were taken with a meter tape. Bedform classification follows that of Boothroyd, 1985 (after Harms et al., 1975) (Table 1'A'). This scheme classifies bedforms primarily according to spacing and secondarily according to height/spacing ratio, flow velocity and velocity asymmetry. The SEPM Bedform and Bedding Structures Research Symposium Classification Scheme (Ashley et al., 1990) is demonstrated in Table 1'B' . A table comparing these two classifications is shown in Table 1'C'.

Trenches

Six trenches were excavated at or near low water in the channel margin linear bar, swash bar and intertidal foreshore environments to determine bedding characteristics and sediment transport directions (Figure 18). Trenches were photographed and the near surface stratigraphy measured with respect to bedding plane direction and dip angles.

Hydrographies

Seven hydrographic surveys were conducted during the study period. In each hydrographic survey, a Marsh-McBirney Model 201D Portable Water Current Meter was used to measure current velocity and direction over one 13 hour period. Current measurements were taken through the water column at 1/4, 1/2 and 3/4 of the total depth and averaged. Velocity measurements and tide pole readings were taken at 30-45 minute intervals. Near a change in tidal phase, tide pole readings were recorded more often in order to closely document the exact position of high or low tide.

Current velocities were recorded at eight stations over six hydrographies during spring, mean and neap tidal conditions (Figure 19). Stations 1-5 were positioned across the inlet throat to determine the flood or ebb current dominance of the inlet throat. Longitudinal profiles

	Ripples	Megaripples	Low-energy sand waves	High-energy sand waves
Spacing	<60 cm	60 cm–10 m	> 6 m	> 10 m
Height/spacing ratio	variable	relatively large	relatively small	very small
Geometry	highly variable	sinuous to highly three-dimensional, prominent scour pits in troughs	straight to sinuous, uniform scour in troughs	straight to sinuous
Characteristic flow velocity	low (> 25–30 cm/sec < 40–50 cm/sec)	high (> 70–80 cm/sec, < 100–150 cm/sec)	moderate (> 30–40 cm/sec, < 70–80 cm/sec)	high (> 70–80 cm/sec, may be 150 cm/sec)
Velocity asymmetry	negligible to substantial	negligible to substantial	usually substantial	small to substantial

A

	Subaqueous Dune			
First Order Descriptors (necessary)				
Size Spacing = Height* =	small 0 6–5 m, 0 075–0 4 m,	medium 5–10 m, 0 4–0 75 m,	large 10–100 m, 0.75–5 m,	very large > 100 m >5 m
Shape 2-Dimensional 3-Dimensional				
Second Order Descriptors (important)				
– Superposition simple or compound (sizes and relative orientation)				
– Sediment characteristics (size, sorting)				
Third Order Descriptors (useful)				
– Bedform profile (stoss and lee slope lengths and angles)				
– Fullbeddedness (fraction of bed covered by bedforms)				
– Flow structure (time-velocity characteristics)				
– Relative strengths of opposing flows				
– Dune behavior-migration history (vertical and horizontal accretion)				

* Height calculated using the equation $H = 0.0677L^{0.5}$ (Flemming 1988)

B

Spacing (m)	0.0 to 0.6	0.6 to 5-6	5 to 10	10 to 100	>100
Boothroyd, 1985 (after Harms et al., 1975)	Ripple	Megaripple	Sandwave	Sandwave	Transverse Bar or Sandwave
Ashley et al., 1990	Ripple	Small Dune	Medium Dune	Large Dune	Very Large Dune

C

Table 1. Bedding classification schemes utilized. A) The primary classification utilized in this paper (Boothroyd, 1985 after Harms et al., 1975). B) References are also made to the scheme recommended by the SEPM Bedforms and Bedding Structures Research Symposium (Ashley et al., 1990). C) Comparison between the two classifications.

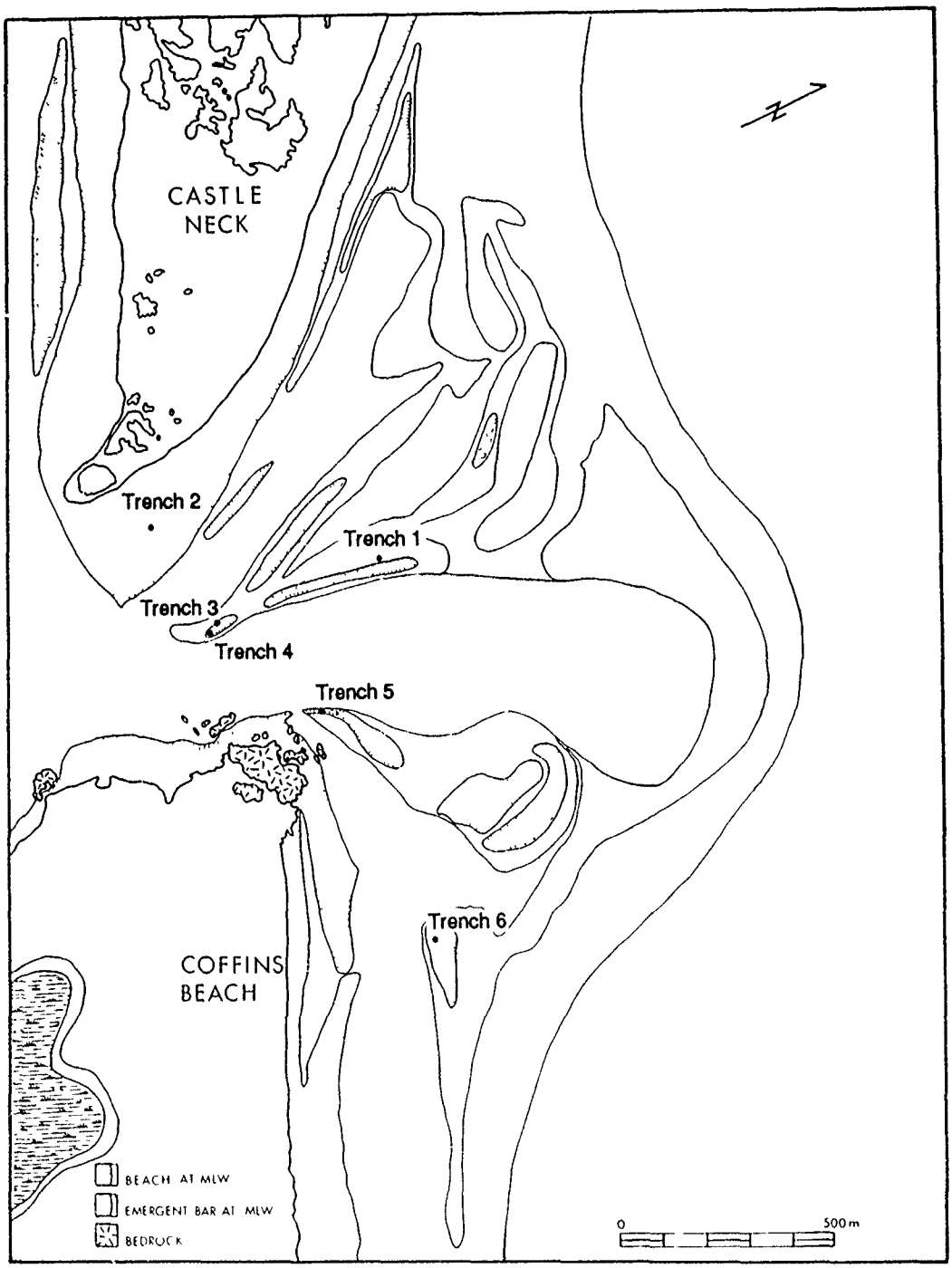

Figure 18. Location of trenches.

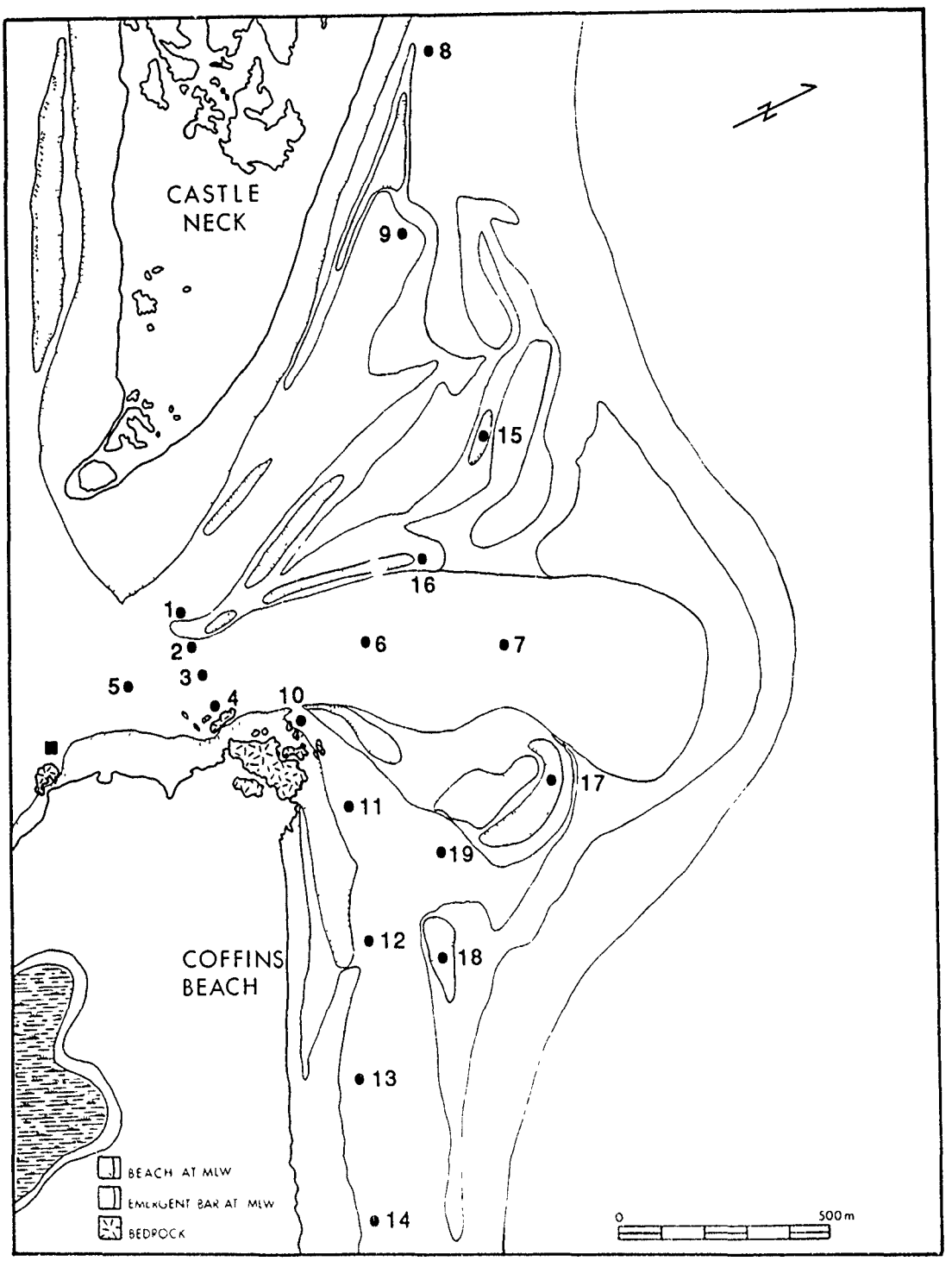

Figure 19 . Location of hydrography stations. The square indicates the location of the tide pole.

of the main ebb channel (stations 6-7) were studied during mean tidal conditions. Current velocities at stations 1 and 10 were also studied to determine the magnitude and dominance of currents in the marginal flood channel.

The magnitude and direction of longshore currents (stations 8-9, 11-14) were monitored during two hydrographies, both of which were conducted during mean tidal conditions. Currents were recorded on the swash platform during a single hydrography (stations 15-18) during mean tidal conditions with average approximate breaker heights of 1.0 m from the northeast.

Aerial Reconnaissance Surveys

Aerial surveys of the study area were performed in a Cessna 152 single engine aircraft on three occasions: 27 May, 1989, 26 August, 1989, and 3 March, 1990. Surveys were scheduled at or near low tide so bedforms and intertidal sand bodies were exposed. Both color and black and white oblique photographs were taken from elevations ranging from 500 - 2,600 m.

Vibra-Cores

Twenty-six vibra-cores were taken in different intertidal and shallow subtidal environments (Figure 20) utilizing the methods as described by Lanesky et al., 1979. Location of each core was determined by taking compass bearings to known locations. Before the cores were extracted from the ground they were marked and oriented with respect to north. Depths of cores ranged from 1.43 to 3.82 m with an average of 2.50 m. Coring was restricted to areas with water depths less than approximately one meter due to equipment limitations.

LABORATORY ANALYSES

Vibra-Core Analysis

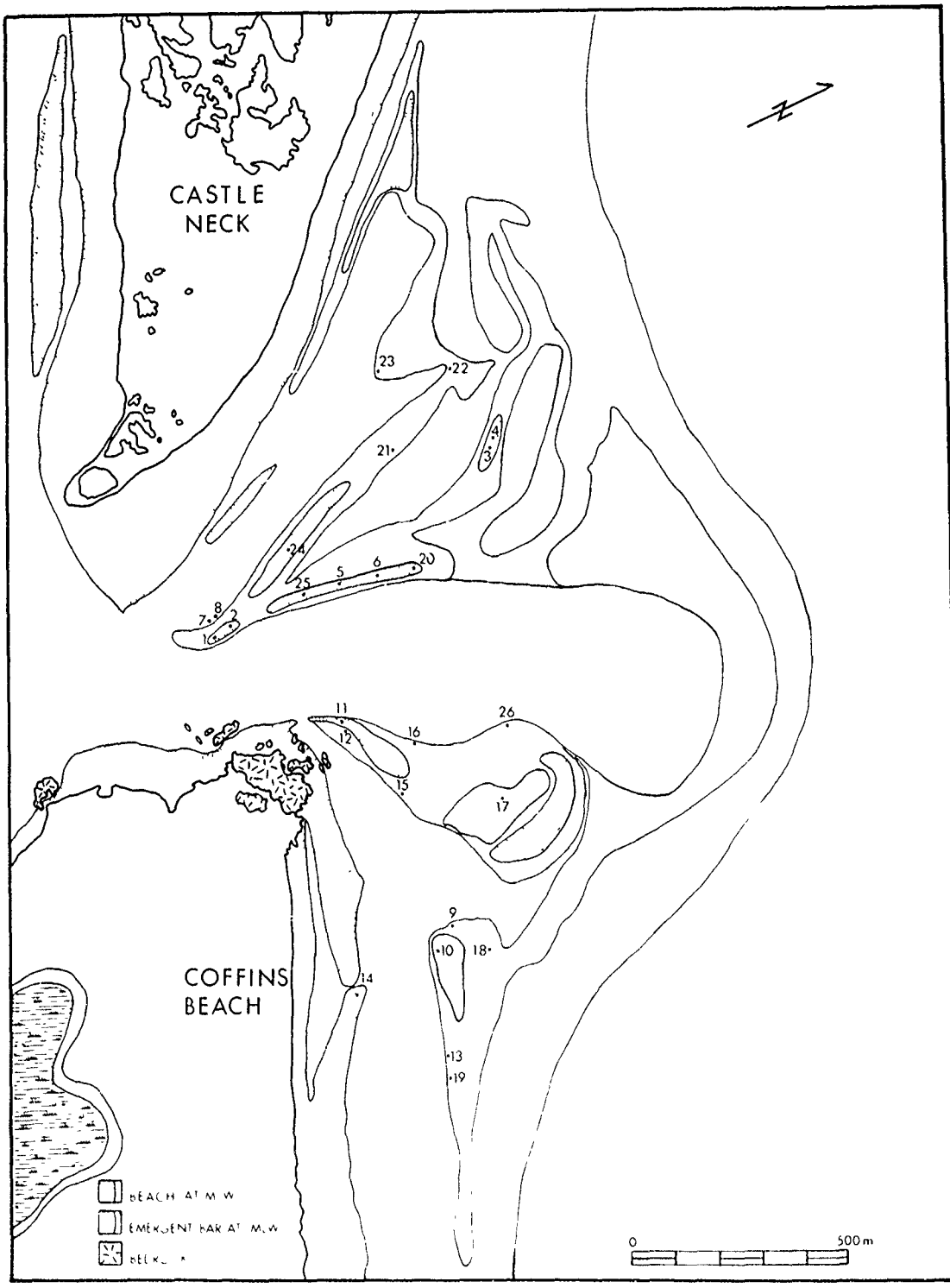

Figure 20 . Location of cores.

Vibra-cores were cut longitudinally into two equal sections (semicircles) using a circular saw. One half was archived while the other half was photographed, logged and sediment samples taken. 107 samples were collected from the cores.

Sections of the cores with visible bedding were preserved using lacquer peels and photographed. A total of 26 peels from 19 cores was produced. For each peel, the depth and orientation were noted with respect to north or onshore/offshore. Analysis of peels included a determination of direction and angle of bedding planes.

Grain Size Analysis

318 sediment samples were analyzed for grain size statistics. Percentages of clay, sand and gravel were determined using the Wentworth grain size scale (Table 2). Approximately 50 grams of each sample were used for analysis while the remainder was stored for possible future analyses. Samples were washed in distilled water in order to remove salt, and then oven dried and cooled. Samples were weighed and then shaken for 10 minutes or more using nested 0.5Ø increment screens ranging from -2.5Ø to 4.0Ø. After shaking, the sediment in each sieve was weighed. These weights were totaled in order to calculate percent sample loss (Folk, 1974). Examination of fines using pipette analysis revealed that samples contained no clay material (<4.0Ø).

Cumulative weight and cumulative percent coarser than were determined so that a cumulative percent frequency graph could be plotted (Folk, 1974).

Two statistcal parameters were used to compare the samples: Graphic mean (Mz) and Inclusive Graphic Standard Deviation (σ_I) (Folk, 1974). Graphic Mean or the average grain size of the sample is determined by using the following formula:

$$\frac{Ø16+Ø50+Ø84}{3}$$

Limiting particle diameter					
mm	φ units		Size class		
2048	−11		Very large	Boulders	GRAVEL
1024	−10		Large		
512	− 9		Medium		
256	− 8		Small		
128	− 7		Large	Cobbles	
64	− 6		Small		
32	− 5		Very coarse	Pebbles	
16	− 4		Coarse		
8	− 3		Medium		
4	− 2		Fine		
2	− 1		Very fine	Granules	
1	0		Very coarse	Sand	
1/2	+ 1	μm 500	Coarse		
1/4	+ 2	250	Medium		
1/8	+ 3	125	Fine		
1/16	+ 4	62	Very fine		
1/32	+ 5	31	Very coarse	Silt	MUD
1/64	+ 6	16	Coarse		
1/128	+ 7	8	Medium		
1/256	+ 8	4	Fine		
1/512	+ 9	2	Very fine		
				Clay	

Table 2. Wentworth Grain Size Scale (from Davis, 1983 after Wentworth, 1922).

Inclusive Graphic Standard Deviation, a measure of sorting, is a measure of the spread of Ø units (Folk, 1974). The formula for Inclusive Graphic Standard Deviation is as follows:

$$\frac{Ø84 - Ø16}{4} + \frac{Ø95 - Ø5}{6.6}$$

Folk, 1974 presents a classification scale for sorting:

<0.35Ø - Very well sorted
0.35Ø - 0.50Ø - Well sorted
0.50Ø - 0.71Ø - Moderately well sorted
0.71Ø - 1.00Ø - Moderately sorted
1.00Ø - 2.00Ø - Poorly sorted
2.00Ø - 4.00Ø - Very poorly sorted
> 4.00Ø - Extremely poorly sorted

Historical Shoreline and Ebb-Tidal Delta Morphologic Change

Nautical charts, vertical and oblique aerial photographs and other historical records were used to create shoreline change maps of Crane Beach, Coffins Beach and the ebb-tidal delta. For this analysis charts and aerial photographs were photographically processed to a common scale.

The shoreline change map was produced by comparing four Coast and Geodetic Survey Nautical Charts from 1855, 1912, 1964 and 1984. The ebb-tidal delta morphologic change map was produced by comparing vertical aerial photographs from 1943, 1952, 1960, 1965, 1972, 1977, 1978, 1979 and 1985. Effort was made to differentiate between subtidal and intertidal sand bodies, and between several accretionary phases of beach ridge development. Additional short-term ebb-tidal delta morphologic changes were determined by comparing oblique aerial photographs.

EBB-TIDAL DELTA CHARACTERISTICS

INTRODUCTION

Numerous studies of ebb-tidal delta processes and morphology exist in the liturature (Hayes, 1975, 1980; Finley, 1975, 1978; Hine, 1975; Hubbard, 1975, 1977; Oertel, 1975; FitzGerald, 1976, 1982, 1984; FitzGerald, Nummedal and Kana, 1976; FitzGerald and Nummedal, 1983; Humphries, 1979; and Sha, 1990). Although Hayes' (1975) morphological ebb-tidal delta model is based on the Essex River Inlet, the dominant physical processes, inlet hydraulics and transport pathways have not been verified. Field data and analyses are presented which consider both short-term and long-term morphologic changes of the Essex River ebb-tidal delta.

An ebb-tidal delta is defined as an accumulation of sediment on the seaward side of a tidal inlet which forms through the interaction of tidal currents and wave activity (FitzGerald, 1984). The Essex River ebb-tidal delta is located on a tide-dominated mixed energy coast (cf. Hayes, 1979) (Figure 5). This coast is chacterized by short, stubby barrier islands and numerous tidal inlets with well developed flood and ebb-tidal deltas. A marsh and tidal creek system separates the barriers from the mainland.

DISCUSSION

Ebb-tidal delta morphology is primarily a function of the interplay between tidal, wave and longshore-generated currents (Hayes, 1975; Oertel, 1975) (Figure 21). Using the classification of Oertel (1975), the Essex River Inlet is dominated by onshore-offshore tidal currents thus resulting in a large offshore extent of 1.4 km as is shown in Example D of Figure 21. While tidal dominance is indicated by its morphology, wave action plays a major role in determining net sediment transport trends.

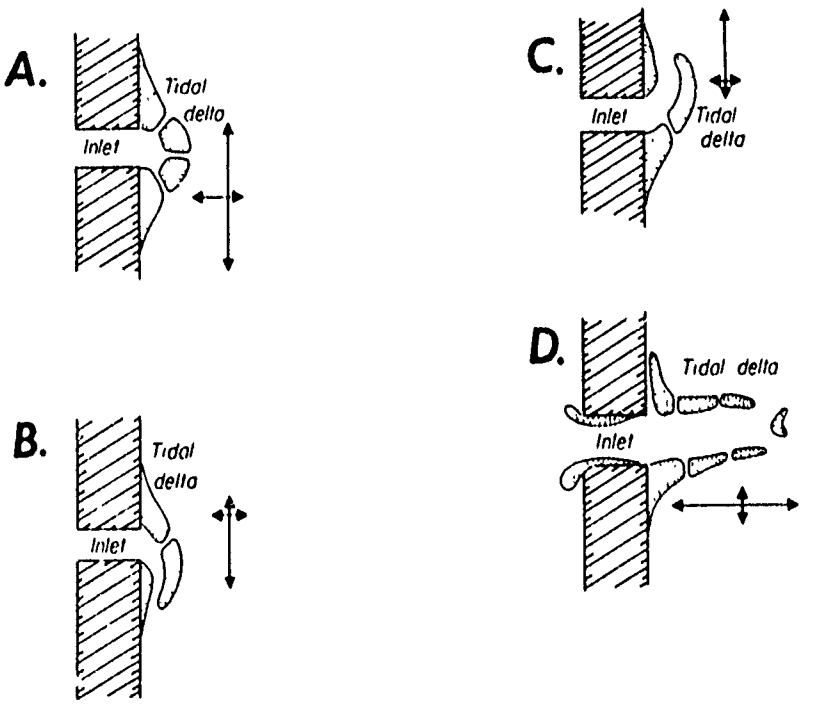

Figure 21. Variations in ebb-tidal delta morphology. Arrows represent relative magnitudes of offshore, onshore and longshore currents. A) Longshore and onshore currents are greater than offshore currents; B) One component of longshore current is greater than the other three currents; C) The other component of longshore current is greater than the other three currents; D) The onshore-offshore currents are greater than the longshore currents. The Essex River inlet-ebb-tidal delta system is best characterized by example D (from Oertel, 1975).

Secondary controls of Essex River ebb-tidal delta morphology include three factors: 1) The inlet tidal prism of 2.01 x 10^7 m^3/cycle (7.06 x 10^8 ft ^{3}/cycle) which has a proportional relationship to ebb-tidal delta sediment volume of 3.54 x 10^6 m^3 (4.63 x 10^6 yd^3). This relationship is shown in Figure 22 where the tidal prism and delta volume plot close to the regression curve on the tidal prism-ebb-tidal delta storage relationship graph for moderately exposed coasts (Walton and Adams, 1976); 2) Bedrock control at Twopenny Loaf on Coffins Beach which anchors the main ebb channel at the inlet throat. Therefore, the flanking channel margin linear bars close to inlet throat are also stable and; 3) The shape of inlet throat (Figure 23) (with cross sectional area of 1.35 x 10^3 m^2 at MLW and 1.77 x $10^3 m^2$ at MSL) which is asymmetric and is positioned along the southern side of the main ebb channel. This is due to the southerly directed longshore sediment transport system and spit formation on the southern end of Crane Beach, and the pattern of tidal channels in the backbarrier as they approach the inlet throat. Seaward, the channel thalweg continues along the southeast side of the channel with no meandering tendancies.

Longitudinally, the main ebb channel shallows and widens from the inlet throat (width of 300 m and depth of 13 m at MSL) to the terminal lobe (approximate main ebb channel width of 400 m and depth of 3.5 m at MSL) (Figure 24). This 1500 m longitudinal cross section distance from the inlet throat to the terminal lobe has a net seaward decrease in depth of 9.5 m. Note also the scouring of the main ebb channel 450 m seaward of the inlet throat. This scouring is due to flood-tidal currents entering the main ebb channel through the southern downdrift marginal flood channel.

The channel margin linear bars are sand bodies which flank the main ebb channel and form from the interaction of ebb and flood-tidal currents with wave-generated currents. Attachment of landward migrating swash bars to distal portions of the channel margin linear bars is another mode of channel margin linear bar formation (cf. FitzGerald, 1976). The channel margin linear bars are dominated by flood currents (Oertel, 1975; FitzGerald, 1976; and Hubbard, 1977). At the

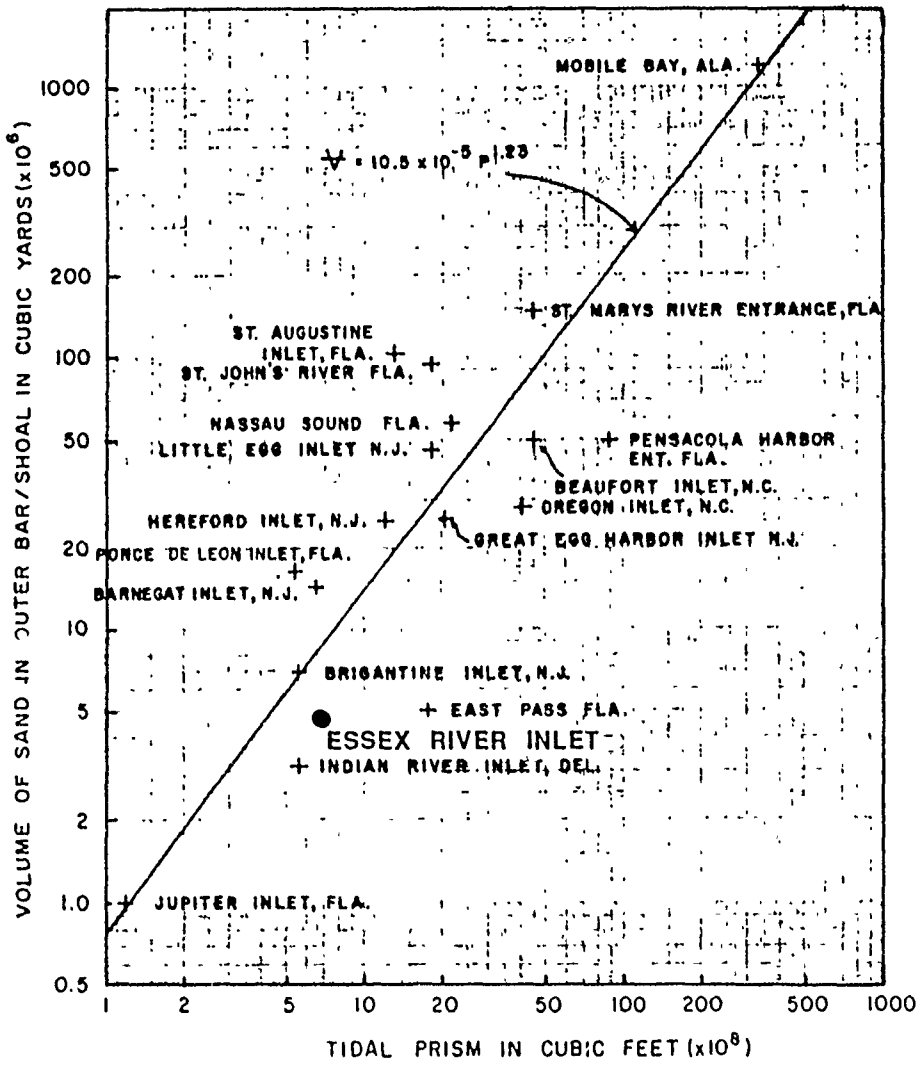

Figure 22. Tidal prism-ebb-tidal delta storage relationship for moderately exposed coasts. Note that the Essex River inlet-ebb-tidal delta system does follow this relationship (Walton and Adams, 1976).

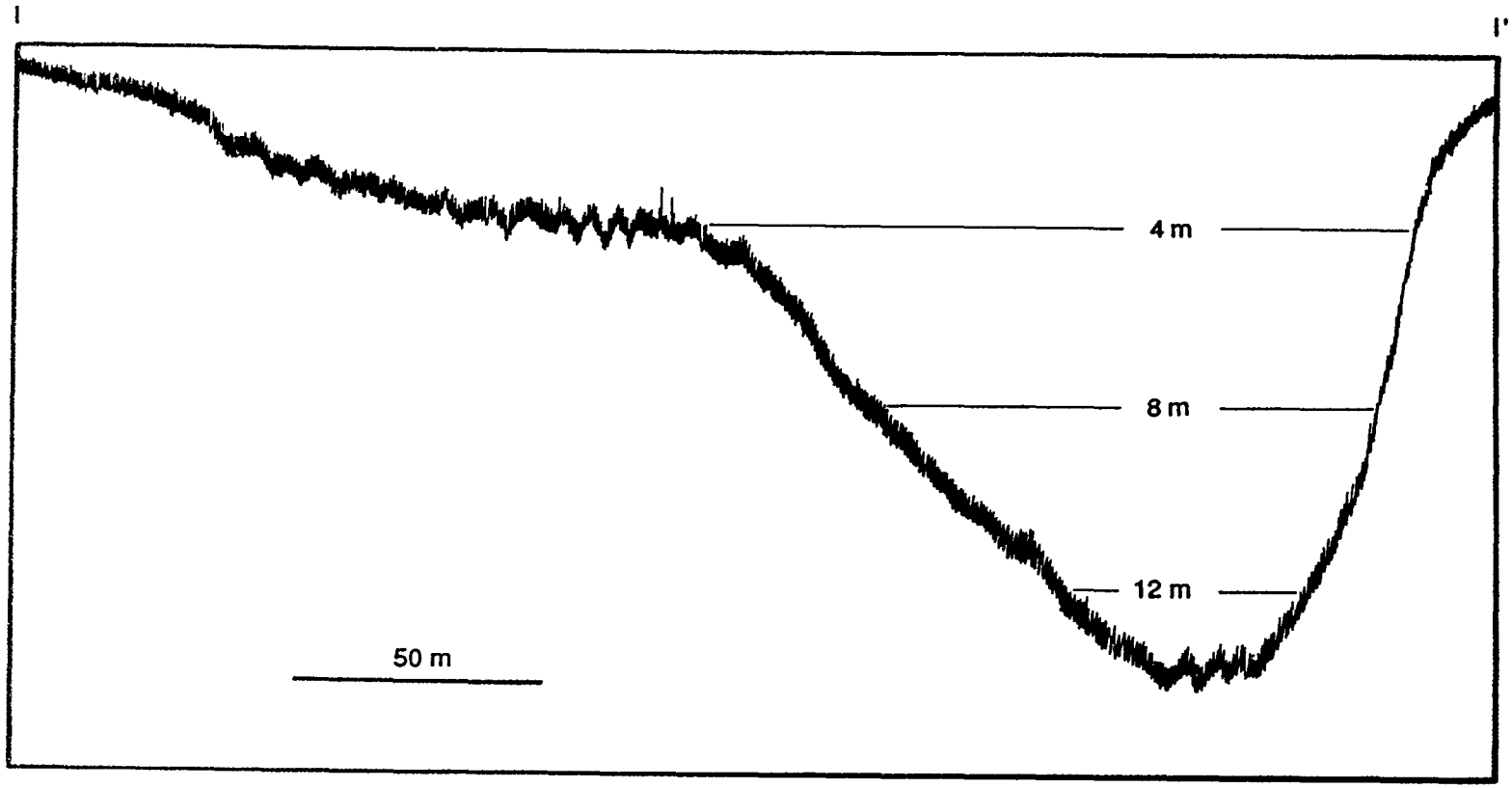

Figure 23. Fathometer cross section of main ebb channel at the inlet throat at MSL. Note the scoured southeast side of the channel. Figure 13 shows the location of the profile.

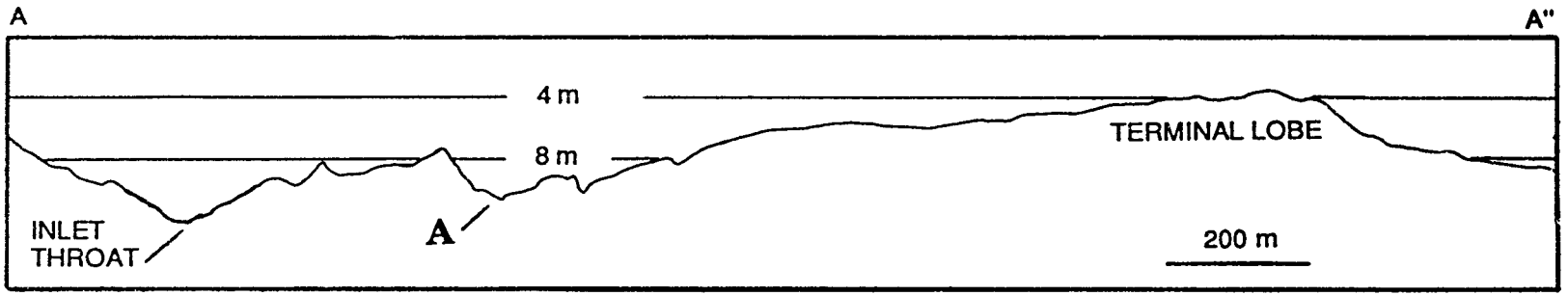

MAIN EBB CHANNEL CROSS SECTIONAL PROFILE

Figure 24. Fathometer profile of the ebb-tidal delta longitudinal cross section with inlet throat and terminal lobe as indicated. Letter 'A' indicates scouring from flood-tidal currents through the southern downdrift marginal flood channel. Figure 13 shows the location of the profile.

Essex River ebb-tidal delta, a spillover lobe was present on the updrift channel margin linear bar during the period June, 1990-January, 1991 which is a direct result of the expansion of the ebb jet (cf. Oertel, 1975).

Flood dominance of tidal currents in the marginal flood channels can be explained by:

1) The momentum of ebb currents continuing to flow through the main ebb channel after low tide. Therefore, flood currents enter through the path of least resistance, which are the marginal flood channels (Hayes, 1975);

2) Intertidal exposure of swash bars at low tide constricts water into swash bar/landward beach confined marginal flood channels (Hubbard, 1977);

3) Marginal flood channels are shorter than the main ebb channel and therefore retain a greater water surface slope until the bars are covered (Hubbard, 1977) and;

4) Waves may cause water to pile up near the distal seaward end of the marginal flood channels and therefore increase the hydraulic head (FitzGerald, 1976).

Cross sections of the marginal flood channels are presented in Figure 25 (Figure 13 shows the locations of the cross sections). The southern downdrift marginal flood channel (profile G-G') has a width of 70 m and a maximum depth of 4.2 m at MSL. The cross sectional area at MSL is 230 m^2. The northern updrift marginal flood channel (profile H-H') has a width of 100 m and a maximum depth of 3.7 m at MSL. The cross sectional area at MSL is 270 m^2.

The channel located between the downdrift channel margin linear bar and the downdrift swash bar, henceforth referred to as the swash platform channel, is dominated by tidal currents. However, the formation of this channel is more a result of constriction between the two surrounding intertidal sand bodies rather than scouring by tidal currents.

The swash platform is the shallow portion of the ebb-tidal delta over which waves break and is therefore dominated by wave swash processes (King, 1972). This wave swash enhances flood-tidal currents but retards

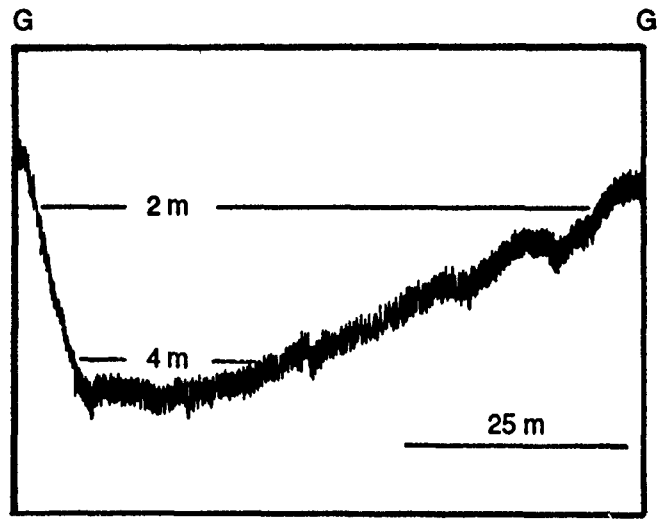

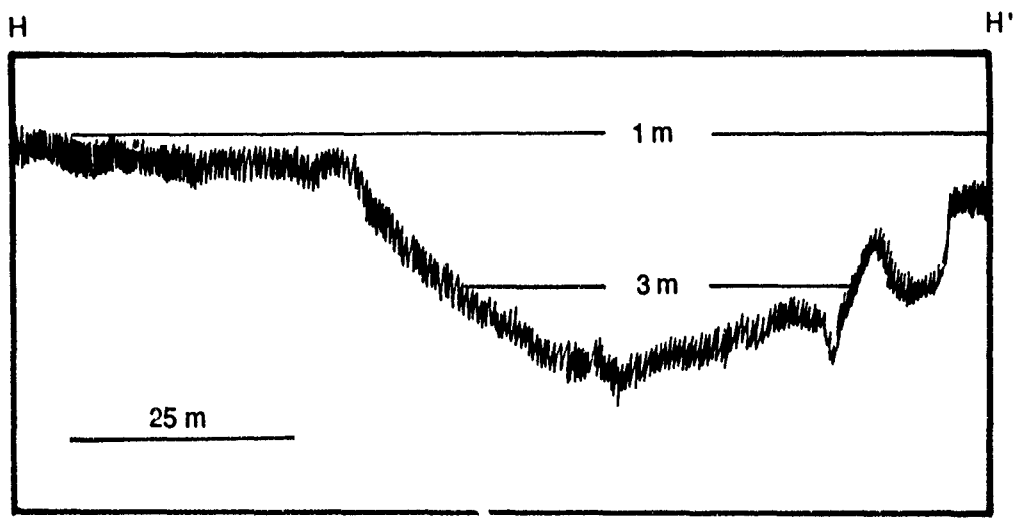

Figure 25. Fathometer cross sectional profile of downdrift marginal flood channel (G-G') and updrift marginal flood channel (H-H') at mean sea leve Cross sectional areas of channels at mean sea level are approximately 230 m^2 and 270 m^2 repectively. Regard Figure 13 for location of profiles.

ebb-tidal currents thereby producing a net landward flow over the platform (FitzGerald, 1982). Atop the swash platform are individual swash bars which migrate landward and whose size is dependent upon sediment input into the delta.

The terminal lobe is the relatively steep, seaward-sloping lobe of sand which fronts the ebb-tidal delta (Hayes, 1975), and represents a zone of equilibrium between wave and tidal processes where sediment settles and is deposited. The depth and position of the terminal lobe is controlled by the tidal prism and the resulting ebb-tidal delta sediment volume, and tidal versus wave energy. Additional changes to the overall terminal lobe position is controlled by storm activity (Van den Berg, 1989).

HYDRODYNAMICS

HYDRODYNAMIC REGIME

RESULTS

The current data for the five stations at the inlet throat (stations 1-5) (Figure 26,27) are shown in Figures 28-32 and summarized in Tables 3-5. At the channel thalweg (station 3), maximum flood velocities ranged from 79 to 109 cm/sec while the maximum ebb velocities ranged from 61 to 104 cm/sec, and mean flood velocities (43 to 59 cm/sec) were similar to mean ebb velocities (35 to 62 cm/sec). These data would seem to indicate a flood-dominated inlet. However, when plotting maximum and mean current velocity versus tidal range (Figure 33), regression lines fitted to these points show that maximum ebb current velocities exceed maximum flood current velocities for tidal ranges greater than mean tide. This indicates that the inlet throat is ebb-dominated.

In addition, statistical analysis of both the flood and ebb maximum velocity regression curves (Figure 33) has shown that the ebb maximum velocity curve is not significant for the 95% confidence level. Thus, the regression lines do not produce a high degree of predictability. Therefore, the maximum ebb current velocity curve cannot be related to the maximum flood current velocity curve. The maximum ebb currents may in fact be greater than the maximum flood currents for tidal ranges below mean tide.

Three separate lines of evidence indicate an ebb-dominance of the inlet. First, bathymetric profiles demonstrate that the inlet throat is floored by ebb-oriented sandwaves with wavelengths up to 40 m and heights up to 1 m which are present throughout the tidal cycle (Profile A-A' of Figure 34). Secondly, aerial photographs have shown that the flood-tidal delta has not grown significantly in size over the past years which would be expected if the inlet were flood-dominated. Thirdly, as noted by

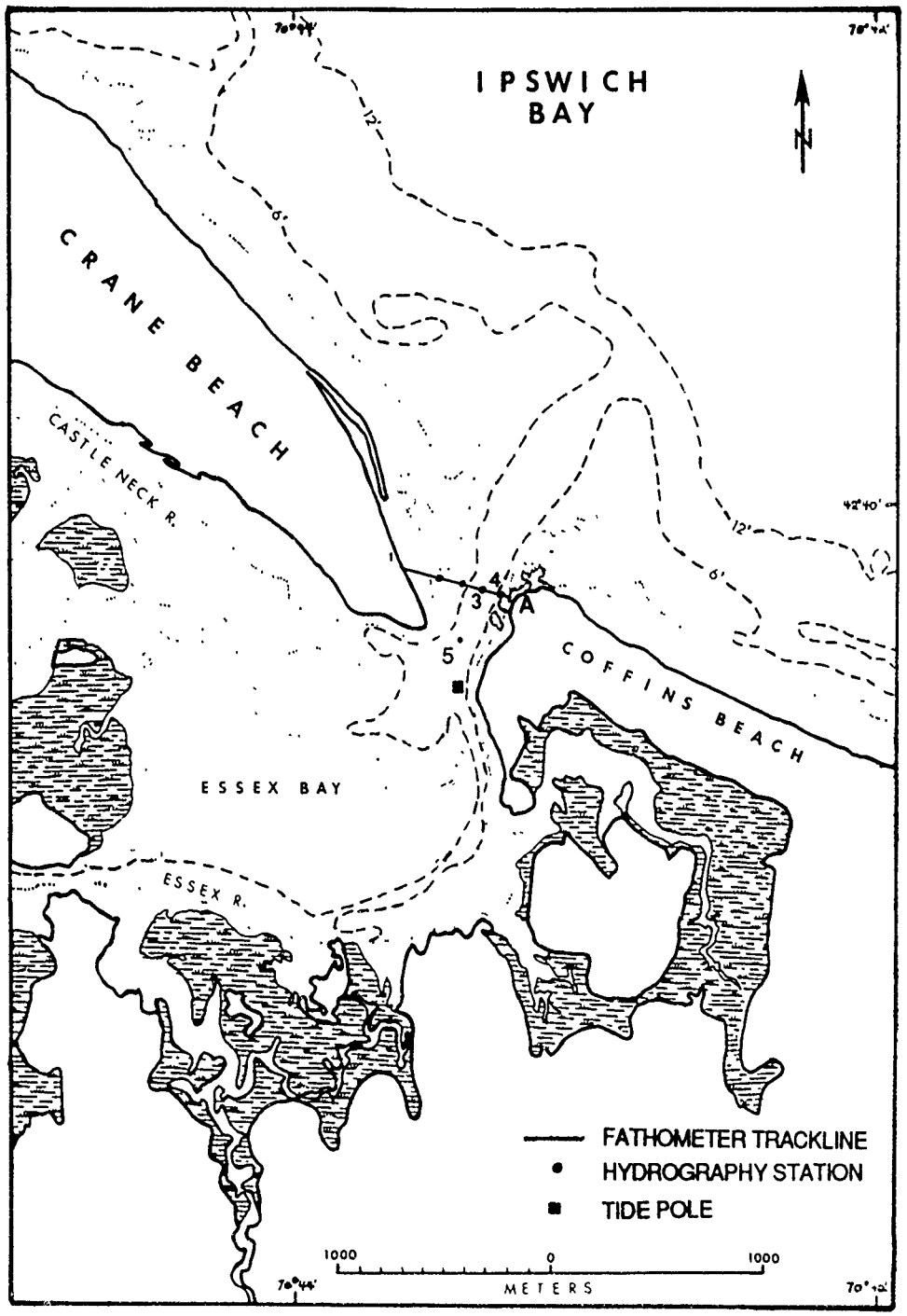

Figure 26. Location of hydrography stations 1-5 utilized to determine inlet hydraulic parameters. Cross section A-A' is shown in Figure 27.

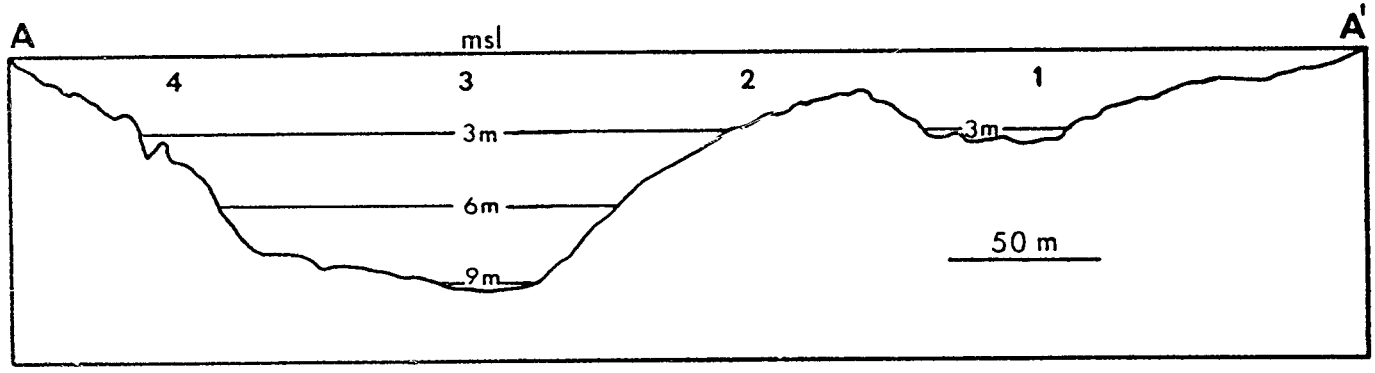

Figure 27. Cross section of inlet channel indicating locations of stations 1-4. Note the marginal flood channel at station 1. Refer to Figure 26 for location of cross section.

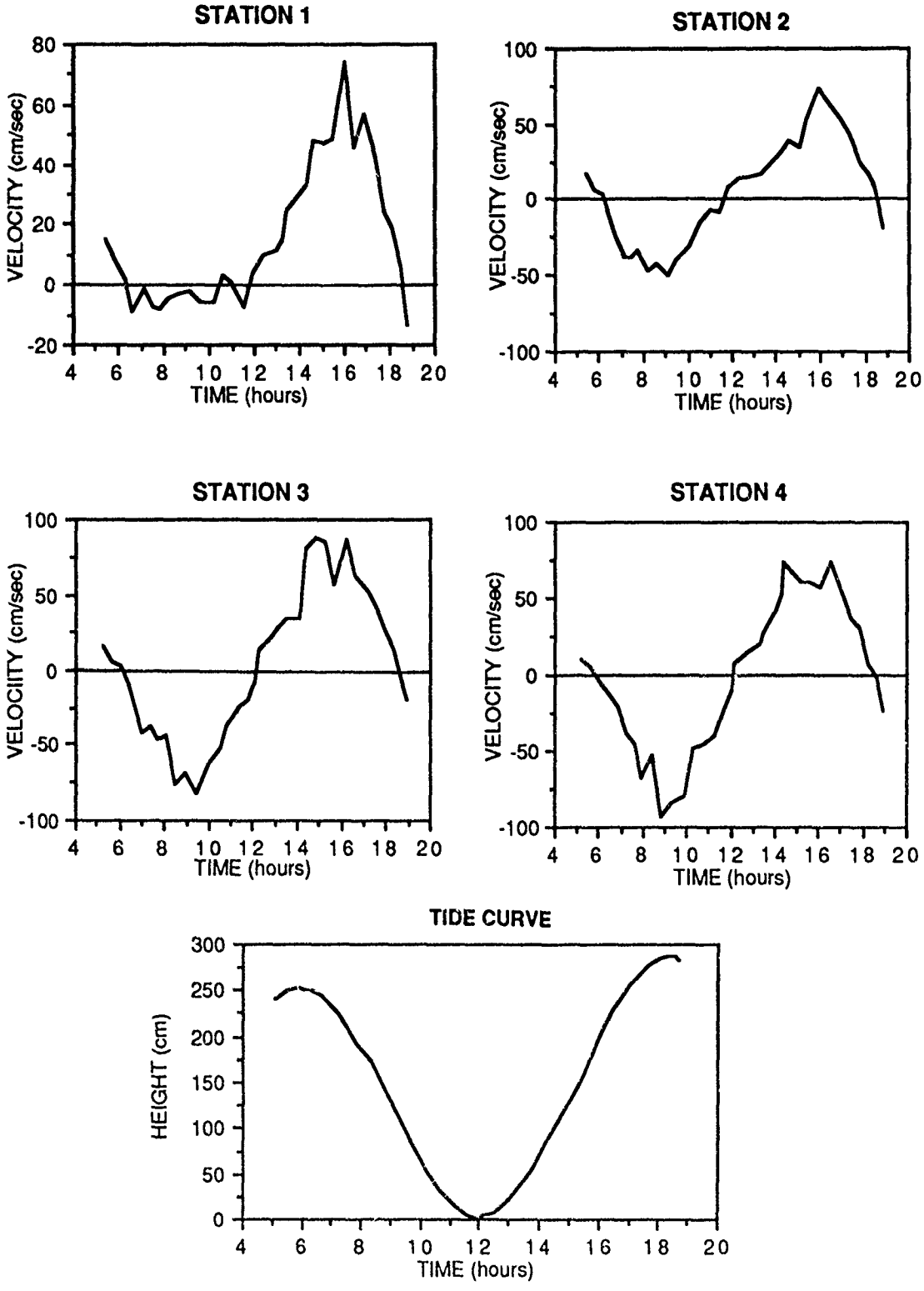

Figure 28 . Velocity-time series and tide curve for stations 1-4 on 26 July, 1989.

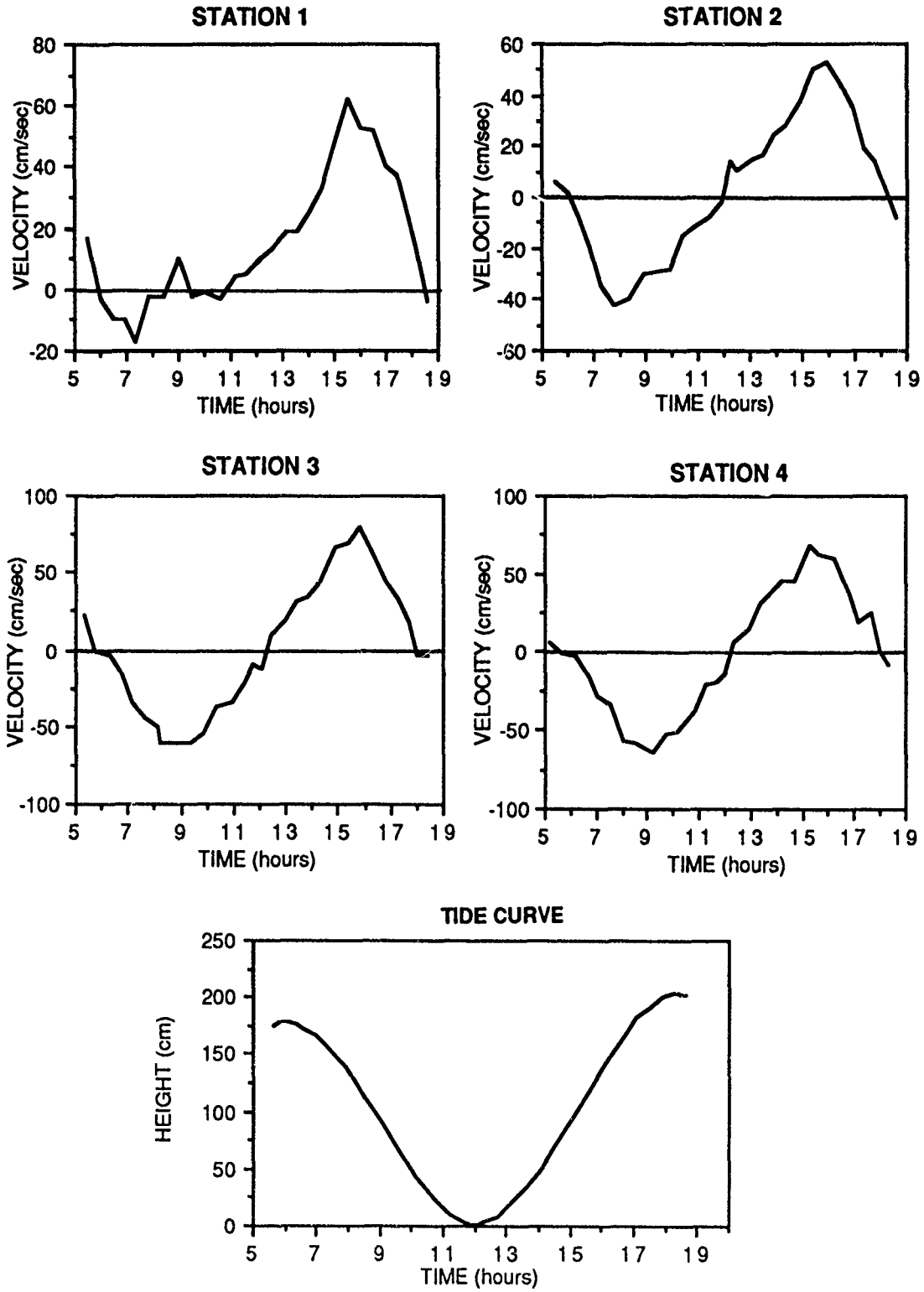

Figure 29. Velocity-time series and tide curve for stations 1-4 on 10 August, 1989.

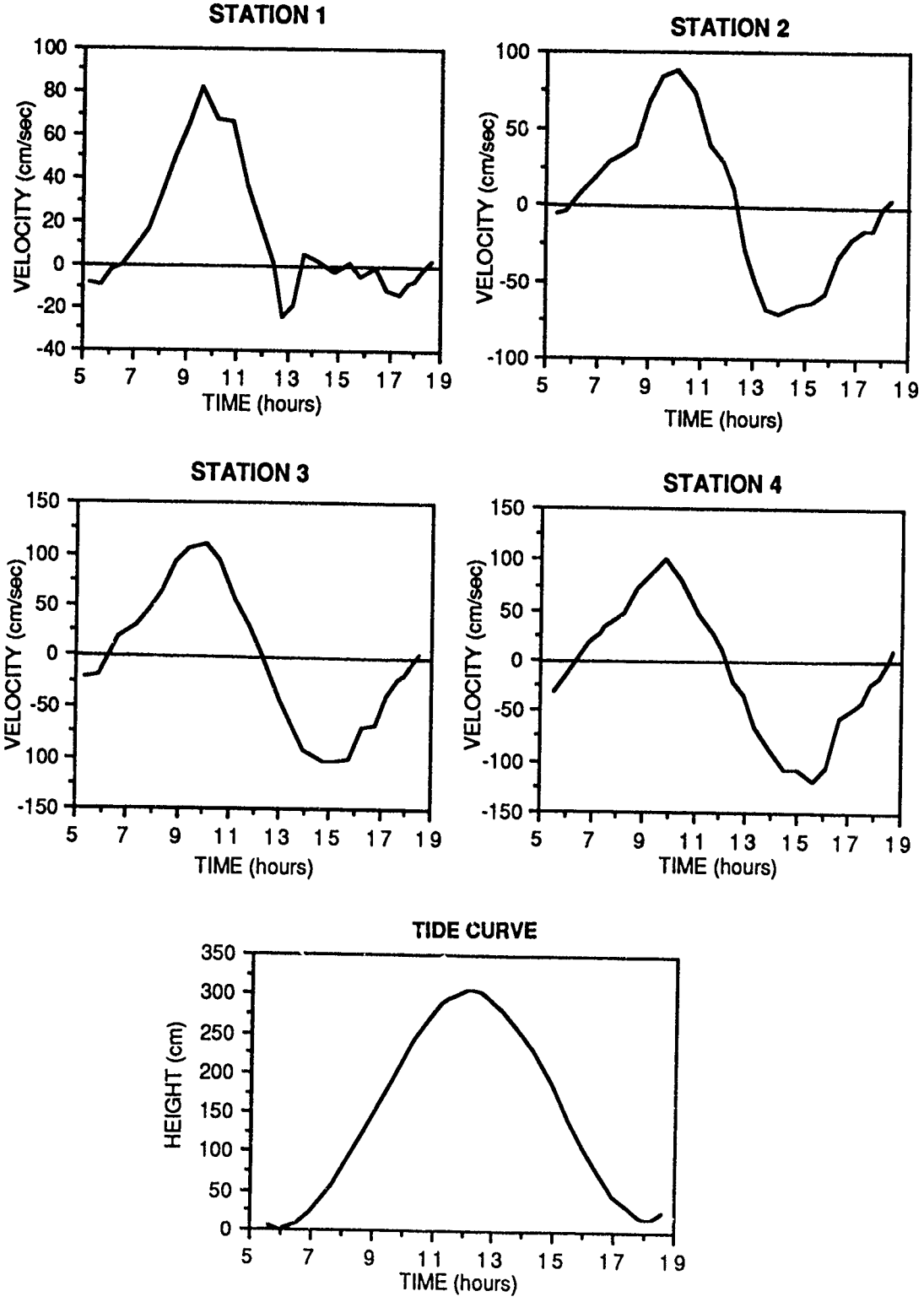

Figure 30. Velocity-time series and tide curve for stations 1-4 on 17 August, 1989.

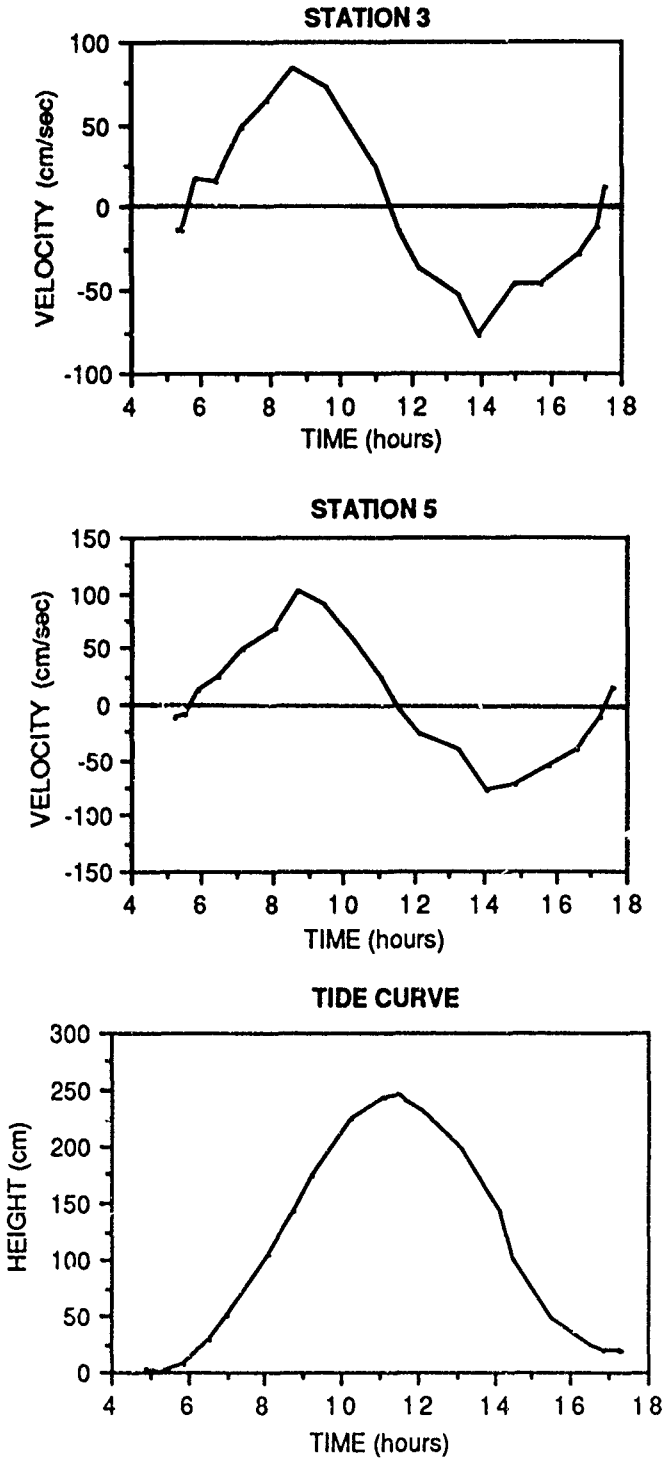

Figure 31 . Velocity-time series and tide curve for inlet throat channel thalweg station (station 5) and channel thalweg station at more seaward position (station 3). Hydrography performed on 05 August, 1990. Although duration of tides are similar for each station, maximum current velocities decrease in a seaward direction.

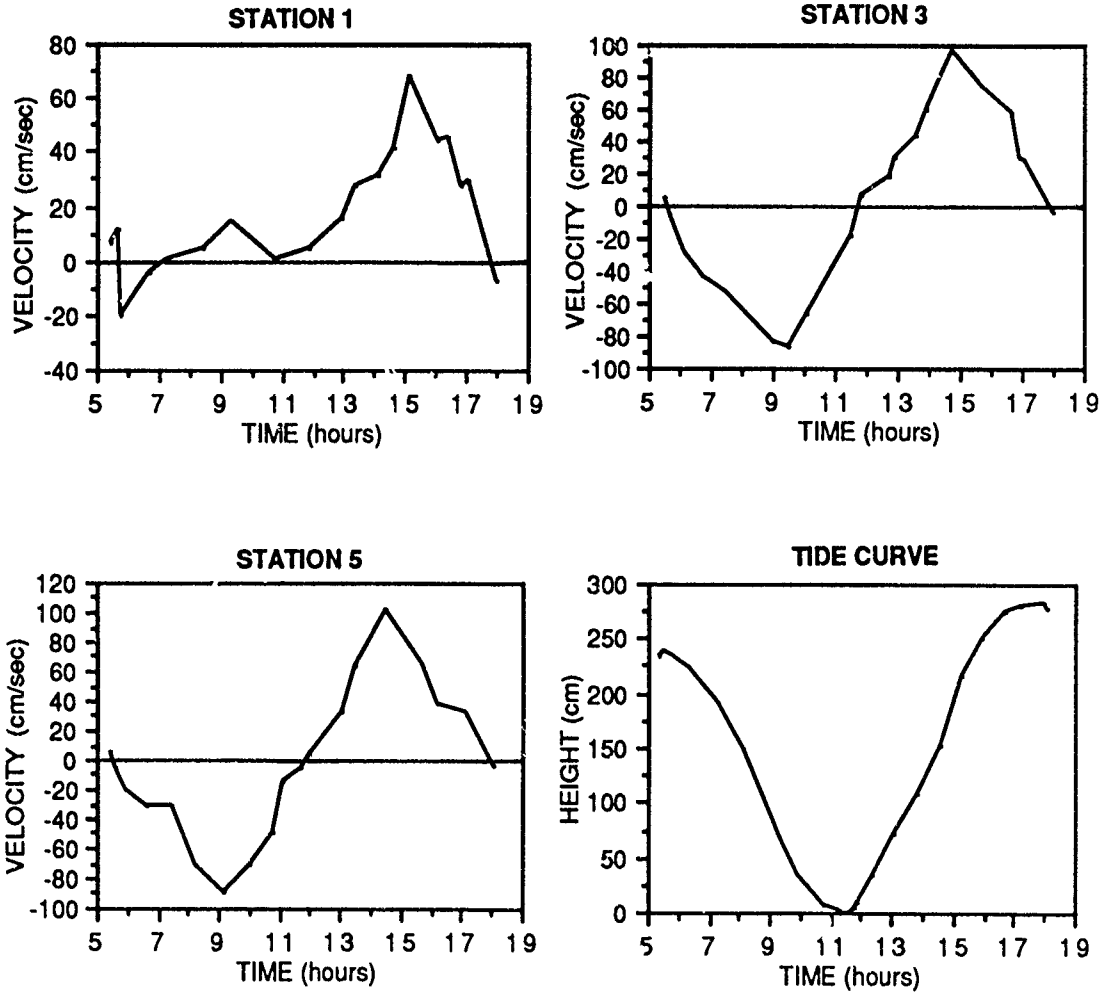

Figure 32. Velocity-time series and tide curve for stations 1, 3 and 5 of inlet channel of 12 September, 1990.

Date	Tidal Cycle	Station 1 (cm/sec)	Station 2 (cm/sec)	Station 3 (cm/sec)	Station 4 (cm/sec)	Station 5 (cm/sec)
26 July 1989	Flood	74	74	88	74	—
	Ebb	9	50	76	92	—
10 Aug. 1989	Flood	62	53	79	69	—
	Ebb	17	42	61	64	—
17 Aug. 1989	Flood	82	88	109	101	—
	Ebb	24	71	104	119	—
05 Aug. 1990	Flood	—	—	84	—	101
	Ebb	—	—	78	—	77
12 Sept. 1990	Flood	68	—	97	—	101
	Ebb	20	—	86	—	89

Table 3 . Su y of maximum currents for stations 1-5.

Date	Tidal Cycle	Station 1 (cm/sec)	Station 2 (cm/sec)	Station 3 (cm/sec)	Station 4 (cm/sec)	Station 5 (cm/sec)
26 July 1989	Flood	29	32	48	42	—
	Ebb	5	30	42	46	—
10 Aug. 1989	Flood	27	30	43	36	—
	Ebb	6	24	35	34	—
17 Aug. 1989	Flood	35	44	59	51	—
	Ebb	7	43	61	68	—
05 Aug. 1990	Flood	—	—	47	—	53
	Ebb	—	—	43	—	46
12 Sept. 1990	Flood	20	—	54	—	48
	Ebb	12	—	51	—	46

Table 4 . Summary of mean currents for stations 1-5.

Date	Tidal Cycle	Tidal Range (cm)	Duration (hr:min)	Maximum Velocity (cm/sec)	Mean Velocity (cm/sec)
26 July 1989	Flood	286	6:23	88	48
	Ebb	253	6:02	76	42
10 Aug. 1989	Flood	203	6:10	79	43
	Ebb	174	6:03	61	35
17 Aug. 1989	Flood	306	6:18	109	59
	Ebb	290	6:08	104	62
05 Aug. 1990	Flood	243	6:10	84	47
	Ebb	225	5:56	78	43
12 Sept. 1990	Flood	282	6:21	97	54
	Ebb	238	5:59	86	51

Table 5 . Summary of hydrographic data for channel thalweg (Station 3).

Date	Tidal Cycle	Station 3 (cm/sec)	Station 5 (cm/sec)	Station 6 (cm/sec)	Station 7 (cm/sec)
26 July 1989	Flood	88	—	—	—
	Ebb	76	—	—	—
10 Aug. 1989	Flood	79	—	—	—
	Ebb	61	—	—	—
17 Aug. 1989	Flood	109	—	—	—
	Ebb	104	—	—	—
12 June 1990	Flood	—	—	27	21
	Ebb	—	—	39	30
05 Aug. 1990	Flood	84	101	—	—
	Ebb	78	77	—	—
12 Sept. 1990	Flood	97	104	—	—
	Ebb	86	89	—	—

Table 6 . Summary of maximum currents for longitudinal inlet throat stations.

Date	Tidal Cycle	Station 3 (cm/sec)	Station 5 (cm/sec)	Station 6 (cm/sec)	Station 7 (cm/sec)
26 July 1989	Flood	48	—	—	—
	Ebb	42	—	—	—
10 Aug. 1990	Flood	43	—	—	—
	Ebb	35	—	—	—
17 Aug. 1989	Flood	59	—	—	—
	Ebb	62	—	—	—
12 June 1990	Flood	—	—	19	13
	Ebb	—	—	21	18
05 Aug. 1990	Flood	47	53	—	—
	Ebb	43	46	—	—
12 Sept. 1990	Flood	54	48	—	—
	Ebb	51	46	—	—

Table 7 . Summary of mean currents for longitudinal inlet channel throat stations.

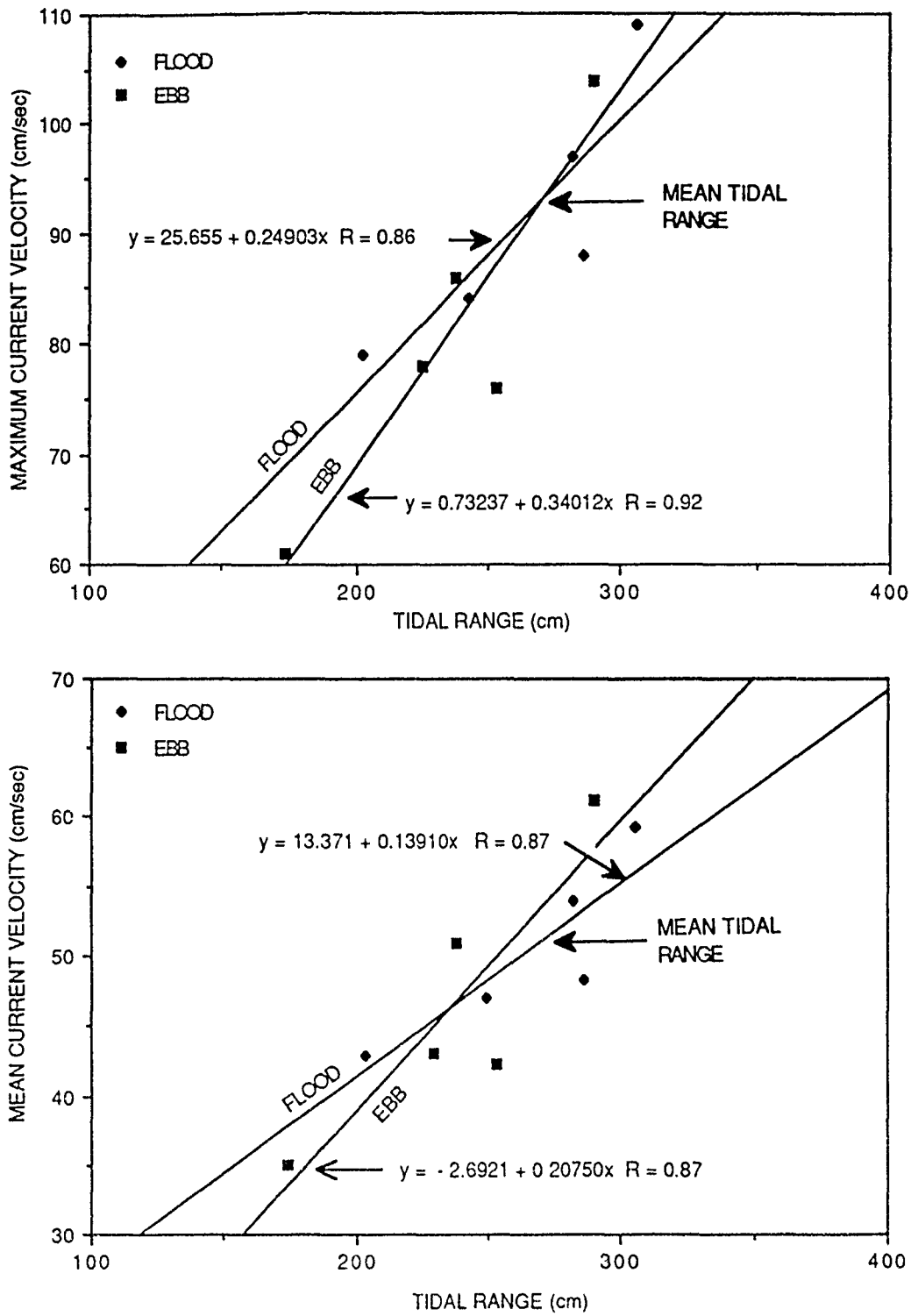

Figure 33 . Regression curves for maximum and mean current velocity versus tidal range at the inlet throat channel thalweg (station 3). Note that the inlet throat is ebb-dominant for tidal ranges greater than mean tidal range (2.7 m).

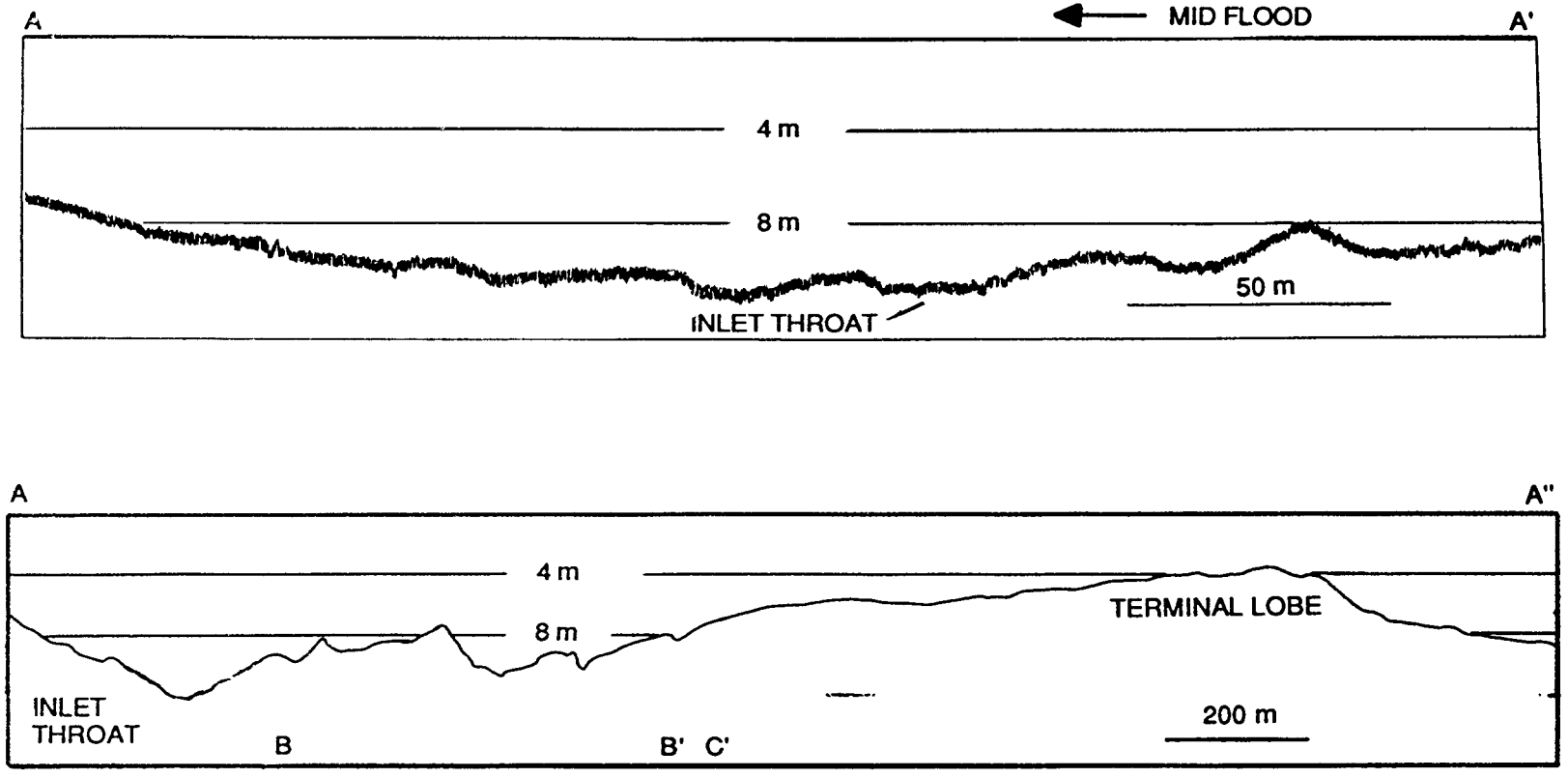

Figure 34 . Fathometer profile of the main ebb channel performed longitudinally in a southwest-northeast direction. Profile A-A' shows well-developed ebb-oriented sandwaves at the vicinity of the inlet throat. Profile A-A" shows the ebb-tidal delta cross section with terminal lobe and inlet throat as indicated. Figure 13 shows the location of the profiles.

Mota Oliveira, (1972) inlets backed by well-developed marshes with sloping channel banks are predicted to be ebb-dominated. Such is the case at the Essex River Inlet where marshes and intertidal areas represent approximately 89% of the backbarrier area (Som, 1990).

Stations 3, 5, 6 and 7 were positioned seaward of the inlet throat along the axis of the inlet channel. Although current velocity measurements at different stations were recorded on different dates, the data clearly demonstrate that there exists a marked decrease in both maximum and mean flood and ebb currents in a seaward direction (Figure 35, Table 6-7). Ebb-oriented sandwaves with wavelengths up to 7.5 m and heights up to 1.25 m as recorded in fathometer profiles B-B' and B-C' indicate the ebb-dominance of the main ebb channel throughout the tidal cycle (Figure 36). Figure 37'A' shows these ebb-oriented bedforms on the flank of the main ebb channel. Profile C'-B" of Figure 36 demonstrates that ebb-oriented sandwaves change orientation just landward of the terminal lobe due to wave-enhanced flood currents. The flood-oriented megaripples at this side have maximum wavelengths of 5.5 m and maximum heights up to 0.75 m.

Current velocity measurements taken in the updrift (stations 1, 9) (Figures 28-30,32,38) and downdrift marginal flood stations (stations 10, 11, 12) (Figures 38,39) and at the downdrift swash platform channel (station 19) (Figure 39) are summarized in Tables 8 and 9. In the updrift marginal flood channel, maximum flood velocities for both stations ranged from 34 to 82 cm/sec while the maximum ebb velocities ranged from 9 to 24 cm/sec. Mean flood velocities ranged from 19 to 35 cm/sec while the mean ebb velocities ranged from 5 to 15 cm/sec. At the downdrift marginal flood channel, maximum flood velocities for the three stations ranged from 29 to 70 cm/sec which compares to 15 to 32 cm/sec for the maximum ebb velocities. Mean flood velocities varied from 16 to 38 cm/sec while the mean ebb velocities ranged from 9 to 17 cm/sec. The dominance of flood currents at both the updrift and downdrift marginal flood channels is more clearly demonstrated by the regression curves of Figures 40 and 41. Although the data do not produce

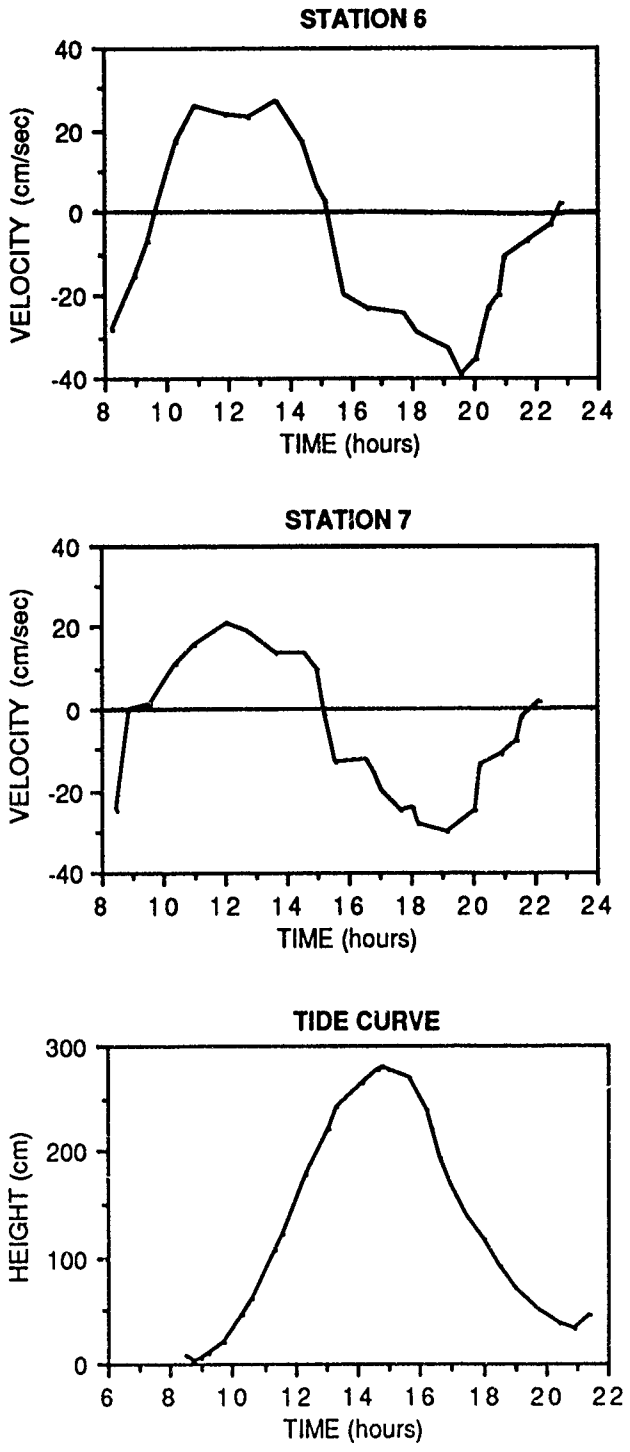

Figure 35 . Velocity-time series and tide curve for stations 6 and 7 located longitudinally in the main ebb channel. Hydrography performed on 12 June, 1990 to determine differential current velocities in the main ebb channel in a seaward direction from the inlet throat.

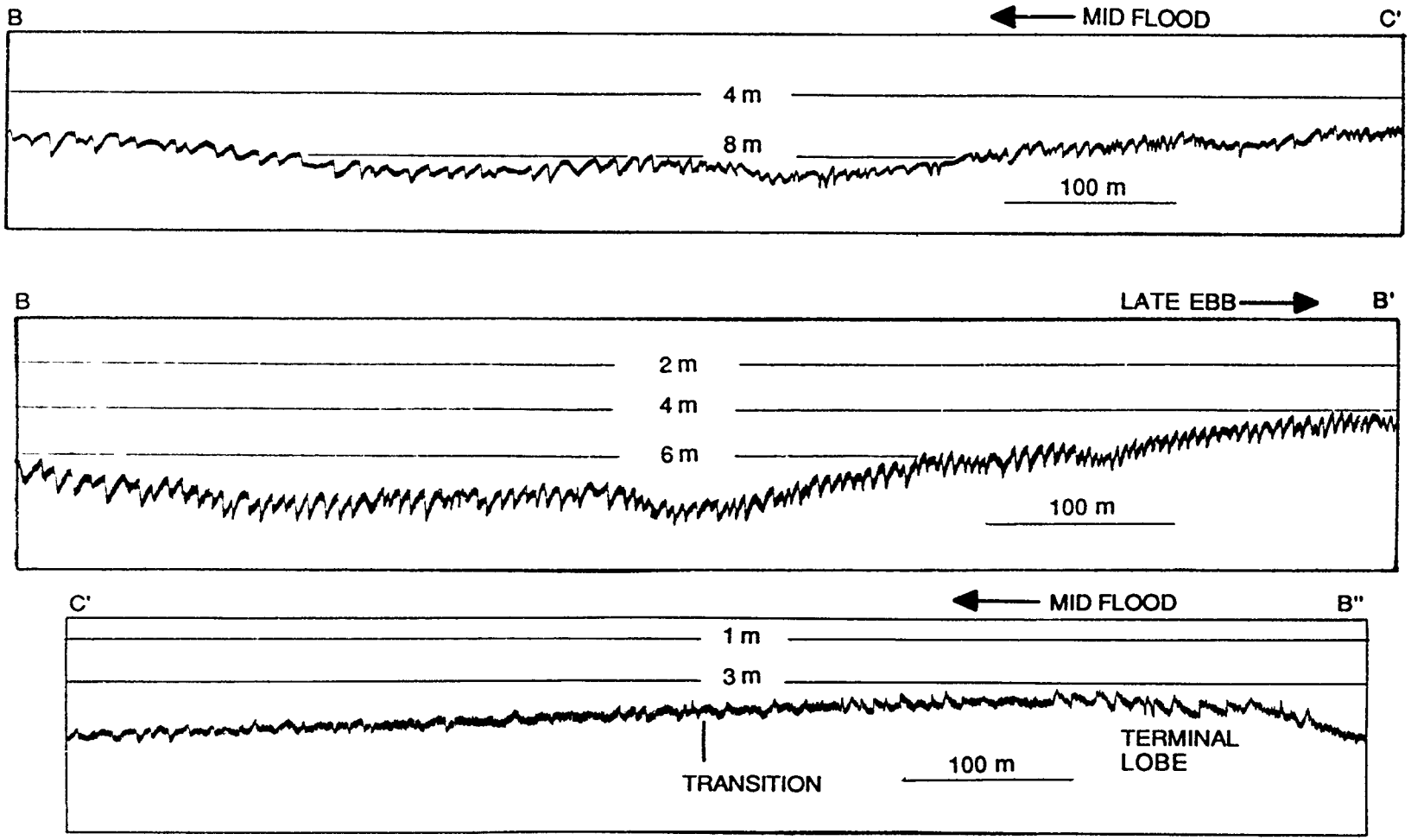

Figure 36. Fathometer profiles of main ebb channel performed longitudinally. Profiles B-B' and B-C' indicate that the proximal main ebb channel is dominated by ebb bedforms during both ebb and flood tides. Profile C'-B" of the distal main ebb channel illustrates the transition in a seaward direction of well-developed ebb-oriented sandwaves to well-developed wave enhanced flood-oriented megaripples .

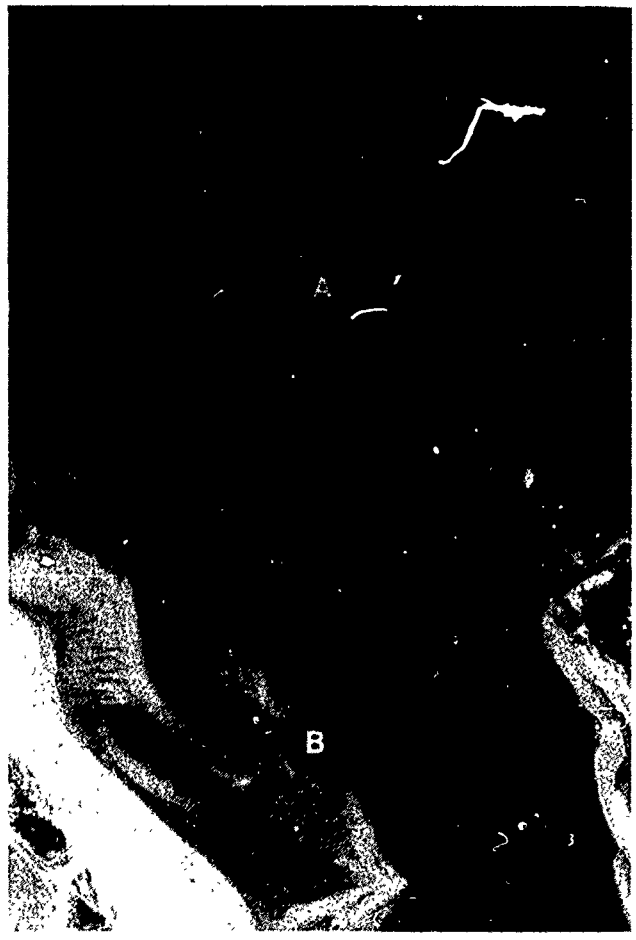

Figure 37. Oblique aerial photograph taken at low tide showing well-developed ebb-oriented sandwaves on outer flanks of main ebb channel. Regard (A) in photograph. Note also the well-developed flood-oriented sandwaves in the updrift marginal flood channel. Regard (B) in photograph.

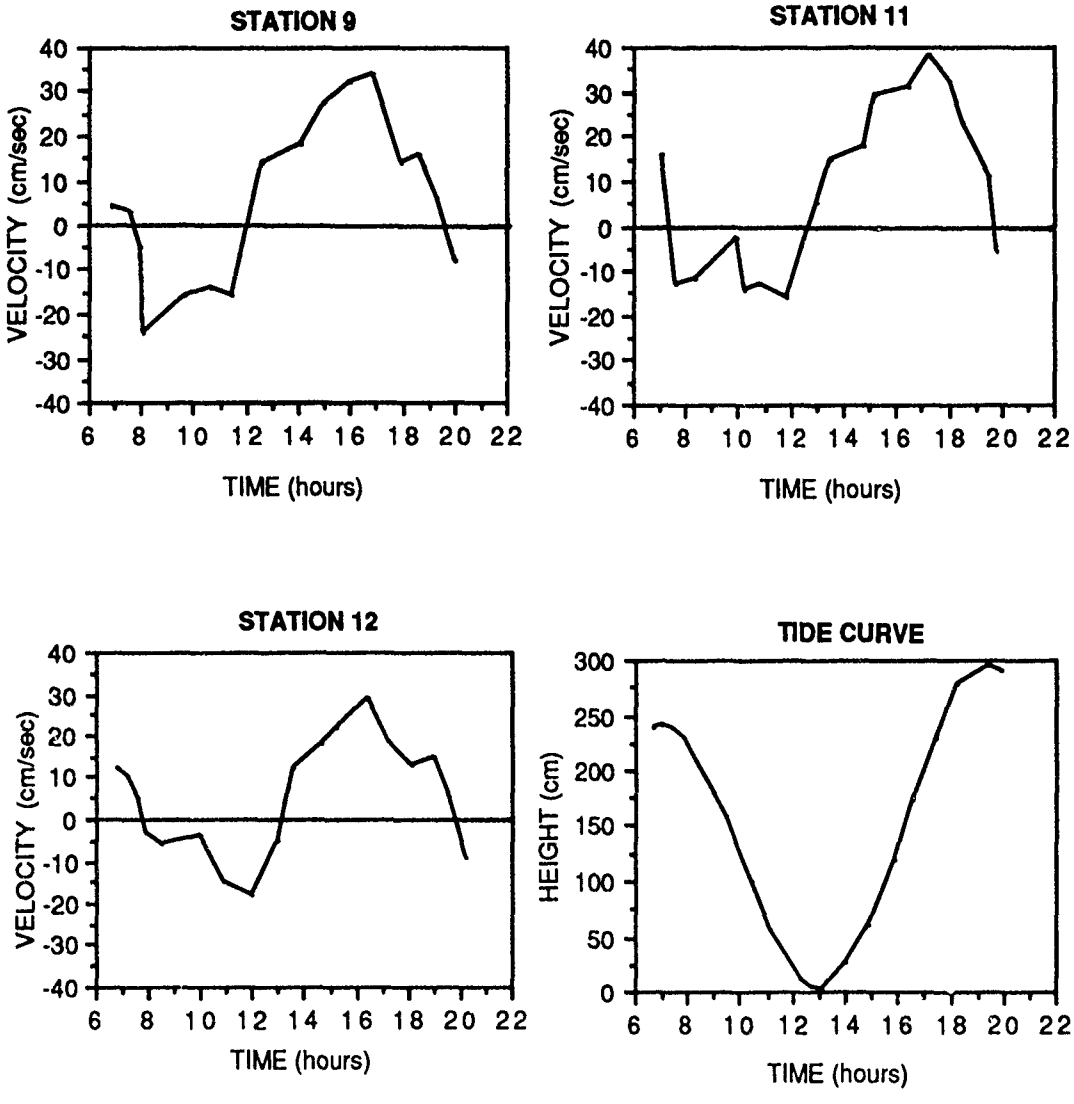

Figure 38. Velocity-time series and tide curve for stations 9 in the updrift marginal flood channel and stations 11, 12 in downdrift marginal flood channel. The hydrography was performed on 17 July, 1990.

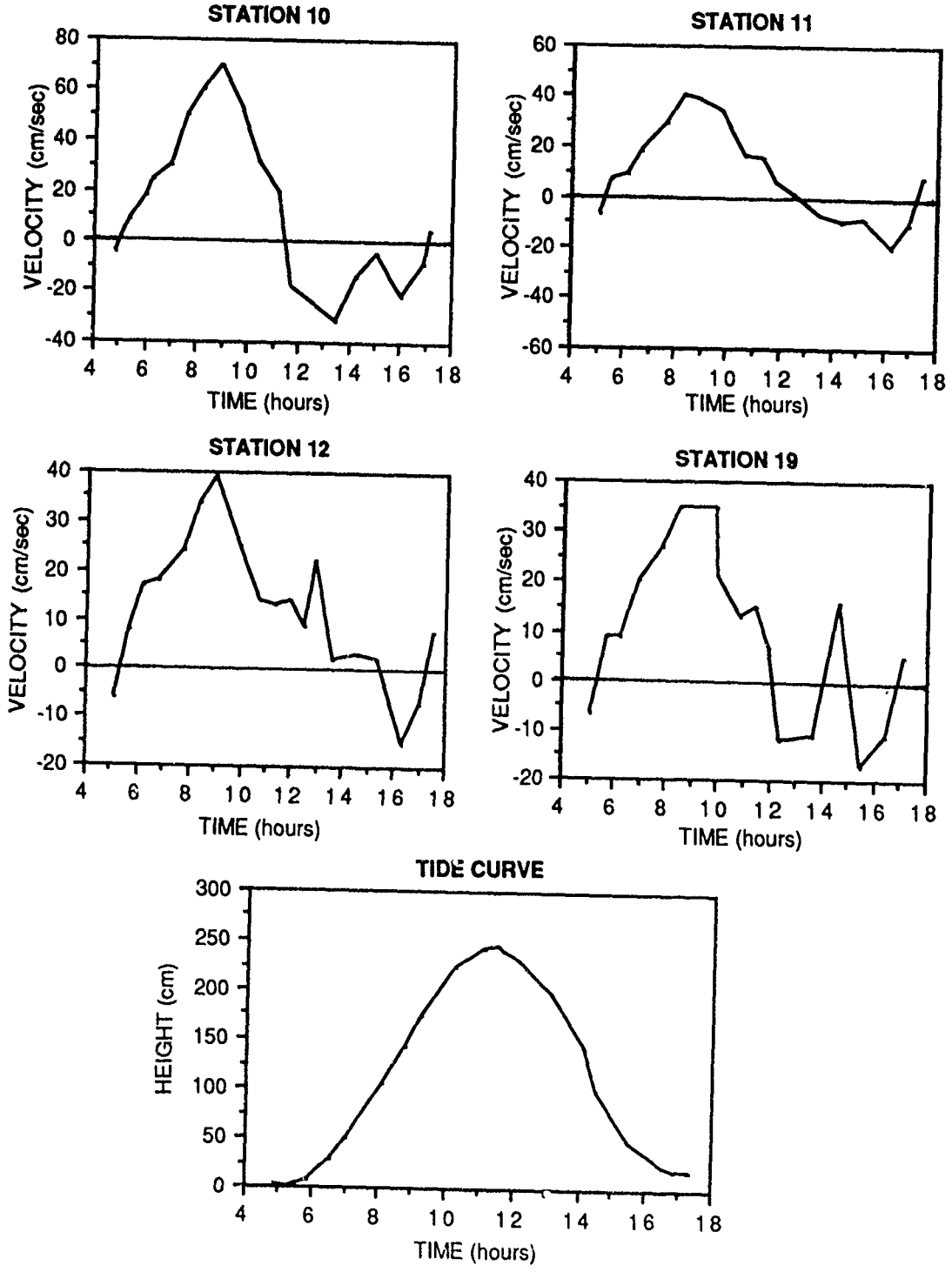

Figure 39. Velocity-time series and tide curve for stations 10, 11, 12 located in the downdrift marginal flood channel and station 19 in the downdrift swash platform channel. The hydrography performed on 5 August, 1990.

Date	Tidal Cycle	Station 1 (cm/sec)	Station 9 (cm/sec)	Station 10 (cm/sec)	Station 11 (cm/sec)	Station 12 (cm/sec)	Station 19 (cm/sec)
26 July 1989	Flood	74	—	—	—	—	—
	Ebb	9	—	—	—	—	—
10 Aug. 1989	Flood	62	—	—	—	—	—
	Ebb	17	—	—	—	—	—
17 Aug. 1989	Flood	82	—	—	—	—	—
	Ebb	24	—	—	—	—	—
17 July 1990	Flood	—	34	—	38	29	—
	Ebb	—	24	—	16	18	—
05 Aug. 1990	Flood	—	—	70	40	39	35
	Ebb	—	—	32	20	15	17
12 Sept. 1990	Flood	68	—	—	—	—	—
	Ebb	20	—	—	—	—	—

Table 8 . Summary of maximum currents for updrift and downdrift marginal flood channel and downdrift swash platform channel stations.

Date	Tidal Cycle	Station 1 (cm/sec)	Station 9 (cm/sec)	Station 10 (cm/sec)	Station 11 (cm/sec)	Station 12 (cm/sec)	Station 19 (cm/sec)
26 July 1989	Flood	29	—	—	—	—	—
	Ebb	5	—	—	—	—	—
10 Aug. 1989	Flood	27	—	—	—	—	—
	Ebb	6	—	—	—	—	—
17 Aug. 1989	Flood	35	—	—	—	—	—
	Ebb	7	—	—	—	—	—
17 July 1990	Flood	—	19	—	23	17	—
	Ebb	—	15	—	10	9	—
05 August 1990	Flood	—	—	38	21	16	18
	Ebb	—	—	17	10	9	10
12 Sept. 1990	Flood	20	—	—	—	—	—
	Ebb	12	—	—	—	—	—

Table 9 . Summary of mean currents for updrift and downdrift marginal flood channel and downdrift swash platform channel stations.

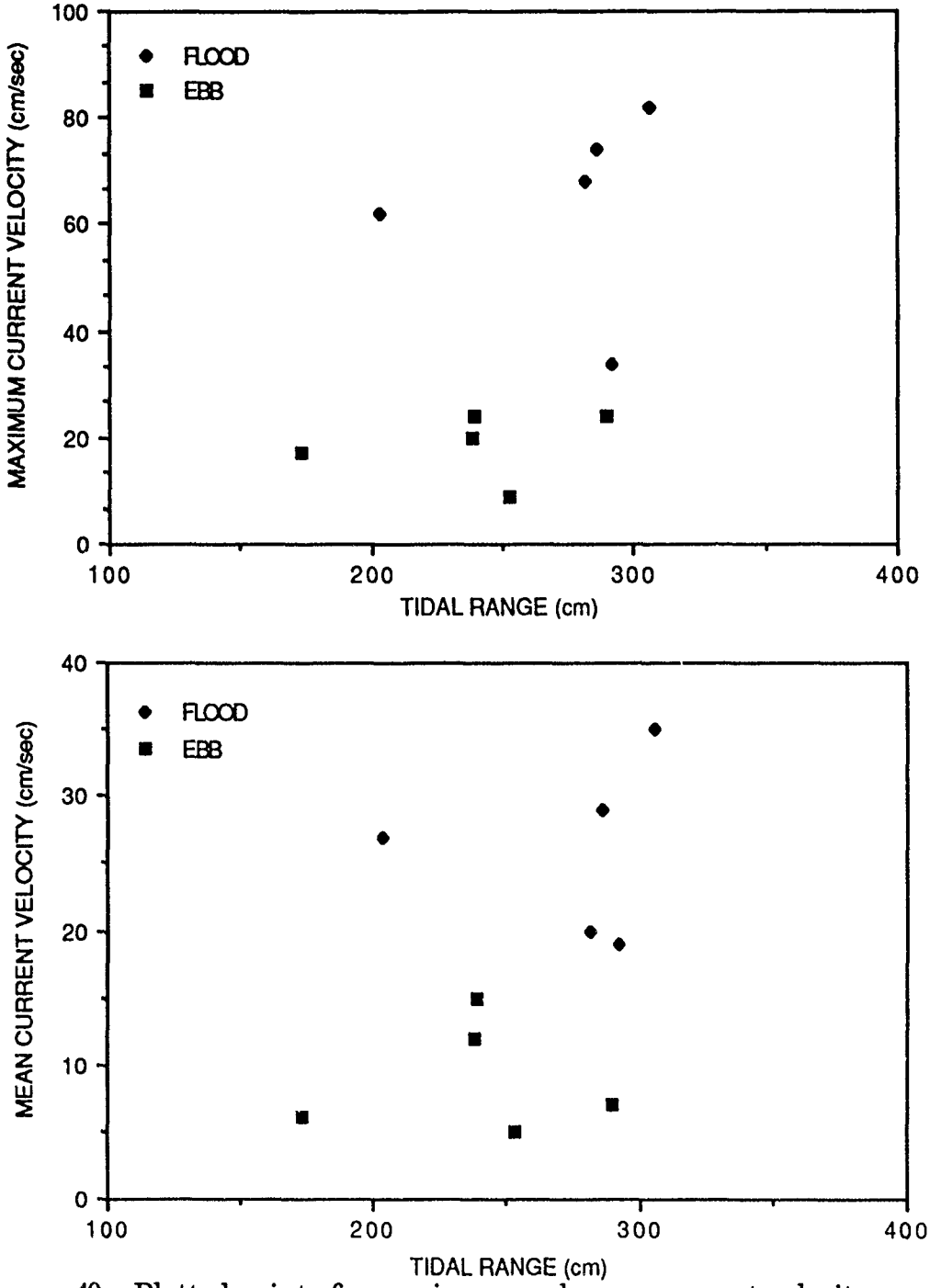

Figure 40. Plotted points for maximum and mean current velocity versus tidal range for updrift marginal flood channel stations (stations 1 and 9) for flood and ebb tidal cycles. Note the clear distinction in both graphs between the stronger flood current velocity points and the ebb current velocity points. This indicates flood dominance of the updrift marginal flood channel.

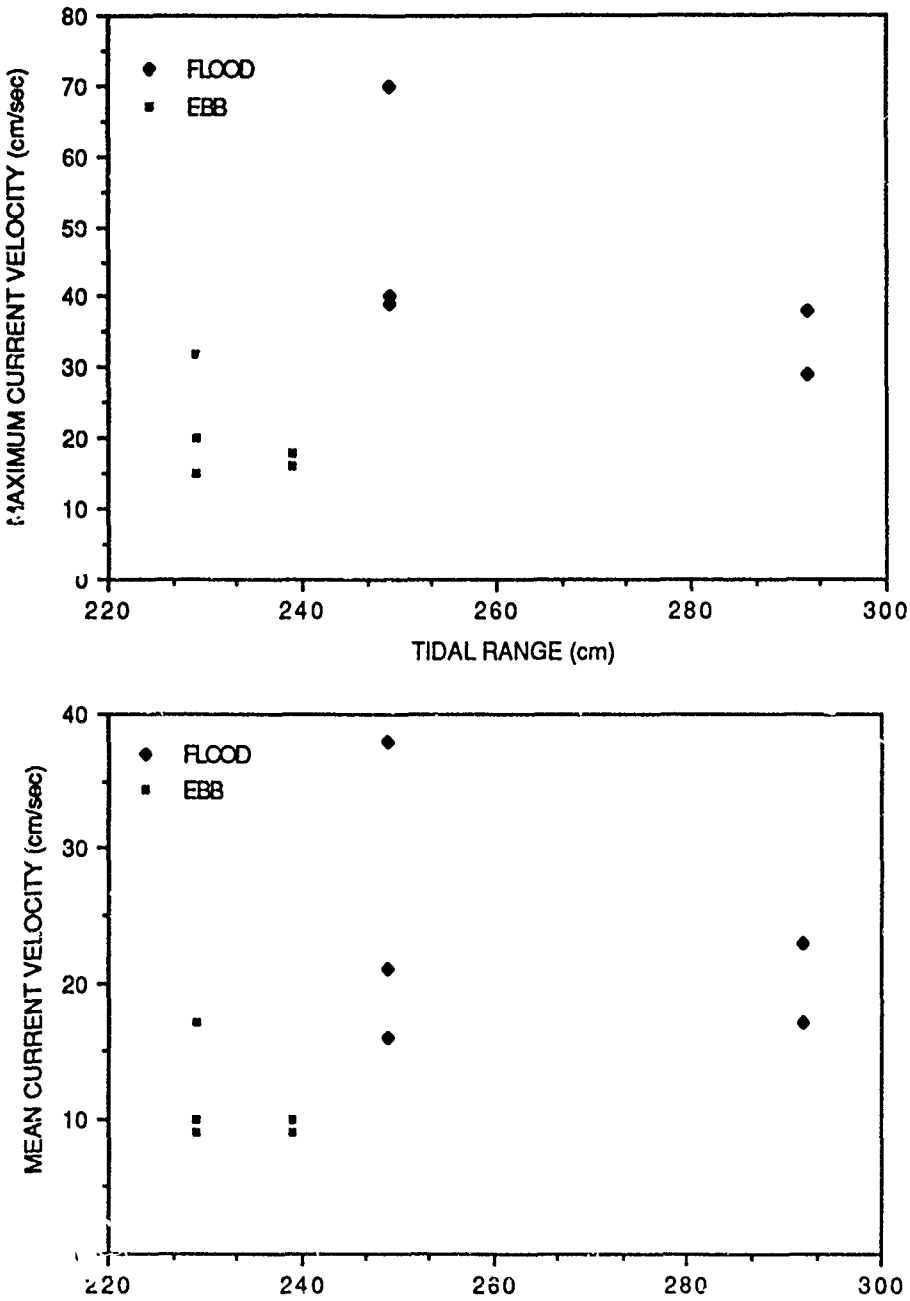

Figure 41. Plotted points for maximum and mean current velocity versus tidal range for downdrift marginal flood channel stations (stations 10, 11, 12) for flood and ebb tidal cycles. A fitted regression line would indicate an inverse relationship between maximum current velocity and tidal range. This trend is explained by plotted points from three stations at different distances from the main ebb channel, each which have differing maximum current velocities at similar tidal ranges. Note the overall trend where maximum flood current velocities are stonger than maximum ebb current velocities. This indicates flood current dominance of the downdrift marginal flood channel.

a high degree of predictability for both maximum and mean velocities, flood currents are stronger than ebb currents for similar tidal ranges. The downdrift swash platform channel is also considered to be flood-dominant as indicated from data from one hydrography. Flood currents had maximum and mean velocities of 35 cm/sec and 18 cm/sec, respectively, which compared to ebb current maximum and mean velocities of 17 cm/sec and 10 cm/sec.

The dominance of flood tidal currents in both marginal flood channels is also demonstrated by channel bottom flood-oriented bedforms. Profiles F-F' and F'-F" of the updrift marginal flood channel illustrate well-developed flood-oriented sandwaves with wavelengths up to 20 m and heights up to 1.5 m which remain flood-oriented throughout the tidal cycle (Figure 42). Figure 37'B' shows these flood-oriented sandwaves of the updrift marginal flood channel. The downdrift marginal flood channel is floored by well-developed flood-oriented sandwaves with wavelengths up to 10 m and heights up to 1 m (Figure 43, Profile D-D'). The downdrift marginal flood channel bedforms are smaller than those of the updrift marginal flood channel due to weaker maximum flood current velocities. These bedforms change orientation only during late ebb stages of the tidal cycle due to ebb currents with maximum velocities of 32 cm/sec (Figure 43, Profile E-E')

Less symmetrical flood-oriented bedforms are found in the distal downdrift marginal flood channel (Figure 44, Profile D'-D") and downdrift swash platform channel (Figure 44, Profile E'-E") However, sandwaves in the distal downdrift marginal flood channel are better defined than in the swash platform channel, thus indicating stronger flood currents.

DISCUSSION

The vector analysis of maximum current velocities at the inlet are depicted in Figure 45. This correlates well with typical ebb-tidal delta

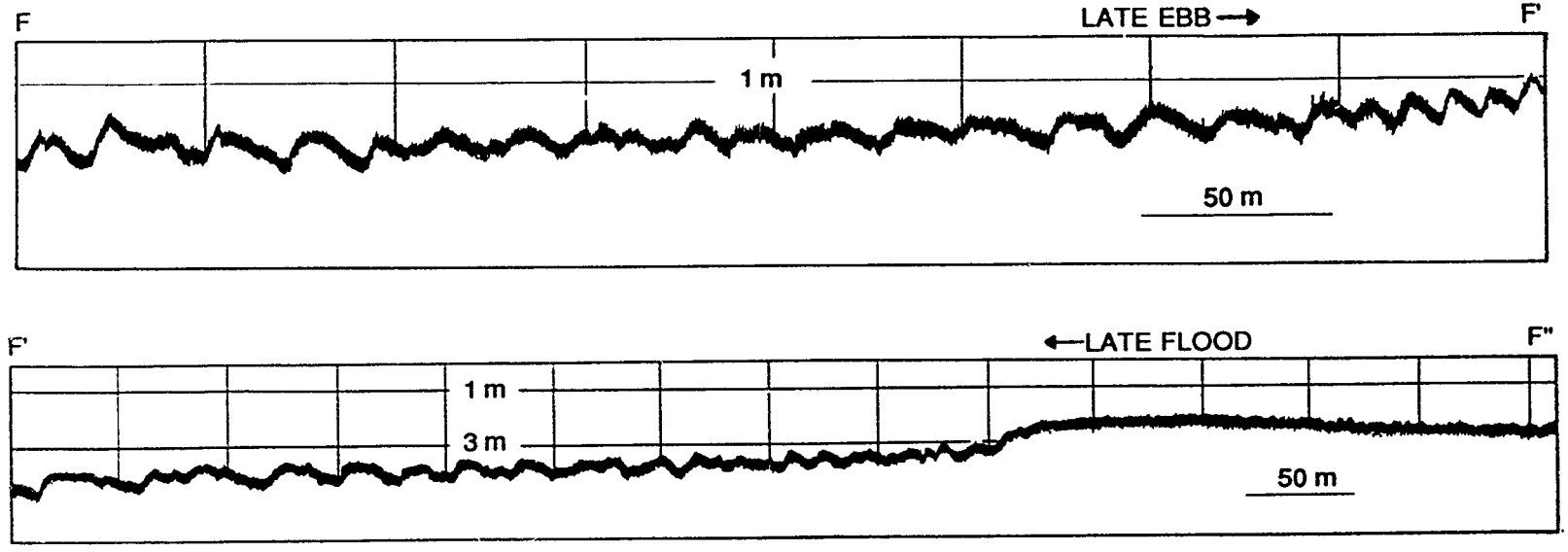

Figure 42. Fathometer profiles of the updrift marginal flood channel. Note the dominance of flood-oriented bedforms during flood tide in the distal portions (F'-F") as well as throughout the tidal cycle as is shown during the late ebb stage (F-F'). Each block represents 50 m of distance. Figure 13 shows the location of the profiles.

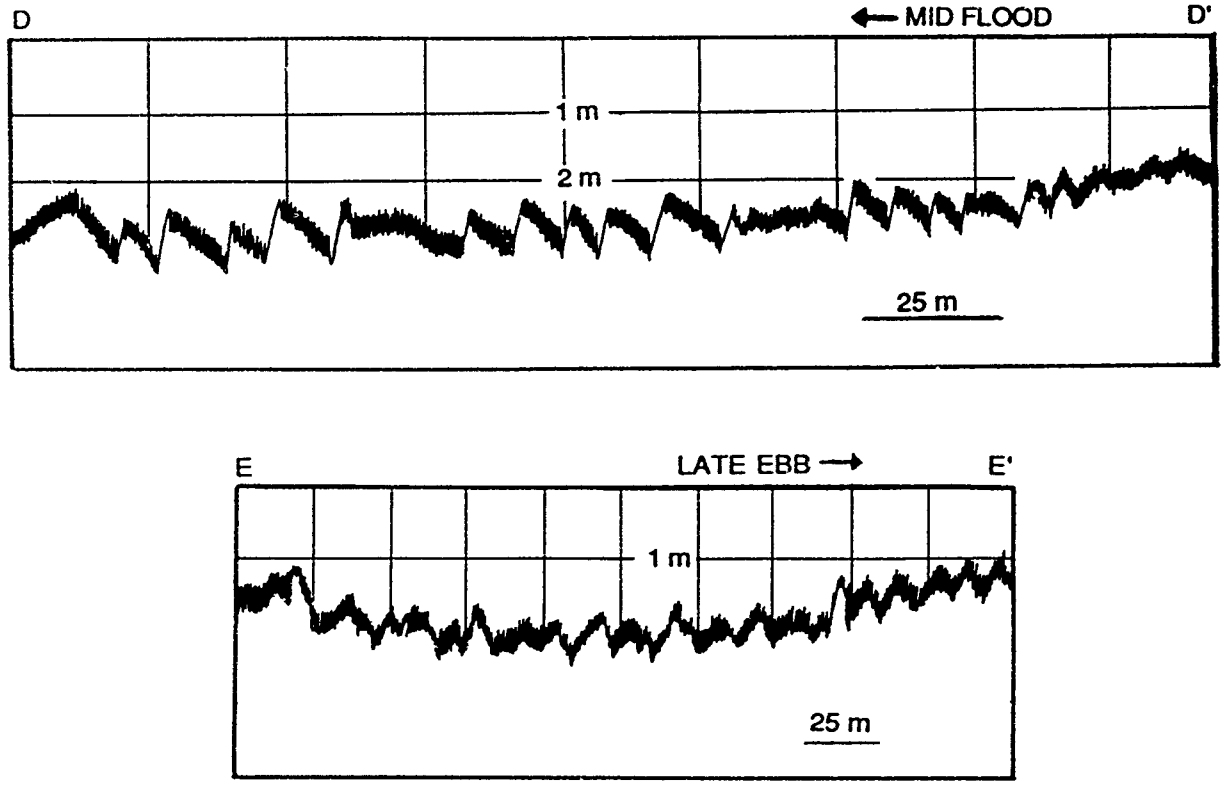

Figure 43. Fathometer profiles of the downdrift marginal flood channel. Profiles D-D' and E-E' performed longitudinally at mid flood and late ebb tides, respectively. Note the flood-oriented sandwaves during the mid flood stage of the downdrift marginal flood channel (D-D'). These bedforms become transitional only at late ebb stage (E-E'). Each block represents 25 m of distance. Figure 13 shows the location of profiles.

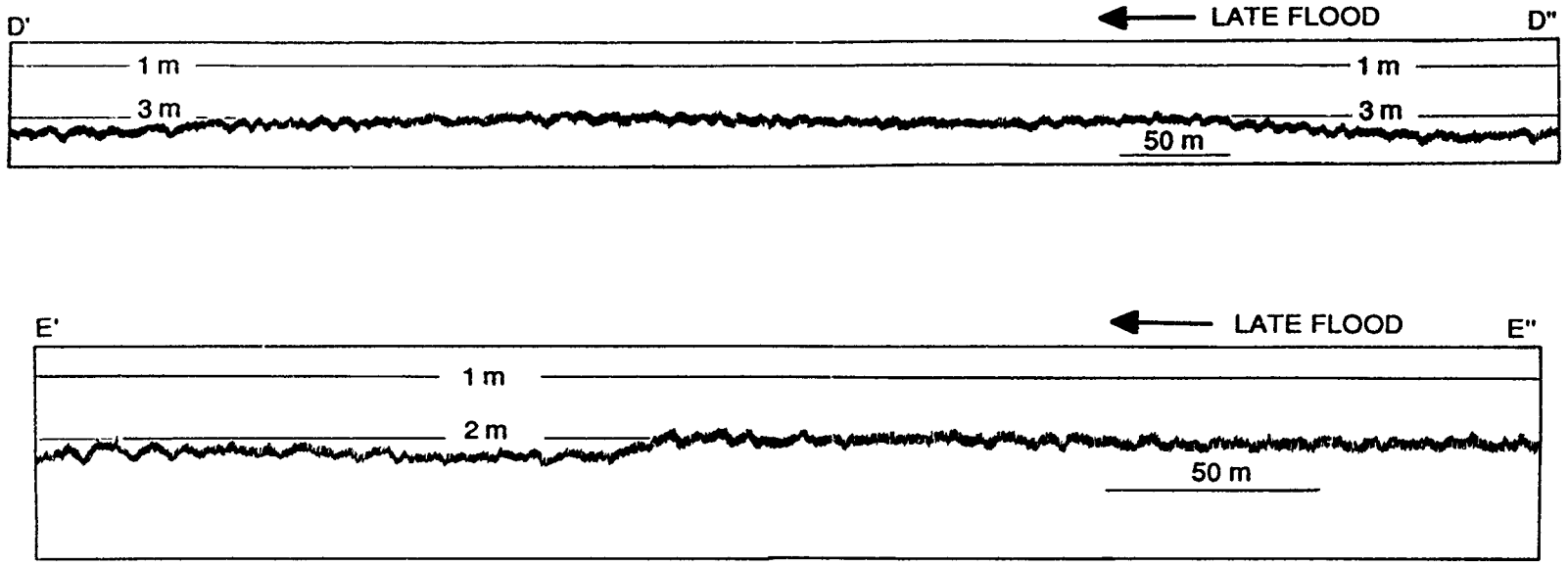

Figure 44. Fathometer profiles of channels downdrift of the main ebb channel at late flood stage of tide. Profile D'-D" of the marginal flood channel shows relatively well-developed flood-oriented sandwaves. Profile E'-E" of the swash platform channel shows poorly developed flood-oriented megaripples. Note better developed flood-oriented bedforms at locations nearer to main ebb channel (E'). Figure 13 shows location of profiles.

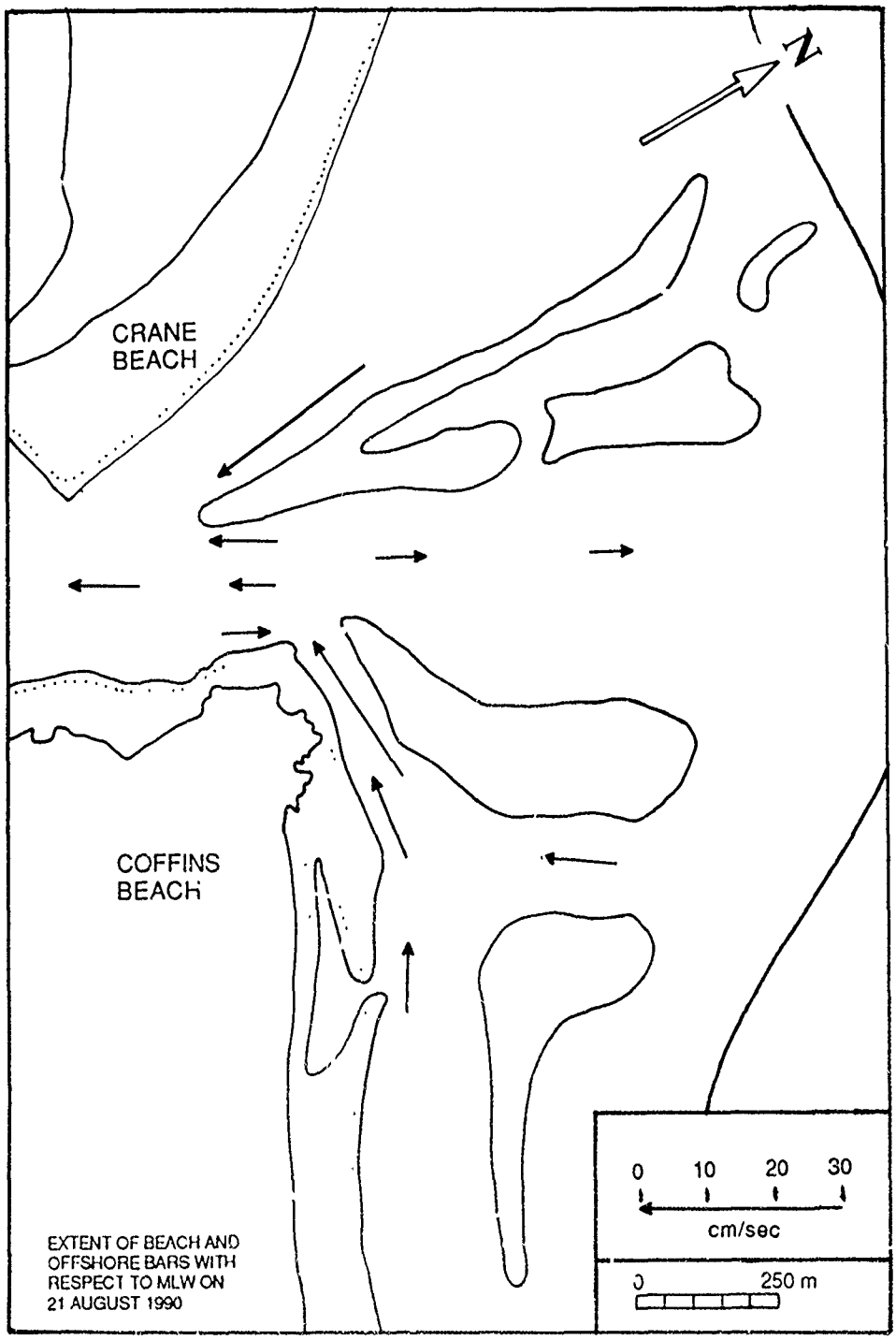

Figure 45. Net direction and magnitude of maximum currents as determined from hydrographic data. Length of stem of arrow measured from base of head to tail indicates net magnitude. One cm of arrow represents a current of 20 cm/sec. Arrow length represents average of maximum currents determined during several hydrographies.

segregation of flow as reported by Hayes (1977) (Figure 46). The segregation of flow is primarily a factor of the hydraulic gradient in a seaward direction associated with the ebb jet. The ebb jet is controlled by changes in inlet cross section and efficiency over the tidal cycle (FitzGerald and Nummedal, 1983), and changes in the backbarrier bay area over the tidal cycle (Keulegan, 1967; Mota Oliveira, 1970). As the tide falls, the rapidly decreasing bay area results in the constriction of water into channels. This results in less friction, greater ebb current velocities which continue to flow past the low water stage of the open ocean, and longer flood tidal durations (Mota Oliveira, 1970). As ebb current velocity decreases, the flood currents follow the path of least resistance which is first through the marginal flood channels and then through the main ebb channel and over intertidal sand bodies (Figure 47).

The ebb jet also produces time-velocity assymetry of currents (Figure 48'A') (Postma 1961; Hayes, 1977) or maximum tidal currents which occur late in the tidal cycle and maximum flow velocities of one tidal stage which are stonger than the other. At the study area, tidal current curves exhibit only velocity assymetry. The inlet throat channel thalweg (station 3) has stronger flood currents than ebb currents (Figure 48'B'). However, maximum ebb currents occur on average only slightly after mid-tide. This is explained by the percentage of marsh surface in the backbarrier and the shallow depth of the channel margin linear bars which are exposed soon after mid tide. This results in the constriction and funneling of the currents earlier in the tidal cycle so maximum currents occur earlier (Hubbard, 1977). Both marginal flood channels demonstrate flood current velocity assymetry (Figure 48'C' and 'D') as is demonstrated by stronger flood currents than ebb currents.

By relating spring tidal prism (3.04×10^7 m^3/tidal cycle) with inlet throat cross sectional area (1.77×10^3 m^2), the Essex River Inlet data plots within the 95% confidence limits for inlets on the Atlantic Coast with one or no jetties (Jarrett, 1976) (Figure 49). This indicates that the inlet is in a state of long term stability or dynamic equilibrium.

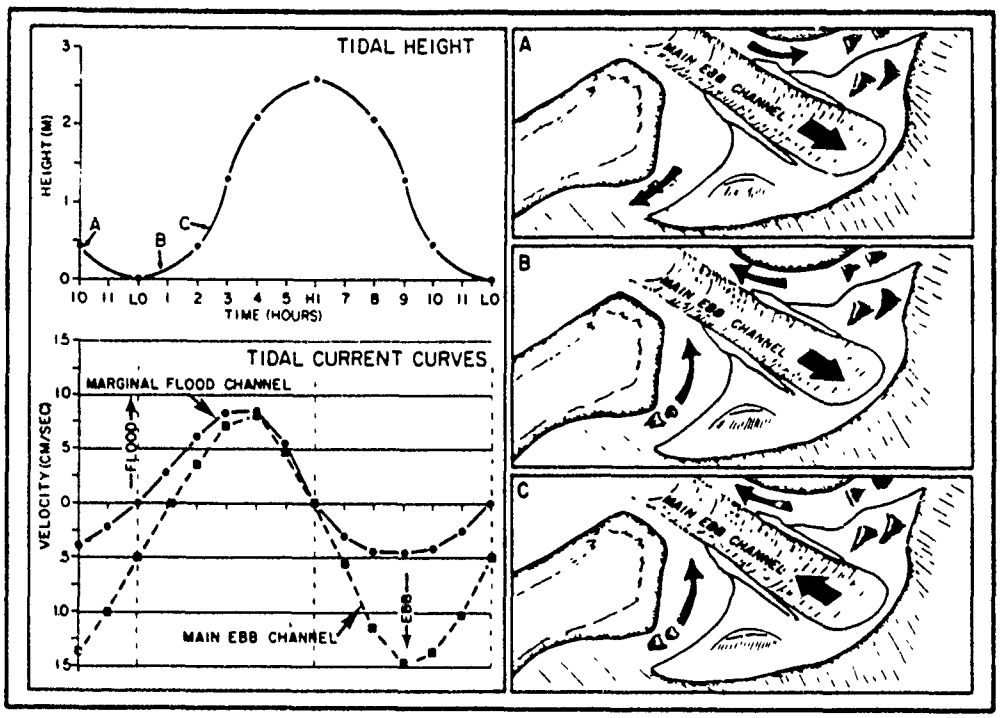

Figure 46. Segregation of flow of ebb-tidal delta and effect on ebb-tidal delta morphology. Note the ebb-dominance of the main ebb channel and the flood-dominance of the marginal flood channels as is shown in the tidal current curves. The initial flooding of the estuary is shown at right. Note the continuation of ebb flow in the main ebb channel past the low water stage in the ocean (Hayes, 1977).

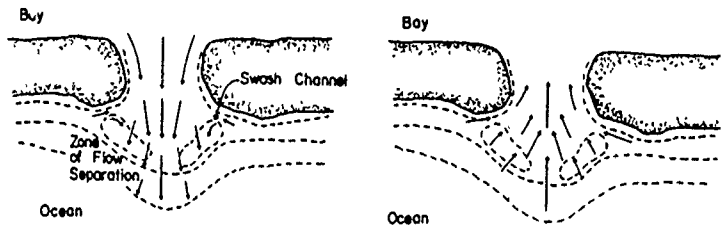

Figure 47. Idealized inlet flow patterns for flood and ebb tidal stages (Dean and Walton, 1975).

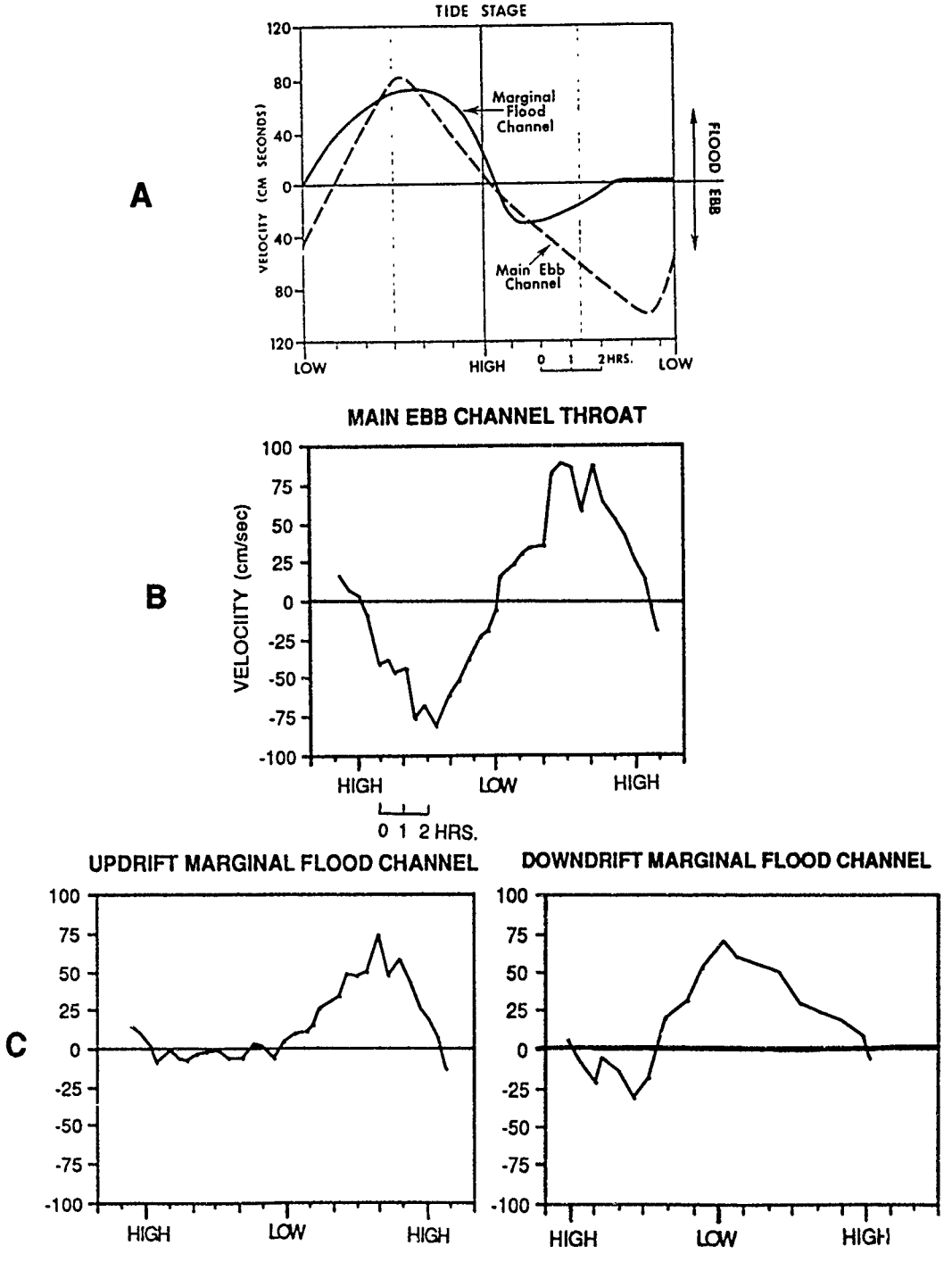

Figure 48 . A) Typical tidal current velocity time-series for a mesotidal ebb-tidal delta, which illustrates the principle of time-velocity assymetry. (Hayes, 1977). Velocity-time series for the study area including B) Main ebb channel and C) Updrift and downdrift marginal flood channels.

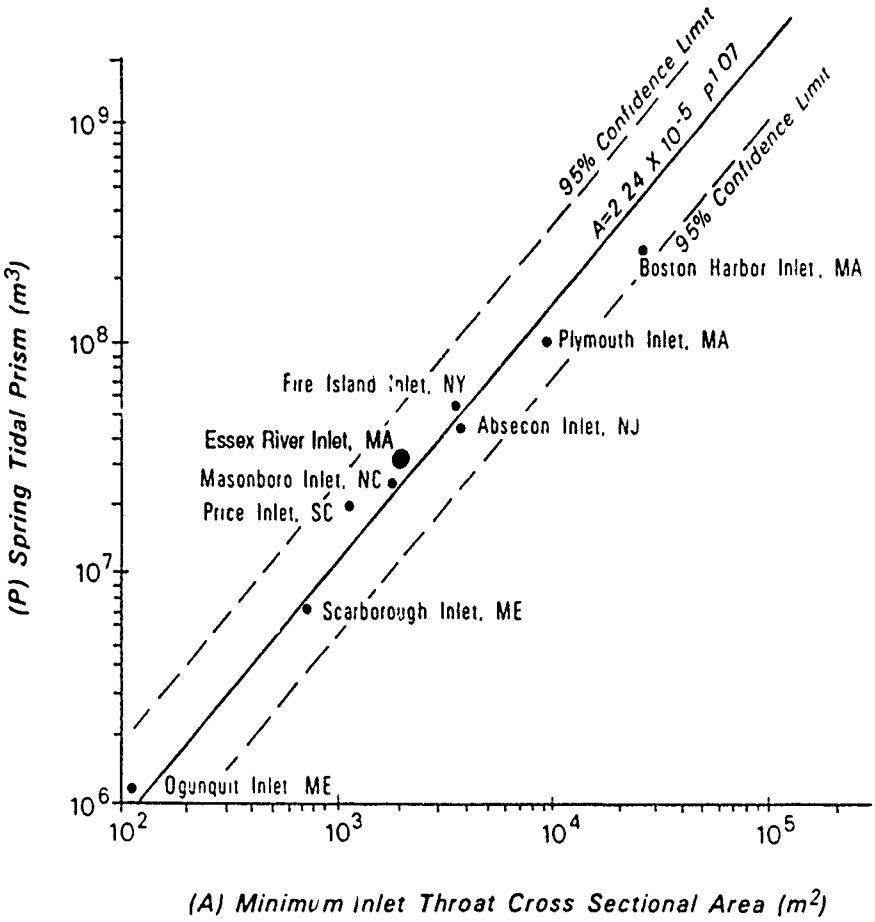

Figure 49. Tidal prism versus minimum inlet cross-sectional area. The Essex River Inlet relationship fits well within the 95% confidence limits (after Jarrett, 1976).

EBB-TIDAL DELTA MORPHODYNAMICS

SEDIMENT CHARACTERISTICS

Generally, the delta is composed of very well to well-sorted (0.21Ø - 0.50Ø) fine to medium sand (1.75Ø - 2.50Ø). The well-sorted nature of the delta sands is indicative of the fine-grained nature of the limited sediment sources.

The sediment source, and wave and tidal energy are the major factors controlling the Essex River ebb-tidal delta grain size characteristics. The sediment source at the Essex River Inlet is derived primarily from longshore currents and is fine to medium sand with very small amounts of coarse-grained material derived from the erosion of drumlins.

Although the delta is composed primarily of well-sorted fine to medium sand, some recognizable grain size trends are present. A seaward grain size fining sequence occurs from the inlet throat thalweg (medium sand-mean grain size 1.70Ø) to the terminal lobe (fine sand-mean grain size 2.00Ø) and is due to the decrease of tidal current energy in a seaward direction (cf. Nelligan, 1982; Sha, 1989). This fining sequence continues seaward from the terminal lobe to the seaward extent of the ebb-tidal delta where the 5 m depth contour parallels the shoreline (very fine sand- mean grain size 2.62Ø with an average sorting coefficient of 0.34Ø).

There is also a difference in grain size characteristics between the tide and wave-dominated environments of the delta. Tide-generated currents are stronger than wave-generated currents and therefore are more competent in winnowing out fine-grained sediment, thus leaving the coarse-grained sediment to settle. Therefore, tide-dominated environments are coarser than wave-dominated environments. Generally, sediments of tide-dominated environments are composed of well-sorted medium sand (mean grain size of 1.94Ø; sorting coefficient of 0.34Ø). Specific tide-dominated environments can be further

differentiated. The mean grain size of main ebb channel sediments is 1.85Ø (medium sand) as compared to 1.94Ø (medium sand) and 2.03Ø (fine sand) for sediments of the downdrift and updrift marginal flood channels, respectively.

Sediments of the wave-dominated environments (swash bars and distal channel margin linear bars) have a mean grain size of 2.11Ø (fine sand) and a sorting coefficient of 0.30Ø (well-sorted). The proximal channel margin linear bar environment has grain size characteristics similar to wave-dominated environments (mean grain size of 2.15Ø (fine sand) and an sorting coefficient of 0.27Ø (very well sorted).

Updrift and downdrift portions of the delta possess different grain size characteristics. The updrift portion of the delta is composed primarily of fine sand as is shown by mean grain size of the delta seaward of the low tide terrace (2.22Ø) and of Crane Beach (2.16Ø). The downdrift portion of the delta is composed of medium sand indicating a mean grain size of the delta seaward of the low tide terrace (1.83Ø) and of Coffins Beach (1.86Ø). This grain size trend may be explained by the inlet channel acting as a coarse-grained sediment trap. Coarser-grained sediment bypasses Crane Beach during storms and enters the inlet system. As sediment is reworked through downdrift portions of the delta and reintroduced into the main ebb channel by residual flood currents through the downdrift marginal flood channel, some coarser-grained material is deposited on the downdrift Coffins beach.

There are also variations in wave energy on Crane Beach which results in a sediment coarsening trend to the southeast towards the inlet. This coarsening sequence of grain size is anomalous to the southeastward fining trend of sediments within the Merrimack Embayment (Schalk, 1936; Goodbred and Montello, 1989). Coffins Beach shows no such sediment trends.

SEDIMENT TRANSPORT PATTERNS

INTRODUCTION

Southerly longshore currents are responsible for bringing sediment to the updrift side of the Essex River ebb-tidal delta. The sediment is subsequently distributed throughout the delta by tidal and wave-generated currents through inlet sediment bypassing. While some of the sediment is reintroduced into the longshore sediment transport system primarily by wave processes along the terminal lobe, much of the sand is reworked and redeposited in the delta itself by a combination of tidal and wave-generated currents acting on the ebb-tidal delta platform.

Sediment transport patterns at the Essex River ebb-tidal delta are dominated by landward transport across the swash platform through the landward migration of swash bars, seaward transport in the main ebb channel, and a transport reversal at downdrift portions of the delta just seaward of Coffins Beach. Morphologic changes to beaches and intertidal offshore sand bodies, and the migration of the distal main ebb channel can be related to these sediment transport patterns.

TIDAL AND WAVE-GENERATED CURRENTS

Inlet Sediment Bypassing

Inlet sediment bypassing at the Essex River ebb-tidal delta follows the model as proposed by Bruun and Gerritsen (1959) and Hine (1975), and refined by FitzGerald (1984). In this model, inlet sediment bypassing at stable inlets occurs through tidal and wave processes which transport sediment from the updrift to the downdrift side of the delta. The input of sediment into the updrift marginal flood channel comes from longshore sediment transport. Tidal and wave-generated currents carry sand through the marginal flood channel and across the channel margin linear bar into the main ebb channel. Net seaward currents of the ebb-

dominated inlet transport sediment seaward to the terminal lobe through sandwave migration. Wave activity then moves the sediment back onshore. At high tide, wave activity is concentrated on the swash bars resulting in their landward migration across the swash platform. At low tide, wave activity is concentrated along the terminal lobe and therefore sediment is transported around the periphery of the delta along the terminal lobe to adjacent beaches. Thus, sediment is both reintroduced into the delta at downdrift portions and is returned into the longshore sediment transport system.

Swash Processes

Landward migration of intertidal swash bars at Essex has been documented for both downdrift and updrift portions of the delta over a 14 month period (May, 1989-August, 1990) by measuring the landward movement of the swash bar slipfaces (Figure 50). During this period, the updrift swash bar (stake 4) migrated onshore 77 m while the downdrift swash bar (stake 7) migrated 117 m (Table 10, Figure 51). The rate of onshore swash bar migration is dependent upon tidal range, wave energy and height of the bar with respect to MLW (FitzGerald, 1984). An aerial view of this downdrift swash bar slipface as well as the two phases of landward migrating swash bars are shown in Figure 52.

Smaller swash bars tend to be ephemeral features which constantly migrate landward and coalesce with larger swash bar complexes. This is demonstrated by the rapid migration (6.6 m/week) and coalescing of an updrift swash bar (stake 12) to a larger updrift swash bar (stake 4).

Current velocity measurements of swash processes at four stations showed the combined effects of wave activity and tidal currents over the swash bars. Velocity-time series (Figure 53) and the summary of hydrographic data (Table 11) indicate that three of the four stations were flood-dominant both in terms of velocity and duration. This net onshore component of currents is explained as a result of waves breaking on or near the swash bars which create bores of water thus retarding ebb currents but enhancing flood currents (cf. FitzGerald, 1982). Thus, the

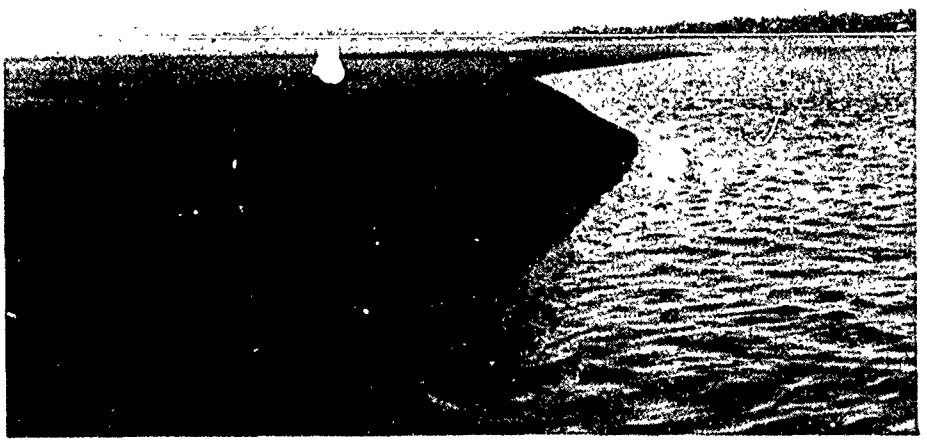

Figure 50. Slipface of downdrift swash bar exposed at low tide of 0.52 m below mean low water. Height of slipface is approximately 1.00 m. Pen on left side of photograph for scale.

LOCATION	DATE OF MEASUREMENT	CUMULATIVE DISTANCE FROM STAKE TO SLIPFACE (m)	CHANGE IN STAKE TO SLIPFACE DISTANCE FROM PREVIOUS MEASURMENT (m)
UPDRIFT			
STAKE 4	29 May 1989	0.0	----
	22 June 1989	6.5	6.5
	19 July 1989	12.3	5.8
	28 April1990	72.0	59.7
	04 May 1990	79.0	7.0
	28 May 1990	103.6	24.6
	24 June 1990	107.0	3.4
	22 July 1990	109.0	2.0
	10 Aug 1990	109.0	0.0
STAKE 11	09 Mar 1990	0.0	----
	27 April 1990	8.4	8.4
	04 May 1990	15.4	7.0
	28 May 1990	40.0	24.6
	24 June 1990	43.4	3.4
	22 July 1990	45.4	2.0
	10 Aug 1990	45.4	0.00
STAKE 12	27 April 1990	0.0	----
	04 May 1990	6.6	6.6
	28 May 1990	*	—
DOWNDRIFT			
STAKE 7	19 June1989	0.0	----
	29 June 1989	0.0	0.0
	07 July 1989	1.1	1.1
	19 July 1989	1.1	0.0
	09 March 1990	55.1	54.0
	24 April 1990	59.5	4.4
	04 May 1990	63.5	4.0
	24 June 1990	65.7	2.2
	22 July 1990	66.9	1.2
	10 Aug 1990	71.5	4.6
STAKE 8	09 Mar 1990	0.0	----
	24 April 1990	4.4	4.4
	04 May 1990	8.4	4.0
	24 June 1990	10.6	2.2
	22 July 1990	11.8	1.2
	10 Aug. 1990	16.4	4.6
STAKE 14	27 April 1990	0.0	----
	04 May 1990	0.0	0.0
	25 May 1990	4.1	4.1
	24 June 1990	14.1	10.0
	22 July 1990	14.1	0.0
	10 Aug. 1990	16.6	2.5
	21 Aug 1990	16.6	0.0
STAKE 13	23 April 1990	0.0	----
	28 May 1990	23.3	23.3

Table 10. Migration of updrift (stakes 4, 11, 12) and downdrift (stakes 7, 8, 14, 13) swash bars as determined by measuring changes in distance between permanent stake and slipface. Positive values of stake migration represent landward migration of swash bar. Asterisk indicates landward migration and coalescing of bar to landward bar.

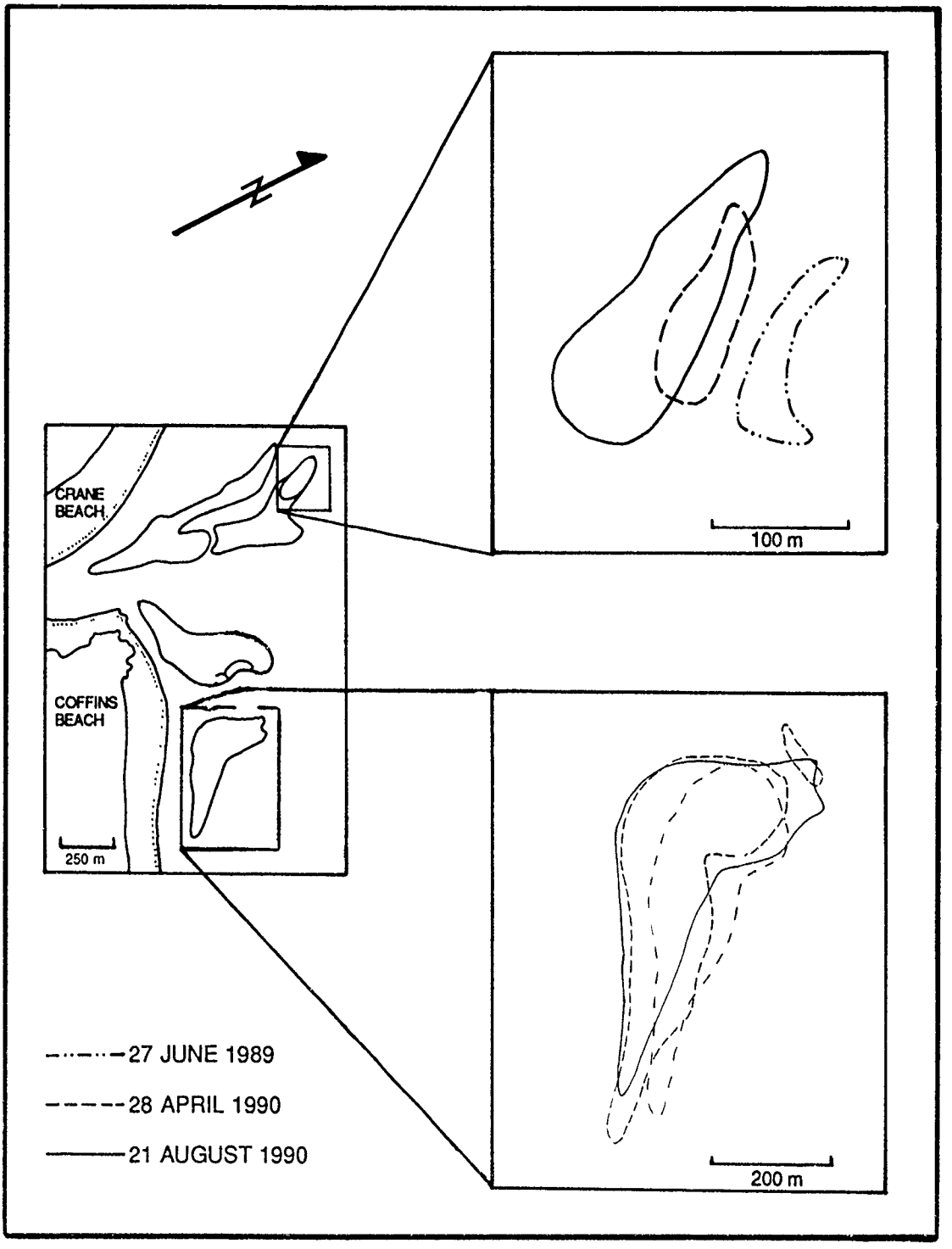

Figure 51. Landward migration of downdrift and updrift swash complexes (stakes 7 and 4, respectively) as determined from mapping on three different dates.

Figure 52. Oblique aerial photograph taken at low tide showing landward migration of the downdrift swash bar. Note particularly the landward slipface as is also shown in Figure 50. Regard 'A' on photograph.

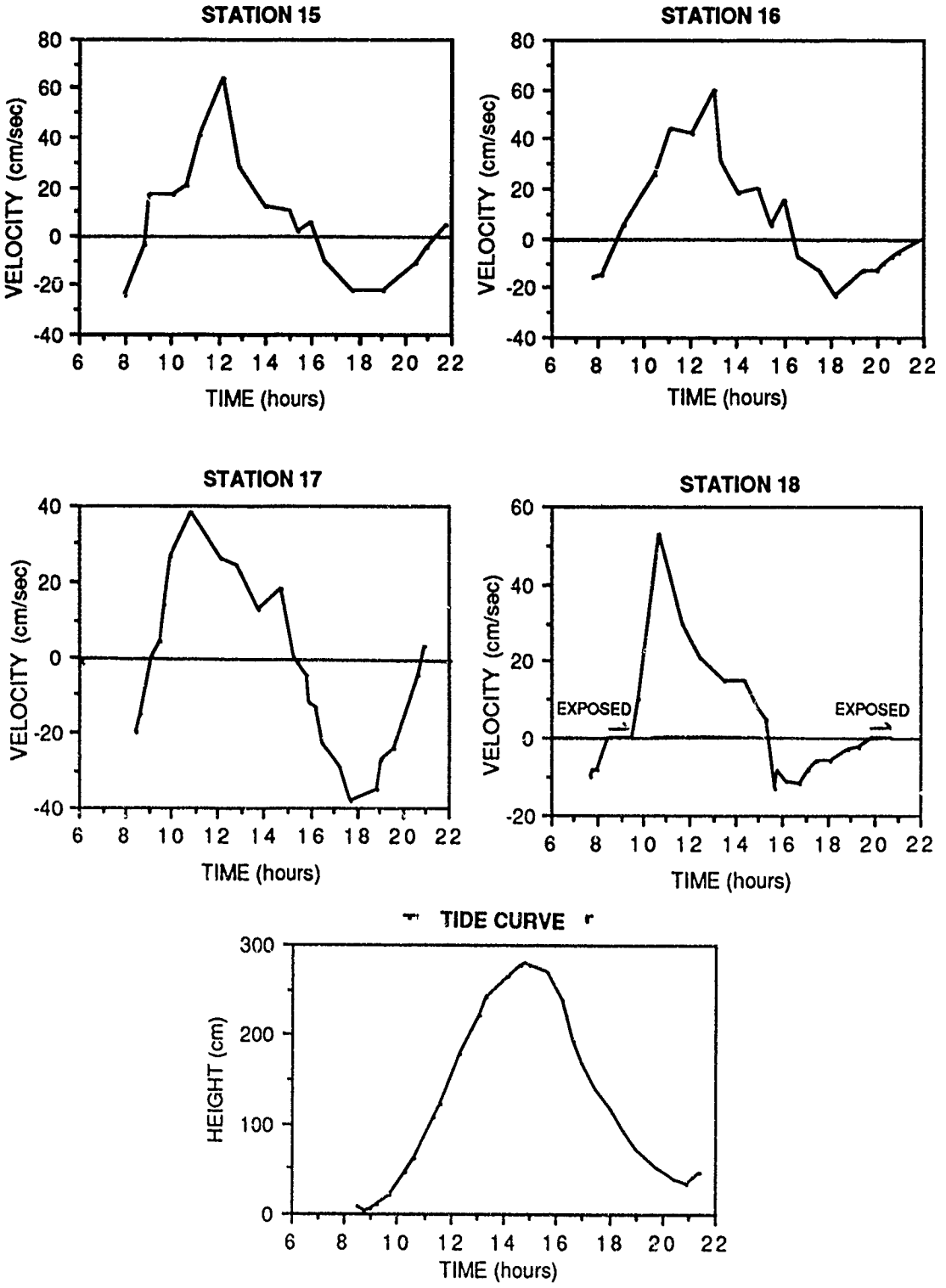

Figure 53. Velocity-time series and tide curve for stations 15-18 associated with the swash process study. Hydrography performed on 12 June 1990. Regard Figure 19 for location of stations.

Station	Date	Tidal Cycle	Tidal Range	Duration (hr:min)	Maximum Velocity (cm/sec)
15	12 June 1990	Flood	277	7:20	64
		Ebb	246	5:05	22
16	12 June 1990	Flood	277	7:15	60
		Ebb	246	5:48	23
17	12 June 1990	Flood	277	6:07	38
		Ebb	246	5:28	38
18	12 June 1990	Flood	277	6:10	53
		Ebb	246	4:24	13

Table 11. Summary of hydrographic data for stations associated with the swash process study (stations 15-18).

swash platform environments experience a net landward transport of sediment resulting in bar migration onshore (cf. Hine, 1975).

Station 17 (Figure 53), which is located on a swash bar that had previously coalesced to the distal downdrift channel margin linear bar, is neither flood nor ebb-dominant due to its proximity to the main ebb channel. In this case the landward-oriented swash processes are offset by ebb currents associated with the slight downdrift offset configuration of the main ebb channel.

Maximum flood current velocities for all stations occur at or just before mid-tide shortly after the bar is covered when waves break directly on the bar. Maximum ebb current velocities occur at mid tide for all stations, except station 18, and therefore have a maximum ebb current velocity earlier in the tidal cycle than that of the typical main ebb channel tidal current time-velocity curve (Figure 48'A')(Hayes, 1977). The maximum ebb current velocity for station 18 occurs earlier in the tidal cycle and is representative of a typical marginal flood channel curve as reported in the liturature by Hayes (1977).

Longshore Sediment Transport Processes

Numerous studies have documented a longshore sediment transport reversal at downdrift portions of the ebb-tidal delta (Hubbard, 1975; FitzGerald, 1976; Finely, 1978; FitzGerald, 1982 and Sha, 1989). Although not conclusive, data collected during three hydrographies (Figures 54-56, Table 12) suggest the presence of a transport reversal in the downdrift portion of the Essex River ebb-tidal delta.

Updrift stations 8 and 9 (updrift of the marginal flood channel proper) are both flood-dominated. This confirms the general longshore current direction to the southeast. Downdrift stations 11-14 show a decrease of channel flood-dominance from the northwest (station 11) to the southeast (station 14). This is demonstrated particularly well by the time-velocity series curves in Figures 54 and 56. The only station which can be considered truly ebb-dominant both in terms maximum velocity and duration is station 14. Thus, the current measurements indicate a

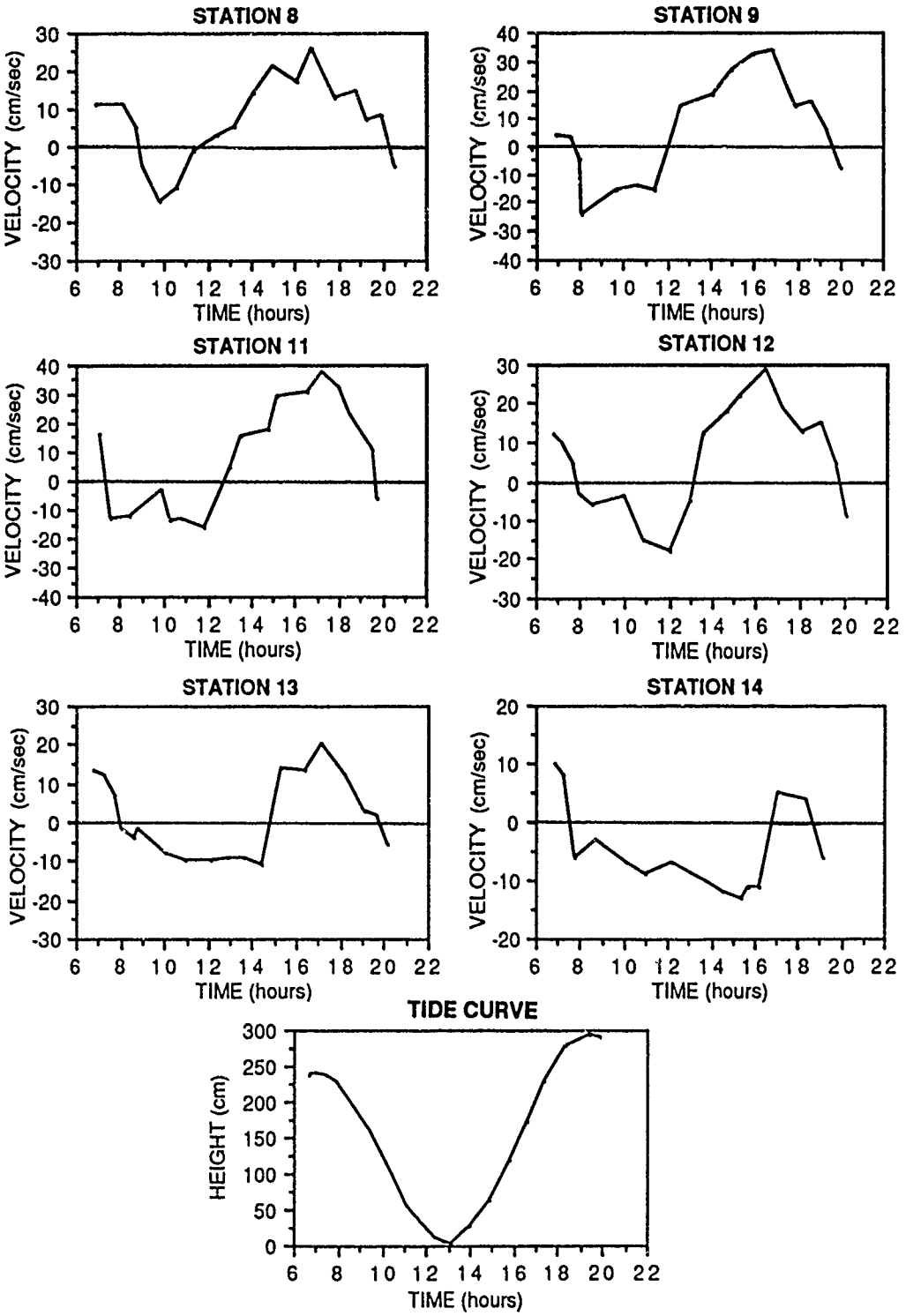

Figure 54. Velocity-time series and tide curve for stations 8-9, 11-14. Hydrography performed on 17 July 1990 to determine longshore currents and the presence of a downdrift transport reversal. Figure 19 shows the location of stations.

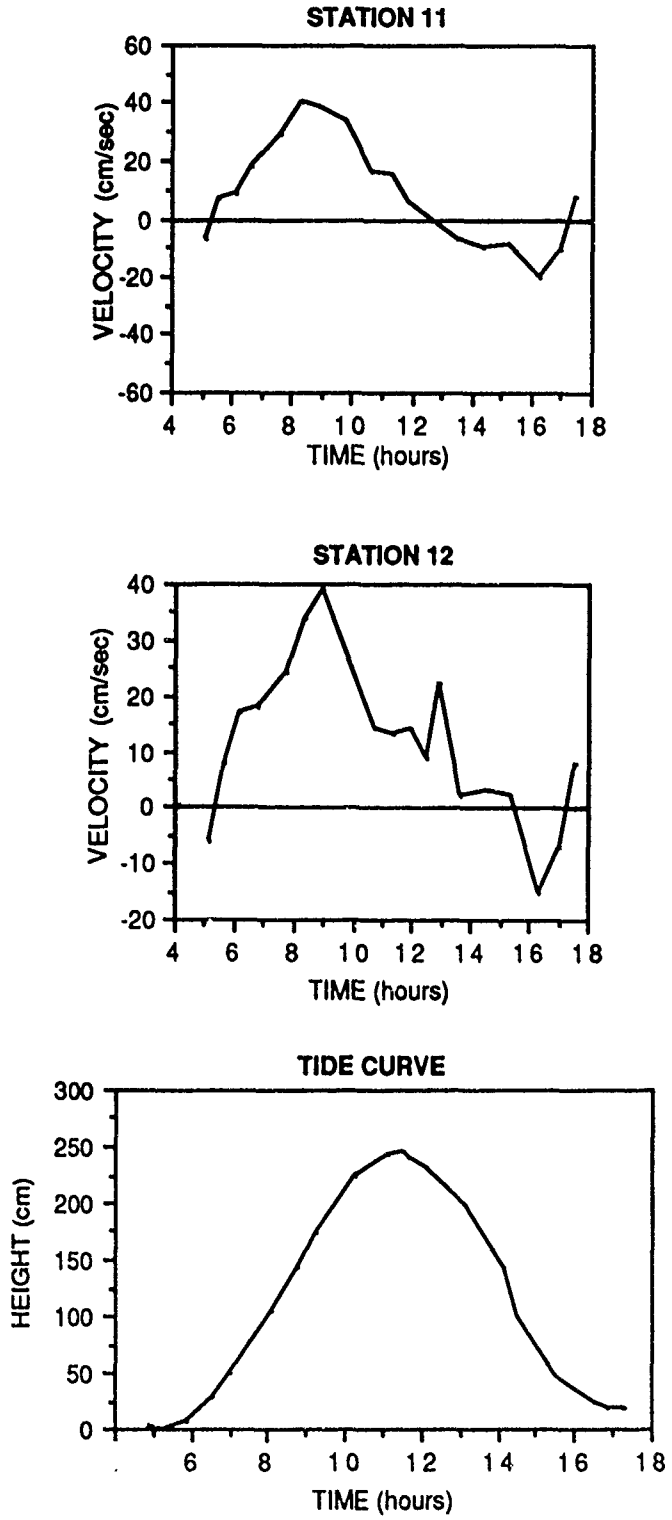

Figure 55. Velocity-time series and tide curve of stations located in downdrift marginal flood channel. Hydrography performed on 5 August 1990 to determine the presence of a downdrift transport reversal.

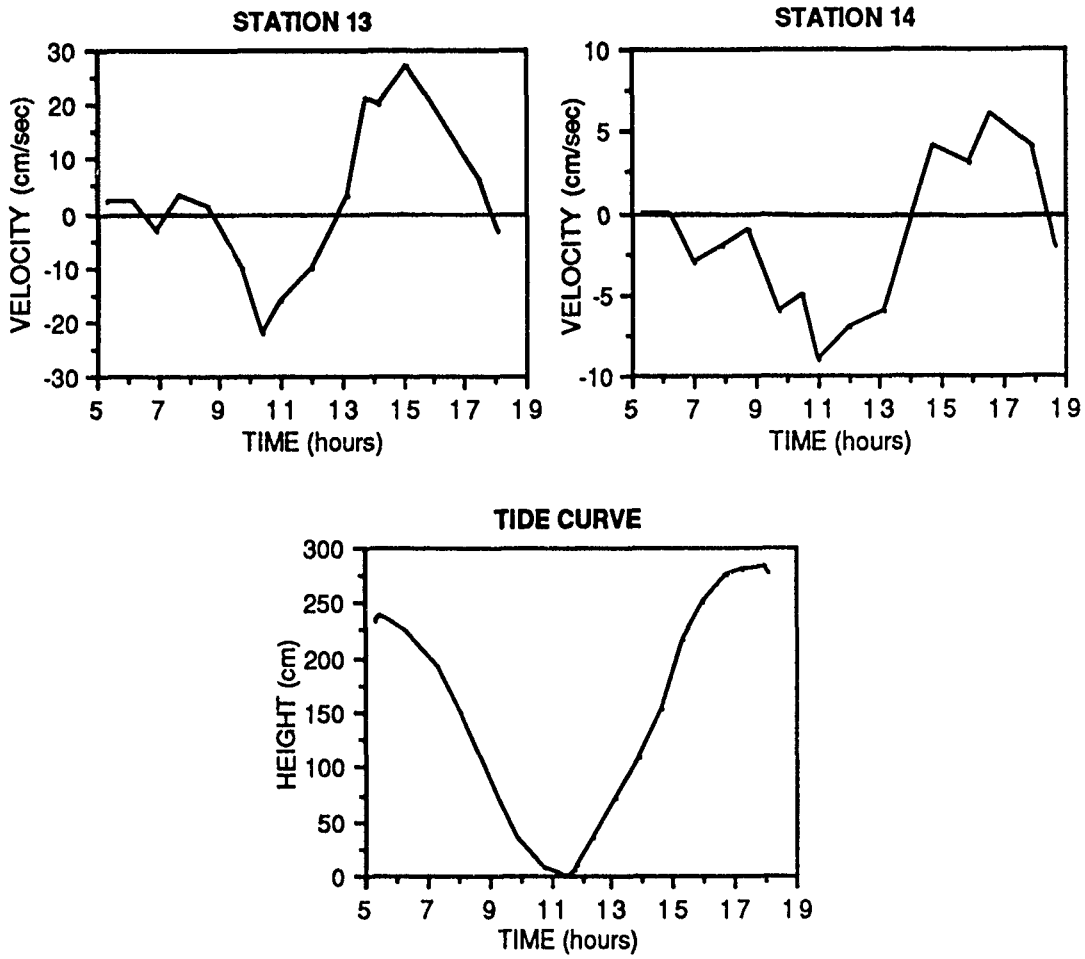

Figure 56. Velocity-time series and tide curve for stations 13 and 14 of downdrift marginal flood channel. Hydrography performed on 12 September 1990 to determine the presence of a downdrift transport reversal.

Station	Date	Tidal Cycle	Tidal Range	Duration (hr:min)	Maximum Velocity (cm/sec)	Mean Velocity (cm/sec)
8	17 July 1990	Flood	292	8:55	26	12
		Ebb	239	2:30	12	6
9	17 July 1990	Flood	292	7:50	34	19
		Ebb	239	4:15	24	15
11	17 July 1990	Flood	292	7:11	38	23
		Ebb	239	5:45	16	10
	05 Aug 1990	Flood	249	7:17	40	21
		Ebb	229	5:07	20	10
12	17 July 1990	Flood	292	7:04	29	17
		Ebb	239	5:32	18	9
	05 Aug. 1990	Flood	249	10:20	39	16
		Ebb	229	2:16	15	9
13	17 July 1990	Flood	292	5:20	20	11
		Ebb	239	7:08	11	8
	12 Sept. 1990	Flood	282	6:45	27	11
		Ebb	238	5:05	22	10
14	17 July 1990	Flood	292	2:37	10	4
		Ebb	239	9:35	13	8
	12 Sept. 1990	Flood	282	4:35	6	4
		Ebb	238	7:50	9	5

Table 12. Summary of hydrographic data for stations associated with longshore current measurement/transport reversal hydrographies.

longshore sediment transport reversal at some point between stations 13 and 14.

Wave directions and orthogonals as determined from analysis of oblique aerial photographs also give evidence for the presence of a longshore sediment transport reversal (Figure 57). Note the divergence of orthogonals at the downdrift extent of the delta due to wave refraction around the large downdrift swash bar (cf. Hine, 1975; cf. FitzGerald, 1984). Orthogonals updrift of this location bend towards the main ebb channel while downdrift orthogonals are directed to the southeast, away from the delta. When the downdrift swash bar is close to shore or has attached to Coffins Beach, orthogonals do not separate and sediment is transported away from the delta to the more southern portions of Coffins Beach.

A generalized sediment transport map utilizing residual current velocities from hydrographies, slip face orientations and wave swash process study velocities is shown in Figure 58.

MORPHOLOGIC CHANGES TO BEACHES AND INTERTIDAL SAND BODIES

Beaches

Morphological characteristics and sediment erosion/accretion trends for Crane and Coffins Beaches have been determined over the period June, 1989-August 1990 through the analysis of beach profiles. A flattening of the beaches occurs in a southeast direction for both Crane and Coffins Beaches. This trend at Crane Beach is due to the effects of greater sediment input from spit accretion at profiles 1A, 1 and 2 of the southeast portion of Crane Beach and greater wave activity at the northwest portions due to protection from wave activity of the southeast portions by the updrift channel margin linear bar.

The flattening of Coffins Beach to the southeast occurs for two reasons. First, there is a greater supply of sediment to the southeast portion due to the landward migration and welding of large swash bars and the movement of sediment back towards the inlet by refracted waves.

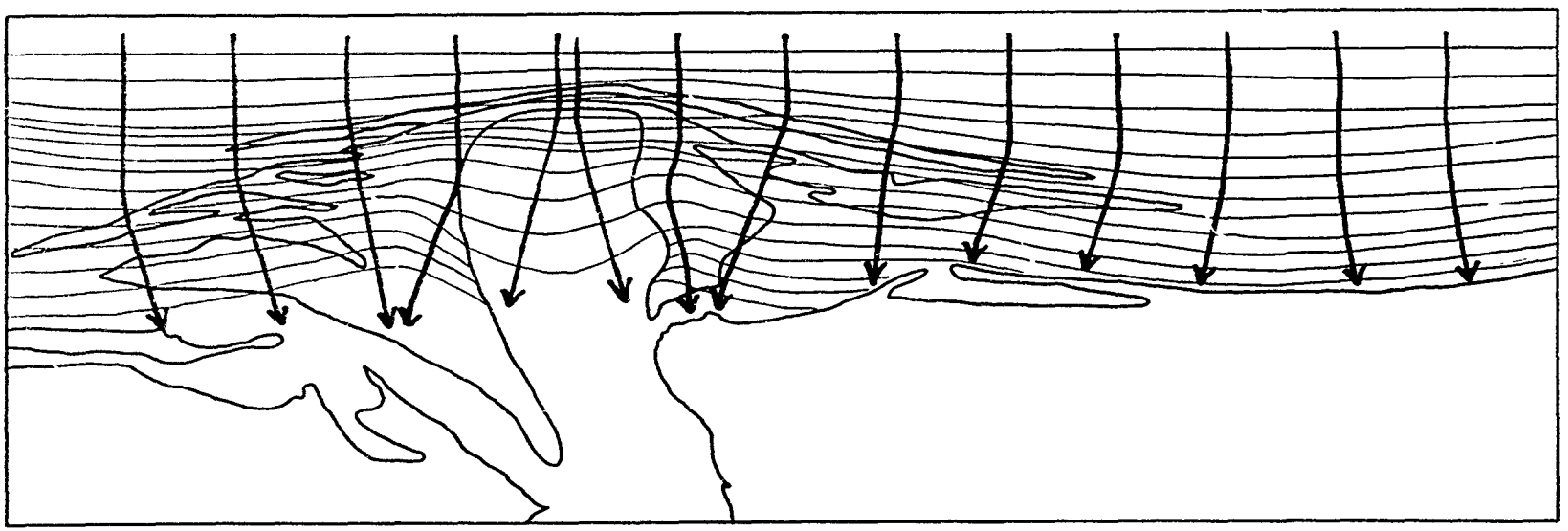

Figure 57. Wave refraction diagram of the ebb-tidal delta. Note the refraction of waves particularly at downdrift portions as they reach the ebb-tidal delta.

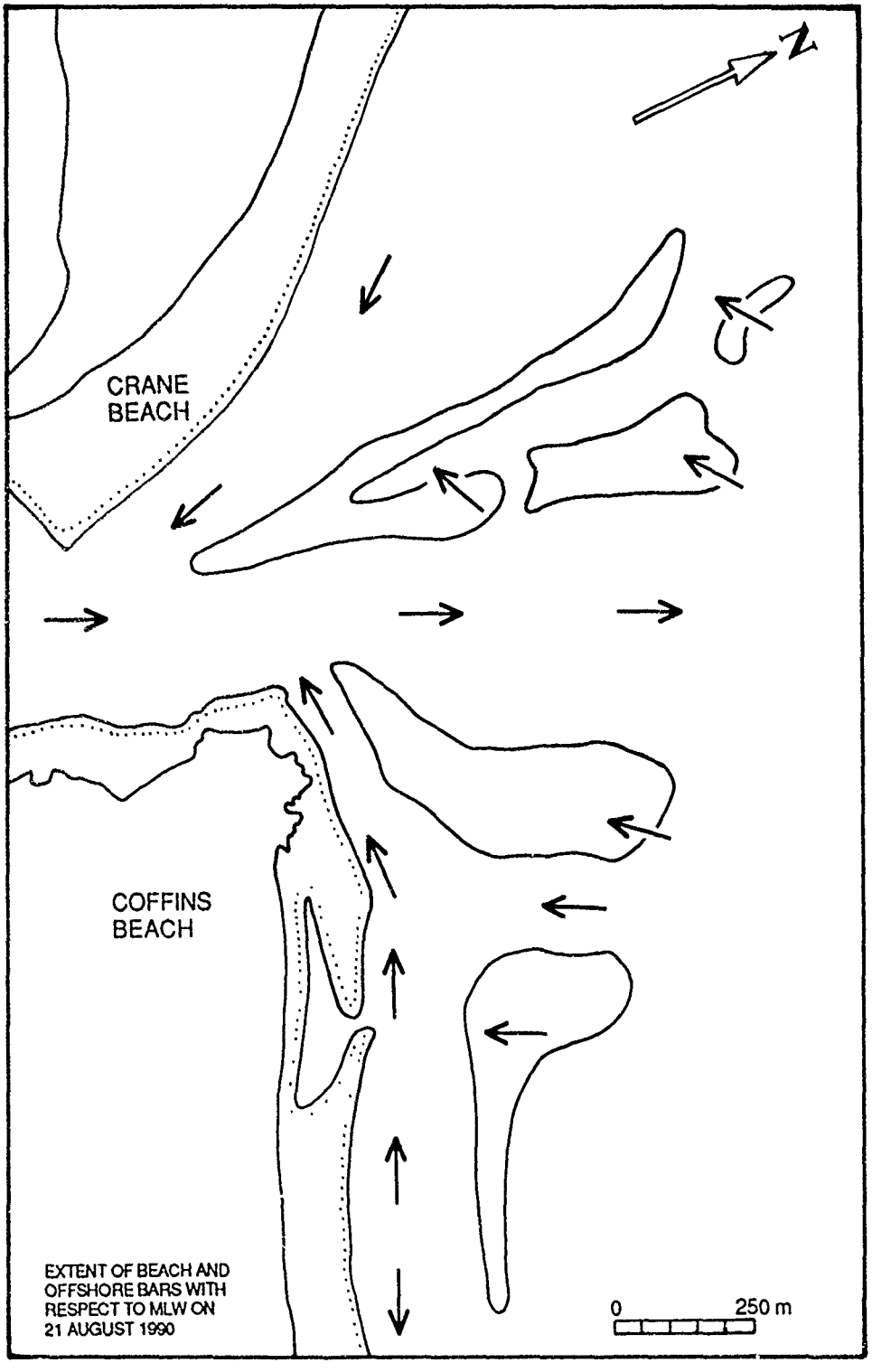

Figure 58. Sediment transport directions as determined from residual current measurements from hydrographies, swash bar slipface orientation and the wave swash process study.

Second, the northwest portion of Coffins Beach is eroded by the flood currents of the downdrift marginal flood channel, thus steepening the beachface.

The net sediment volume loss for Crane and Coffins Beaches during the entire field investigation period was 188 m^3/m and 37 m^3/m, respectively (Table 13). This loss of sediment during the winter of 1989-1990 exposed bedrock along the low tide terrace of the Coffins Beach near to profile 9. In addition, a total of eight out of thirteen profiles incurred a net sediment depletion.

Beach volume changes can be broken down into three periods of erosion and accretion. During the first phase (June, 1989 - December, 1989), increases in sediment volume for Crane and Coffins Beaches were 128 m^3/m and 13 m^3/m, respectively. During the second phase (December, 1989 - February, 1990), Crane Beach eroded 85 m^3/m while Coffins Beach accreted slightly (10 m^3/m). This results in a net sediment loss during this period of 48 m^3/m. The third phase (February, 1990 - August, 1990) also represents a period of beach erosion. During this period, nine out of eleven profiles eroded for an average sediment loss of 153 m^3/m. Note the substantial sediment loss of 231 m^3/m on Crane Beach where five out of six profiles eroded. On Coffins Beach four out of five profiles eroded for an average sediment loss of 60 m^3/m. Thus, during the entire fifteen month study period, the average sediment loss for both Crane and Coffins Beaches was 118 m^3/m.

Further anlaysis of profile data has indicated that areas closer to the inlet have eroded while areas farther from the inlet have accreted. Southeastern Crane Beach (profiles 1-3), nearer to the inlet, experienced net erosion during the study while northwestern Crane Beach (profiles 4-7) underwent net accretion with the exception of profile 7, located furthest from the inlet (Figure 59).

Northwestern Coffins Beach (profiles 8-10), which is nearer to the inlet experienced a net erosion during the study while southeast Coffins Beach (profiles 11-12) underwent net accretion (Figure 60).

Intertidal Offshore Sand Bodies

	August (June), 1989- Nov. (Dec.), 1989	Nov. (Dec.), 1989- February, 1990	February, 1990- August, 1990	Net Change Over the Entire 15 Month Period - August (June), 1989- August, 1990
CRANE BEACH	5/8 prof.= Accretion Ave. Accretion = 128 m^3/m	6/8 prof.= Erosion Ave. Erosion = 85 m^3/m	5/6 prof. = Erosion Ave. Erosion = 231 m^3/m	5/8 prof. = Erosion Ave. Erosion = 188 m^3/m
COFFINS BEACH	2/5 prof. = Accretion Ave. Accretion = 13 m^3/m	3/5 prof. = Accretion Ave. Accretion = 10 m^3/m	4/5 prof. = Erosion Ave. Erosion = 60 m^3/m	3/5 = Erosion Ave Erosion = 37 m^3/m
TOTAL	8/13 prof. = Accretion Ave. Accretion = 83 m^3/m	8/13 prof. = Erosion Ave. Erosion = 48 m^3/m	9/11 prof. = Erosion Ave. Erosion = 153 m^3/m	8/13 = Erosion Ave Erosion = 118 m^3/m

Table 13 . Amount of accretion and erosion at Crane and Coffins Beaches as determined by change in volume over time. Note general sediment accretion from August (June), 1989 to November (December), 1989 and general sediment erosion in the two periods from November (December), 1989 to February, 1990 and February, 1990 to August, 1990. The last column on the right denotes net change over the entire 15 month period June, 1989-August, 1990. Months in parentheses denote that profiles on Coffins Beach were performed on a different date than profiles on Crane Beach. Average accretion/erosion represents total change in sediment volume over the time period.

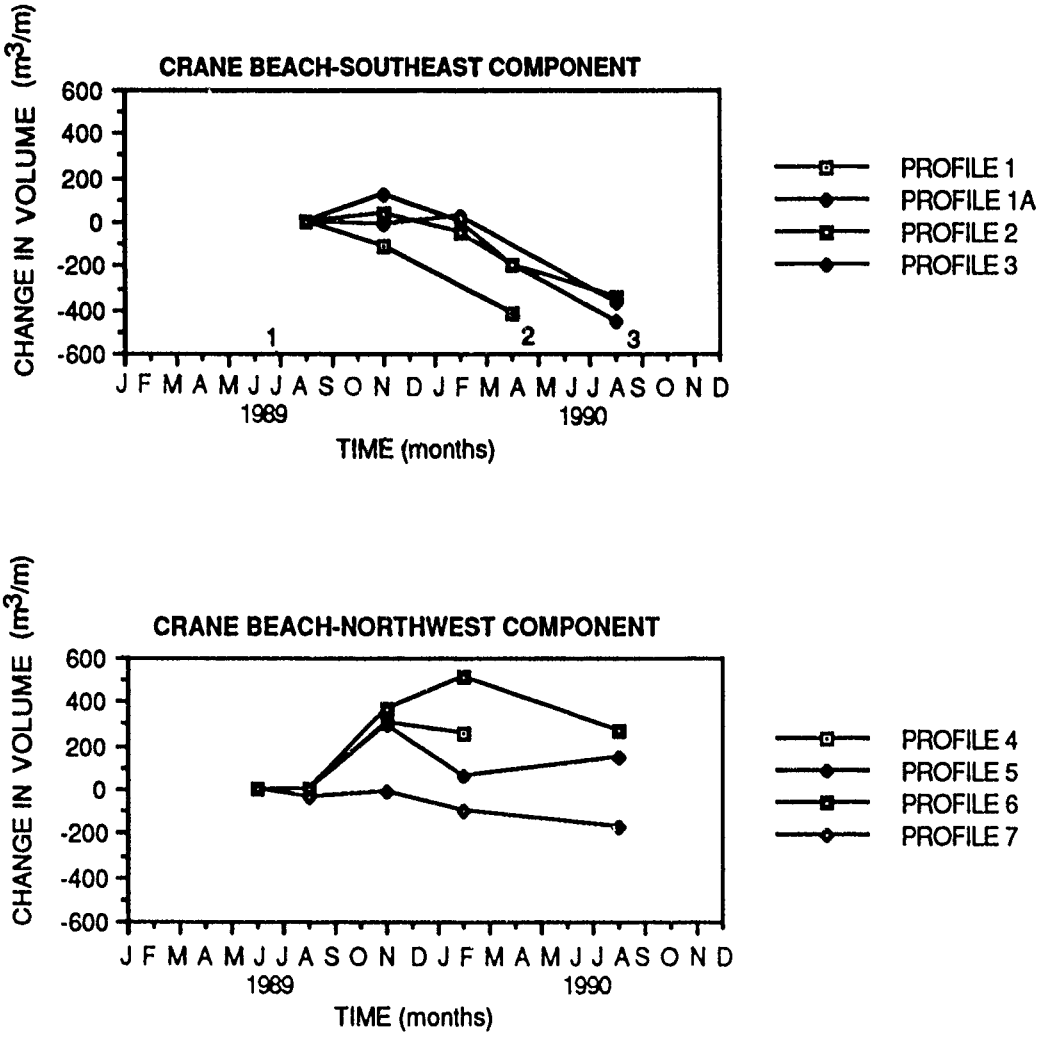

Figure 59. Changes in volume (m^3/m) over time for Crane Beach from June, 1989 to August, 1990. Datum of 0 m^3/m started in June, 1989. Two compartments have been determined. The southeast compartment (Profiles 1-4) nearer to Essex River Inlet has decreased in volume over the time period while the northwest compartment (profiles 5-7) has increased in volume over the time period (except for profile 7). Numbers above time axis on southeast compartment graph indicate dates of mapping of intertidal offshore sand bodies.

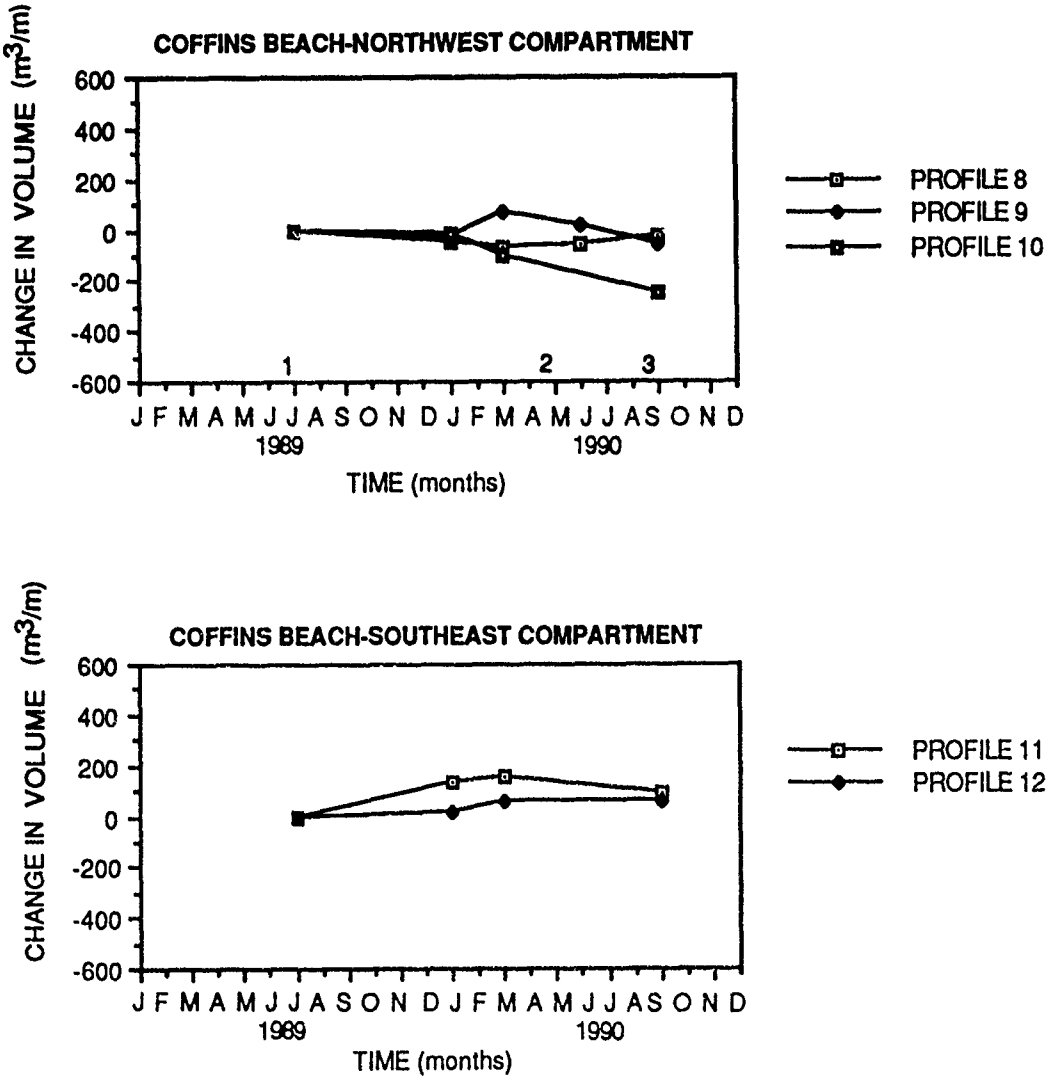

Figure 60. Changes in volume (m^3/m) over time for Coffins Beach from June, 1989 to August, 1990. Datum of 0 m^3/m started in June, 1989. Two compartments have been determined. The northwest compartment (profiles 8-10) nearer to Essex River Inlet has decreased in volume over the time period while the southeast compartment (profiles 11-12) has increased in volume over the time period. Numbers above time axis on the northwest compartment graph indicate dates of mapping of intertidal offshore sand bodies.

Significant changes to the offshore sand bodies including migrations and changes in sand body area have resulted primarily from sediment input/output and channel migration patterns (Table 14). Overall, three major trends are present including: 1) a southerly migration of both the updrift and downdrift channel margin linear bars; 2) an onshore migration of swash bars along both the updrift and downdrift portions of the ebb-tidal delta and; 3) an overall enlargement of the intertidal portions of the ebb-tidal delta complex (Figure 61).

The updrift channel margin linear bar increased in area and migrated to the south over the fourteen month period from June, 1989 to August, 1990. These changes are attributed mostly to an increase in sediment to this environment through southerly longshore currents, and interplay between wave activity and ebb-oriented tidal currents through the main ebb channel. Evidence for this increase is the connection that formed between the distal channel margin linear bar and updrift swash bar complex between 28 April, 1990 and 21 August, 1990.

This increase of sediment to the updrift channel margin linear bar is responsible for the deflection and resulting southerly migration of the distal main ebb channel as is demonstrated by aerial photographs in Figure 62. This migration of the main ebb channel and expansion of the ebb jet (as is shown by ebb-oriented bedforms on the distal downdrift channel margin linear bar-Figure 63) have resulted in the southerly migration of the entire downdrift channel margin linear bar. Distal portions of the downdrift channel margin linear bar migrated up to 100 m to the south during the study period.

The large downdrift swash bar increased in area of nearly 200 m^2 and is likely a function of sediment input associated with the migration of the downdrift channel margin linear bar. Sediment increases to this swash bar also increases sediment input to the slipface, thus resulting in the present onshore migration.

Location	Area (m^2) on 27 June 1989	Area (m^2) on 28 April 1990	Area(m^2) on 21 August 1990
Updrift Channel Margin Linear Bar	1026	1589	1815
Downdrift Channel Margin Linear Bar	1080	992	1078
Downdrift Swash Bar	609	795	807

Table 14. Change in surface area over time of updrift and downdrift channel margin linear bars and downdrift swash bar as determined by pace and Brunton mapping.

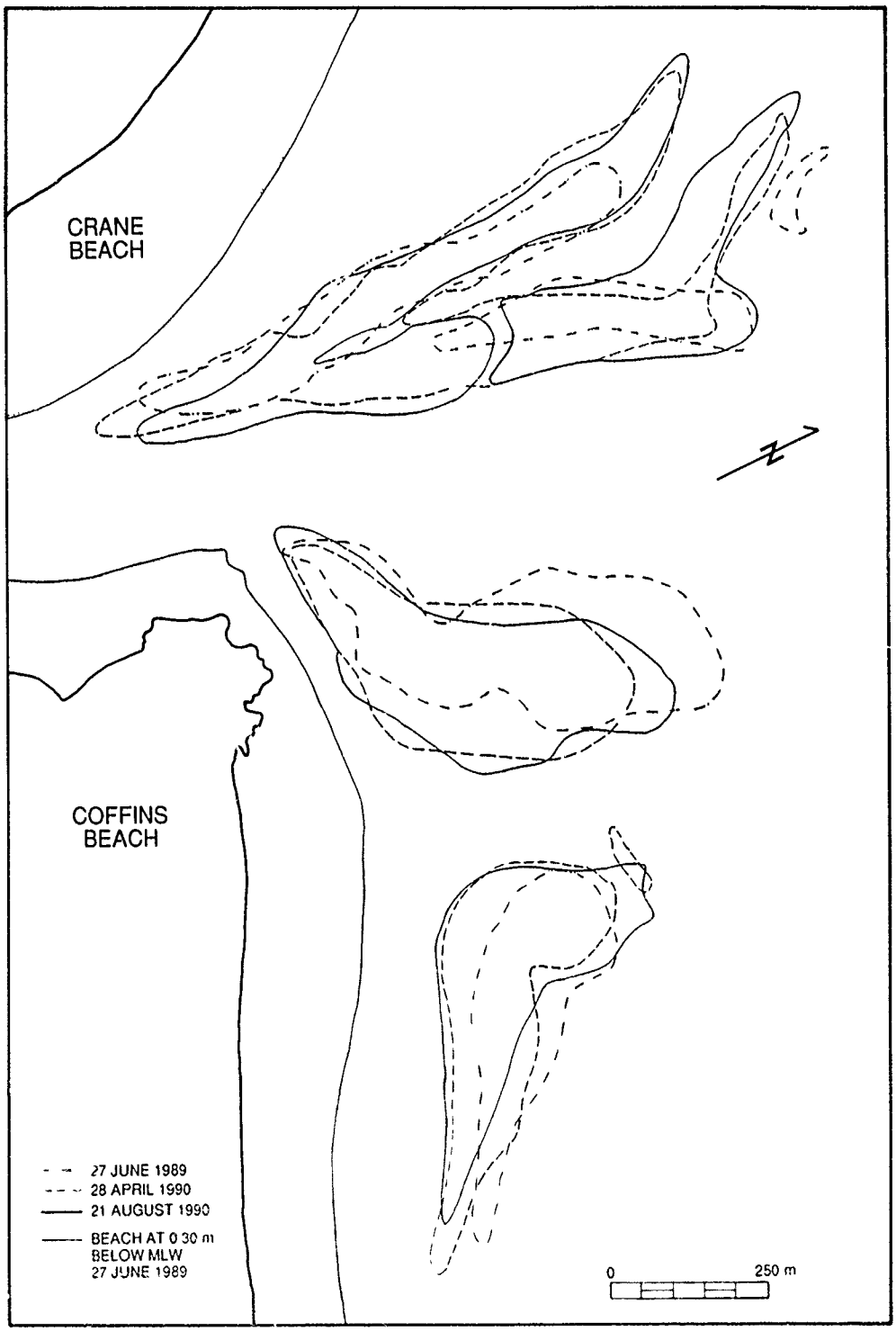

Figure 61. Location and size of sand bodies at 0.30 m (1.0') below mean low water as determined from pace and brunton mapping. Note the increase in size of channel margin linear bars during the 4 month period 28 April, 1990 - 21 August, 1990 and the landward migration of swash bars.

A

B

Figure 62. Oblique aerial photographs on (A) 27 May, 1989 and (B) 3 March, 1990. Note the migration of the outer main ebb channel to a downdrift offset position during this ten month period.

Figure 63. Ebb-oriented scour megaripples on distal portion of downdrift channel margin linear bar. Photograph taken following spring tidal range of 3.57 m. Average wavelength and height of the bedforms is 2.75 m and 0.16 m, respectively. Pen for scale.

STRATIGRAPHY

INTRODUCTION

Although numerous studies have addressed ebb-tidal delta processes and morphology, few field studies have addressed ebb-tidal delta stratigraphy with the exception of Nelligan (1983), Imperato (1988) and Sha (1990). Most studies of ebb-tidal delta stratigraphy are based mainly on surficial sedimentological processes and near surface sedimentary structures from which only hypothetical subsurface stratigraphic models are proposed (Kumar and Sanders, 1974; Moslow, 1977; Barwis and Hayes, 1978; and Hubbard, Oertel and Nummedal, 1979). Seismic reflection profiles of deltas indicate that large scale ebb-tidal delta internal stratification is dominated by large-scale gently-dipping seaward and landward-oriented cut and fill accretionary beds associated with main ebb channel migration, marginal flood channel accretion and swash bar migration (FitzGerald and Nummedal, 1977).

The detailed stratigraphy of the Essex River ebb-tidal delta has been determined for the upper 3.5 m. A stratigraphic framework for the Essex River ebb-tidal delta below 3.5 m is difficult to determine due to shallow core penetration. Only 4 cores (Core 1, 5, 14, and 19) penetrated deeper than 3.0 m and possibly through the ebb-tidal delta sediments into the underlying shoreface deposits; it is hard to distinguish between the two units due to similarities in grain size and bedding structures. This shallow depth of the cores (average depth of 2.50 m) usually only penetrated one unit of a particular facies. Therefore, it was difficult to distinguish between and correlate different units of the delta. In addition, due to a number of processes occurring at a given locality, bedding structures as preserved in cores and peels may not necessarily indicate dominance of the process at that locality. For instance, both main ebb channel and marginal flood channel tidal currents occur at the proximal ends of the channel margin linear bars. Core 11, located adjacent to the main ebb channel, is dominated by flood-oriented

bedforms while core 12, located adjacent to the marginal flood channel, is dominated by ebb-oriented bedforms.

GENERAL

STRATIGRAPHY

The thickness of the Essex River ebb-tidal delta ranges from 3-5 m at distal portions to greater than 10 m at proximal portions adjacent to the main ebb channel. The ebb-tidal delta sediments are underlain by shoreface deposits which in turn are underlain by diamict (non-compact sandy glacial till) (Rhodes, 1973). Glaciomarine deposits are absent under Crane Beach but do underlie the 15 m thick barrier island deposits of Plum Island (Rhodes, 1973).

The dominant processes which affect the overall stratigraphic framework of the Essex River ebb-tidal delta include:

1) main ebb channel migration and associated cut and fill accretionary beds. A study of historical aerial photographs (1943-1985) indicates migrations of the distal portion of the main ebb channel of up to 700 m as measured just landward of the terminal lobe;
2) abandoned marginal flood channel deposits which are a result of infilling of the marginal flood channel by fine-grained organic material and micaeous sediment from the backbarrier, and landward migrating swash bars and;
3) migration of swash bars which coalesce with distal channel margin linear bars and migrate into abandoned marginal flood channel environments.

This has also been sugested in studies of other ebb-tidal deltas by FitzGerald and Nummedal (1977) and Nelligan (1983).

NEAR SURFACE STRATIGRAPHY

Near surface depositional environments were defined primarily by surficial bedforms and associated subsurface bedding structures (cf. Harms et al., 1979). Bedform measurements and trench excavations on intertidal sand bodies at Essex River Inlet show that the near surface stratigraphy of the Essex River ebb-tidal delta is dominated by landward-oriented cross beds (Table 15)(cf. Hayes, 1980). This dominance of landward-oriented bedforms is explained by wave swash enhancing flood-tidal currents but retarding ebb-tidal currents. In addition, ebb currents through the main ebb channel are confined during lower tidal stages due to the exposure of flanking channel margin linear bars (cf. FitzGerald, 1976, 1982). However, ebb-oriented bedforms are present on the channel margin linear bars adjacent to the main ebb channel.

Bedform measurements were taken throughout the delta following both extreme tidal conditions (tidal range of 4.0 m on 28 April, 1990) and extreme wave conditions (following four days of 10-20 knot east to northeast winds associated with a storm on 25 May, 1990)(Figures 64 and 65). During extreme tidal conditions, the majority of bedforms are oriented in a seaward direction associated with main ebb channel ebb currents. During extreme wave conditions, the majority of bedforms are landward-oriented. Thus, bedform orientation and resulting sediment transport is highly dependent upon tidal versus wave influences. Figure 66 shows final sediment transport directions as determined from bedform measurements, and direction and dip of bedding in trenches.

Additional information defining near surface environments include unit thickness, grain size, structures such as graded bedding, and sedimentary deposits such as shell or coarse sediment lags and storm deposits as preserved in trenches, cores and peels. Fining-upward sequences and basal channel lags of medium-coarse sand to very fine gravel are found throughout the ebb-tidal delta. Channel lags were noted both in cores and at the inlet throat as determined from sediment sampling. These lags were found in both the main ebb and marginal

LOCATION	DATE OF MEASUREMENT	BEDFORM TYPE	AVERAGE ORIENTATION (True N)	MEAN WAVELENGTH (m)	MEAN HEIGHT (m)
SPIT PLATFORM	09 Mar. 1990	Linear ripples	N 126 W	0.11	0.02
		Ladderback ripples	S 16 E	0.04	0.01
	28 April 1990				
	-Loc. A	Cuspate megaripples	Flood	5.50	0.36
	-Loc. B	Cuspate megaripples	Ebb	3.00	0.19
	-Loc.C	Cuspate megaripples	Ebb	2.50	0.17
UPDRIFT CHAN. MARG.	02 Aug. 1989	Linear sandwaves	Flood	7.00	0.37
		Linear megaripples	Flood	5.00	0.27
LINEAR BAR	28 April 1990	Linear sandwaves	Flood	8.00	0.40
(PROXIMAL)	24 June 1990	Cuspate megaripples	Flood	4.21	0.27
(MARG FLD.	22 July 1990	Linear sandwave	Flood	7.70	0.12
CHAN SIDE)	10 Aug. 1990	Linear sandwave	Flood	7.20	0.34
UPDRIFT	02 Aug 1989	Cuspate megaripples	Ebb	4.31	0.20
CMLB	28 April 1990	Linear sandwaves	Ebb	8.00	0.40
(PROXIMAL)	24 June 1990	Cuspate megaripples	Ebb	4.56	0.32
(MAIN EBB		Ladderback ripples	N 14 E	0.05	0.02
CHAN. SIDE)	22 July 1990	Linear megaripples	Ebb	1.60	0.12
		Cuspate/ linear ripples	N 56 W	0.18	0.02
	10 Aug. 1990	Cuspate megaripples	Ebb	5.30	0.29
UPDRIFT	29 May 1989	Plane beds	—	—	—
CMLB		Linear sandwaves	S 96 E	—	—
(STAKE 5)	22 June 1989	Plane beds	—	—	—
		Linear sandwaves	S 34 E	—	—
	19 July 1989	Plane beds	—	—	—
		Linear sandwaves	S 46 E	—	—
UPDRIFT	29 May 1989	Plane beds	—	—	—
CMLB		Linear sandwaves	S 96 E	—	—
(STAKE 6)	22 June 1989	Plane beds	—	—	—
		Linear sandwaves	S 22 E	—	—
	19 July 1989	Plane beds	—	—	—
	02 Aug 1989	Plane beds	—	—	—
		Linear sandwaves	S 60 E	—	—
UPDRIFT	29 May 1989	Plane beds	—	—	—
CMLB		Linear sandwaves	S 46 E	—	—
(STAKE 3)	22 June 1989	Plane beds	—	—	—
		Linear sandwaves	S 34 E	—	—

Table 15. Bedform measurements at specific environments. See Figure 16 for noted stake locations and Figure 64 for specific locations (A,B,C) on spit platform. Wavelength and height of sandwaves in some areas could not be measured as bedform trains were not present.

LOCATION	DATE OF MEASUREMENT	BEDFORM TYPE	AVERAGE ORIENTATION	MEAN WAVELENGTH (m)	MEAN HEIGHT (m)
UPDRIFT CMLB (STAKE 3) (cont.)	19 July 1989	Plane beds	—	—	—
		Linear sandwaves	S 34 E	—	—
	02 Aug 1989	Plane beds	—	—	—
		Linear sandwaves	S 34 E	—	—
	09 Mar. 1990	Plane beds	—	—	—
		Current lineations	towards MEC	—	—
		Linear sandwaves	—	—	—
	27 April 1990	Plane beds	—	—	—
		Current lineations	NW - SE	—	—
	25 May 1990	Plane beds	—	—	—
		Current Lineations	N 05 E	—	—
		Cuspate megaripples	Ebb	2.30	0.15
	22 July 1990	Plane beds	—	—	—
		Linear sandwaves	N 76 W	10.50	0.30
	10 Aug 1990	Plane beds	—	—	—
		Linear sandwaves	N 76 W	10.00	0.30
		Cuspate megaripples	Ebb	2.00	0.13
		Linear ripples	N 80 W	0.05	0.02
		Linear ripples	N 61 W	0.10	0.03
UPDRIFT CMLB (STAKE 10)	09 Mar 1990	Linear sandwaves (washed out)	S 06 W	30.00	0.11
		Cuspate ripples	N 125 W	0.13	0.02
	27 April 1990	Linear sandwaves	N 61 W - Ebb	10.00	0.30
		Cuspate megaripples	N 40 W	4.05	0.17
		Linear Ripples	N 125 W	0.06	0.01
	25 May 1990	Cuspate megaripples	Ebb	5.60	0.21
		Linear megaripples	N 136 W	0.08	0.02
	24 June 1990	Cuspate megaripples	Ebb	1.00	0.10
		Ripples (wave-generated)	N106 W	0.06	0.01
	22 July 1990	Plane beds	—	—	—
		Current lineations	NW-SE	—	—
		Ripples (wave generated)	N 91 W	0.09	0.02
	10 August 1990	Plane beds	—	—	—
		Ripples (wave generated)	N 106 W	0.08	0.01
DOWNDRIFT CMLB (PROXIMAL)	02 Aug 1989	Cuspate megaripples	Ebb	3.40	0.18
	09 Mar 1990	Cuspate sandwaves	Ebb	27.00	0.15
		Cuspate ripples	S 16 E	0.15	0.03
	27 April 1990	Cuspate megaripples	Ebb	6.50	0.27
	25 May 1990	Cuspate megaripples	Ebb	3.75	0.23
		Linear ripples	S 26 E	0.12	0.03
	24 June 1990	Cuspate megaripples	Ebb	3.20	0.16
		Ripples (ladderback)	N 14 E	0.07	0.01
	22 July 1990	Cuspate megaripples	Ebb	2.36	0.18
		Ripples (ladderback)	N 04 E	0.05	0.01
	10 Aug 1990	Cuspate megaripples	E b b	—	—

LOCATION	DATE OF MEASUREMENT	BEDFORM TYPE	AVERAGE ORIENTATION	MEAN WAVELENGTH (m)	MEAN HEIGHT (m)
DOWNDRIFT CMLB (STAKE 1)	22 June 1989	Plane beds	—	—	—
		Linear sandwaves	S 31 E	—	—
	07 July 1989	Plane beds	—	—	—
		Linear sandwaves	S 34 E	—	—
	17 July 1989	Plane beds	—	—	—
		Linear sandwaves	S 26 E	—	—
	02 Aug. 1989	Plane beds	—	—	—
		Linear sandwaves	S 46 E	—	—
	04 May 1990	Plane beds	—	—	—
		Linear sandwaves	S 21 E	—	—
	22 July 1990	Plane beds	—	—	—
		Linear sandwaves	S 31 E	—	—
DOWNDRIFT CMLB (STAKE 2)	29 May 1989	Plane beds	—	—	—
		Linear sandwaves	S 21 E	—	—
	22 June 1989	Plane beds	—	—	—
		Linear sandwaves	—	—	—
	07 July 1989	Plane beds	—	—	—
		Linear sandwaves	—	—	—
	19 July 1989	Plane beds	—	—	—
		Linear sandwaves	—	—	—
	02 Aug. 1989	Plane beds	—	—	—
		Linear sandwaves	—	—	—
	04 May 1990	Plane beds	—	—	—
		Linear sandwaves	—	—	—
DOWNDRIFT CMLB (DISTAL)	26 May 1990	Cuspate megaripples	Ebb	2.75	0.16
		Linear ripples	S 14 W	0.06	0.01
	10 Aug 1990	Cuspate megaripples	Ebb	1.85	0.11
		Linear ripples	S14W	0.09	0.02
DOWNDRIFT CMLB DISTAL SWASH BAR (STAKE 9)	09 Mar 1990	Cuspate ripples	N 49 E	0.08	0.01
	27 April 1990	Cuspate megaripples	Ebb	2.00	0.15
	25 May 1990	Plane beds	—	—	—
		Current lineations	S 45 W	—	—
		Cuspate megaripples	Ebb	1.80	0.08
		Ripples (wave generated)	S 40 W	0.10	0.03
	24 June1990	Cuspate megaripples	Ebb	1.00	0.08
	22 July 1990	Cuspate megaripples (washed out)	Ebb	0.76	0.10
		Linear ripples	N84E	0.10	0.02
UPDRIFT SWASH (STAKE 11)	09 Mar. 1990	Plane beds	—	—	—
		Ripples (wave generated)	N 136 W	0.10	0.01
	24 April 1990	Plane bed	—	—	—
		Ripples (wave generated)	N 136 W	0.08	0.01

LOCATION	DATE OF MEASUREMENT	BEDFORM TYPE	AVERAGE ORIENTATION (True N)	MEAN WAVELENGTH (m)	MEAN HEIGHT (m)
UPDRIFT SWASH (STAKE 11) (cont.)	04 May 1990	Plane beds	—	—	—
		Ripples (wave generated)	N 136 W	0.08	0.01
	25 May 1990	Plane bed	—	—	—
		Ripples (wave generated)	N 136 W	0.07	0.01
	24 June 1990	Plane beds	—	—	—
		Ripples (wave generated)	N 66 W	0.11	0.03
	22 July 1990	Plane beds	—	—	—
		Ripples (wave generated)	N 74 E	0.09	0.01
DOWNDRIFT SWASH (STAKE 8)	09 Mar. 1990	Plane bed	—	—	—
		Ripples (wave generated)	N 141 W	0.16	0.01
	24 April 1990	Plane bed	—	—	—
		Current lineations	N123 W	—	—
		Ripples (wave generated)	N141 W	0.15	0.02
	03 May 1990	Plane beds	—	—	—
		Ripples (wave generated)	N 141 W	0.16	0.01
	25 May 1990	Plane beds	—	—	—
		Current lineations	S 50 W	—	—
		Cuspate megaripples (washed out)	S 37 W	2.55	0.11
	24 June 1990	Plane beds	—	—	—
		Ripples (wave generated)	N 36 E	0.11	0.02
		Ladderback ripples	S 06 E	0.03	0.01

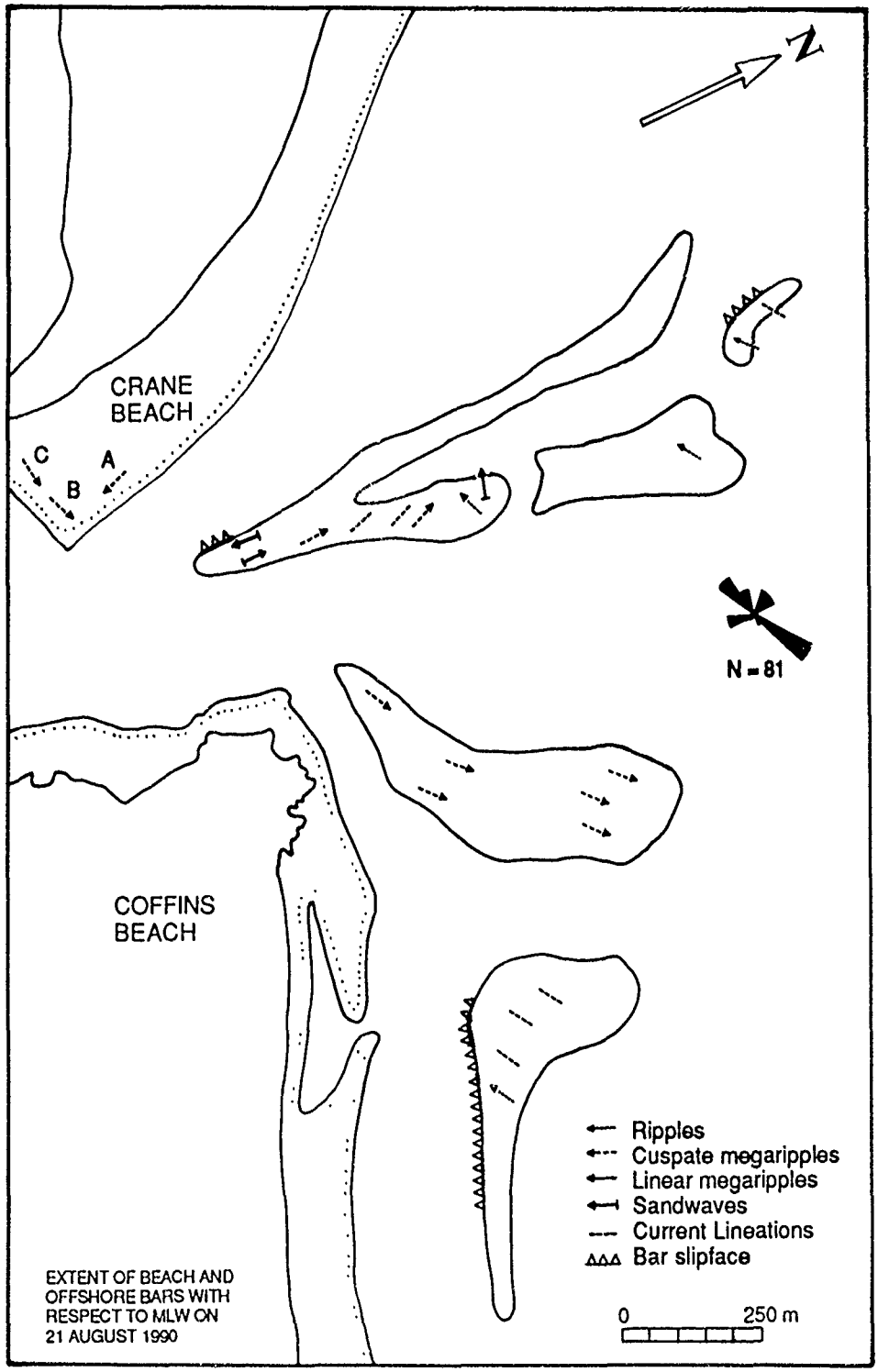

Figure 64. Bedform measurements taken at low tide on 28 April, 1990 following extreme tidal conditions (ebb tidal range of 4.0 m). Letters on spit platform note the location of bedform measurement stations as mentioned in Table 15 .

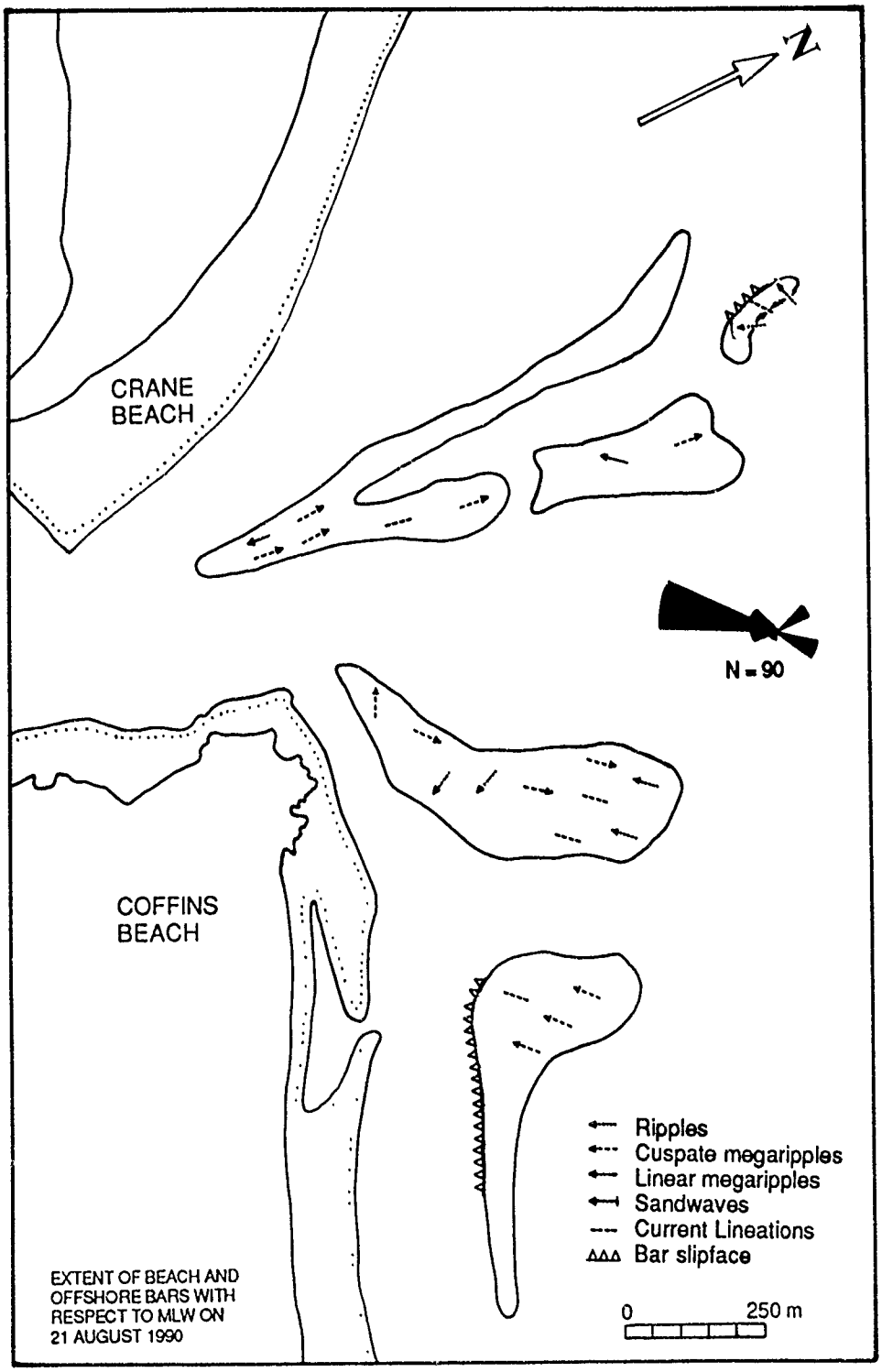

Figure 65. Bedform measurements taken at low tide on 25 May, 1990 following four days of strong northeast winds associated with a low pressure system to the south.

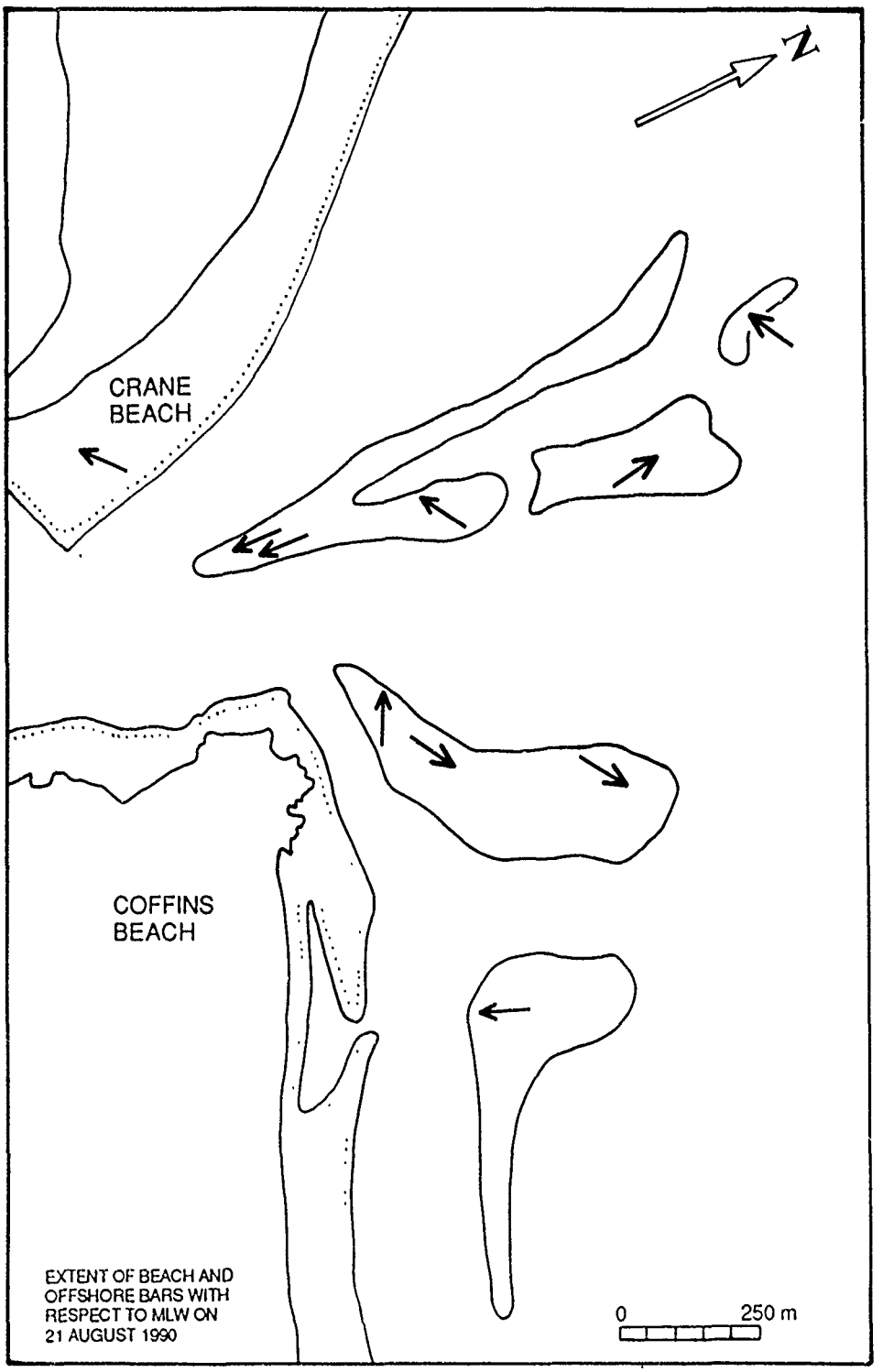

Figure 66. Direction of sediment transport as determined from bedform measurements and dip angle and direction of bedding in trenches.

flood channels at varying depths and are coarser and more frequent in the marginal flood channel environment. Storm deposits, which are signified by steeply dipping beds with fining-upward sequences, are found occasionally in cores but are similar to fining-upward sequences in channels which result from decreasing tidal current velocities (cf. Sha, 1989).

These parameters have enabled wave versus tide-dominated environments to be differentiated. Although exceptions do occur, wave-dominated environments are characterized by planar horizontal and high-angle landward-oriented unidirectional cross-bedding. Sediments tend to be fine-grained and well to very well-sorted. Tide-dominated environments are characterized by both trough and planar high-angle bidirectional cross-bedding. Sediments of the tide-dominated environments tend to be slightly coarser-grained then those of wave-dominated environments but have similar sorting characteristics.

SEDIMENTARY FACIES

Six environments of the Essex River ebb-tidal delta have been defined: 1) spit platform; 2) main ebb channel; 3) marginal flood channel; 4) swash platform channel; 5) swash bar and; 6) channel margin linear bar (Figure 67). Each environment has characteristic features which differentiate it from other environments.

1. SPIT PLATFORM

The spit platform at the southeast end of Crane Beach is dominated by ebb-oriented cuspate megaripples near the throat (locations B and C)(Table 15, Figure 64). Flood-oriented cuspate megaripples dominate the region nearer to the marginal flood channel (location A). Away from the influence of tidal currents of the inlet, a trench of a migrating

Figure 67. Sedimentary environments of the Essex River ebb-tidal delta. Numbers correspond to specific environments: 1) Spit Platform; 2) Main Ebb Channel; 3) Marginal Flood Channel; 4) Swash Platform Channel; 5) Swash Bar and; 6) Channel Margin Linear Bar.

ridge of a ridge and runnel system indicates landward transport of sand on Crane Beach (Trench 2 of Figure 68).

2. MAIN EBB CHANNEL

The large-scale framework of main ebb channel facies is dominated by cut and fill accretionary beds associated with main ebb channel migration (Figure 69). The smaller scale internal stratification of the active main ebb channel facies is dominated by bedding structures associated with bedform migration and includes deep and shallow main ebb channel deposits. The deep main ebb channel deposits are characterized by medium to coarse sand with large-scale seaward-oriented trough cross-bedding produced by ebb-oriented megaripples migrating over sandwaves. Overlying this unit are the shallow main ebb channel deposits which include fine to medium sands with smaller scale bidirectional trough and planar cross-bedding. Numerous reactivation surfaces are present in both deposits (Barwis and Hayes, 1978; Hubbard et al., 1979; and Sha, 1990).

Characteristics of the main ebb channel facies are inferred from subtidal bedforms and sedimentary structures in Cores 12, 16, 25 and 26. Figure 20 illustrates the location of cores and Appendix C shows stratigraphic columns of the cores.

Core 12 is most representative of sedimentary structures associated with the active main ebb channel facies. The majority of this 2.0 m deep core is dominated by low-angle ebb-oriented trough cross-bedding and bidirectional low-angle trough cross-bedding. Reactivation surfaces separate these units from smaller scale flood-oriented high-angle trough cross-bedding associated with tidal reversals. Note also the 0.25 m thick fining-upward sequence from coarse sand with fine pebbles at base to medium sand.

Further classification of the active main ebb channel environment is based on sedimentary structures in peels. Peel 1 of Core 12 (1.04 m-1.56

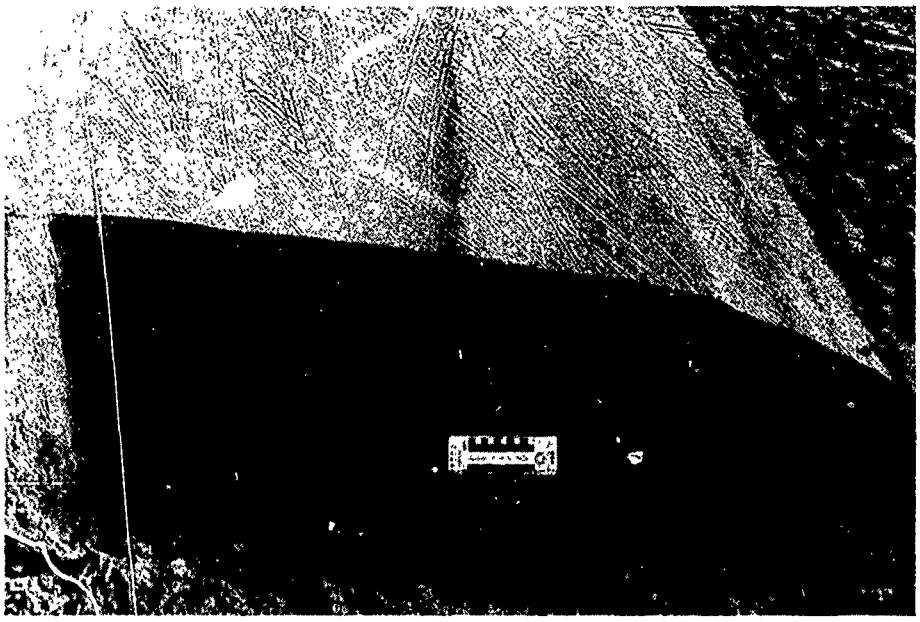

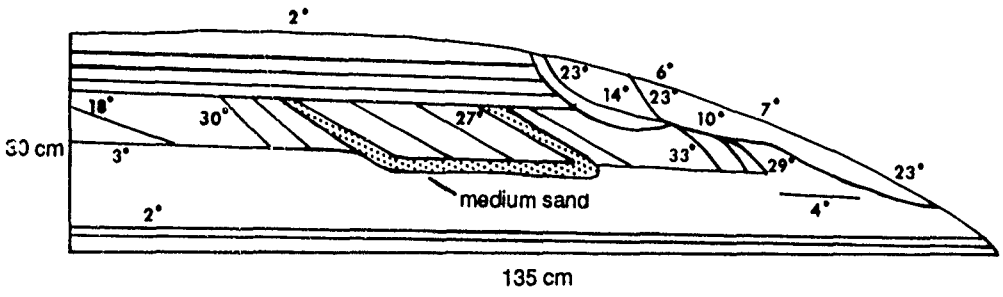

Figure 68. Trench #2 cut through a migrating ridge of a ridge and runnel system on Crane beach. Land is to the right. Note the high-angle (18^{0} - 33^{0}) landward-oriented cross-beds becoming tangential at top and truncated at bottom by nearly horizontal bedding surfaces. The bar is composed of fine sand with layer of medium sand as indicated. Figure 18 shows location of trench.

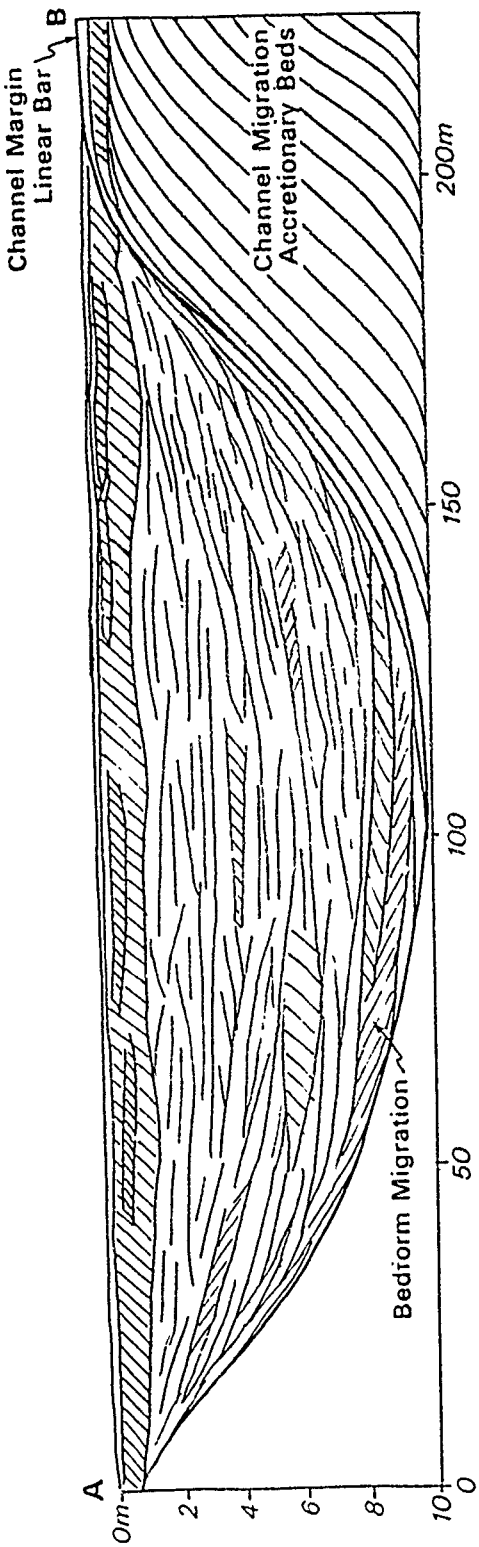

Figure 69. Cut and fill accretionary beds associated with main ebb channel migration.

m) (Figure 70) exhibits high-angle trough and planar (32°) ebb-oriented bedding (1.37 m-1.52 m) and a coarse sand unit with flood-dominated bidirectional planar cross-bedding (1.10 m-1.27 m). This unit probably represents migrating flood-oriented megaripples associated with a high-energy storm event overlying migrating ebb-oriented sandwaves in the main ebb channel. Numerous reactivation surfaces occur throughout the peel.

A facies model of the Essex River ebb-tidal delta active main ebb channel includes the following units in ascending order:

1) Basal channel lag of medium to coarse-grained sand (1 cm-3 cm thick);
2) Active main ebb channel deposits of medium-grained sand with high-angle bidirectional trough cross-bedding with dominant offshore orientation due to ebb-tidal currents. Fining-upward sequences and numerous reactivation surfaces are present. Some units of medium to coarse sand associated with high energy events are also present. Little to no shell matter is present. (2 m thick);
3) Main ebb channel fill unit of reworked channel margin linear bar and swash bar sands which have migrated into the sides of the main ebb channel (3 m thick).

3. MARGINAL FLOOD CHANNEL

Characteristics of the marginal flood channel facies have been determined from subtidal bedforms and sedimentary structures in Cores 7, 8, 11, 14 and 23. Sedimentary structures for both marginal flood channels are similar, although the downdrift marginal flood channel has a stronger ebb-tidal component.

The marginal flood channel facies can be divided into the active marginal flood channel fill and abandoned marginal flood channel fill, both of which are present in Core 8. The active marginal flood channel

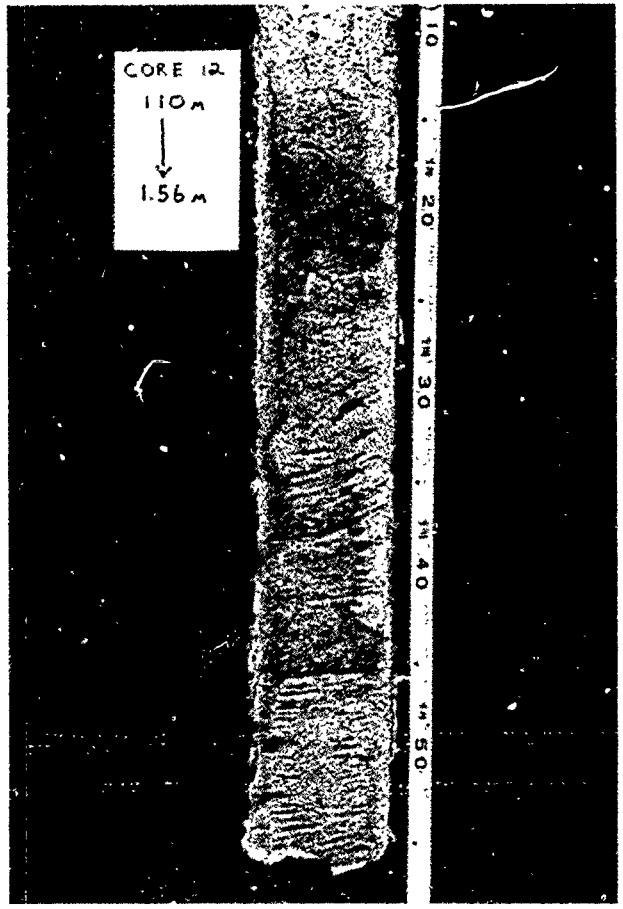

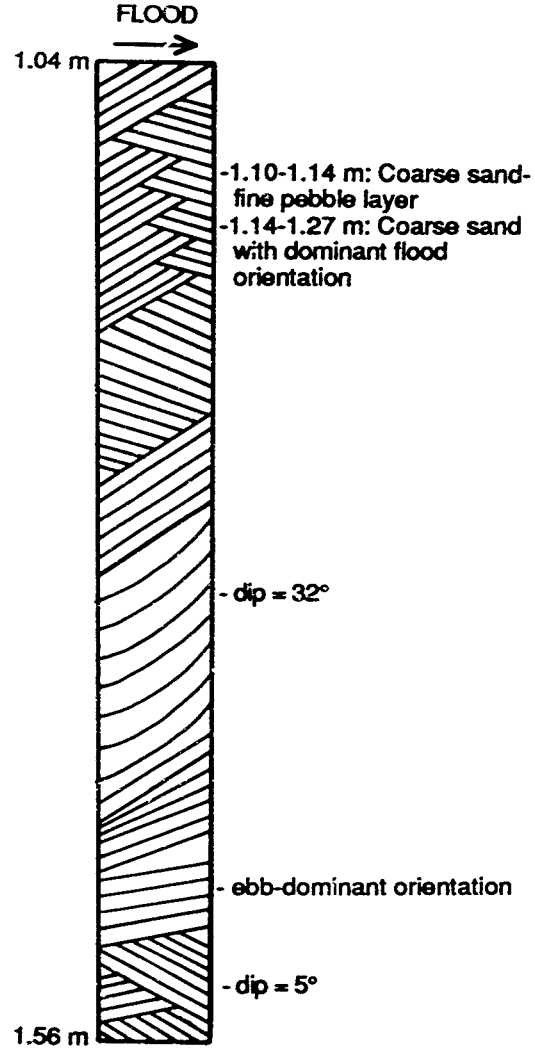

Figure 70. Peel 1 of Core 12 (1.04 m-1.56 m) showing internal stratification of the main ebb channel environment. Note the dominance of ebb-oriented high-angle trough cross-bedding and ebb-dominated low-angle bidirectional cross-bedding.

unit from 1.07-2.40 m is dominated by flood-oriented, high-angle planar cross-bedding and flood-dominated bidirectional low-angle planar cross-bedding. Layers of coarse sand, occasional fine gravel and shell matter, and two fining-upward sequences from fine-medium to coarse sand demonstrate the strong tidal currents which occur in this environment. Overlying this unit from 1.06 m to the surface is a thick structureless unit of fine sand with occasional organic wood and mica which is characteristic of the abandoned marginal flood channel unit. A coarse sand layer separates the active and abandoned marginal flood channel units signifying a high energy event.

Structures of the active marginal flood channel facies are also seen in Core 14 (1.22 m-3.65 m) which is dominated by low-angle flood-oriented planar and bidirectional cross-bedding and has a 0.50 m thick fining-upward sequence of fine to coarse sand with a layer of coarse pebbles at the base. Both cores 8 and 14 have numerous reactivation surfaces.

Peel 2 of Core 8 (1.90 m-2.25 m) (Figure 71) demonstrates the dominance of flood currents in the marginal flood channel as is indicated by high-angle flood-oriented planar cross-bedding intersperced with some trough cross-bedding. The peel is composed of fine sand with occasional layers of coarse sand from 2.11 m-2.14 m. The angles of dip of cross-beds are 4° from 1.90 m-1.94 m and 20° from 1.94 m-2.20 m. Bedding is planar except for trough from 2.10 m-2.17 m which coincides with a coarse sand layer.

Peel 3 of Core 11 (1.82 m-2.24 m)(Figure 72) also demonstrates the flood dominance of currents of the marginal flood channel. Note the dominance of high-angle flood-oriented planar and trough cross-bedding and associated numerous reactivation surfaces, and the coarse sand layer from 1.82 m-1.85 m. Some of the dip angles of the beds in this peel exceed 50° which may be partially explained by the disturbance of sediments during core penetration.

Peel 4 of Core 11 (2.50 m-2.95 m)(Figure 73) is only 25 cm deeper than Peel 3. However, this peel shows a dominant seaward-orientation of

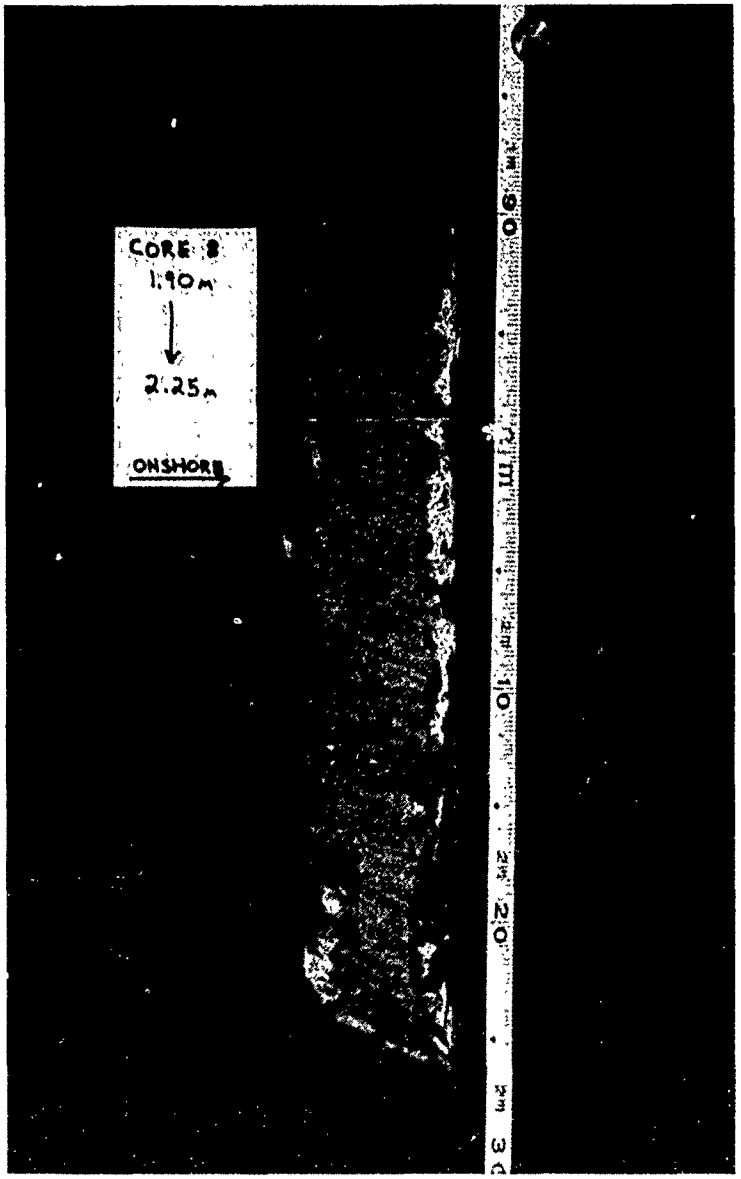

Figure 71. Peel 2 of Core 8 (1.90 m-2.25 m) showing dominant flood-oriented bedding horizons of marginal flood channel environment.

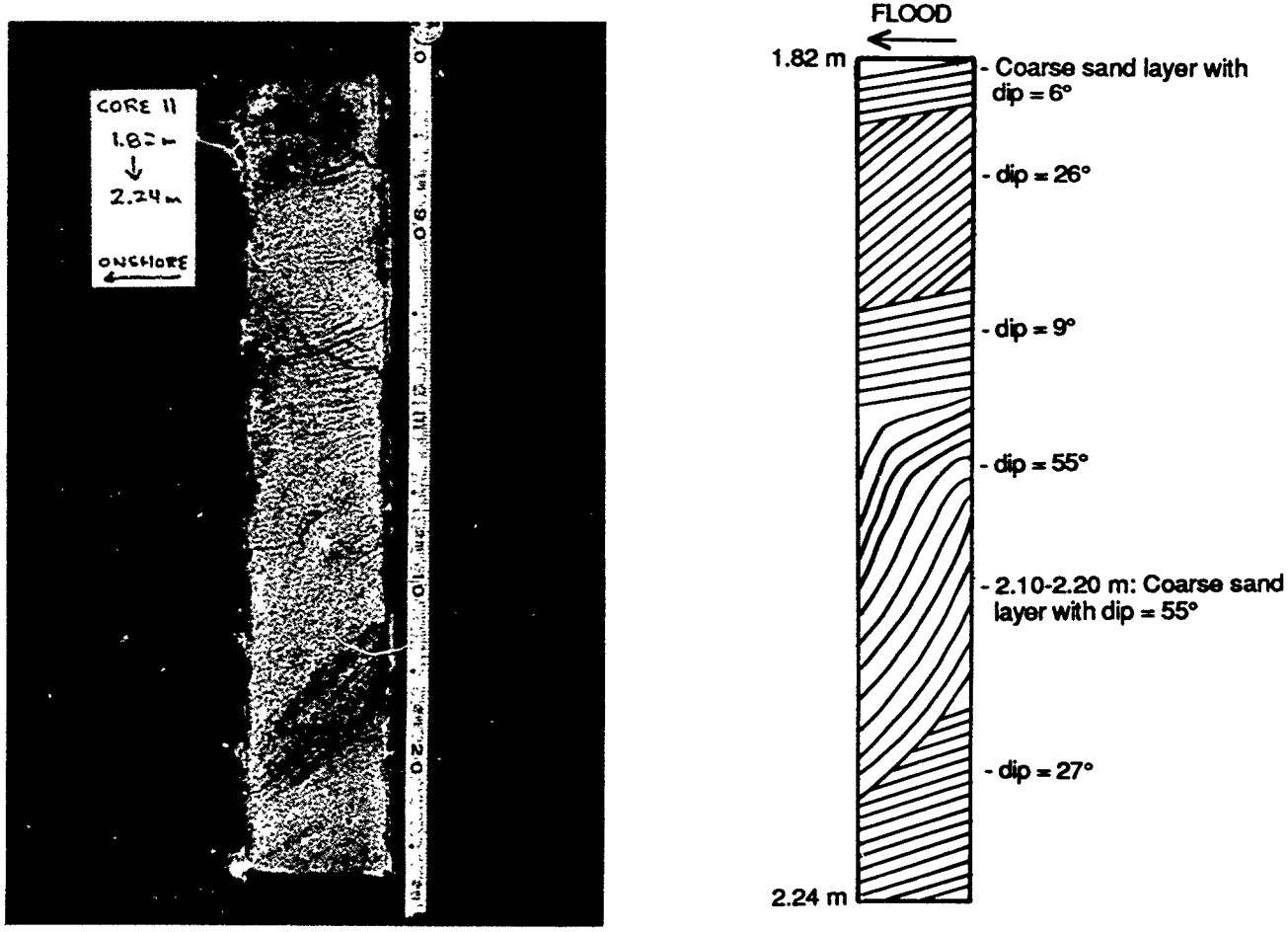

Figure 72. Peel 3 of Core 11 (1.82 m-2.24 m) demonstrating characteristic internal stratification bedding horizons of the marginal flood channel environment.

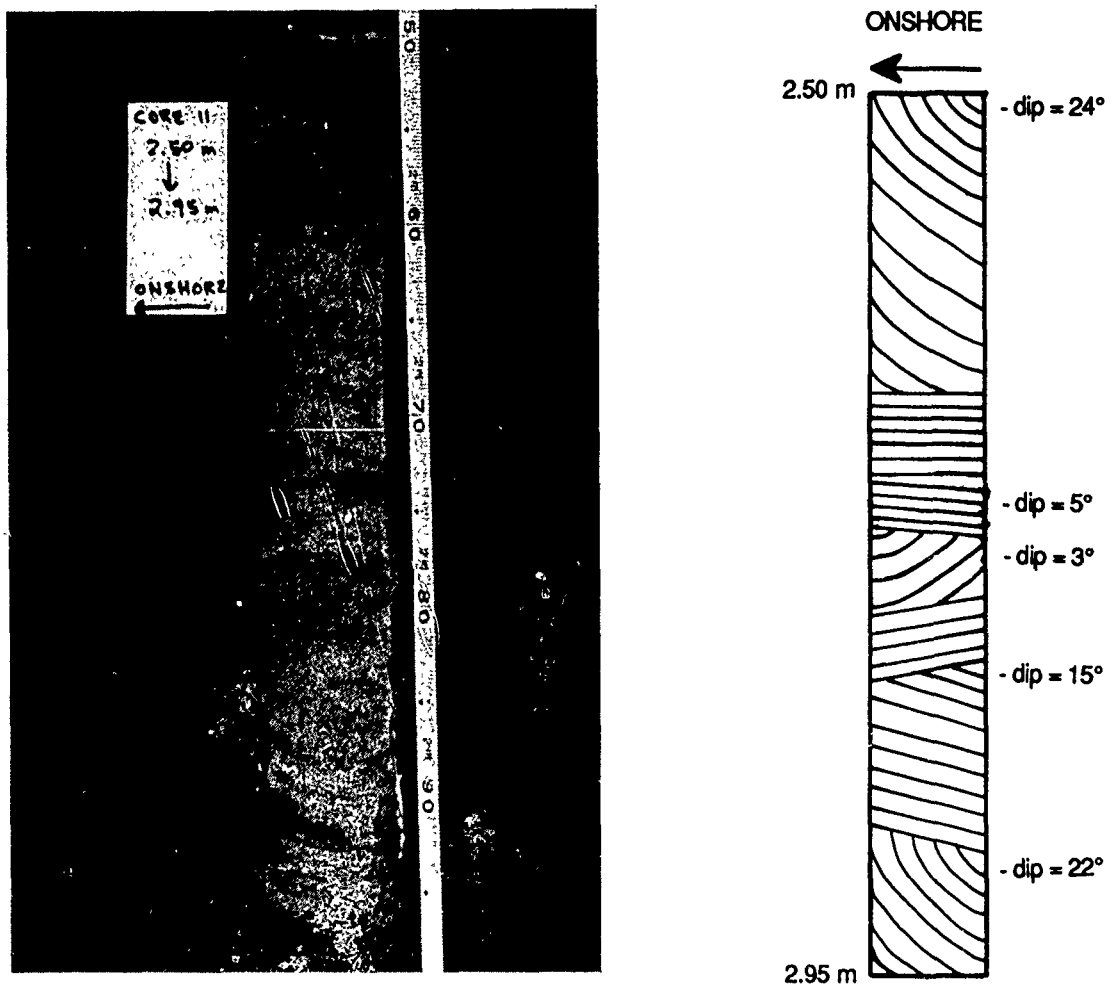

Figure 73. Peel 4 of Core 11 (2.50 m-2.95 m) with characteristic bedding horizons of the marginal flood channel environment.

cross bedding and is finer-grained than Peel 3 except for a layer of coarse sand from 2.77 m-2.79 m. Layers of mica from 2.89 m-2.92 m and overlying fine-grained low-angle ebb-oriented cross-beds from 2.82 m-2.86 m are indicative of an abandoned marginal flood channel deposit. Unconformably overlying this deposit is a unit of flood-oriented low-angle trough cross-bedding indicating active marginal flood channel deposits. Dip angles of these deposits range from 22°-24° at the top and bottom of the sequence to 3°-5° in the middle of the sequence. Although the marginal flood channel environment is dominated by flood currents, this peel indicates that this environment does have seaward-migrating bedforms during some stages of the tidal cycle.

At Essex River ebb-tidal delta, a complete marginal flood channel facies model is composed of the following units from bottom to top:

1) Shoreface deposits;
2) Basal channel lag consisting of shell matter and coarse sand to fine gravel (1 cm-3 cm);
3) Active marginal flood channel fill unit (thickness of approximately 2 m) of fine to medium sand with low-angle flood-dominated bidirectional planar and trough cross-bedding. This bidirectionality is due to migration of megaripples during dominant flood-tidal phases and subsequent modification during subordinate ebb cycles. Reactivation surfaces are common. Occasional layers of coarse sand/fine gravel in fining-upward sequences occur and are associated with high energy events. These coarse layers are coarser and more frequent than those associated with the main ebb channel. Shell matter is limited. Mica is also present and is believed to be a result of ebb currents carrying fine-grained material seaward from the backbarrier and;
4) Abandoned marginal flood channel unit of fine-grained structureless sand sheets with abundant mica and organic matter (wood pieces) (2.5 m).

4. SWASH PLATFORM CHANNEL

Characteristic features of the swash platform channel facies are inferred from subtidal bedforms and revealed in the sedimentary structures of Cores 9 and 15, both of which are located on the edges of the swash platform channel on channel margin linear bar and swash bar margins.

The 3.0 m deep Core 15 and 1.6 m deep Core 9 include fine sand with horizontal planar and high-angle planar cross-bedding oriented onshore with numerous reactivation surfaces. Core 15 also shows a predominance of seaward-oriented cross-bedding, which is likely associated with strong ebb currents during spring tidal events. The bidirectional nature of currents in this environment is demonstrated by three units of Core 15: 1) the bottommost unit from 2.50 m-2.78 m of fine sand with horizontal to low-angle landward-oriented planar and trough cross-bedding with organic and micaceous sand; 2) the 1.77 m-1.87 m unit of fine-grained landward-oriented high-angle cross-bedding and; 3) the 1.42 m-1.60 m unit of seaward-oriented high-angle planar cross-bedding.

Peel 5 of core 15 (2.50 m-2.75 m)(Figure 74), is believed to be representative of deposits from either the active or abandoned swash platform channel facies and shows the bidirectional transport of sand occurring in this environment. The flood-oriented bedding associated with wave-enhanced flood-tidal currents is demonstrated by the fine-grained onshore-oriented planar to trough cross-bedding from 2.75 m-2.78 m. The fine-grained horizontal planar beds from 2.50 m-2.55 m are associated with wave swash. The presence of ebb currents are shown by the overall seaward-oriented nature of the peel as well as units of micaceous sand at 2.56 m-2.62 m. The unit from 2.65 m- 2.69 m has mica but is composed primarily of steeply-dipping coarse sand beds (22°) deposited by ebb currents during spring tidal conditions.

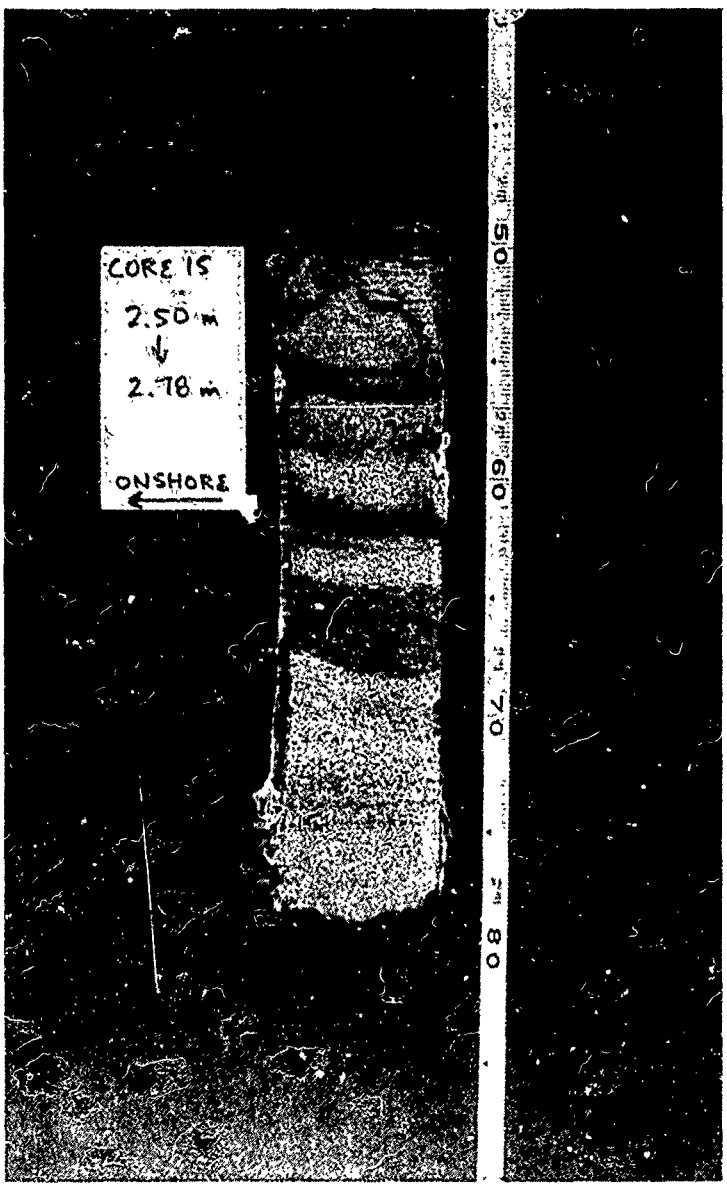

Figure 74. Peel 5 of Core 15 (2.50 m-2.78 m) demonstrating internal stratification associated with the swash platform channel.

Although this peel indicates that seaward forces are dominant in this environment, bedding structures of other peels and cores indicate that flood-dominant forces mostly control bedding horizons at this environment.

In summarizing, since this environment is influenced by wave-generated flood-tidal and ebb-tidal currents, a variety of sedimentary structures are produced which include: 1) bidirectional trough cross-bedding with dominant high-angle flood-oriented planar cross-bedding and planar horizontal bedding; 2) numerous reactivation surfaces as dominant flood-tidal currents are interrupted by either ebb-tidal currents and associated erosion or slack currents; 3) fine-grained nature of sediments (very fine to fine sand) and; 4) deposition wood matter and mica. There is no indication of any fining-upward sequences in this environment.

A complete swash platform channel facies model consists of these units in ascending order:

1) Shoreface deposits;
2) Active swash platform channel deposits of fine sand with dominantly flood-oriented planar and trough cross-bedding with numerous reactivation surfaces. Some micaceous sand is also present (1 m);
3) Channel fill deposits of fine to medium sand associated with the growth and input of sediment from the adjoining channel margin linear bar and (2 m);
4) Abandoned swash platform channel deposits of fine sand with horizontal planar to low-angle landward-oriented cross-bedding, and homogeneous, massive sheets of sand all of which are associated with wave activity. Significant interbedded layers of wood matter and mica deposited during the ebb-tidal stage are present (1 m).

5. SWASH BAR

Characteristics of the swash bar facies have been determined from analysis of intertidal bedforms and sedimentary structures of Cores 3, 4, 10, 13, 18, 19, 21 and 22 which were taken on both updrift and downdrift swash bar complexes as well as on wave-dominated distal channel margin linear bar environments. Bedforms on both the updrift (stake 11 from Table 15) and downdrift (stake 8) swash bars are dominated by plane beds and wave-generated ripples. The landward transport of sediment at the downdrift swash bar produces the low-angle dominant landward-oriented cross bedding as seen in Trench 6 (Figure 75). Deposition of sediment during storm events is demonstrated in this trench by high-angle (22°-34°) landward-oriented cross-beds (cf. Sha, 1989).

Two types of sedimentary structures associated with the swash bar facies as preserved in cores 3, 4, 13, 18 and 22 are noted. Core 3 shows high-angle landward-oriented planar cross-beds with numerous reactivation surfaces associated with migration of the landward slipface, and horizontal planar beds associated with vertical accretion plane bed deposition. Only one 0.50 m unit (2.15 m-2.65 m) of bidirectional planar cross-bedding deviates from this dominant landward-oriented bedding. Core 4 also shows this dominant landward orientation of bedding. Core 22 shows a conformable sequence of high-angle landward-oriented planar beds of the slipface directly overlain by low-angle landward oriented cross-beds associated with vertical accretion deposits (1.38 m-1.98 m). Core 13 shows low-angle seaward-oriented planar beds associated with vertical accretion interbedded by units of high-angle landward-oriented planar beds associated with slipface migration.

Two storm deposit layers (0.93 m-1.20 m and 1.30 m-1.55 m) of core 18 are indicated by: 1) a fining-upward sequence of coarse to fine sand with low-angle bidirectional trough cross-bedding and; 2) an overlying unit of medium to coarse sand with occasional fine pebble clast and shell

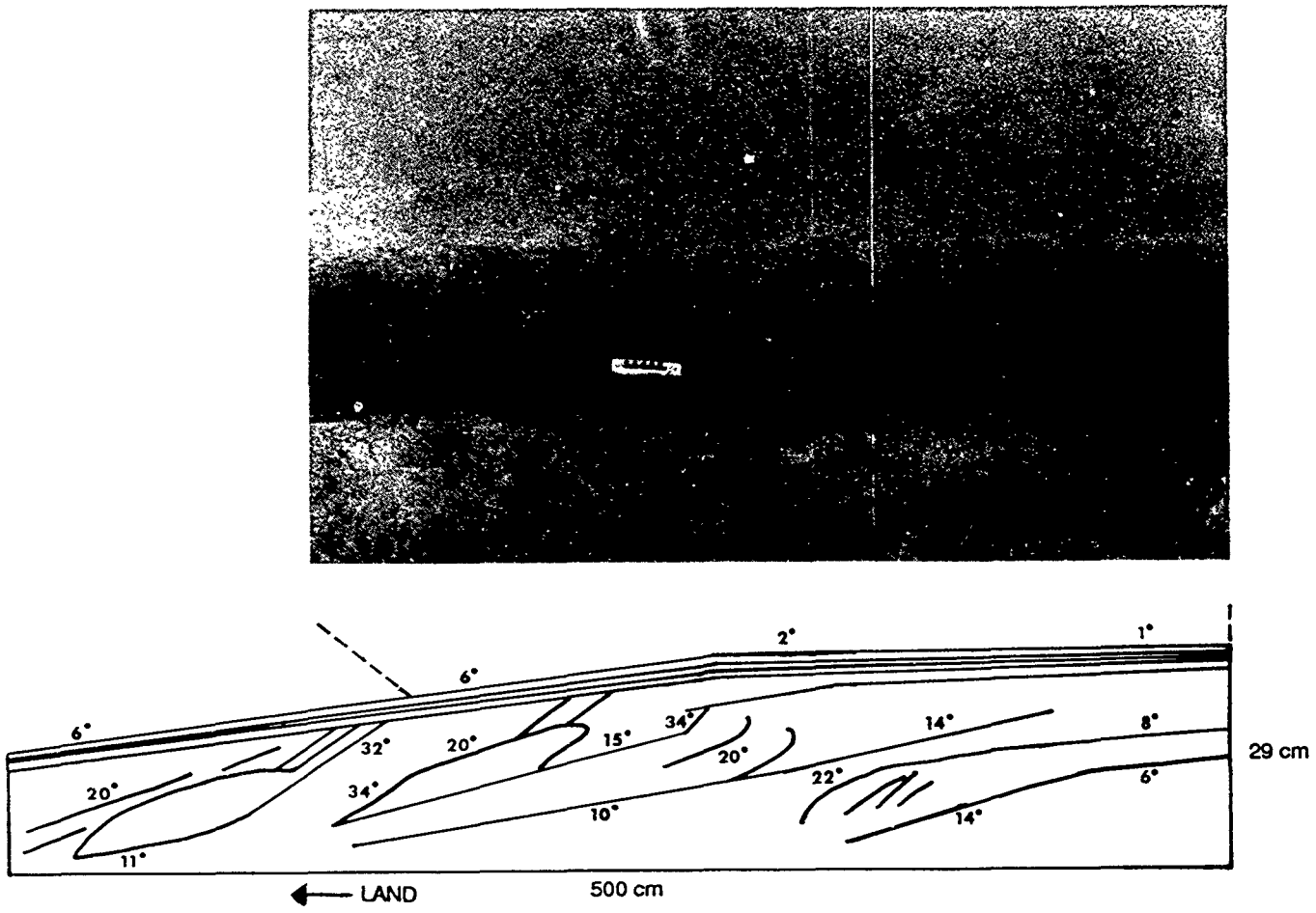

Figure 75. Trench #6 located on a landward migrating bar atop the downdrift swash bar. Land is to the left. Note the dominant landward dip of both low-angle and high-angle cross-beds denoting landward transport of sediment into the marginal flood channel.

matter with landward-oriented low-angle planar cross bedding. Core 19 also contains two consecutive fining-upward sequences.

Two peels show the two major processes associated with swash bar migration. Peel 6 of Core 3 (2.60 m-2.88 m) (Figure 76) show high-angle landward-oriented cross-beds associated with the slipface of the swash bar. Note the numerous high-angle planes of dip (1°-25°) and the numerous reactivation surfaces.

Peel 7 of Core 19 (2.44 m-2.87 m) (Figure 77) shows fine sand with horizontal planar beds and homogeneous, massive sand sheets associated with vertical accretion. Two medium sand units occur, one of which has landward-oriented planar cross-beds which dip at an angle of 15° (2.54 m-2.58 m). This unit is most likely associated with onshore migration of a smaller swash bar atop the swash complex. Note that the structureless sand unit lies directly above this unit. Bedding horizons of this peel appear to be convex (regard fine grained sediment layer at 2.65 m) which is due to disturbance of sediments during core penetration.

In summary, the near surface stratigraphy of the swash bar facies include high-angle planar landward-dipping cross-beds associated with slipface migration, and horizontal to low-angle planar seaward-dipping cross-beds and homogeneous, massive, structureless deposits associated with vertical accretion on the swash bar surface (cf. FitzGerald, 1976 and Nelligan, 1983). Planar and trough seaward-oriented bidirectional cross-bedding is also present and is most likely a function of ebb currents of the main ebb and marginal flood channels. Other characteristic features of the swash bar facies include: 1) numerous reactivation surfaces; 2) the lack of subsurface records of ripples as they are washed out by plane beds; 3) well-sorted fine sand and; 4) layers of medium-coarse sand and shell matter associated with fining-upward sequences of storm deposits.

A complete swash bar facies includes the following units in ascending order:

1) Shoreface deposits;

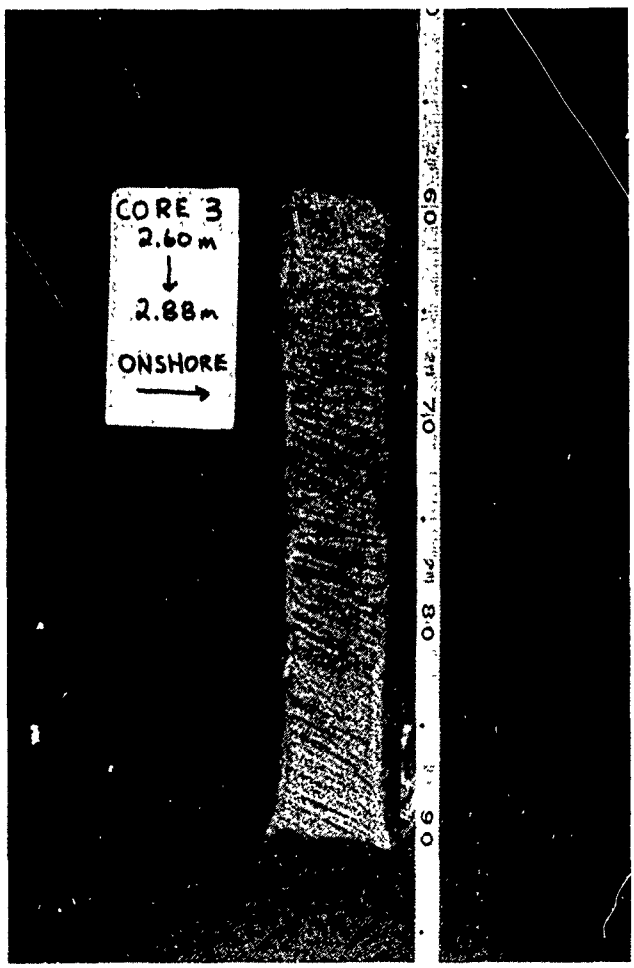

Figure 76. Peel 6 of Core 3 (2.60 m-2.81 m) showing landward-oriented high-angle cross-bedding of migrating slipface of swash bar.

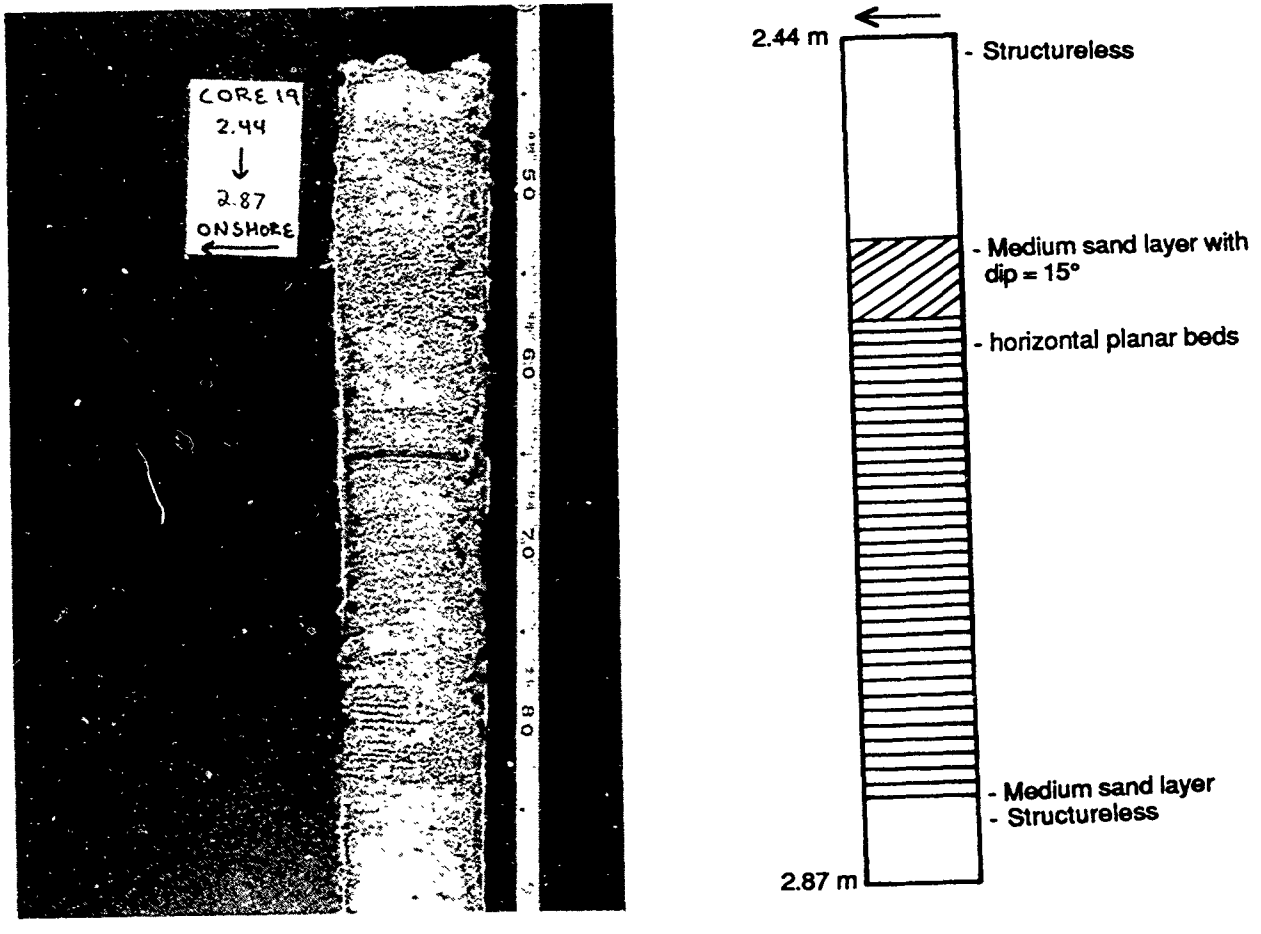

Figure 77. Peel 7 of Core 19 (2.44 m-2.87 m) showing characteristic horizontal planar beds and homogeneous massive sand sheets associated with plane beds on the surface of the swash bar.

2) Landward-oriented high-angle planar cross-bedding composed of fine sand associated with the landward migrating swash bar slipface. Numerous reactivation surfaces are present (1.0 m-1.5 m);
3) Vertical accretion unit of fine sand with planar horizontal to low-angle seaward-oriented cross-bedding and massive homogeneous sand sheets (0.5 m-1.0 m).

6. CHANNEL MARGIN LINEAR BAR

The channel margin linear bar facies have been determined from analysis of intertidal bedforms and sedimentary structures preserved in Cores 1, 2, 5, 6, 17, 20, 24.

The sedimentary structures of this environment are dominated by landward-oriented bedding but vary depending upon the interaction of main ebb channel ebb-tidal currents and wave-enhanced flood-tidal currents. The majority of bedforms on the interior portions of the channel margin linear bar environment are plane beds with current lineations associated with wave activity, and ripples. This dominance of landward-oriented currents is demonstrated by the high-angle (14°-24°) landward-dipping cross-bedding of the landward-oriented slipface of the updrift channel margin linear bar (Trench 1 of Figure 78).

On the extreme ends of the updrift channel margin linear bar, megaripple and sand wave trains are the dominant type of bedform (cf. FitzGerald, 1976 and Hubbard, 1977) but differ with respect to orientation and dimensions at proximal versus distal channel margin linear bar locations. Therefore, this environment is divided into two subenvironments.

Surficial bedforms of the proximal channel margin linear bar environment include both ebb and flood-oriented megaripples and sandwaves (Figure 79, 80). These bedforms are dominantly flood-oriented due to wave-generated flood-tidal currents through the

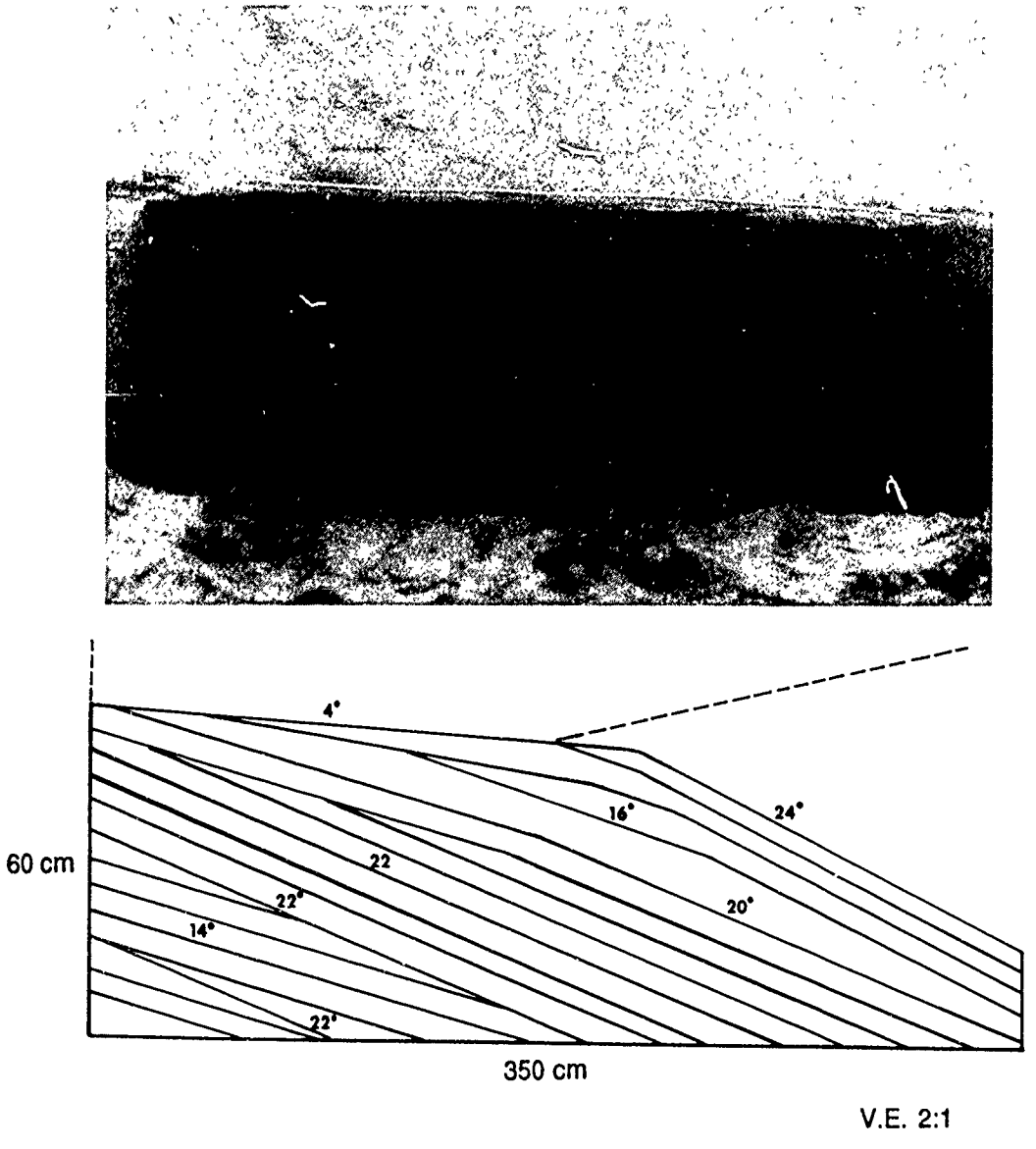

Figure 78. Trench #1 located on northwest side of updrift channel margin linear bar. Land is to the right. Note the landward-oriented cross-bedding which is a result of landward-oriented wave activity. Figure 18 shows the location of all trenches.

Figure 79. Ebb-oriented sandwaves on the proximal updrift channel margin linear bar formed by ebb-tidal currents. The average wavelength and height of these bedforms are 8.0 m and 0.40 m, respectively. The scale is 10 cm.

Figure 80. Flood-oriented sandwaves at the proximal updrift channel margin linear bar formed by flood-tidal currents. The average wavelenth and height of these bedforms are 8.0 m and 0.40 m, respectively. The scale is 10 cm.

marginal flood channel. Although ebb-tidal currents do affect this environment, the majority of ebb-tidal currents and the maximum ebb-tidal currents occur when this environment is exposed. Therefore, this environment is flood-dominated.

Trenches reveal the near surface stratigraphy of both flood and ebb-oriented sand waves. A flood-oriented sandwave located adjacent to the marginal flood channel shows low-angle (7°-12°) landward-oriented cross-bedding truncated by high-angle (10°-31°) landward-oriented cross-bedding (Trench 3 of Figure 81). The internal stratification of a ebb-oriented sand wave located adjacent to the main ebb channel is dominantly landward-oriented (dip of 10°-30°) although the surficial outline of the bedform is ebb-oriented (Trench 4 of Figure 82). This indicates an overall landward transport of sediment.

Landward-oriented bidirectional bedforms also dominate the proximal downdrift channel margin linear bar. The near surface stratigraphy of cores and trenches also indicate that the proximal channel margin linear bar environment is dominated by landward-oriented bidirectional high-angle trough and planar cross-bedding. For instance, low-angle (7°-13°) landward-oriented cross-bedding dominates Trench 5 (Figure 83). Other characteristic features of this environment include numerous reactivation surfaces and fining-upward sequences but no subsurface signature of ripples as they tend to be washed out by plane beds. Due to stability of the main ebb channel at proximal channel margin linear bar environments, there is an absence of main ebb channel cut and fill deposits.

The proximal channel margin linear bar facies includes the following units in ascending order:

1) Main ebb channel active channel deposits (2 m);
2) Interfingering deposit between: a) active main ebb channel and active marginal flood channel deposits which wash over the channel margin linear bar environment at higher tidal stages and; b) wave swash deposits of homogeneous, massive sand

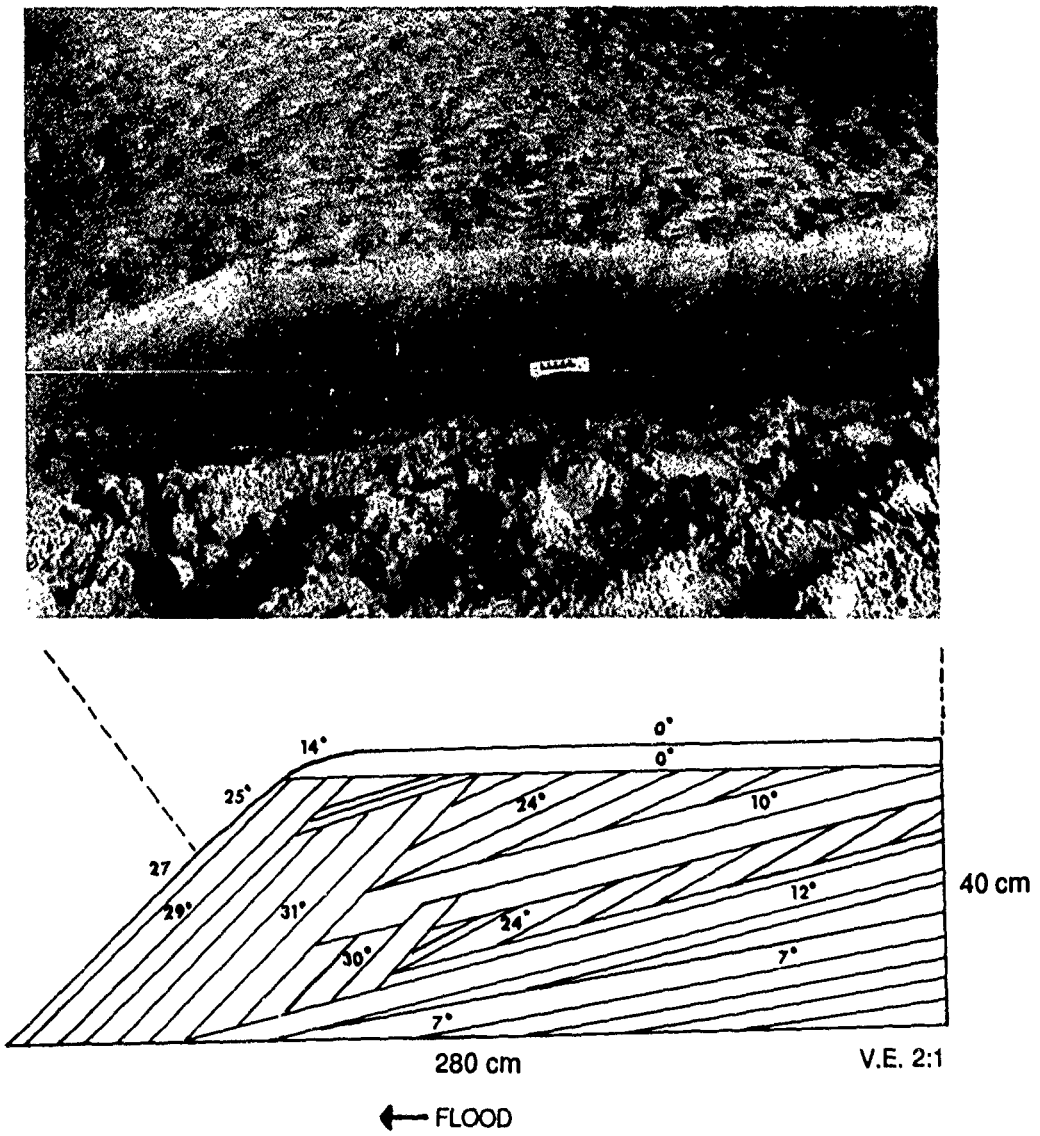

Figure 81. Trench #3 dissecting a flood-oriented bedform on the proximal updrift channel margin linear bar near the marginal flood channel. Note low angle (7°-12°) landward-oriented cross-bedding truncated by high-angle (24°-31°) landward-oriented cross-bedding.

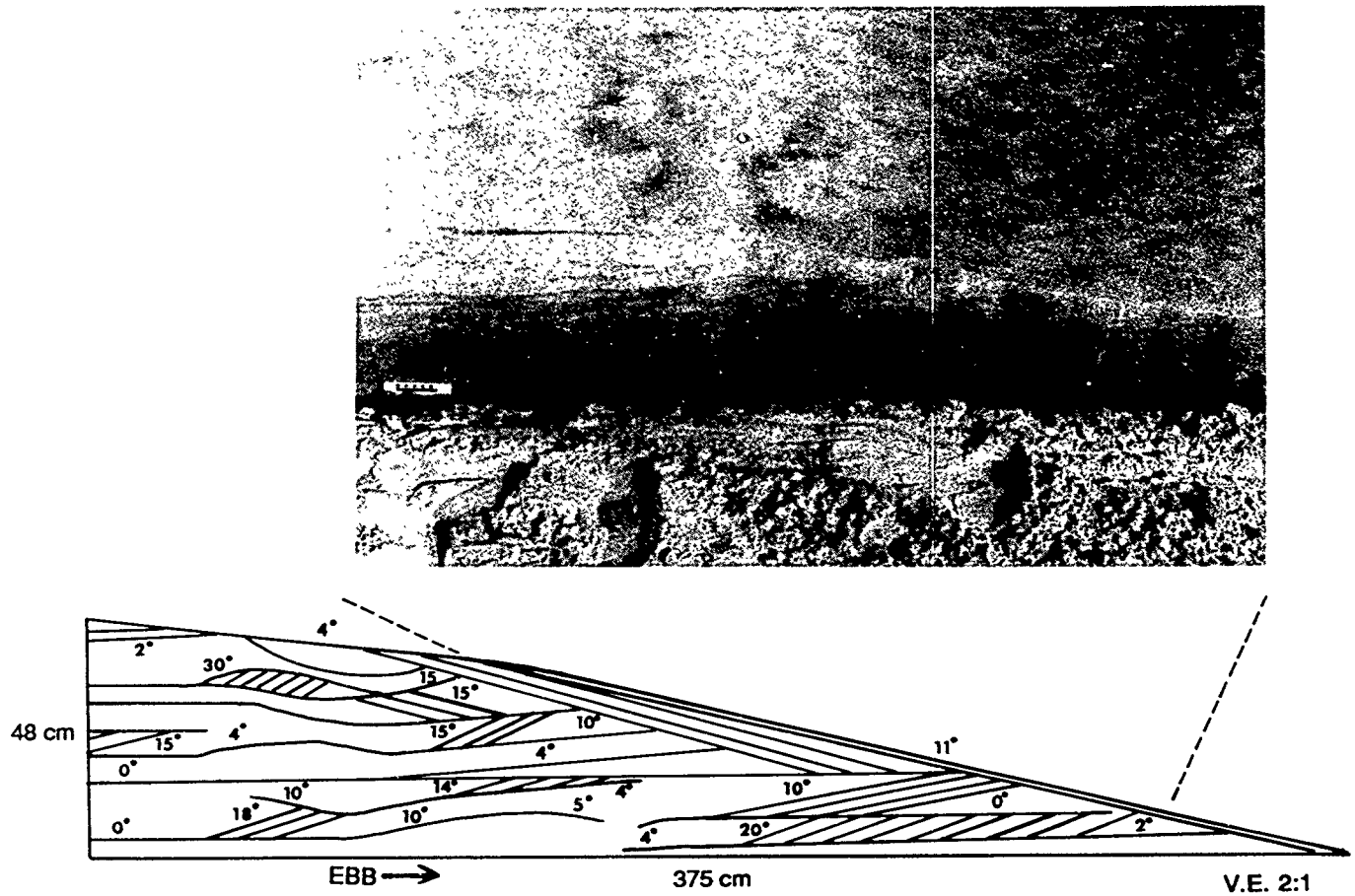

Figure 82. Trench #4 located adjacent to trench #3 on the proximal updrift channel margin linear bar near the main ebb channel. Note the overall ebb orientation of the bedform. However, dominant internal features indicate flood-oriented cross-bedding with numerous truncation of beds and reactivation surfaces.

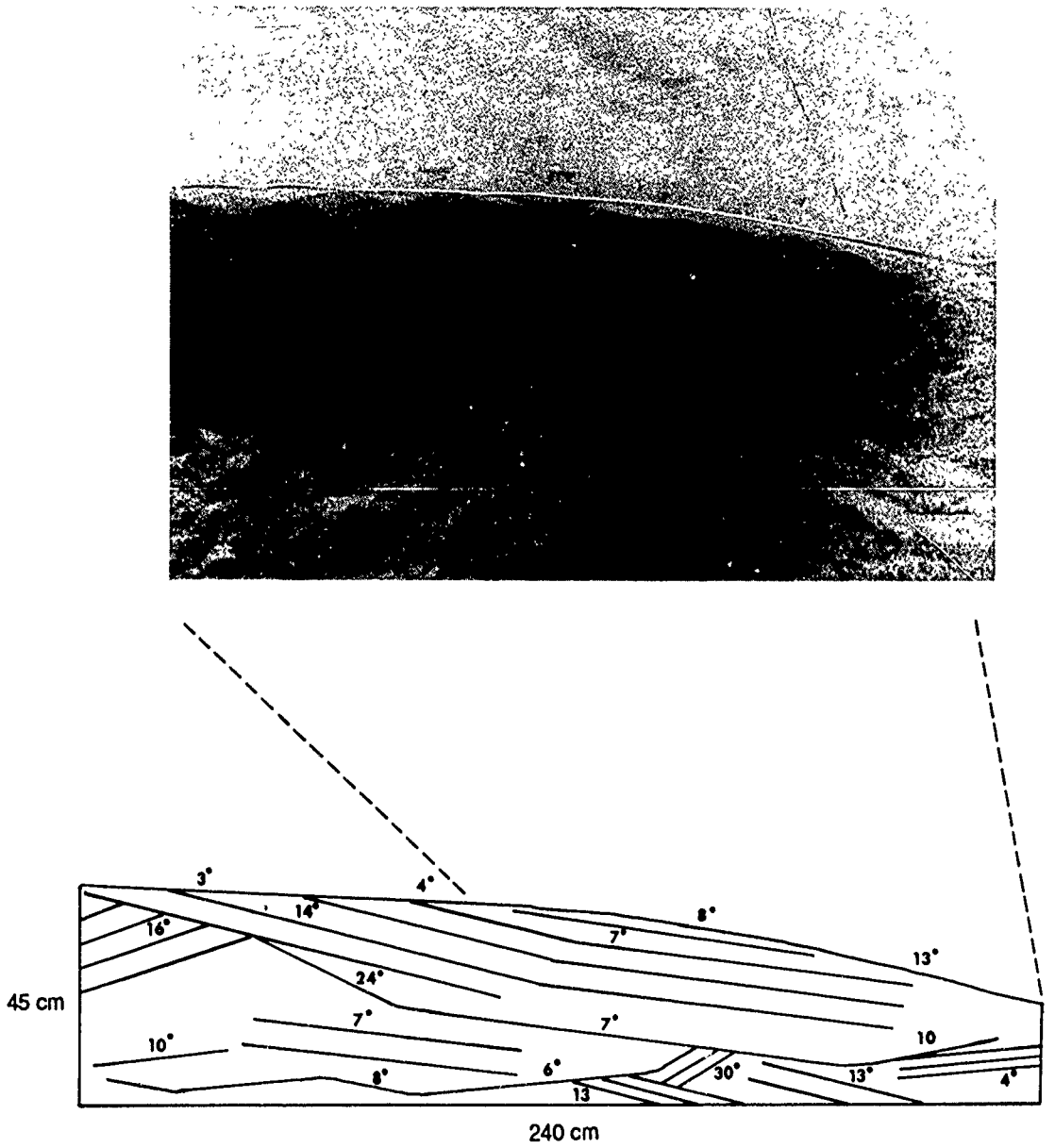

Figure 83. Trench #5 located at the main ebb channel scour slipface on the northwest side of the proximal downdrift channel margin linear bar. Note the dominant dip of low-angle crossbeds to the right towards the main ebb channel. These beds formed from the transport of sediment by flood-tidal currents over the channel margin linear bar and into the main ebb channel.

sheets and horizontal planar to low-angle landward-oriented cross-beds associated with vertical accretion (2 m).

The distal channel margin linear bar facies has been determined by analysis of intertidal bedforms and cores. Distally, the channel margin linear bar is dominated by plane beds and current lineations associated with wave-generated flood-tidal currents, and ebb-oriented cuspate megaripples associated with spillover lobe deposits and the expansion of the ebb jet during late ebb stage periods (Figure 63).

Horizontal planar and landward-oriented bidirectional low-angle planar cross-beds of Cores 6, 17 and 20 support the bidirectional nature of bedforms. Cores 6 and 17 are dominated by landward-oriented bidirectional planar cross-bedding, while Core 20 is dominated by seaward-oriented planar and trough cross-bedding.

Two peels of these cores are presented in Figure 84 and 85. Peel 8 of Core 6 (1.80 m-2.24 m) indicates vertical accretion associated with wave-generated flood-tidal currents and planar cross-beds associated with migrating ebb-oriented megaripples. Landward-oriented currents are demonstrated by two units of landward-oriented high-angle (15°-20°) planar cross-beds from 1.94 m-2.00 m and 2.18 m-2.24 m. Seaward-oriented low-angle (7°-10°) planar and trough cross-beds are demonstrated in units from 1.80 m-1.85 m and 2.10 m-2.18 m. Note also the bidirectional cross-bedding from 1.85 m-1.94 m and from 2.00 m-2.10 m and associated numerous reactivation surfaces. Dips of these bidirectional cross-beds range from 7°-10°. The sediment is fine-grained throughout the sequence.

Peel 9 of Core 17 (1.07 m-1.50 m) shows high-angle seaward-oriented trough cross-bedding from ebb-tidal currents (dip of 15°-20°)(1.40 m-1.50 m) and two interbedded sets of landward-oriented wave-enhanced flood-tidal planar cross-bedding with dips of 10°-12° and 25°-30° (1.07 m-1.28 m). The high-angle seaward-dominated bidirectional cross-bedding (1.28 m-1.40 m) is noteworthy as it is composed of coarse sand and therefore represents a high energy tidal event.

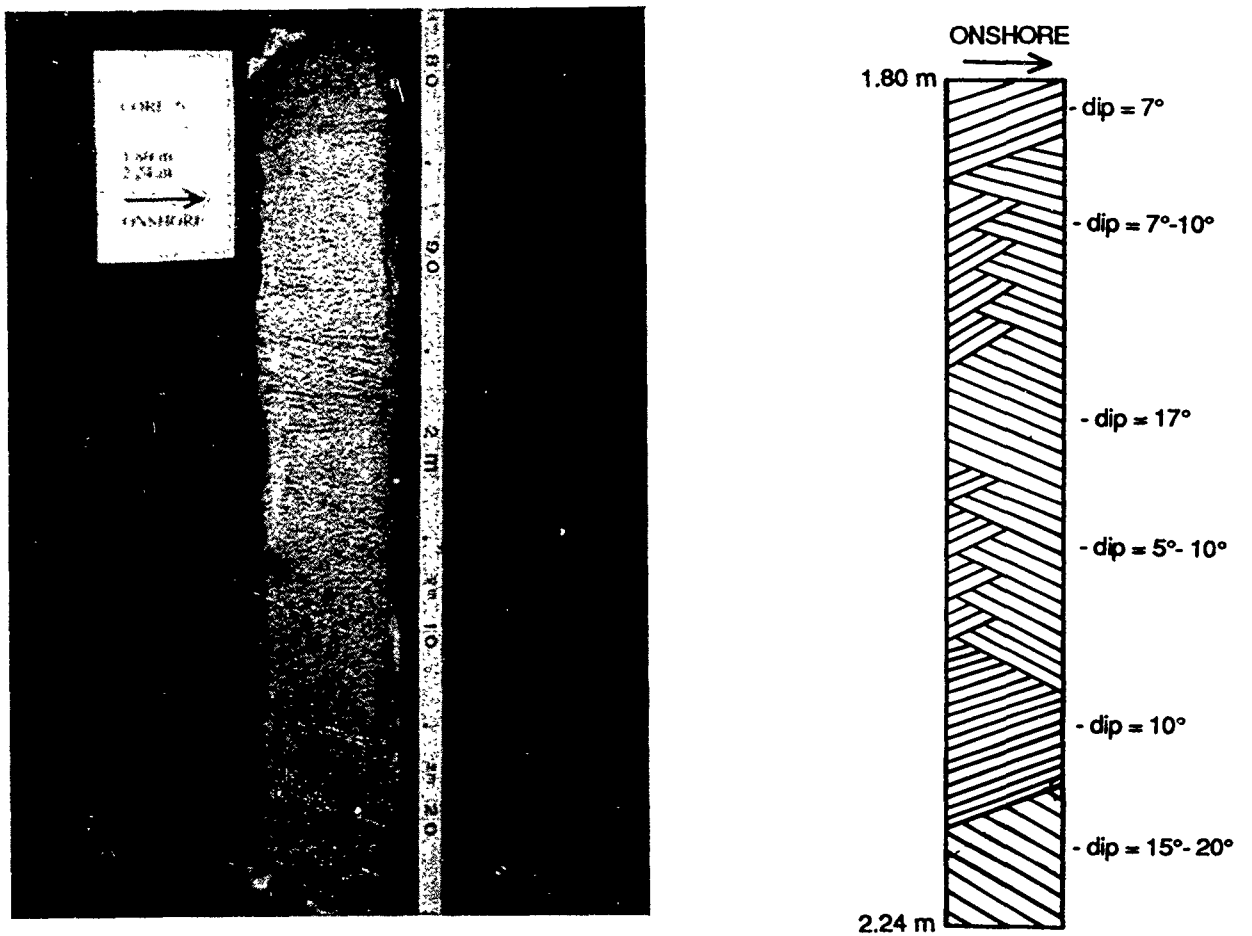

Figure 84. Peel 8 of Core 6 (1.80 m-2.24 m) of the distal channel margin linear bar environment. Note the landward dominated bidirectional planar cross-beds associated with wave-enhanced flood-tidal currents and main ebb channel ebb-tidal currents.

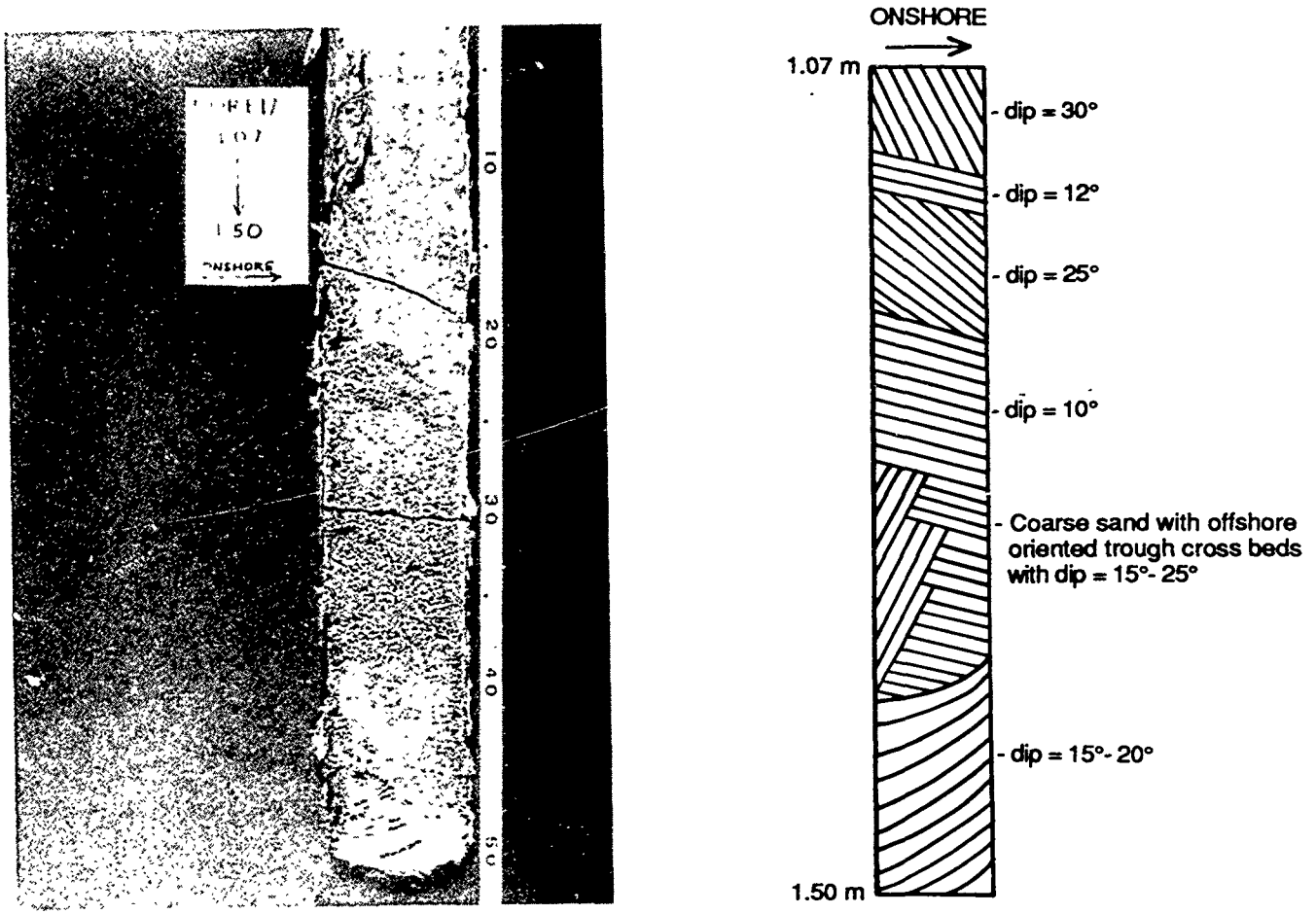

Figure 85. Peel 9 of Core 17 (1.07 m-1.50 m) showing characteristic internal stratification of the distal channel margin linear bar environment.

A distal channel margin linear bar facies is composed of the following deposits in ascending order:

1) Main ebb channel active channel deposits (2 m);
2) Main ebb channel cut and fill deposits associated with channel migrations (3 m);
3) Seaward-oriented low-angle trough to planar cross-beds associated with spillover lobe deposits and expansion of the ebb jet during higher phases of tides (1 m);
4) Active swash bar deposits (0.5 m-1.0 m).

DISCUSSION

SEDIMENT TRANSPORT

PROCESSES AND PATHWAYS

Inlet sediment bypassing is the process whereby sediment from the updrift side of the Essex River Inlet shoreline is transported to the downdrift side. Three methods of inlet sediment bypassing are described by Bruun and Gerritsen (1959): 1) through the transport of sand in channels by tidal currents; 2) by the migration of tidal channels and sand bars and; 3) through wave-induced sand transport along the terminal lobe. FitzGerald (1982) has indicated that sediment bypassing at non-migrating tide-dominated mixed energy tidal inlets occurs through stable inlet processes. Essex River Inlet, which has a stable inlet throat and proximal main ebb channel, is dominated by stable inlet processes. Although all three methods of inlet sediment bypassing are operative, the primary means at the Essex River Inlet is sand transport in channels by tidal currents, and the migration of tidal channels and sand bars. The volume of sediment transport is dependent upon: 1) the velocity and duration of ebb and flood-tidal currents through the main ebb and marginal flood channels and associated inlet throat tidal prism and; 2) the sediment-water interface surface area of the inlet throat (cf. Bruun, 1966).

Transport pathways by inlet sediment bypassing at the Essex River Inlet are dominated by two sediment transport gyres for both updrift and downdrift portions (Figure 86). These gyres, whose sediment is first introduced to updrift portions of the delta by southerly longshore transport currents, transport sediment through the marginal flood channel and over the channel margin linear bar into the main ebb channel, seaward through sandwave migration in the main ebb channel and subsequently back onshore through swash processes along the

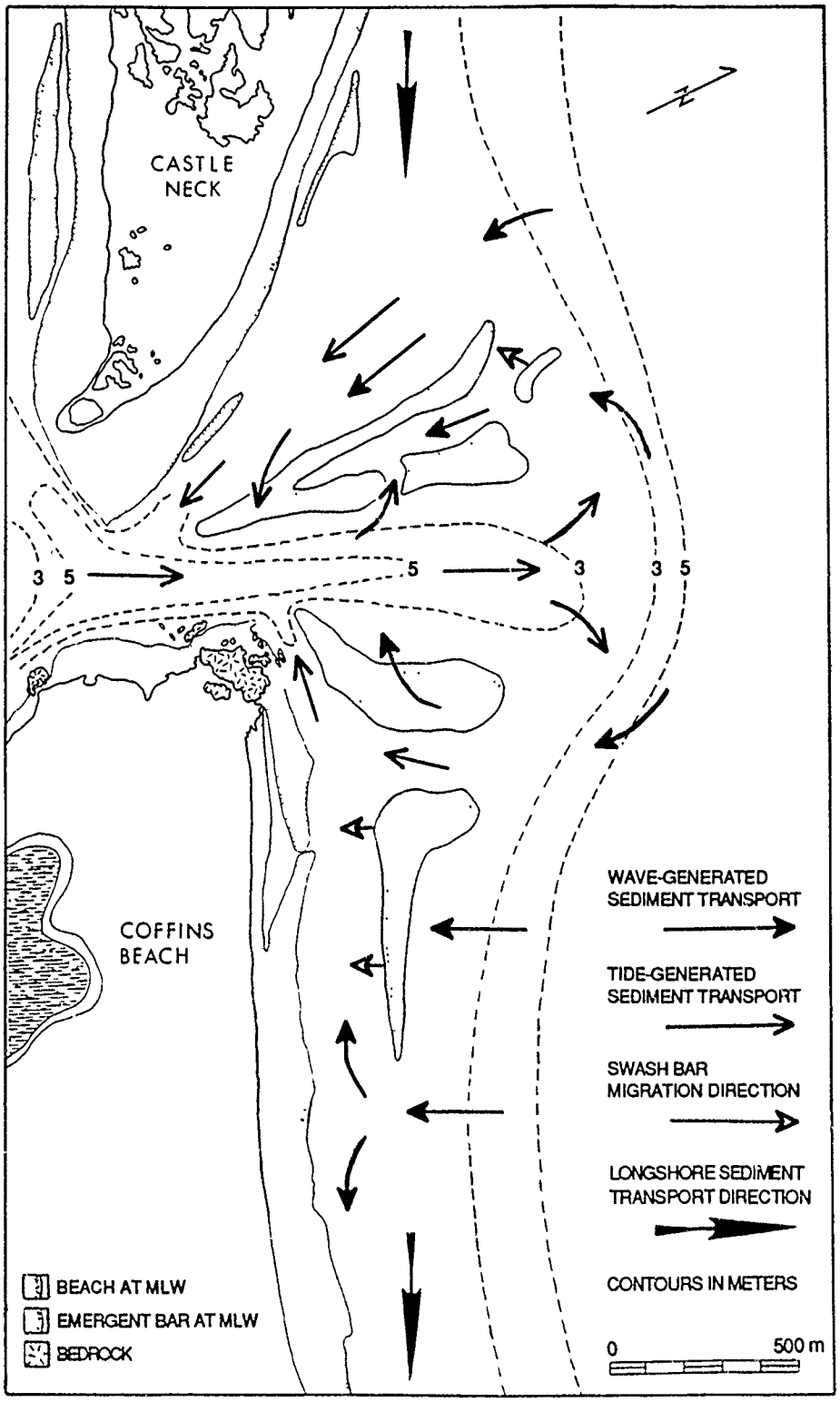

Figure 86. Sediment transport gyres associated with both updrift and downdrift portions of the delta. Note different arrow types to denote wave or tide-generated sediment transportation.

terminal lobe. The updrift counterclockwise gyre is completed as small, ephemeral swash bars migrate landward eventually attaching to Crane Beach in indiscrete packages.

In the downdrift clockwise gyre, sediment transported to the south along the terminal lobe by longshore currents is augmented by sediment moving out the main ebb channel. Southerly migrations of the main ebb channel also contribute sediment thus resulting in the growth of the large downdrift swash platform. Associated swash bars migrate landward and ultimately weld to Coffins Beach in discrete events. Wave refraction around this bar produces a transport reversal thereby reintroducing sand into the main ebb channel. Sand is also transported downdrift of the delta to more southerly portions of Coffins Beach.

POTENTIAL TRANSPORT RATES

Potential sediment transport at the inlet was determined by utilizing Maddock's equation (1969) which states that the total bedload sediment transport rate is equal to the cube of the maximum current velocity:

$$\text{Load (in } m^3/\text{sec}) = 15.244\ V^3/1600$$

Suspended load is not accounted for in this equation and is considered to be negligible at Essex River Inlet because the channel is floored by medium to coarse sand with little or no fine-graind sand.

Using the velocity as determined from the regression curve for maximum current velocity versus tidal range (Figure 33), during mean tidal conditions, a potential sediment transport rate of 7.5×10^6 m^3/year is exchanged through the inlet (Figure 87). At these tidal conditions, since maximum flood and ebb current velocities are equal, there will be no net sediment transport in or out of the inlet. However, at spring tidal ranges the regression curve indicates that the inlet throat is ebb-dominant. Since the strongest currents through the inlet occur during

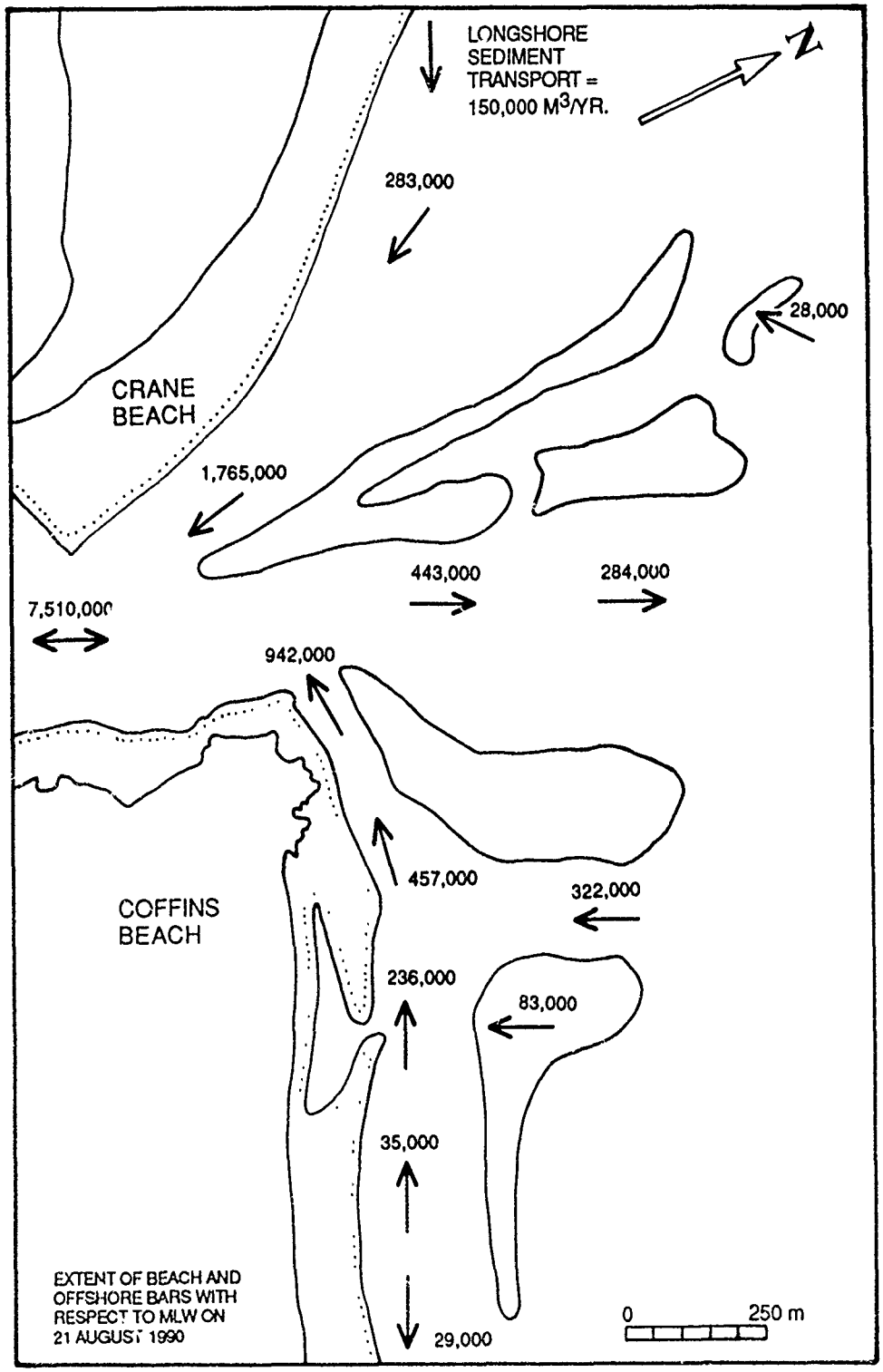

Figure 87. Potential net sediment transport directions as determined from Maddock's equation (1969) using current measurements from hydrographies and the swash process study. Longshore transport rate is 150,000 m^3/ year. All figures in m^3/year.

spring tidal conditions and sediment transport is a factor of the maximum velocity, there exists a net seaward transport of sediment through the inlet throat on a yearly basis.

Potential sediment transport rates were also calculated for locations in the main ebb channel seaward of the inlet throat and for both marginal flood channels. Distally, sediment transport rates through the main ebb channel decrease to 4.43×10^5 m^3/year and 2.84×10^5 m^3/year (Figure 87). This decrease results from an expansion of the ebb jet and an increase in the cross section of the channel. Sediment rates for the updrift and downdrift marginal flood channels are 1.76×10^6 m^3/year and 9.42×10^5 m^3/ year, respectively. Thus, the updrift marginal flood channel introduces 8.23×10^5 m^3 more sediment per year into the main ebb channel than does the downdrift marginal flood channel. This is due to the greater input of sediment as well as the more flood-dominant nature of the updrift marginal flood channel.

Net bedload transport rates for each swash bar were determined by multiplying the distance the slipface has migrated over a yearly period of each bar by the bar length and thickness. Migration rates of the updrift and downdrift swash bars were 2.80×10^4 m^3/year and 8.30×10^4 m^3/year, respectively (Figure 87).

However, several errors may be associated with determination of potential sediment transport rates. First, the equation utilized by Maddock (1969) was originally derived for fluvial environments and therefore is only a qualitative estimation of sediment transport in a marine environment such as the Essex River Inlet. These sediment transport rates through channels represent potential maximum rates. Conversely, rates of bar migration are minimal estimates of sediment transport rates as some of the sediment may have been transported by longshore transport currents and therefore would not be calculated as part of the migrating swash bar. This is demonstrated in Figure 87 where sediment transport rates associated with swash bar migration are much lower than the rates associated with sediment transport through channels. Note in particular the downdrift swash bar where 8.30×10^4

m^3/year of sediment is added into the downdrift marginal flood channel through swash bar migration. This figure is substantially less than the 2.36×10^5 m^3/year which is transported through the marginal flood channel into the main ebb channel. A second indication of these unequal rates is that net potential sediment transport through both marginal flood channels of 2.70×10^6 m^3/year is substantially less than the 7.51×10^6 m^3/year transported through the inlet throat. This difference of 4.80×10^6 m^3/year is not totally explained by the flood-tidal transport of sediment over the channel margin linear bar into the main ebb channel.

VOLUMETRIC CHANGES

A comparison between field data and historical aerial photographs indicate that the Essex River ebb-tidal delta undergoes volumetric changes. These changes are a direct result of the processes previously discussed including inlet sediment bypassing, the longshore transport of sediment into the inlet and the sediment transport gyres.

These volumetric changes are explained by a bar migration model for a South Carolina Inlet (FitzGerald, 1984) (Figure 88). In applying this model to the Essex River Inlet, the ebb-tidal delta undergoes a 5-7 year cycle of volume changes of 15%-20%. The model is divided into four stages.

The first stage in this ebb-tidal delta cycle occurs after the bars have welded to both Crane and Coffins Beaches. At this time, the sediment volume of the delta is small and no offshore bars exist to protect beaches from wave activity. Thus, wave activity and swash processes on Crane Beach transport sediment to the delta through longshore transport processes.

Stage 2 is characterized by increases in delta sediment volume, and formation, growth and onshore migration of swash bars, some of which coalesce with channel margin linear bars. In this stage, little sediment is being added to landward beaches, resulting in their overall decrease in

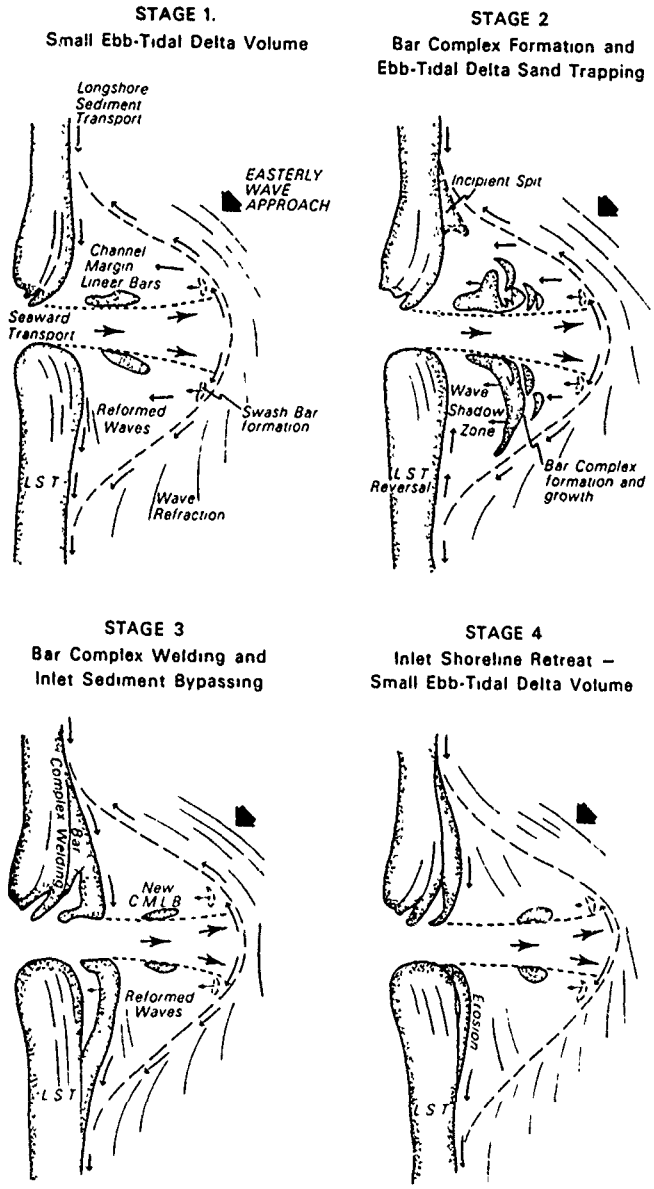

Figure 88. Model of onshore migration of bar complexes and attachment to Crane and Coffins Beaches. Stage 1 and 2 are growth stages where swash bars form and coalesce into large bar complexes resulting in increases in volume of the channel margin linear bars and entire ebb-tidal delta. At this time, waves refracting around the bars cause a transport reversal along the downdrift shoreline, which serves to trap most of the sediment entering in the vicinity of the inlet. After the bars weld to the landward beaches (stage 3), shoaling and reformed waves break along the downdrift inlet shoreline and transport sediment away from the inlet. This process results in erosion of the downdrift shoreline and a release of sediment to the shoreline downdrift of the delta (stage 4) (after FitzGerald, 1984).

volume. A transport reversal at downdrift portions of the delta occurs due to wave refraction around the downdrift offshore swash bar. The increased ebb-tidal delta sediment volume will be maintained as long as the sediment transport reversal and related recirculation of sediment through the ebb-tidal delta system exist. The Essex River ebb-tidal delta is presently in this stage.

The third stage occurs as landward migrating swash bars attach to both Crane and Coffins Beach. The longshore sediment transport reversal is disrupted, thus leaving inlet sediment bypassing as the only contributor of sediment to the delta. The delta now has a small volume and is mostly subtidal, thus resulting in greater wave energy expended to the beaches.

The fourth stage is a period of shoreline retreat as sediment from Crane and Coffins Beach is eroded do to wave activity. The volume of the delta is still small. This cycle then repeats itself.

Three lines of evidence support this bar migration model. First, the areal changes of intertidal offshore sand bodies have a direct correlation to volumetric changes of beaches. Table 16 demonstrates that during the 14 month period (June, 1989-August, 1990), as offshore sand bodies increased in area, the beach sediment volume decreased. Secondly, overall intertidal sand body area has increased substantially over the 14 month study period (Figure 61). This increase in area is interpreted as resulting from processes similar to stage 2 of the bar migration model.

The third and most supportive piece of evidence are the morphologic changes to the ebb-tidal delta over a 42 year period associated with a historical study of nine series of aerial photographs (1943-1985) (Figure 89)(Table 17). Shoreline changes were also determined from four nautical charts (1855-1985)(Figure 90).

The major morphologic features of the ebb-tidal delta considered during this historical study include: 1) changes in sediment volume of the entire ebb-tidal delta as well as area of intertidal sand bodies (channel margin linear bar and swash bar); 2) stability of the inlet throat and proximal main ebb channel with slight migrations at distal portions; 3)

LOCATION	August (June), 1989-August, 1990
UPDRIFT	
Updrift Channel Margin Linear Bar	Increase 789 m^2
Cranes Beach	Decrease 188 m^3/m
DOWNDRIFT	
Downdrift Channel Margin Linear Bar	Decrease 2 m^2
Downdrift Swash Bar	Increase 198 m^2
Coffins Beach	Decrease 118 m^3/m

Table 16. Changes in sediment volume for Crane and Coffins Beach and in area for intertidal offshore sand bodies. Figures are indicative of trends in sediment accretion/erosion.

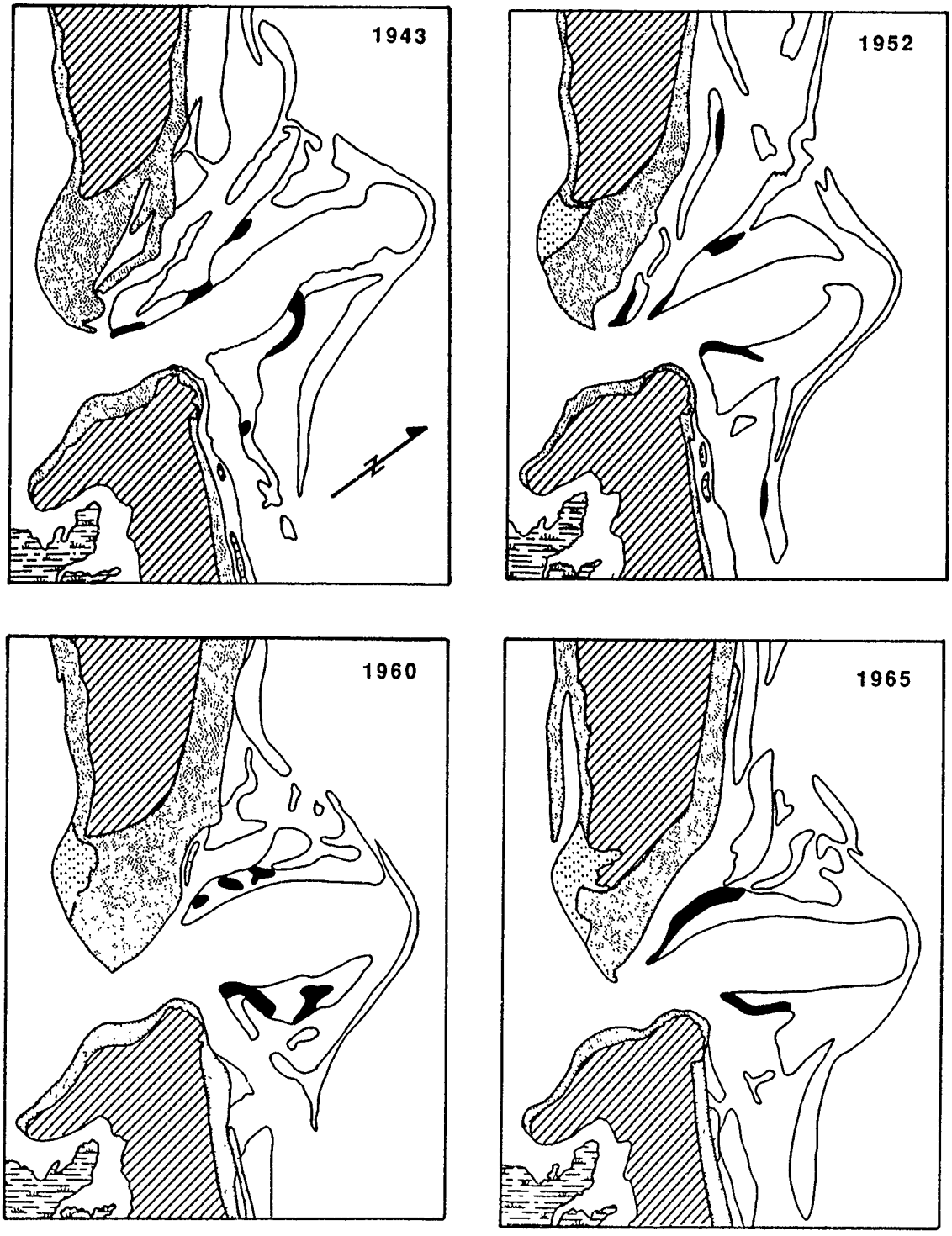

Figure 89. Morphologic changes to Essex River ebb-tidal delta as determined from vertical aerial photographs. Note the stability of the inlet throat, migration of outer main ebb channel and overall accretion of both Crane Beach and Coffins Beach during the study period.

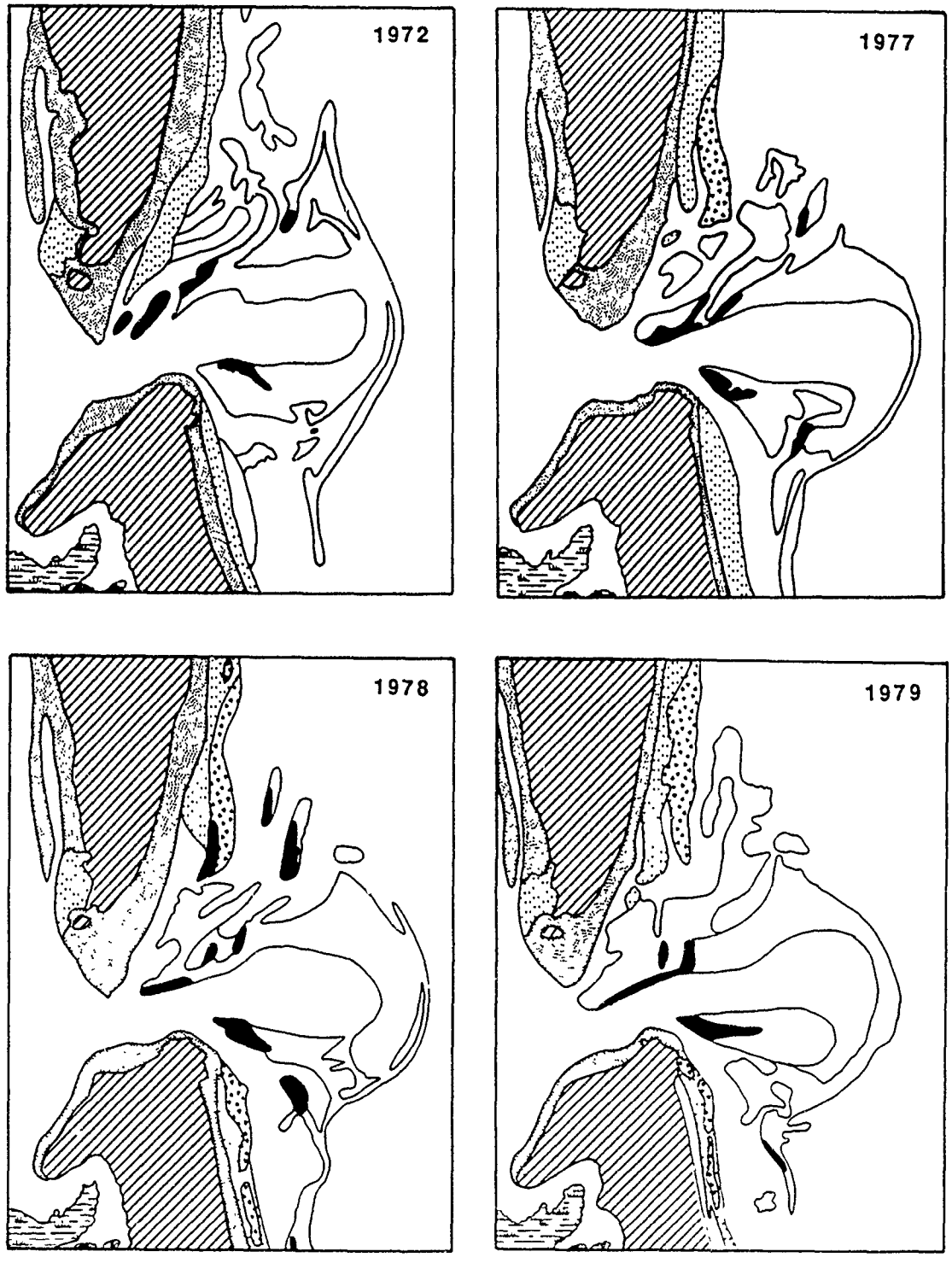
1972
1977
1978
1979

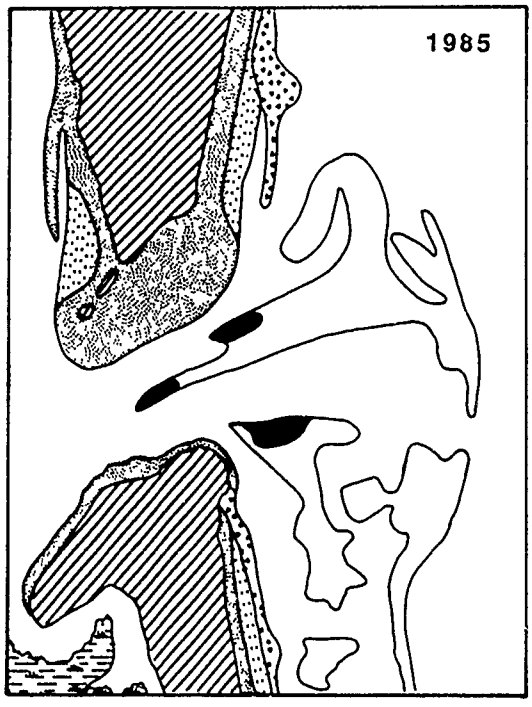

STABILIZED BEACH AND DUNE RIDGES

MARSH

SUBTIDAL SAND BODIES

INTERTIDAL SAND BODIES

ACCRETIONARY PHASES OF BEACH RIDGE DEVELOPMENT

0 500 1000 m

DATE	OVERALL INTERPRETATION	MAIN EBB CHANNEL CONFIGURATION	MARGINAL FLOOD CHANNEL/ SWASH PLATFORM CHANNEL CHARACTERISTICS
07 July 1943	Small sediment volume of ETD. Majority of sediment is offshore but is migrating onshore. Well defined marginal flood channel (MFC).	Most seaward extent of MEC during period (1.47 km from Coffin Beach headland). Entire main ebb channel (MEC) has slight updrift-offset position.	Well-defined updrift and downdrift MFC. Swash platform channel (SPC) in between downdrift CMLB and downdrift swash bar is non-existent.
26 July 1952	Great ETD volume as sand moves onshore and CMLB increase in size.	Less seaward extent of MEC (1.25 km) MEC has shore normal orientation and is wider at distal portions.	Well-defined updrift and downdrift MFCs. SPC is non-existent.
19 May 1960	Swash bar migration has resulted in great sediment volume at proximal portions. Accretionary phases at both beaches. Distal MEC has downdrift-offset configuration.	Near similar seaward extent of MEC (1.22 km). Channel has shore normal orientation and has similar width to 1952. Outer MEC has slight downdrift-offset configuration.	MFCs are well defined. Swash platform channel is present and separates downdrift CMLB from downdrift swash bar.
04 April 1965	Great volumes of sediment at proximal portions of ETD and at CMLB. Both beaches have depleted greatly in sediment. Distal MEC has downdrift-offset configuration.	Near similar seaward extent of MEC (1.23 km). Distal MEC has more downdrift-offset configuration.	Well-defined updrift MFC but poorly defined downdrift MFC. Downdrift swash channel is non-existent; swash bar is migrating onshore in its place.
13 May 1972	Great sediment volume throughout system. Distinct phases of swash bar migration, particularly updrift. Outer MEC is at extreme downdrift-offset position. Well defined MFCs and swash platform channel.	Similar seaward extent of MEC with greater downdrift offset configuration. Outer MEC is at farthest downdrift-offset position of entire historical study.	Well-defined updrift and downdrift MFCs and downdrift swash platform channel.

Table 17. Historical morphological changes to Essex River ebb-tidal delta and surrounding environments.

DATE	SWASH BAR POSITION AND SIZE	CHANNEL MARGIN LINEAR BAR MORPHOLOGY	BEACH MORPHOLOGY
07 July 1943	Distinct phases of onshore migration of swash bars, both updrift and downdrift. Position of swash bars is well offshore. Downdrift swash bar is connected to downdrift CMLB.	Updrift CMLB has large intertidal area and is aligned in an updrift position due to updrift-offset alignment of MEC. Downdrift CMLB has small size with intertidal portions at distal end.	Crane Beach is wide near inlet and spit but narrows to the northwest. Coffins Beach is narrow with slight bulge about 350 m to southeast of bedrock at Twopenny Loaf.
26 July 1952	Distinct phases of swash bar migration onshore and welding to beach. Second set of downdrift swash bars well offshore of Coffins Beach.	Updrift CMLB has small intertidal portion but overall increase in size. Downdrift CMLB has more downdrift position with intertidal position closer to Coffins Beach adjacent to MFC.	Beach morphology similar to 1943. Swash bars near to and nearly accreted onto beaches.
19 May 1960	No distinct phase of onshore swash bar migration.	Updrift and downdrfit CMLB has remained constant in size with similar intertidal areas as 1952.	Width of Crane and Coffins Beaches has increased due to welding of swash bars previously. Second phase of beach ridge development present.
04 April 1965	Distinct phase of onshore migration of swash bars for both updrift and downdrift portions. Position of swash bars are relatively far offshore.	Both updrift and downdrift CMLB are large in size with majority of sediment at proximal locations. Downdrift CMLB connected to downdrift swash bar	Coffins Beach, Crane Beach and spit system on southern end of Crane Beach substantially decrease in sediment.
13 May 1972	Distinct phase of swash bar migration onshore. Note five phases of swash bar migration in updrift portions of ETD. Downdrift, one large swash bar lies well offshore.	Both updrift and downdrift CMLB are large in size with greatest intertidal portions landward near MFCs. Downdrift CMLB connected to downdrift swash bar.	Substantial welding of swash bars to both Crane and Coffins Beaches. Spit system still has small sediment volume.

DATE	OVERALL INTERPRETATION	MAIN EBB CHANNEL CONFIGURATION	MARGINAL FLOOD CHANNEL/ SWASH PLATFORM CHANNEL CHARACTERISTICS
01 April 1977	Great amounts of sediment in proximal portions but little sediment distally.	Similar seward extent of MEC (1.23 km). MEC has widened since 1972 but still has slight downdrift-offset configuration.	Well-defined downdrift MFC. Poorly developed updrift MFC and swash platform channel.
28 April 1978	Relatively small amounts of sediment throughout system. Greatest sediment at proximal portions of CMLBs noted by accretionary phase of beach development. Distal MEC has downdrift-offset configuration.	Similar seaward extent of MEC. Distal MEC has downdrift-offset configuration.	Well-defined downdrift MFC. Updrift MFC interrupted by distinct phases of swash bar migration. Poorly developed SPC.
20 June 1979	Sediment decrease at proximal portions ETD, especially at Coffins Beach. Small amount of sediment moving on-shore via bar migration. Complete re-alignment of distal MEC to shore normal orientation.	Similar seaward extent of MEC (1.17 km). Realignment of distal MEC to shore normal position.	Well-defined downdrift MFC. Re-establishment of updrift MFC. Poorly-defined swash platform channel.
29 Sept, 1985	Majority of ETD sediment is in distal locations. Beaches have small sediment volume. No distinct phase of swash bar migration.	Similar seaward extent of MEC. Distal MEC has slight downdrift-offset configuration.	Well-defined updrift and downdrift MFCs. Swash platform channel just present.

DATE	SWASH BAR POSITION AND SIZE	CHANNEL MARGIN LINEAR BAR MORPHOLOGY	BEACH MORPHOLOGY
01 April 1977	Distinct phase of swash bar migration onshore for both updrift and downdrift portions. Great southeastern extent of downdrift swash bar.	Updrift CMLB is similar in size to 1972. Intertidal portions of CMLB are landward near MFC. Distally, downdrift CMLB is depleted of sediment but has great amount intertidal portions abutting MFC.	Swash bars welding to beach especially on Crane Beach. Spit system has increased in area substantially.
28 April 1978	Distinct phase of swash bar migration onshore for both updrift and downdrift portions. Two phases of swash bar migration are occurring downdrift. Great southeastern extent of downdrift swash bar.	Overall small size of both updrift and downdrift CMLBs. Greater intertidal portions are closer to shore.	Welding of swash bars to both beaches resulted in accretionary phase to beaches. Majority of spit system is intertidal.
20 June 1979	Updrift, some degree of swash bar migration. Downdrift, one bar is present. Less southeastern extent of downdrift swash bar.	Updrift CMLB has large size. Size of downdrift CMLB has increased in volume since 1978 with intertidal portion proximal and abutting MFC. Downdrift CMLB is connected to downdrift swash bar at distal portions.	Extreme width of beaches updrift due to welding of swash bars. Coffins Beach width has diminished.
29 Sept 1985	Less distinct phase of swash bar. migration than in previous years. Swash bars are mostly offshore for both updrift and downdrift portions.	Updrift CMLB is slightly smaller than in 1979. Majority of CMLB sediment is in distal portions. Downdrift CMLB is very small but does connect to downdrift swash bar.	Narrowing of both Crane and Coffins Beach.

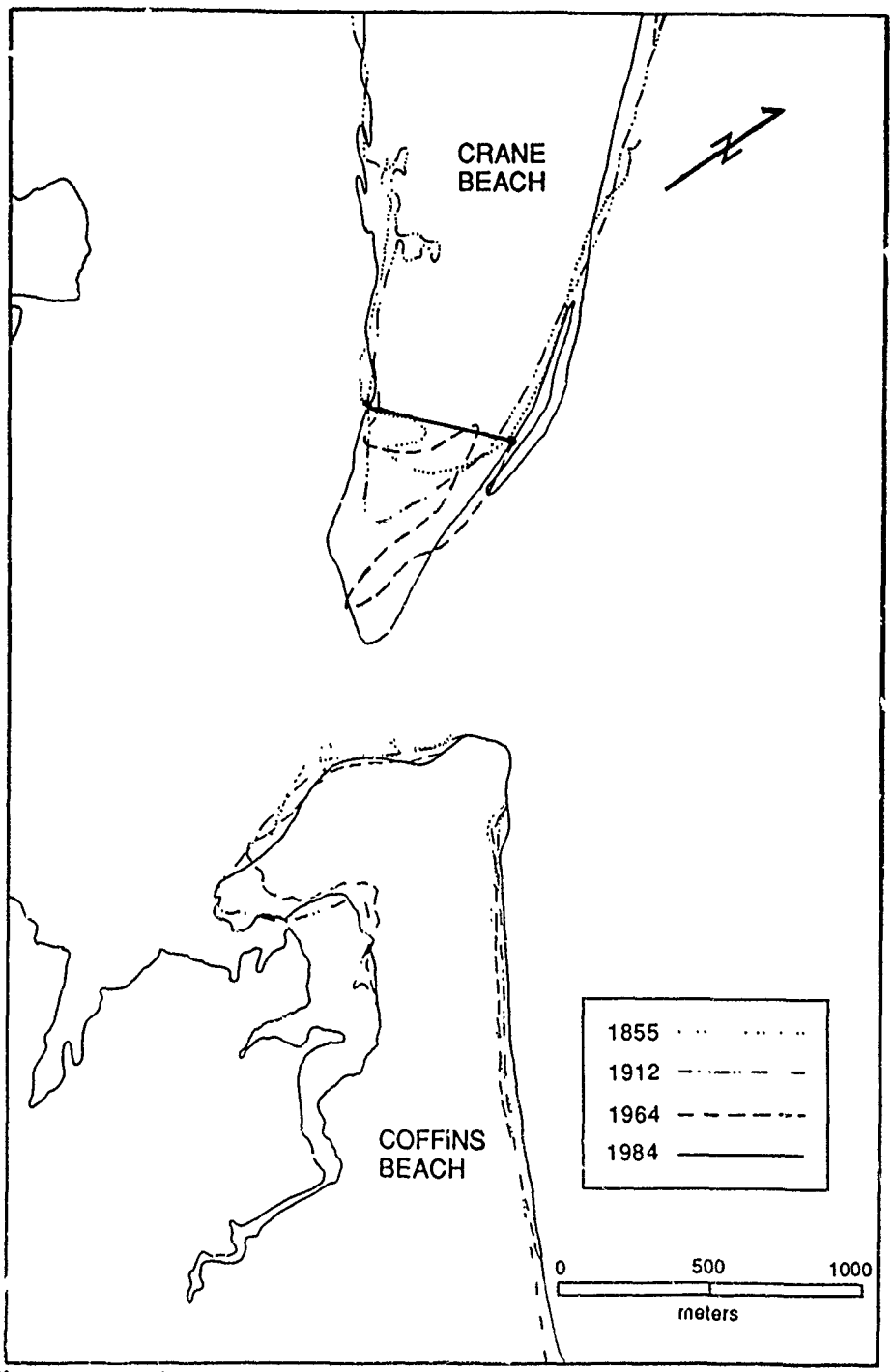

Figure 90. Historic shoreline changes of Crane Beach and Coffins Beach as determined from four different coastal charts. Extent of beach is measured at MLW. Noticeable changes during this 129 year study include fluctuations of beach width up to 120 m on Crane Beach and 60 m on Coffins Beach and spit elongation on the southern end of Crane Beach. (Note dissection line on Crane Beach utilized to determine the change in area of the spit).

development (scour characteristics and width) of the marginal flood channel and swash platform channel; 4) migration and attachment of swash bars to both updrift and downdrift beaches and; 5) increases in beach and spit platform volume.

During the 42 year historical aerial photograph study, the inlet throat and proximal main ebb channel have been stable and have maintained an approximate shore normal orientation due to bedrock control at Twopenny Loaf on Coffins Beach, and tidal dominance of the channel. However, between 1943 and 1977, a clockwise downdrift migration of the main ebb channel of 25° has reoriented the channel from a northeasterly to a more easterly configuration (Figure 89). The seaward extent of the main ebb channel (1.22 km +/- 0.05 km) has not fluctuated greatly during the 42 year historical aerial photograph study except in 1943 when the seaward extent of the channel was 1.47 km.

Both of the channel margin linear bars have undergone considerable changes over the historical aerial photograph study which is due in part to changes in the orientation of the distal main ebb channel, but primarily to changes in sediment input and resulting volume of the ebb-tidal delta. For instance, in 1978 the small channel margin linear bar size reflects the small ebb-tidal delta volume. In addition, a more downdrift configuration of the main ebb channel resulted in the depletion and downdrift migration of sediment from the distal downdrift channel margin linear bar (refer to the 1978 diagram of Figure 89, Table 17 and Figure 62). Conversely, in 1965 and 1972, the channel margin linear bars were larger in size which correlates to the greater ebb-tidal delta volume. In addition, location and size of channel margin linear bar intertidal area changed with respect to the stage of the bar migration model. For instance, in 1965 the greatest channel margin linear bar intertidal area was located at proximal portions. This correlates well with sediment maximums at proximal locations associated with the bar migration model (midway between Stages 2 and 3 of Figure 88).

Extent of downdrift channel margin linear bar size and marginal flood channel development (scouring characteristics and width) are primarily responsible for morphological changes to the swash platform channel. For example, a well-developed distal downdrift marginal flood channel indicates that the majority of the tidal currents to the downdrift portions of the delta flow through the distal marginal flood channel. Therefore, less tidal currents and less scouring will occur in the swash platform channel. Examples of this correlation are shown in the diagrams of 1943, 1952, 1977, 1978, 1979 and 1985 (Figure 89).

Landward migration and attachment of swash bars to beaches have occurred periodically over the 42 year historical aerial photograph study. The ultimate attachment of these landward migrating swash bars to Coffins Beach occurs in discrete events while attachment of migrating swash bars to Crane Beach is less obvious. Two other characteristics of swash bar morphology are: 1) swash bar size and; 2) downdrift extent of the entire downdrift swash bar complex. The usual downdrift extent of this swash bar complex is 0.77 km +/- 0.16 km as measured from a line drawn in a shore-normal orientation from Twopenny Loaf. However, in 1978 the bar complex had a downdrift extent of 1.40 km. Both of these morphological characteristics are dependent upon the size of the ebb-tidal delta.

Both Crane and Coffins Beach have increased in width during the 130 year historical shoreline change study (1855-1985) by 120 m and 60 m, respectively (Figure 90). This increase in width is due to accretionary phases of beach ridge development which is primarily a result of the attachment of landward migrating swash bar complexes to the beach (Figure 89)(Table 17).

Significant increases in the volume of the southern end of Crane Beach have also occurred through spit accretion. From 1855 to 1984, this spit has increased from 3.70×10^4 m^3 to 2.43×10^5 m^3 (volume at MLW), an increase of 6.5 times its original volume (Figure 90). This spit accretion has narrowed and deepened the inlet throat. However, it is assumed that the cross sectional area of the inlet throat has not changed

due to similar tidal range and associated tidal prism throughout the time period.

Successive stages of the bar migration model are demonstrated in diagrams of the first three photographs (1943, 1952 and 1960). It is important to note that these three photographs do not depict consecutive stages of the bar migration model as this 17 year period is much longer than the estimated average 5-7 year bar migration cycle that occurs at Essex River Inlet.

The 1943 photograph, indicative of Stage 1, depicts a small ebb-tidal delta volume where channel margin linear bar volume is small, the majority of intertidal swash bars are offshore and no distinct accretionary phases of beach ridge development occur.

Stage 2 of the bar migration model is depicted in the 1952 photograph which shows an increase in ebb-tidal delta sediment volume and channel margin linear bar size and the proximal location of the majority of intertidal offshore sand bodies.

The 1960 photograph is indicative of Stage 3 as offshore sand bodies continue to decrease in size due to landward migration of sediment through swash bar migration and subsequent attachment to the beach. This attachment is demonstrated by the accretionary phase of beach ridge development at Coffins Beach.

STRATIGRAPHY

An overall ebb-tidal delta stratigraphic sequence model for the Essex River ebb-tidal delta is based upon comparison of general sedimentary structures recorded at the inlet with additional information from other studies including Moslow (1977) and Barwis and Hayes (1978) (Figure 91).

The thickness of the sequence is based upon the thickness of ebb-tidal delta sediments (3-5 m at MSL) and scouring depth of the main ebb and marginal flood channels. Despite the well-sorted nature of the entire

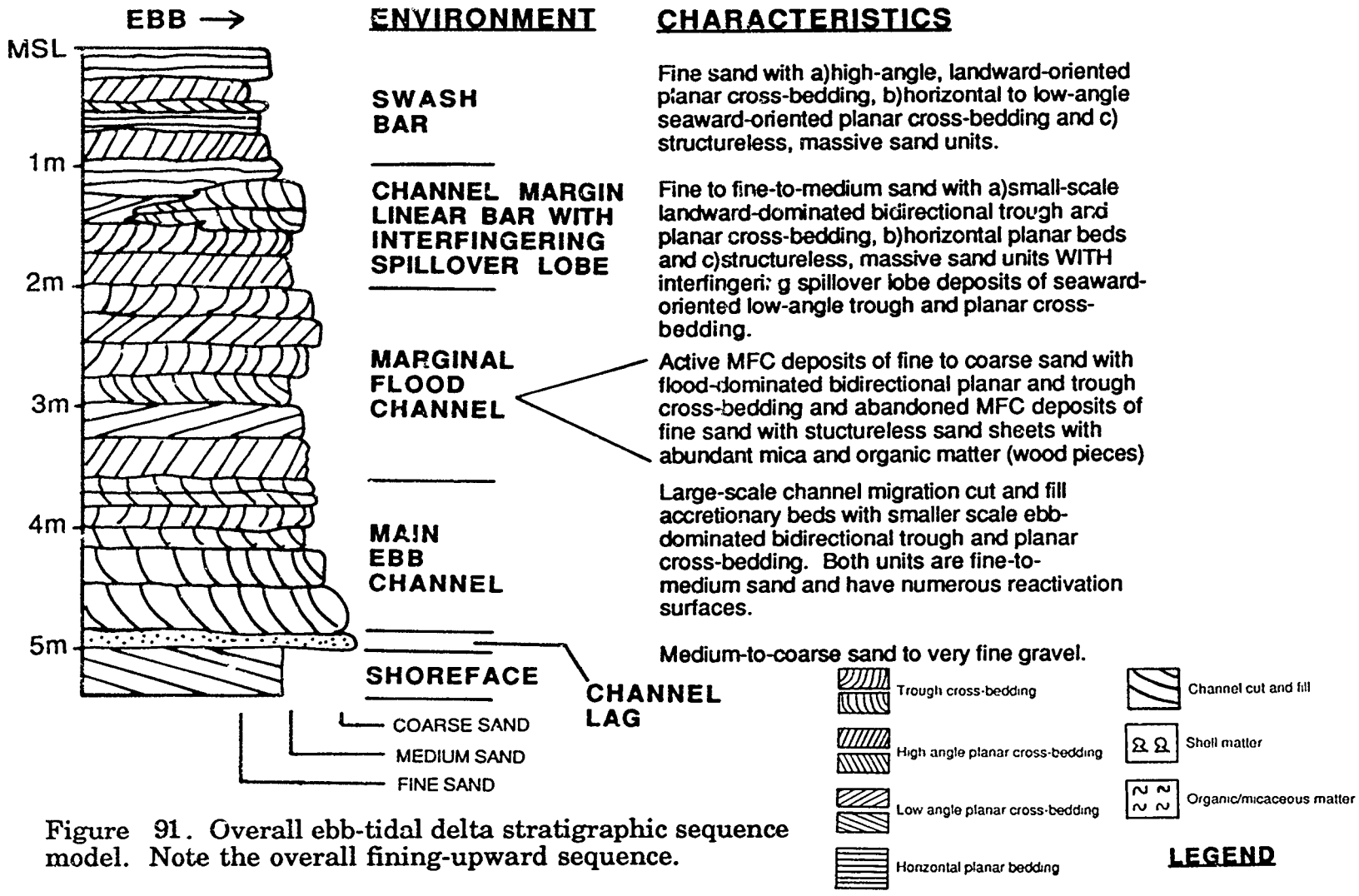

Figure 91. Overall ebb-tidal delta stratigraphic sequence model. Note the overall fining-upward sequence.

ebb-tidal delta, there exists a fining-upward sequence with increased sorting through the column which is a function of the less tidal and greater wave dominance of facies up the sequence.

At the base of the sequence, the channel lag at the Essex River ebb-tidal delta is not well-developed due to the lack of a coarse-grained source material. The main ebb channel facies is characterized by large-scale channel migration cut and fill accretionary beds and smaller scale high-angle ebb-dominated bidirectional cross-bedding. Numerous reactivation surfaces are present. This facies is the thickest and the most preservable part of the overall ebb-tidal delta sequence as it is stratigraphically deepest and therefore the least likely to be reworked (Barwis and Hayes, 1978). The marginal flood channel facies is characterised by flood-dominated bidirectional planar and trough cross-bedding associated with flood-dominant tidal currents. Numerous reactivation surfaces occur throughout this facies.

Wave-dominated facies of the ebb-tidal delta sequence model include the shallow channel margin linear bar facies which is ephemeral compared to the tide-dominated facies due to reworking of sediments by swash processes. This facies is characterized by: 1) landward-dominated bidirectional trough and planar cross-bedding associated with wave-enhanced flood-tidal currents; 2) horizontal planar beds and massive sand sheets associated with swash processes and; 3) seaward-oriented low-angle planar and trough cross-bedding associated with interfingering spillover lobe deposits and expansion of the ebb jet. The sequence is capped by the swash bar facies, which also tends to be reworked by wave activity. This facies is characterized by landward-oriented high-angle planar cross-bedding associated with slipface migration, and horizontal to low-angle offshore-oriented planar cross-bedding associated with vertical accretion.

The stratigraphy of the Essex River ebb-tidal delta can further be divided into updrift, downdrift and distal stratigraphic sequences whose characteristics are dependent upon different sedimentary processes occurring at each locality. Three major processes include: 1) main ebb

channel migration and associated cut and fill accretionary beds associated with migrations of the distal main ebb channel; 2) abandoned marginal flood channel accretion and; 3) swash bar migration.

The updrift ebb-tidal delta stratigraphic sequence model is dominated by main ebb channel cut and fill large-scale gently dipping accretionary cross beds (Figure 92). The 6 m depth of this column, which scours below the 5 m depth of the ebb-tidal delta deposits, is a result of the maximum depth of main ebb channel scouring at updrift portions of the delta. These cut and fill deposits are overlain by thin channel margin linear bar (1 m) and swash bar (1m) facies, both of which are dominated by landward-oriented cross-beds associated with wave-augmented flood-tidal currents. The thickness of the swash bar facies is dependent upon the scouring depth as indicated by the height of the updrift swash bar slipface (0.5-1.0 m). Note the absence of marginal flood channel facies in this sequence as the updrift marginal flood channel is stable.

The downdrift ebb-tidal delta stratigraphic sequence model (Figure 93) is dominated by abandoned marginal flood channel and swash bar facies due to the landward migration of the large downdrift swash bar into the marginal flood channel. Note the absence of main ebb channel cut and fill accretionary beds as the main ebb channel does not migrate into this environment.

The thin overall thickness of this sequence (3.5 m) is dependent upon migrations and associated scouring depth of the downdrift marginal flood channel which is a function of position and size of the landward migrating swash bar. The 1.25 m thick abandoned marginal flood channel deposits are composed of gently-dipping large-scale accretionary sand wedges associated with deposition of sediment from the swash bar and downdrift channel margin linear bar and settling of fine-grained sediment (including mica and organic (wood) matter) believed to be deposited by ebb-currents from the backbarrier. The 2 m thick swash bar deposits are much thicker than the swash bar deposits of the updrift swash bar due to the greater scouring depth.

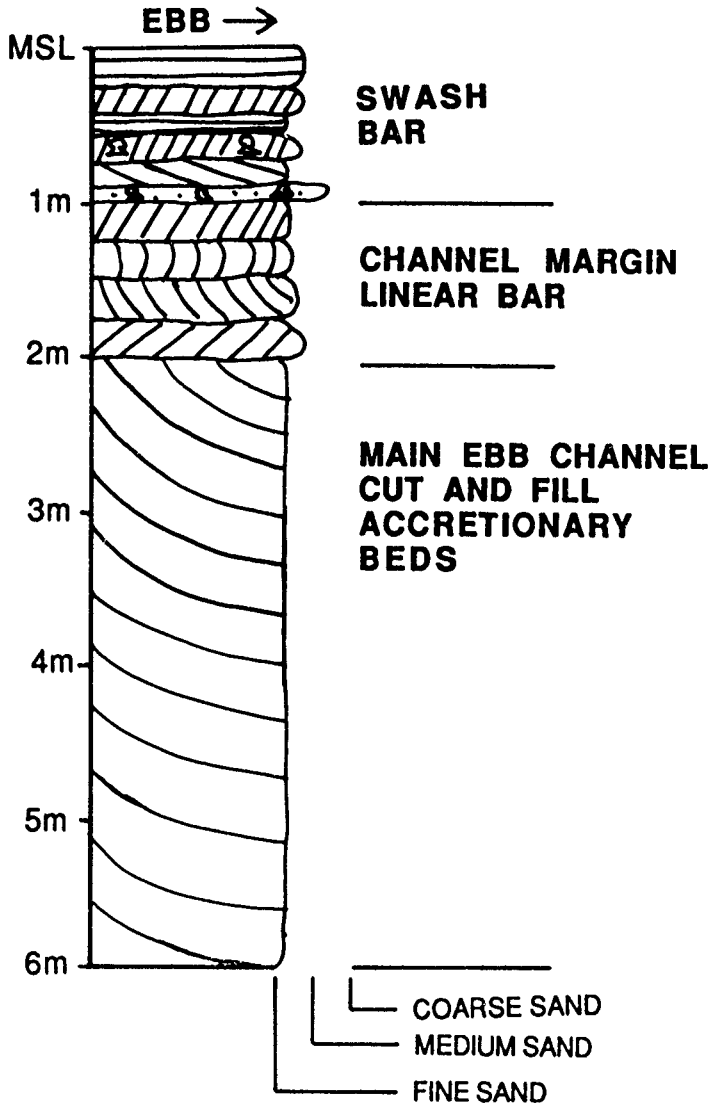

Figure 92. Stratigraphic sequence model for the updrift portion of the Essex River ebb-tidal delta. Note the dominance of main ebb channel cut and fill accretionary beds in this sequence.

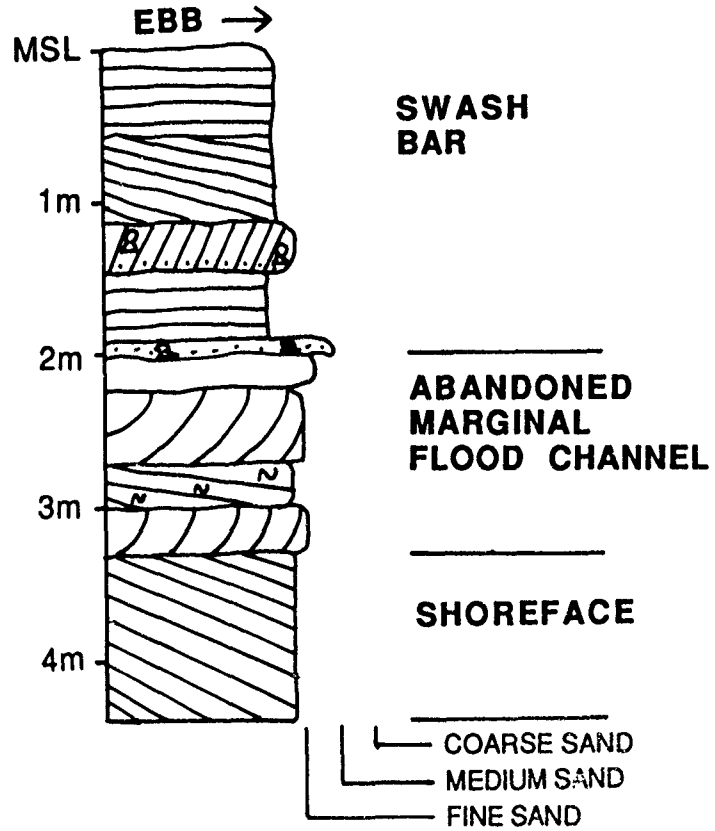

Figure 93. Stratigraphic sequence model for the downdrift portion of the Essex River ebb-tidal delta. Note the dominance of swash bar deposits in this sequence.

The distal ebb-tidal delta stratigraphic sequence is similar to the overall ebb-tidal delta sequence but is dominated by 1.5 m thick main ebb channel cut and fill accretionary bed deposits (Figure 94). This facies overlies tidally-derived active main ebb channel deposits. The sequence is floored by a channel lag. Overlying the main ebb channel cut and fill facies are wave-dominated channel margin linear bar and swash bar deposits. Sorting characteristics improve slightly in wave-dominated units as does the greater amount of shell matter. Note the slight fining-upward sequence which occurs over the entire column.

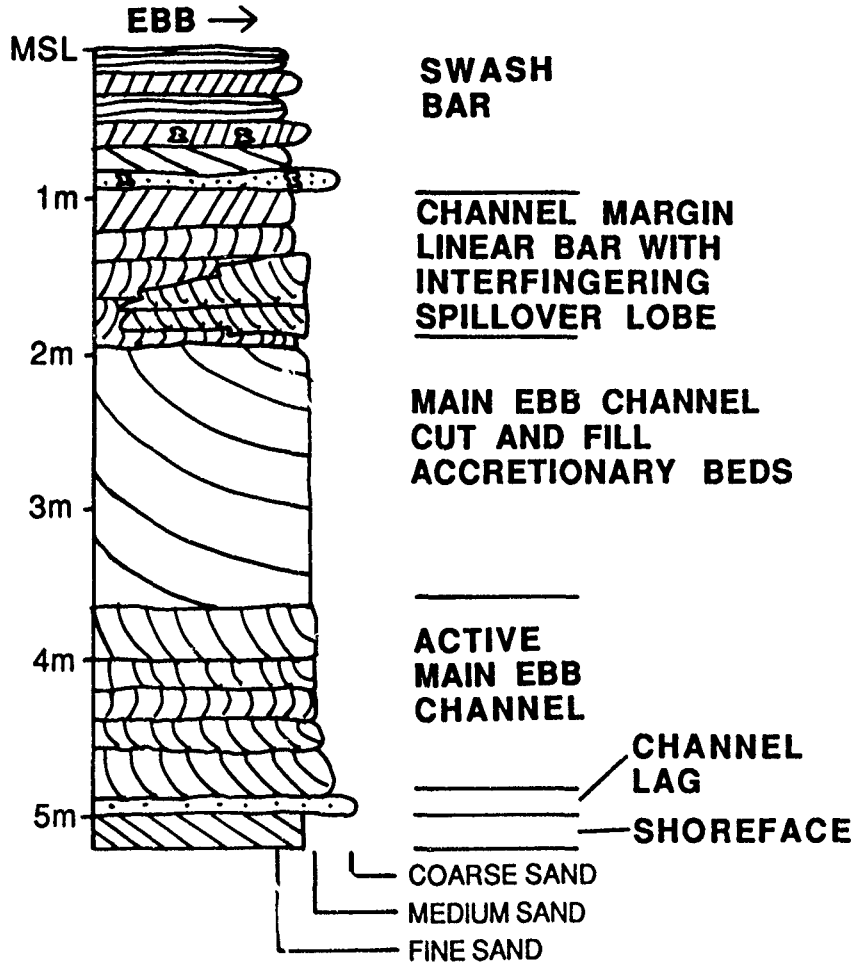

Figure 94. Stratigraphic sequence model for the distal portion of the Essex River ebb-tidal delta. Note the overall fining-upward sequence over the entire 5 m column.

CONCLUSIONS

1) The Essex River Inlet, with a mean tidal range of 2.7 m and a deepwater wave height of 1.2 m is classified as a mixed energy, tide-dominated inlet (cf. Hayes, 1979). The stability of the inlet throat and proximal main ebb channel is due to the presence of bedrock at Twopenny Loaf on Coffins Beach. Migrations of the distal main ebb channel of up to 700 m over a 42 year period (1943-1985) are the result of the southerly longshore transport system and sediment input into the system.

2) Inlet sediment bypassing through stable inlet processes (cf. FitzGerald, 1984) is the major process which transports sand from the updrift side of the Essex River Inlet shoreline to the downdrift side. Patterns of sediment transport within the ebb-tidal delta are dominated by gyres for both updrift and downdrift portions of the delta. These gyres, whose sediment is first introduced to updrift portions of the delta by southerly longshore currents, transport sediment through the marginal flood channel and over the channel margin linear bar into the main ebb channel, seaward through sandwave migration in the main ebb channel and subsequently back onshore through swash processes along the terminal lobe and swash bar migration. The updrift counterclockwise gyre is completed as small, ephemeral swash bars migrate landward eventually attaching to Crane Beach in indiscrete packages. These swash bars have slipfaces on the order of 0.25-0.50 m in height and have migrated over 5 m/week associated with one storm event.

In the downdrift clockwise gyre, sediment moving out the main ebb channel is added to sand delivered by southerly longshore sediment transport along the terminal lobe. Southerly migrations of the main ebb channel also contribute sediment thus resulting in the growth of a large downdrift swash bar. This swash bar, which has slipfaces of up to 1.0 m in height, migrates landward 70 m/year and ultimately welds to Coffins Beach in discrete welding events. Wave refraction around this bar

produces a transport reversal which introduces sand back into the main ebb channel and downdrift of the delta to more southerly portions of Coffins Beach.

Ebb-tidal delta volumetric changes occur in a 5-7 year cycle where swash bars form, migrate and attach to the landward beach. These changes, as shown in a bar migration model (cf. FitzGerald, 1984) demonstrate that the ebb-tidal delta volume is directly related to the size and position of the swash bars and holds an inversely proportional relationship to beach sediment volume.

3) Current patterns and subtidal bedforms at the Essex River Inlet suggest that the inlet throat and the main ebb channel are dominated by ebb-tidal currents. The inlet throat has maximum velocities of 1.0 m/s for mean tidal ranges and ebb-oriented sandwaves with wavelengths up to 40 m and waveheights up to 2 m. The marginal flood channels are dominated by flood-tidal currents as maximum flood currents of up to 0.80 m/s are twice as strong as maximum ebb currents. The swash platform channel is slightly flood-dominant.

Intertidal sand bodies are dominated by landward-oriented currents. The proximal channel margin linear bars are dominated by flood-oriented sandwaves and megaripples associated with flood-tidal currents. Distal and internal channel margin linear bars, and swash bars are dominated by plane beds and landward-oriented current lineations associated with wave-generated flood currents. The distal channel margin linear bars also have ebb-oriented megaripples associated with the expansion of the ebb jet.

4) The delta is composed of very well to well-sorted (0.21Ø - 0.50Ø) fine to medium-grained sand (1.75Ø - 2.50Ø). Three overall grain size trends of the delta are present. First, tidal channel environments tend to be the coarsest-grained followed by environments with both wave and tidal components (i.e. proximal channel margin linear bar). The wave-dominated environments (i.e. swash bar, distal channel margin linear

bar) are the finest-grained environment. Second, a fining trend in grain size occurs from the inlet throat to offshore areas seaward of the terminal lobe. Lastly, the updrift portion of the delta is composed primarily of fine sand (2.19Ø) while the downdrift portion of the delta is composed of medium sand (1.84Ø). This latter grain size trend may be explained by the Essex River Inlet acting as a coarse-grained sediment trap.

5) The sedimentary sequences of tide versus wave-dominated settings can be differentiated. Tide-dominated settings are dominated by bidirectional trough cross-bedding with some planar cross-bedding. Wave-dominated settings are dominated by a) homogeneous, structureless sand sheets and horizontal to low-angle seaward-dipping planar cross beds and b) high-angle planar cross-beds associated with slipface migration.

6) The stratigraphic framework of the Essex River ebb-tidal delta is based upon three dominant processes: 1) main ebb channel migration and associated cut and fill accretionary beds; 2) abandoned marginal flood channel accretion and; 3) swash bar migration. Environments can be further differentiated by smaller scale subsurface sedimentary structures which are formed from the migration of surficial bedforms. An overall ebb-tidal delta stratigraphic sequence divides the Essex River ebb-tidal delta into five units. Overlying the shoreface deposits in ascending order are the following units: 1) Basal channel lag; 2) Main ebb channel; 3) Marginal flood channel; 4) Channel margin linear bar with interfingering spillover lobe and; 5) Swash bar. A fining-upward trend occurs throughout the sequence.

The stratigraphy of the Essex River ebb-tidal delta can be divided further into three stratigraphic sequence models whose characteristics are a result of different sedimentary processes occurring at each locality. The updrift ebb-tidal delta sequence is dominated by main ebb channel cut and fill accretionary beds. Channel margin linear bar and swash bar deposits overlie this unit. The downdrift ebb-tidal delta sequence is dominated by abandoned marginal flood channel and swash bar

migration deposits. Distally, the ebb-tidal delta is dominated by an active main ebb channel and overlying main ebb channel cut and fill accretionary bed unit. The sequence is capped by channel margin linear bar and swash bar deposits.

REFERENCES

Abele, R.W., 1977, Analysis of short-term variations in beach morphology for summer and winter periods, 1971-72, Plum Island, Massachusetts, U.S. Army Corps of Engineers, Coastal Engineering Research Center, Fort Belvoir, VA. Miscellaneous Report # 77-5, 101 p.

Ashley, G.M., 1990, Classification of large scale subaqueous bedforms: A new look at an old problem: Journal of Sedimentary Petrology, vol. 60, no. 1, p.160-172.

Barosh, P.J., 1979, Paleozoic plate boundary conditions in southeastern New England: Geological Society of America Abstracts with Programs, vol. 11, no. 1, p.?-3.

_____, 1984, Regional Geology and tectonic history of Southeastern New England in Hanson, L., ed., Geology of the Coastal Lowland, Boston to Kennebunk, Maine, 76th Annual meeting of the New England Intercollegiate Geological Conference, p. I1-I35.

Barwis, J.H. and Hayes, M.O., 1978, Regional patterns of barrier island and tidal inlet deposition applied to hydrocarbon exploration in Saxena, R., ed., Stratigraphic Concepts in Hydrocarbon Exploration: Short Course sponsored by GCAGS and NOGS, New Orleans, La.

Boothroyd, Jon C., 1985, Tidal inlets and deltas in Davis, R.A., ed. Coastal Sedimentary Environments: New York, Springer-Verlag, p.445-525.

Boyd, R., Hall, R.K. and Bowen, A.J., 1987, An evolutionary model for transgressive sedimentation on the eastern shore of Nova Scotia in FitzGerald, D.M. and Rosen, P., eds., Glaciated Coasts: New York, Academic Press, p.87-114.

Bruun, P., 1966, Tidal inlets and littoral drift: Vol. 2, Universitalsforlaget, Oslo, 193 p.

Bruun, P. and Gerritsen, F., 1959, Natural bypassing of sand at coastal inlets: American Society of Civil Engineers, Waterways and Harbors Division Journal, vol. 85WW4, Paper 2301, p. 75-107.

Cameron, B. and Naylor, R.S., 1976, General geology of southeastern New England in Cameron, B., ed., Geology of Southeastern New

England, 68th Annual meeting of the New England Intercollegiate Geological Conference, p.13-37.

Chute, N. E., 1940, Surficial geologic map of the Gloucester Quadrangle, Massachusetts: U.S. Geological Survey Geologic Quadrangle.

Corson, W.D., Resio, D.T., Brooks, R.M., Ebersole, B.A., Jensen, R.E., Ragsdale, D.S., Tracy, B.A., 1982, Atlantic Coast Hindcast, Phase II Wave Information: WIS Report 6, U.S. Army Corps of Engineers, Hydraulics Laboratory, Vicksburg, MS.

Davies, J.L., 1964, A morphogenetic approach to world shorelines: Zeits fur Geomorphologie, vol. 8, p.127-142.

Davis, R. A., 1983, Depositional Systems: A Genetic Approach to Sedimentary Geology: Englewood Cliffs, Prentice-Hall, 669 p.

DeAlteris, J.T. and Byrne, R.J., 1975, The recent history of Wachapreague Inlet, Virginia in Cronin, L.E., ed. Estuarine Research: Vol. 2, Geology and Engineering: New York, N.Y., Academic Press, p.167-181.

Dean, R.G., and Walton, T.L., 1975, Sediment transport patterns in the vicinity of inlets with special reference to sand trapping in Cronin. L.E., ed., Estuarine Research: Vol. 2, Geology and Engineering: New York, N.Y., Academic Press, p. 129-149.

Farrell, S.C., 1969, Growth cycle of a small recurved spit, Plum Island, Massachusetts in Hayes, M. O., ed., Coastal Research Group, Coastal Environments, northeast Massachusetts and New Hampshire, Cont. No. 1-CRG, Geology Department, University of Massachusetts, p. 316-336.

Finley, R.J., 1975, Hydrodynamics and tidal deltas of North Inlet, South Carolina in Cronin, L.E., ed., Estuarine Research: Vol. 2, New York, N.Y., Academic Press, p. 277-292.

_____, 1976, Hydraulics and dynamics of North Inlet, South Carolina, 1974-75: General Investigation of Tidal Inlets, Report 10, U.S. Army Corps of Engineers, Coastal Engineering Research Center, Fort Belvoir, Virginia, 188 p.

_____, 1978, Ebb-tidal delta morphology and sediment supply in relation to seasonal wave energy flux, North Inlet, South Carolina: Journal of Sedimentary Petrology, vol. 48, p. 227-238.

FitzGerald, D.M., 1976, Ebb-tidal delta of Price Inlet, South Carolina: Geomorphology, physical processes and associated changes in inlet shape in Hayes, M.O. and Kana, T.W., eds. Terrigenous Clastic Depositional Environments Report # 11-CRD, Coastal Research Division, Dept. of Geology, Univ.of South Carolina, p.II-143 - II-157.

FitzGerald, D.M., 1982, Sediment bypassing at mixed energy tidal inlets: Proceedings 18th Coastal Engineering Conference, American Society of Civil Engineers, Cape Town, South Africa, p. 1094-1118.

FitzGerald, D.M., 1984, Interactions between the ebb-tidal delta and landward shoreline: Price Inlet, South Carolina: Journal of Sedimentary Petrology vol. 54, no.4, p.1303-1318.

FitzGerald, D.M., Nummedal, D. and Kana, T.W., 1976, Sand circulation patterns at Price Inlet, South Carolina: Proc. 15th Coastal Eng. Conference, American Society of Civil Engineers, Honolulu, Hawaii, July 11-17, 1976, p.1868-1880.

FitzGerald, D.M. and FitzGerald, S.A., 1977, Factors influencing tidal inlet throat geometry: Proc. of Coastal Sediments, 1977, Am. Soc. of Civ. Eng., Charleston, South Carolina, Nov. 2-4, 1977, p. 563-581.

FitzGerald, D.M. and Nummedal, D., 1977, Ebb-tidal delta stratification in: Nummedal, D., ed., Beaches and Barriers of the Central Carolina Coast: Coastal Sediments 1977, Field Trip Guidebook.

FitzGerald, D.M. and Nummedal, D., 1983, Response characteristics of an ebb-tidal delta inlet channel: Journal of Sedimentary Petrology, vol. 53, p. 833-845.

Folk, R.L, 1980, Petrology of Sedimentary Rocks: Austin, Texas, Hemphill publishing Co.,184 p.

Goodbred, S.L. and Montello, T.M., 1989, A study of the morphological characteristics of Plum Island, Crane, Coffins and Wingaersheek Beaches, MA.: Dept. Geology, Boston Univ. unpublished report, 15 p.

Harms, J.C., Southard, J.B., Spearing, D.R., and Walker, R.G., 1975, Depositional environments as interpreted from primary sedimentary structures and stratification sequences: Lecture Notes, Soc. of Econ. Paleo. and Min. Short Course 2, Dallas, TX, 161 p.

Hayes, M.O., 1975, Morphology of sand accumulation in estuaries: An introduction to the symposium: in Cronin, L.E. ed., Estuarine

Research: Vol. 2, Geology and Engineering, New York, Academic Press, p.3-22.

Hayes, M.O., 1977, Part 1-Lecture notes in Hayes, M.O., and Kana, T.W., eds.,Terrigenous Clastic Depositional Environments, Technical Report No. 11-CRD, Coastal Research Division, Dept. of Geology, Univ. of South Carolina, Columbia, South Carolina, p. I-1 - I-74.

Hayes, M.O., 1979, Barrier island morphology as a function of tidal and wave regime: in Leatherman, S.P., ed., Barrier Islands from the Gulf of St. Lawrence to the Gulf of Mexico: New York, Academic Press, p.3-22.

Hayes, M.O., 1980, General morphology and sediment patterns in tidal inlets: Journal of Sedimentary Petrology, vol. 26, p. 139-156.

Hayes, M.O., Hubbard, D.K. and FitzGerald,D.M., 1973, Investigation of beach erosion probelems at Revere, Winthrop and Nantasket Beaches, Massachusetts: Final Report for Boston Metropolitan District Commission, 149 p.

Hine, A.C., 1975, Bedform distribution and migration patterns on tidal deltas in the Chatham Harbor estuary, Cape Cod, Massachusetts in Cronin, L.E., ed. Estuarine Research: Vol. 2, Geology and Engineering: New York, Academic Press, p. 235-252.

Hine, A.C., Snyder, S.W., and Neumann, A.C., 1979, Coastal plain and inner shelf structure, stratigraphy and geologic history: Bogue Banks area, North Carolina: Part 3- The Holocene high sedimentation interval-A hypothesis: A Final Report to the North Carolina Science and Technology Committee, p.1-18.

Hubbard, D.K., 1975, Morphology and hydrodynamics of the Merrimack River ebb-tidal delta in Cronin, L.E., ed. Estuarine Research: Vol. 2, Geology and Engineering: New York, Academic Press, p. 253-266.

Hubbard, D.K., 1976, Changes in inlet offset due to stabilization: Proceedings of the 15th Coastal Engineering Conference, Am. Soc. Civ. Eng., Honolulu, Hawaii, July 11-17, 1976, p. 1812-1823.

Hubbard, D.K., 1977, Variations in tidal inlet processes and morphology in the Georgia Embayment: Technical Report No. 14-CRD, Coastal Research Division, Dept. of Geology, Univ. of South Carolina, Columbia, South Carolina, 79 p.

Hubbard, D.K., Barwis, J.H. and Nummedal, D., 1977, Sediment transport in four South Carolina Inlets: Proceedings of Coastal Sediments 1977, American Society of Civil Engineers, Charleston, South Carolina, Nov. 2-4, 1977 p. 582-601.

Hubbard, D.K., Oertel, G.F. and Nummedal, D., 1979, The role of waves and tidal currents in the development of tidal sedimentary structures and sand body geometry: examples from North Carolina, South Carolina and Georgia: Journal of Sed. Petrology, V. 49, p.1073-1092.

Humphries, S.M., 1977, Morphologic equilibrium of a natural tidal inlet: Coastal Sediments 1977, Proceedings of the Fifth Symposium, WPCO Division, American Society of Civil Engineers, Charleston, South Carolina, November 2-4, 1977, p. 734-753.

Imperato, D.P., Sexton, W.J. and Hayes, M.O., 1988, Stratigraphy and sediment characteristics of a mesotidal ebb-tidal delta, North Edisto Inlet, South Carolina, Journal of Sed. Pet., vol. 58, no. 6, p.950-958.

Jarrett, J.T., 1976, Tidal prism-inlet area relationships: U.S. Army Corps of Engineers GITI Report 3, 55 p.

Jensen, R.E., 1983, Atlantic coast hindcast shallow water significant wave information: WIS Report 9, U.S. Army Corps of Engineers, Hydraulics Laboratory, Vicksburg, MS.

Kaye, C.A., 1964, Outline of the Pleistocene geology of Martha's Vineyard, Massachusetts: U.S. Geological Survey Prof. Paper 501-C, p. C134-C139.

Keulegan, G.H., 1967, Tidal flows in entrances: water level fluctuations of basins in communication with seas: Technical Bulletin 14, Committee on Tidal Hydraulics, U.S. Army Corps of Engineers, p. 1827-1844.

King, C.A.M., 1972, Beaches and Coast: London, England, Edward Arnold, 2nd edition, 570 p.

Komar, P.D., 1976, Beach Processes and Sedimentation: Englewood Cliffs, N.J., Prentice-Hall, 429 p.

Kumar, N. and Sanders, J.E., 1974, Inlet sequences: A vertical succession of sedimentary structures and textures created by the lateral migration of tidal inlets: Sedimentology, vol. 21, p. 491-533.

Lanesky, D.B., Logan, B.W., Brown, R.G. and Hine, A.C., 1979, A new approach to portable vibra-coring underwater and on land: Journal of Sedimentary Petrology, vol. 49, p. 654-657.

Maddock, T. Jr., 1969, The behavior of straight open channels with moveable beds: U.S. Geological Survey Prof. Paper 622-A, 70 p.

Moslow, T.F., 1977 Internal stratification of tidal delta deposits in Nummedal, D., ed., Beaches and Barriers of the Central South Carolina Coast, Coastal Sediments 1977, Field trip Guidebook, p.45-51.

Mota-Oliveira, I.B., 1970, Natural flushing ability in tidal inlets: Proceedings 12th Coastal Engineering Conference, American Society of Civil Engineers, p. 1827-1844.

McIntyre, W.G. and Morgan, J.P., 1963, Recent geomorphic history of Plum Island and adjacent coasts: Coastal Study Series, Louisiana State University, LSU Press, Baton Rouge, Louisiana.

Nelligan, D., 1983, Ebb-tidal delta stratigraphy: Geology Department, University of South Carolina, unpublished masters thesis, 178 p.

Newman, W.S., Marcus, L.F., Pardi, R.P., Paccione, J.A. and Tomecek, S.M., 1980, Eustasy and deformation of the geoid: 1000-6000 radiocarbon years BP in Morner, N.A., ed., Earth Rheology, Isostasy and Eustasy: John Wiley and Sons, Chicestern England, p.555-567.

Nummedal, D., and Fischer, I., 1978, Process-response models for depositional shorelines, the German and Georgia Bights: Proc. of the 16th Coastal Engineering Conference, Am. Soc. of Civ. Eng., Hamburg, Germany, Aug. 27-Sept. 3, 1978, p. 1215-1232.

Oertel, G.F., 1975, Ebb-tidal deltas in Georgia estuaries in Cronin, L.E., ed., Estuarine Research: vol. 2, Geology and Engineering , New York, N.Y., Academic Press, p.267-276.

Oldale, R.N., 1985, Late Quaternary sea-level history of New England: a review of the published sea-level data: Northeastern Geology, vol. 7, no. 3/4, p.192-200.

Oldale, R.N., Wommack, L.E., and Whitney, A.B., 1983, Evidence for a postglacial low relative sea level stand in the drowned delta of the Merrimack River, Western Gulf of Maine: Quaternary Research, vol. 33, p.325-336.

Postma, H., 1961, Transport and accumulation of suspended matter in the Dutch Wadden Sea: Netherlands Journal of Sea Research, Vol. 1, p. 148-190.

Pratt, R.M, and Schlee, J.S., 1969, Glaciation on the continental margin off New England: Geological Society of America Bulletin, vol. 80, p. 2335-2342.

Rhodes, E.G, 1973, Pleistocene-Holocene sediments interpreted by seismic refraction and wash bore sampling, Plum Island-Castle Neck, MA.: Technical memo No. 40, U.S. Army Corps of Engineers Coastal Engineering Research Center, Vicksburg, MS., 75 p.

Schafer, J.P. and Hatrshorn, J.H., 1965, The Quaternary of New England in Wright, H.E. and Frey, D.G., eds., The Quaternary of the United States: Princeton, New Jersey, Princeton University Press, p.113-128.

Schnitker, D., 1984, Postglacial emergence of the Gulf of Maine: Geological Society of America Bulletin, vol. 85, p.491-494.

Sha, L.P., 1989, Sand transport patterns in the ebb-tidal delta off Texel Inlet, Wadden Sea, The Netherlands: Marine Geology, vol. 86, p.137-154.

Sha, L.P., 1989, Variation in ebb-tidal delta morphologies along the West and East Frisian Islands, The Netherlands and Germany: Marine Geol., vol. 89, p. 11-28.

Sha, L.P., 1990, Surface sediments and sequence models in the ebb-tidal delta of Texel Inlet, Wadden Sea, the Netherlands in Sha, L.P., ed. Sedimentological studies of the Ebb-Tidal Deltas Along the West Frisian Islands, the Netherlands: Geologica Ultraiectina No. 64.

Shalk, M.A., 1936, A textural study of certain New England Beaches: Division of Geological Sciences, Harvard University, unpublished Doctorate Thesis.

Som, M.R, 1990, Stratigraphy and the evolution of a backbarrier region along a glaciated coast of New England: Castle Neck-Essex Bay, MA.: Geology Department, Boston University, unpublished Master's Thesis, 185 p.

Stone, B.D., and Peper, J.D., 1982, Topographic control of the deglaciation of eastern Massachusetts: ice lobation and the marine incursion in Larson, G.J. and Stone, B.D., eds., Late Wisconsin

Glaciation of New England, Kendall/Hunt Publishing Co., Dubuque, Iowa, p.145-166.

Sverdrup Corporation, 1990, Subsurface exploration report for inter-island tunnel: Deer Island, Boston, Massachusetts: Mass. Water Resources Authority Contract # 5494.

Swift, D.J.P., 1975, Barrier island genesis: Evidence from the Central Atlantic Shelf, Eastern U.S.A.: Sedimentary Geology, vol.14, p. 1-43.

U. S. Army Corps of Engineers, 1984, Shore Protection Manual: U.S. Army Corps of Engineers, Coastal Engineering Research Center, Vicksburg, MS.

Van den Berg, J.H., 1989, The Oosterschelde ebb-tidal delta in Nio, S.D. and Yang, C.S., eds., Recognition of Tidally In fluenced Facies and Environments: Short Course Note Series #1, Part 4, p.151-154.

Van Veen, J., 1936, Onderzoekingen in de Hoofden: Landsdrukkerij, Den Haag, 252 p.

Walton, T.L. and Adams, W.D., 1976, Capacity of inlet outer bars to store sand: Proceedings of the 15th Coastal Engineering Conference, July 11-17, 1976, Honolulu, Hawaii, p.1919-1937.

Wentworth, C.K., 1922, A scale of grade and class terms for clastic sediments: Journal of Geology, vol. 30, p. 377-392.

APPENDIX A:

BEACH PROFILE DATA

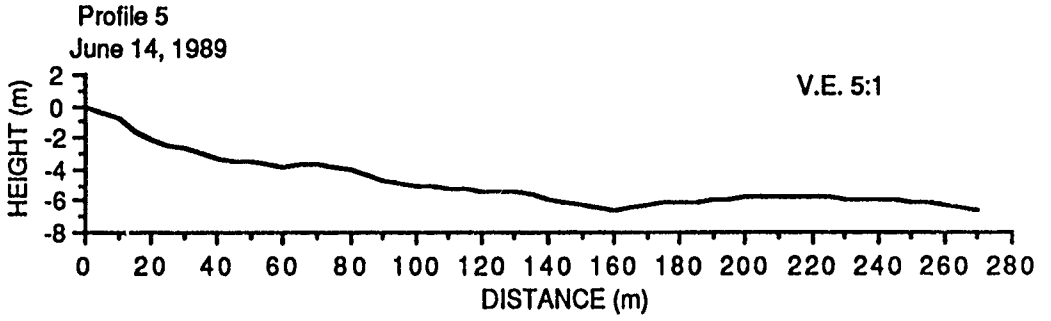
Profile 5
June 14, 1989
V.E. 5:1
HEIGHT (m)
2
0
-2
-4
-6
-8
0 20 40 60 80 100 120 140 160 180 200 220 240 260 280
DISTANCE (m)

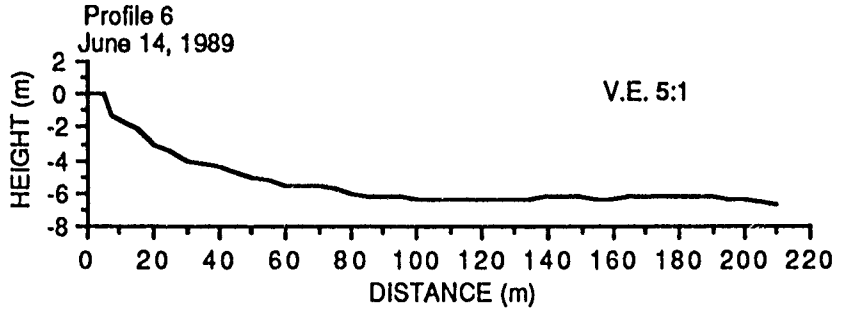
Profile 6
June 14, 1989
V.E. 5:1
HEIGHT (m)
2
0
-2
-4
-6
-8
0 20 40 60 80 100 120 140 160 180 200 220
DISTANCE (m)

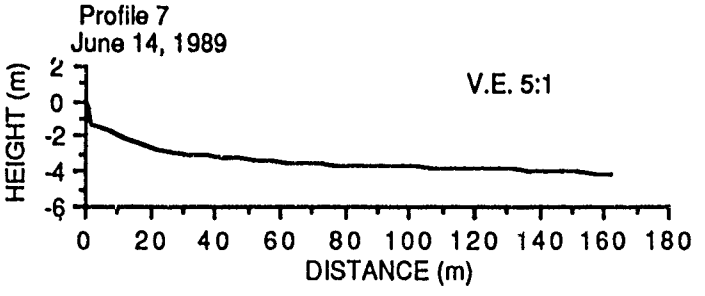
Profile 7
June 14, 1989
V.E. 5:1
HEIGHT (m)
2
0
-2
-4
-6
0 20 40 60 80 100 120 140 160 180
DISTANCE (m)

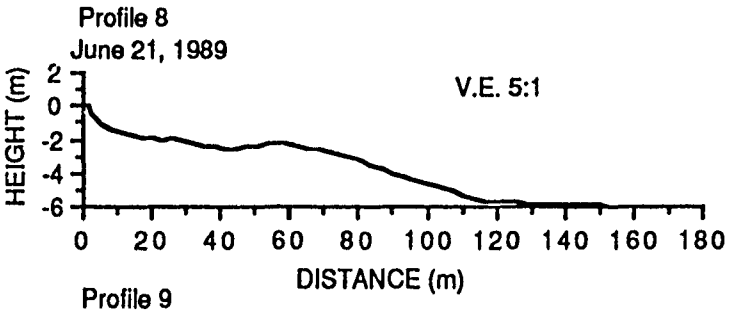
Profile 8
June 21, 1989
V.E. 5:1
HEIGHT (m)
2
0
-2
-4
-6
0 20 40 60 80 100 120 140 160 180
DISTANCE (m)

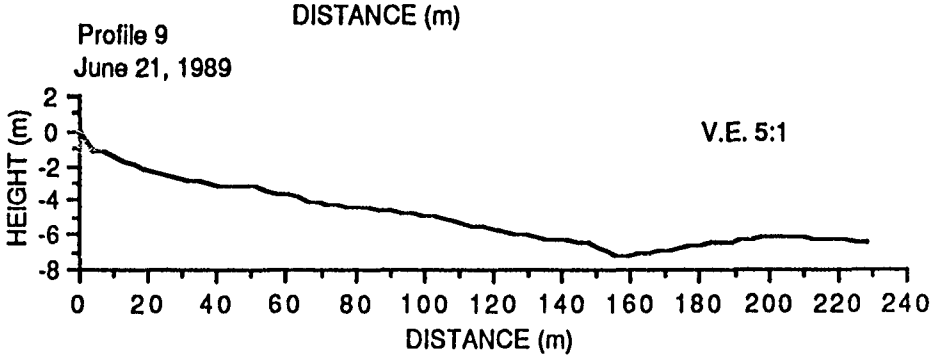
Profile 9
June 21, 1989
V.E. 5:1
HEIGHT (m)
2
0
-2
-4
-6
-8
0 20 40 60 80 100 120 140 160 180 200 220 240
DISTANCE (m)

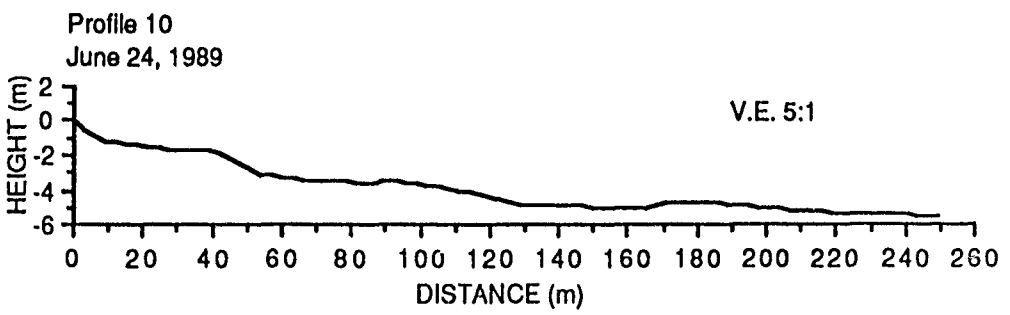
Profile 10
June 24, 1989
V.E. 5:1
HEIGHT (m)
2
0
-2
-4
-6
0 20 40 60 80 100 120 140 160 180 200 220 240 260
DISTANCE (m)

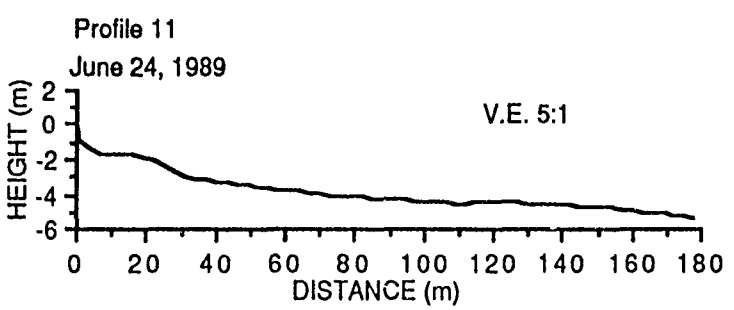
Profile 11
June 24, 1989
V.E. 5:1
HEIGHT (m)
2
0
-2
-4
-6
0 20 40 60 80 100 120 140 160 180
DISTANCE (m)

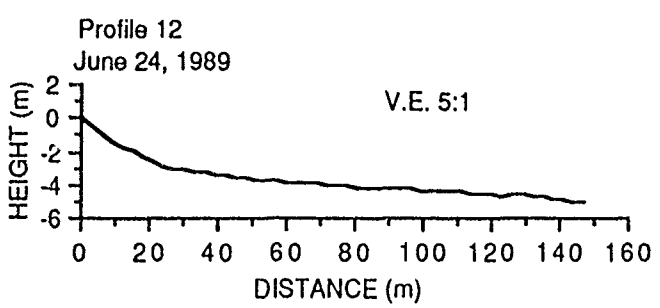
Profile 12
June 24, 1989
V.E. 5:1
HEIGHT (m)
2
0
-2
-4
-6
0 20 40 60 80 100 120 140 160
DISTANCE (m)

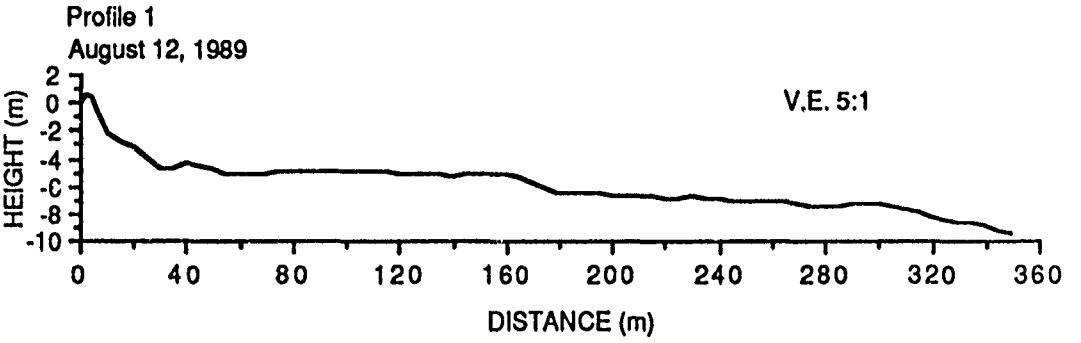
Profile 1
August 12, 1989
V.E. 5:1
HEIGHT (m)
2
0
-2
-4
-6
-8
-10
0
40
80
120
160
200
240
280
320
360
DISTANCE (m)

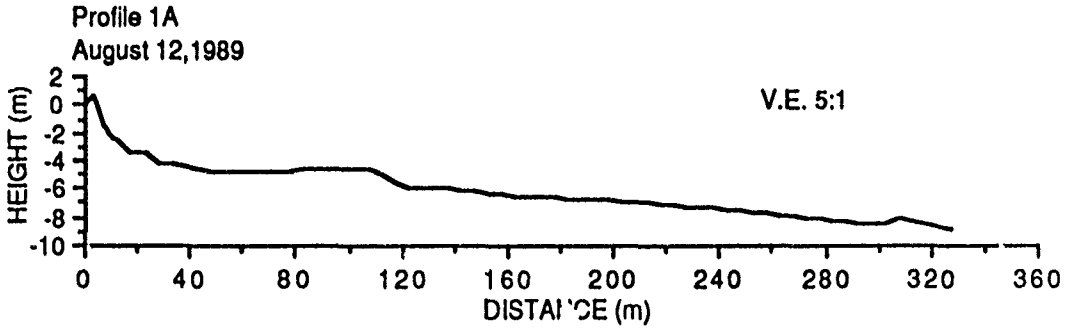
Profile 1A
August 12,1989
V.E. 5:1
HEIGHT (m)
2
0
-2
-4
-6
-8
-10
0
40
80
120
160
200
240
280
320
360
DISTANCE (m)

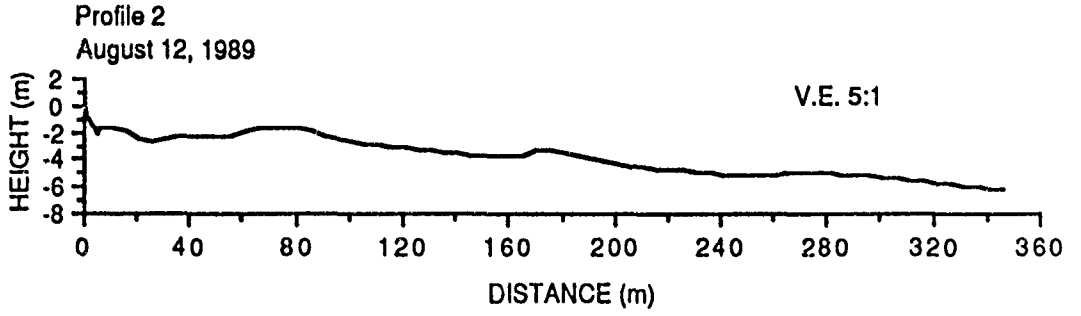
Profile 2
August 12, 1989
V.E. 5:1
HEIGHT (m)
2
0
-2
-4
-6
-8
0
40
80
120
160
200
240
280
320
360
DISTANCE (m)

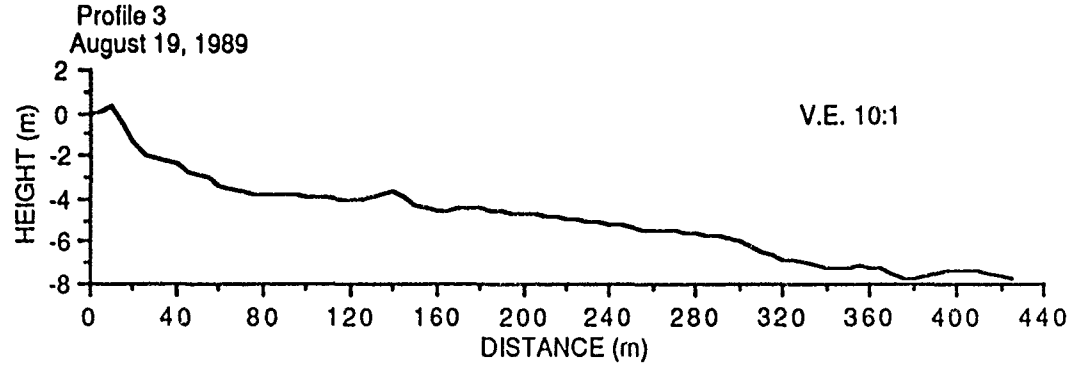
Profile 3
August 19, 1989
V.E. 10:1
HEIGHT (m)
2
0
-2
-4
-6
-8
0
40
80
120
160
200
240
280
320
360
400
440
DISTANCE (m)

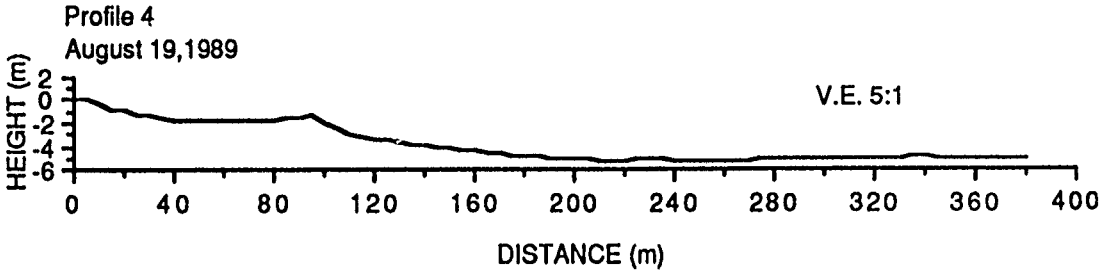
Profile 4
August 19,1989
V.E. 5:1
HEIGHT (m)
2
0
-2
-4
-6
0
40
80
120
160
200
240
280
320
360
400
DISTANCE (m)

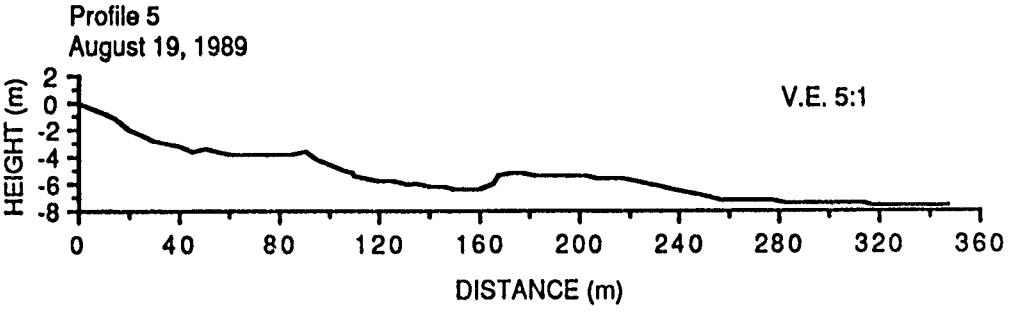
Profile 5
August 19, 1989
V.E. 5:1
HEIGHT (m)
2
0
-2
-4
-6
-8
0
40
80
120
160
200
240
280
320
360
DISTANCE (m)

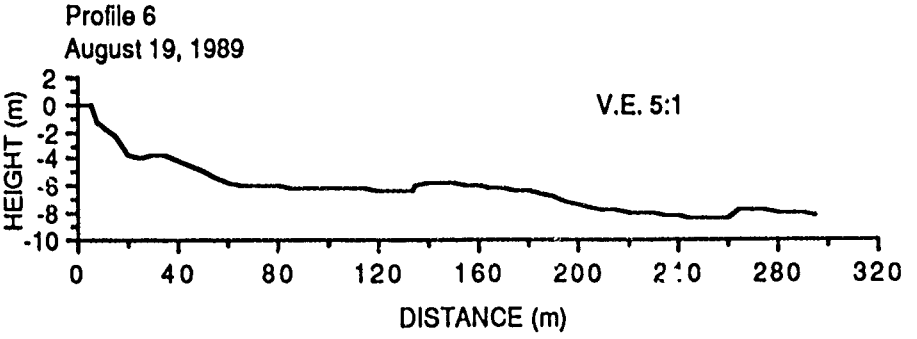
Profile 6
August 19, 1989
V.E. 5:1
HEIGHT (m)
2
0
-2
-4
-6
-8
-10
0
40
80
120
160
200
240
280
320
DISTANCE (m)

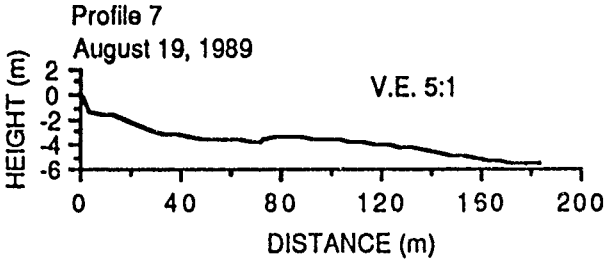
Profile 7
August 19, 1989
V.E. 5:1
HEIGHT (m)
2
0
-2
-4
-6
0
40
80
120
160
200
DISTANCE (m)

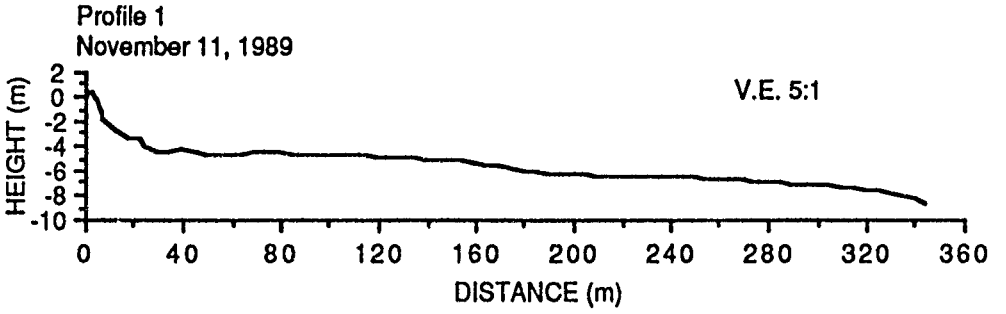
Profile 1
November 11, 1989
V.E. 5:1
HEIGHT (m)
2
0
-2
-4
-6
-8
-10
0
40
80
120
160
200
240
280
320
360
DISTANCE (m)

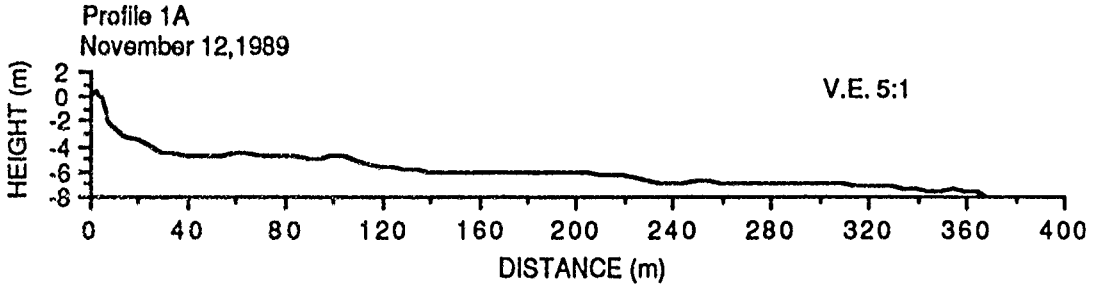
Profile 1A
November 12,1989
V.E. 5:1
HEIGHT (m)
2
0
-2
-4
-6
-8
0
40
80
120
160
200
240
280
320
360
400
DISTANCE (m)

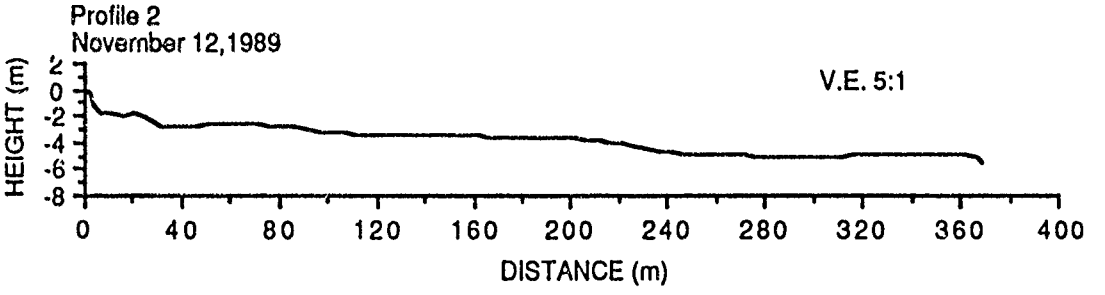
Profile 2
November 12,1989
V.E. 5:1
HEIGHT (m)
0
-2
-4
-6
-8
0
40
80
120
160
200
240
280
320
360
400
DISTANCE (m)

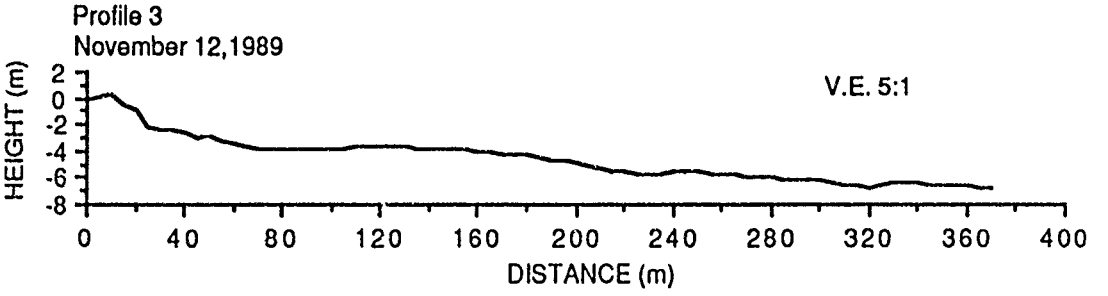
Profile 3
November 12,1989
V.E. 5:1
HEIGHT (m)
2
0
-2
-4
-6
-8
0
40
80
120
160
200
240
280
320
360
400
DISTANCE (m)

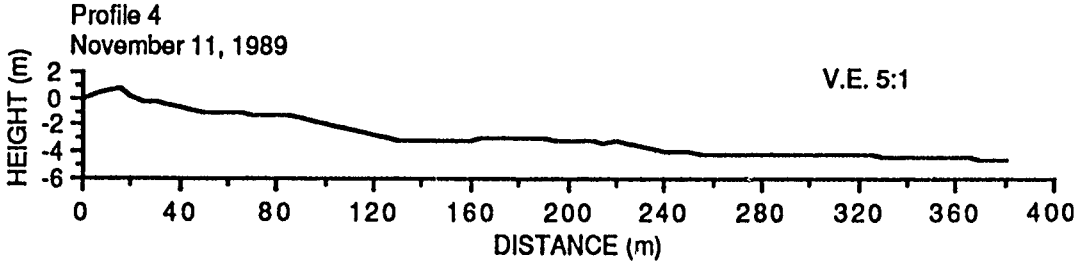
Profile 4
November 11, 1989
V.E. 5:1
HEIGHT (m)
2
0
-2
-4
-6
0
40
80
120
160
200
240
280
320
360
400
DISTANCE (m)

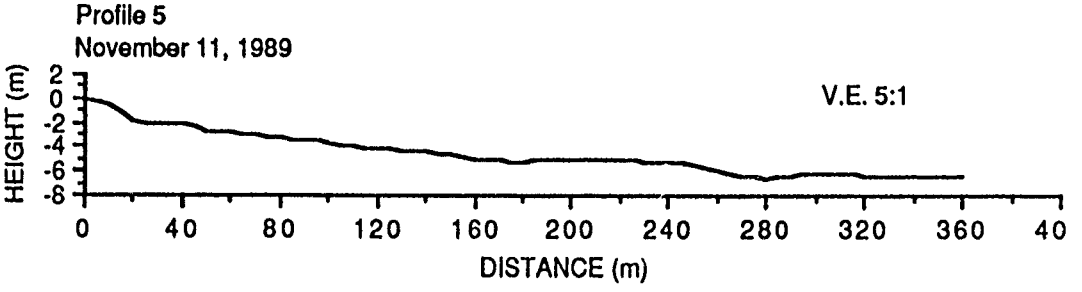
Profile 5
November 11, 1989
V.E. 5:1
HEIGHT (m)
2
0
-2
-4
-6
-8
0
40
80
120
160
200
240
280
320
360
40
DISTANCE (m)

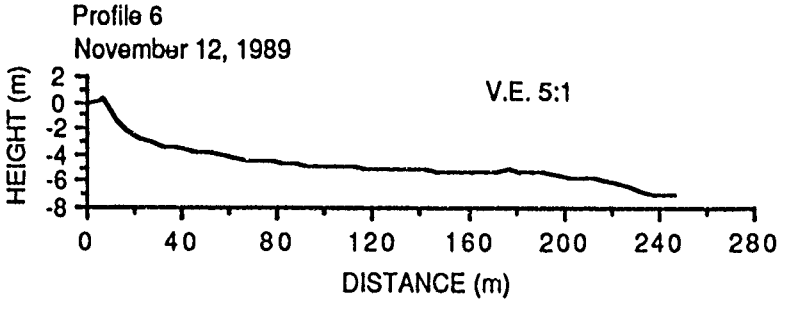
Profile 6
November 12, 1989
V.E. 5:1
HEIGHT (m)
2
0
-2
-4
-6
-8
0
40
80
120
160
200
240
280
DISTANCE (m)

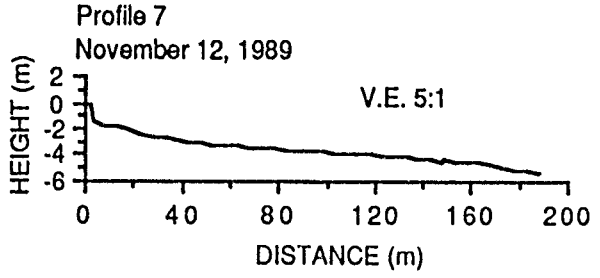
Profile 7
November 12, 1989
V.E. 5:1
HEIGHT (m)
2
0
-2
-4
-6
0
40
80
120
160
200
DISTANCE (m)

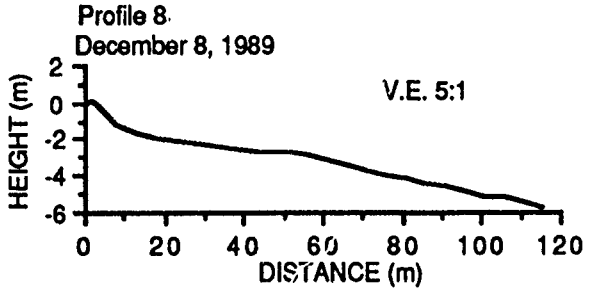
Profile 8
December 8, 1989
V.E. 5:1
HEIGHT (m)
2
0
-2
-4
-6
0
20
40
60
80
100
120
DISTANCE (m)

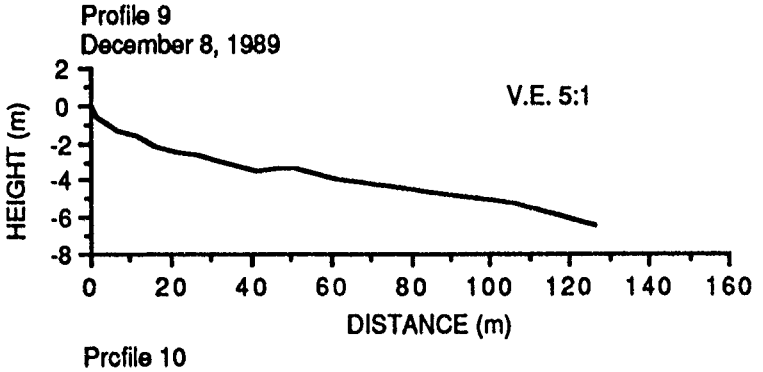
Profile 9
December 8, 1989
V.E. 5:1
HEIGHT (m)
2
0
-2
-4
-6
-8
0
20
40
60
80
100
120
140
160
DISTANCE (m)

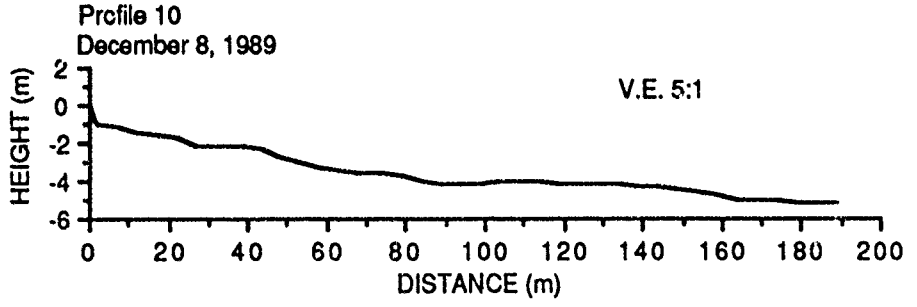
Profile 10
December 8, 1989
V.E. 5:1
HEIGHT (m)
2
0
-2
-4
-6
0
20
40
60
80
100
120
140
160
180
200
DISTANCE (m)

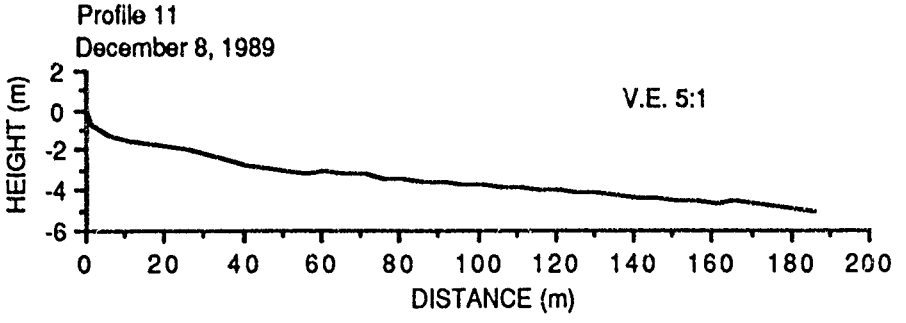
Profile 11
December 8, 1989
V.E. 5:1
HEIGHT (m)
2
0
-2
-4
-6
0
20
40
60
80
100
120
140
160
180
200
DISTANCE (m)

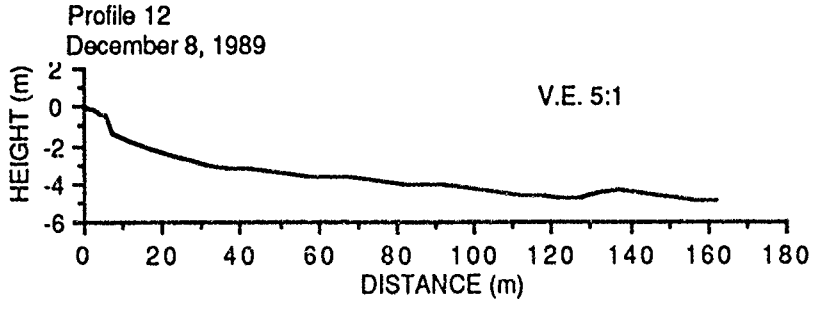
Profile 12
December 8, 1989
V.E. 5:1
HEIGHT (m)
2
0
-2
-4
-6
0
20
40
60
80
100
120
140
160
180
DISTANCE (m)

Profile 8
February 28, 1990

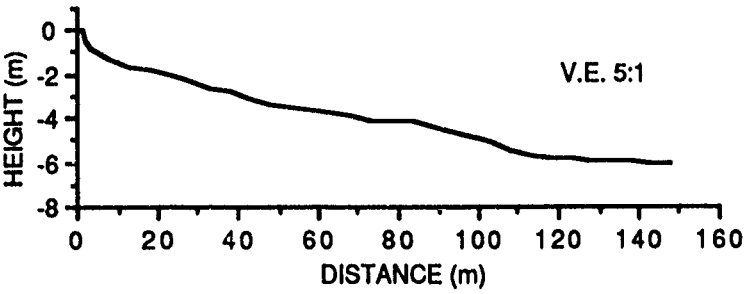

Profile 9
February 28, 1990

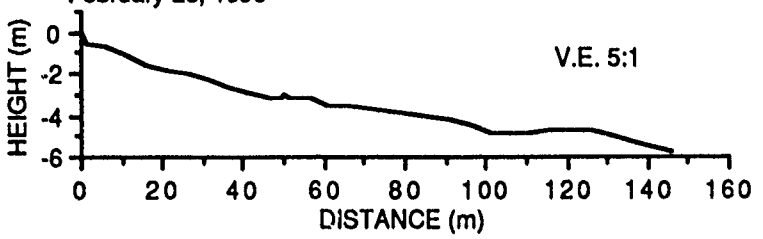

Profile 10
February 28, 1990

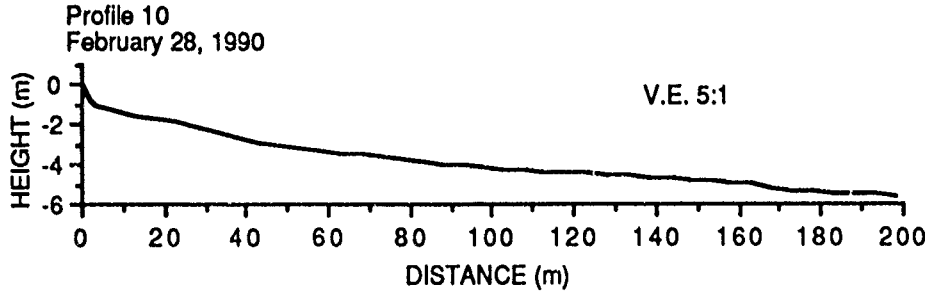

Profile 11
February 28, 1990

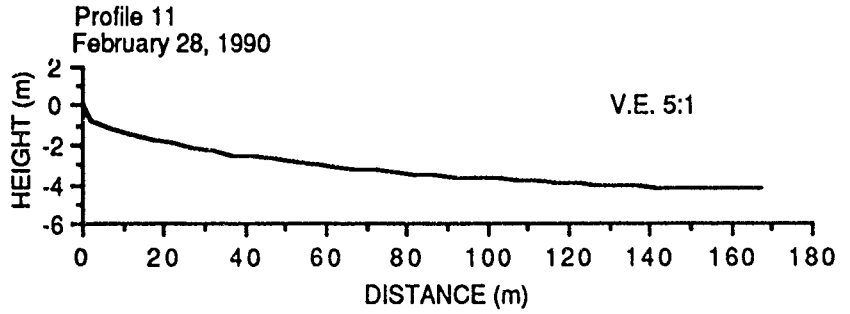

Profile 12
February 28, 1990

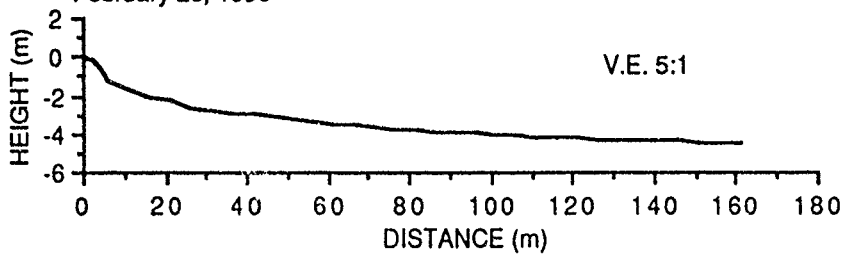

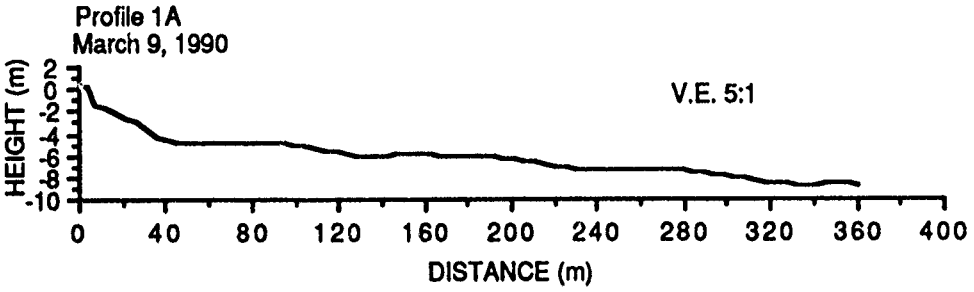
Profile 1A
March 9, 1990
V.E. 5:1
HEIGHT (m)
2
0
-2
-4
-6
-8
-10
0
40
80
120
160
200
240
280
320
360
400
DISTANCE (m)

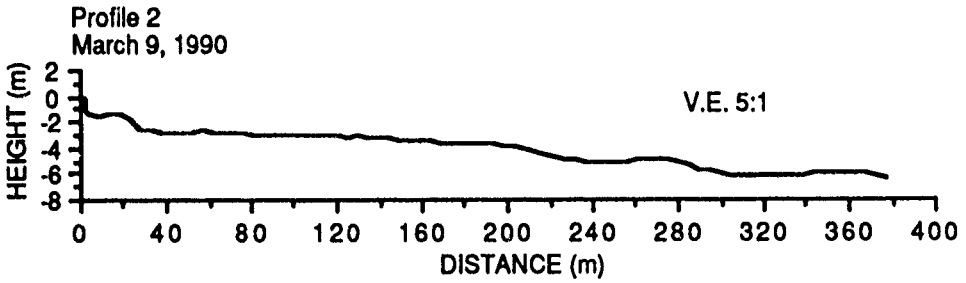
Profile 2
March 9, 1990
V.E. 5:1
HEIGHT (m)
2
0
-2
-4
-6
-8
0
40
80
120
160
200
240
280
320
360
400
DISTANCE (m)

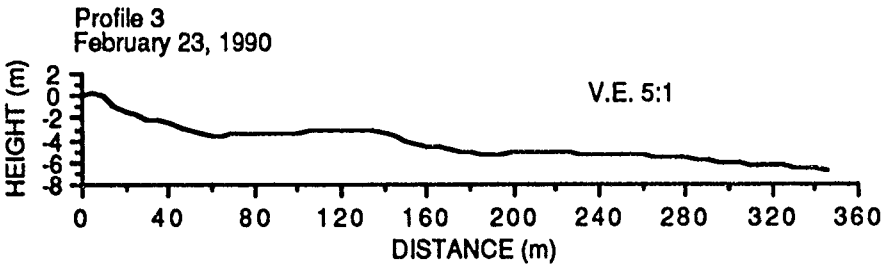
Profile 3
February 23, 1990
V.E. 5:1
HEIGHT (m)
2
0
-2
-4
-6
-8
0
40
80
120
160
200
240
280
320
360
DISTANCE (m)

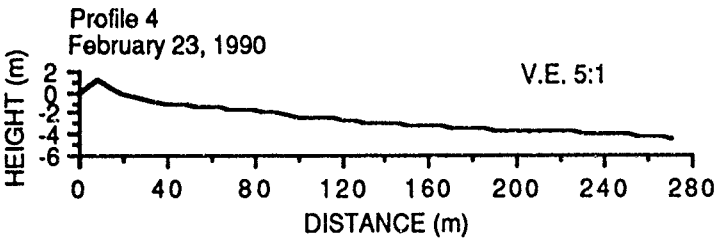
Profile 4
February 23, 1990
V.E. 5:1
HEIGHT (m)
2
0
-2
-4
-6
0
40
80
120
160
200
240
280
DISTANCE (m)

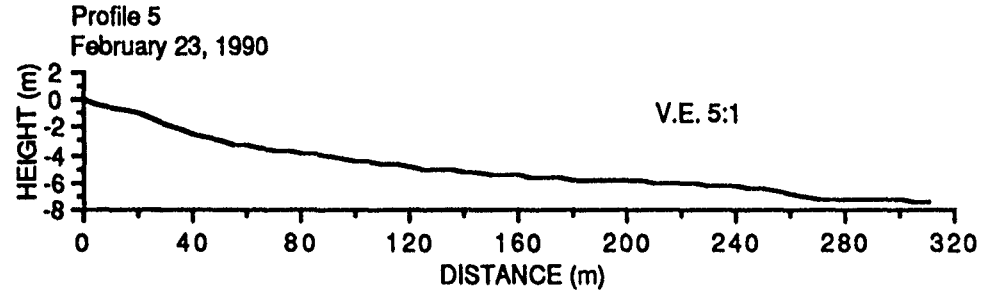
Profile 5
February 23, 1990
HEIGHT (m)
2
0
-2
-4
-6
-8
V.E. 5:1
0
40
80
120
160
200
240
280
320
DISTANCE (m)

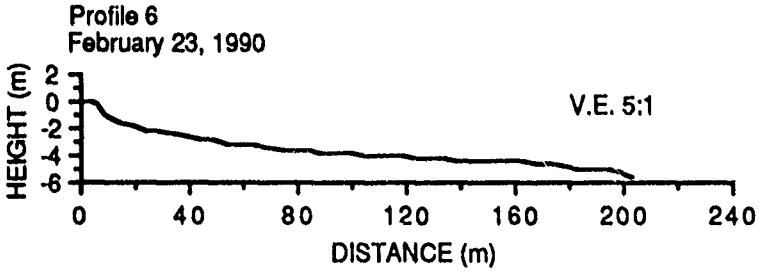
Profile 6
February 23, 1990
HEIGHT (m)
2
0
-2
-4
-6
V.E. 5:1
0
40
80
120
160
200
240
DISTANCE (m)

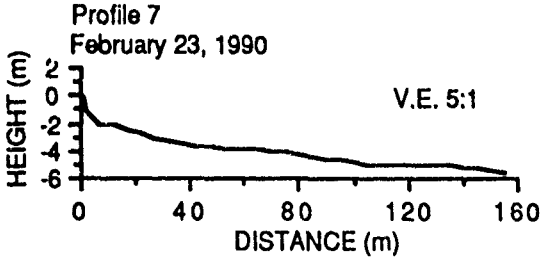
Profile 7
February 23, 1990
HEIGHT (m)
2
0
-2
-4
-6
V.E. 5:1
0
40
80
120
160
DISTANCE (m)

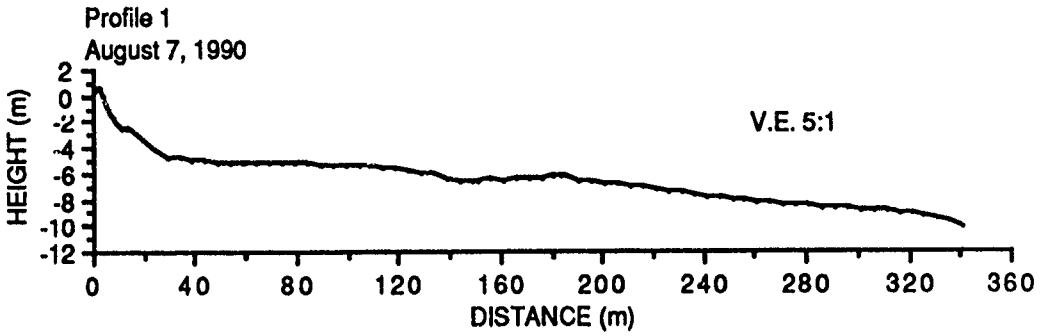
Profile 1
August 7, 1990
V.E. 5:1
HEIGHT (m)
2
0
-2
-4
-6
-8
-10
-12
0
40
80
120
160
200
240
280
320
360
DISTANCE (m)

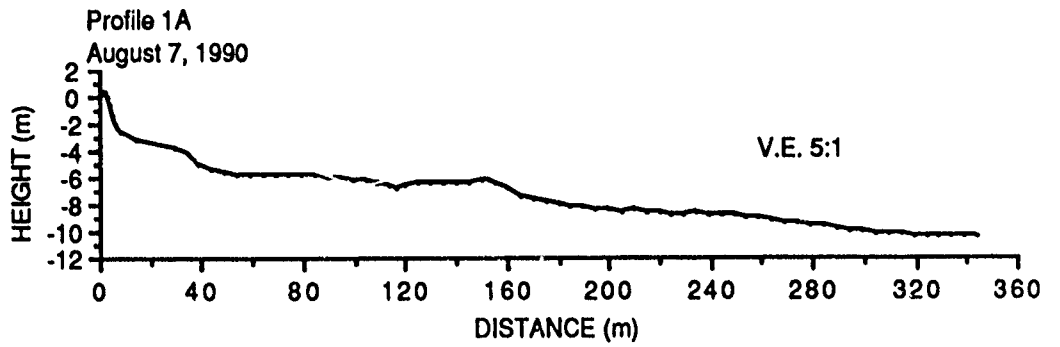
Profile 1A
August 7, 1990
V.E. 5:1
HEIGHT (m)
2
0
-2
-4
-6
-8
-10
-12
0
40
80
120
160
200
240
280
320
360
DISTANCE (m)

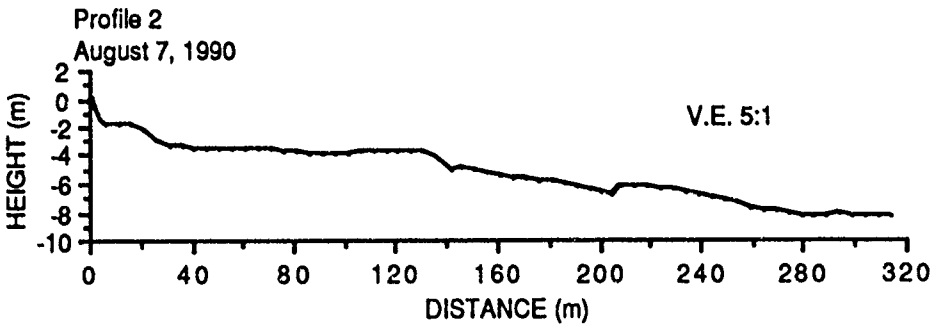
Profile 2
August 7, 1990
V.E. 5:1
HEIGHT (m)
2
0
-2
-4
-6
-8
-10
0
40
80
120
160
200
240
280
320
DISTANCE (m)

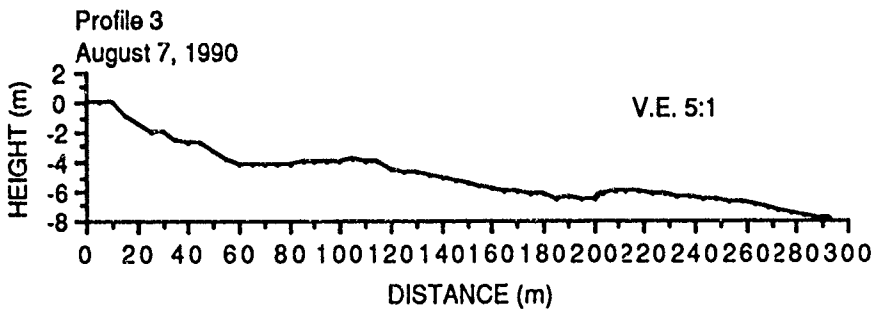
Profile 3
August 7, 1990
V.E. 5:1
HEIGHT (m)
2
0
-2
-4
-6
-8
0 20 40 60 80 100 120 140 160 180 200 220 240 260 280 300
DISTANCE (m)

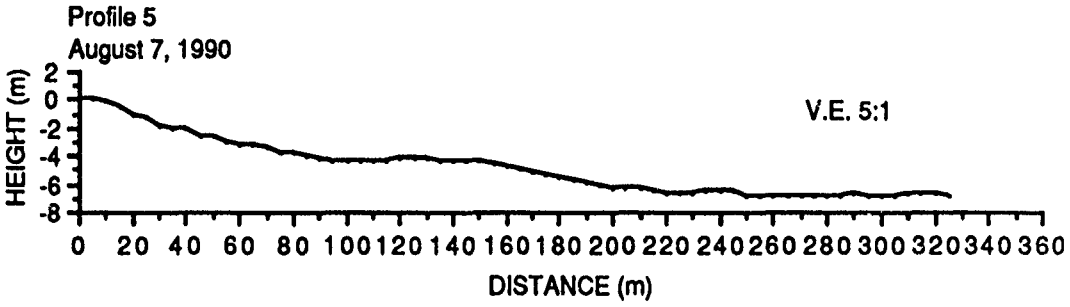
Profile 5
August 7, 1990
V.E. 5:1
HEIGHT (m)
2
0
-2
-4
-6
-8
0 20 40 60 80 100 120 140 160 180 200 220 240 260 280 300 320 340 360
DISTANCE (m)

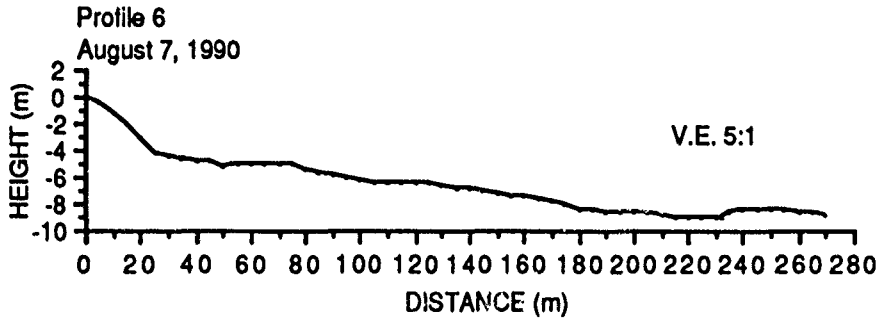
Profile 6
August 7, 1990
V.E. 5:1
HEIGHT (m)
2
0
-2
-4
-6
-8
-10
0 20 40 60 80 100 120 140 160 180 200 220 240 260 280
DISTANCE (m)

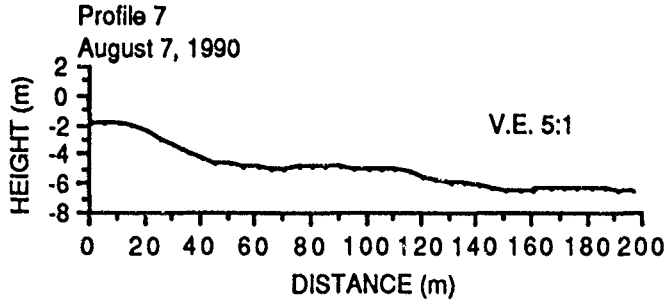
Profile 7
August 7, 1990
V.E. 5:1
HEIGHT (m)
2
0
-2
-4
-6
-8
0 20 40 60 80 100 120 140 160 180 200
DISTANCE (m)

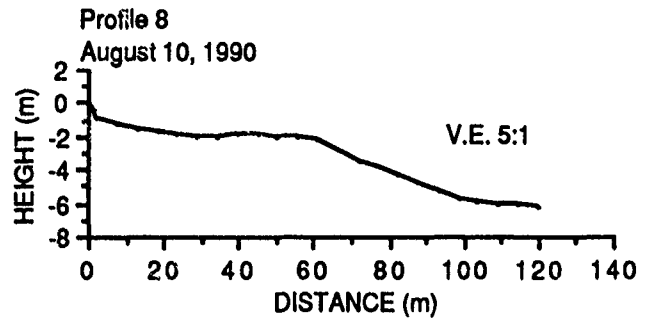
Profile 8
August 10, 1990
V.E. 5:1
HEIGHT (m)
2
0
-2
-4
-6
-8
0
20
40
60
80
100
120
140
DISTANCE (m)

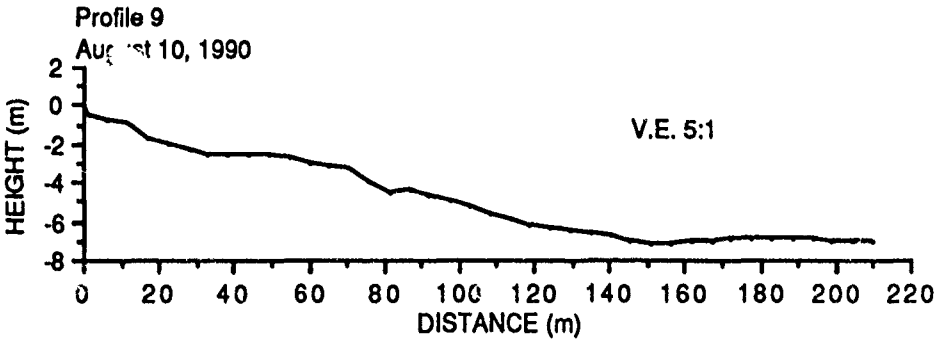
Profile 9
August 10, 1990
V.E. 5:1
HEIGHT (m)
2
0
-2
-4
-6
-8
0
20
40
60
80
100
120
140
160
180
200
220
DISTANCE (m)

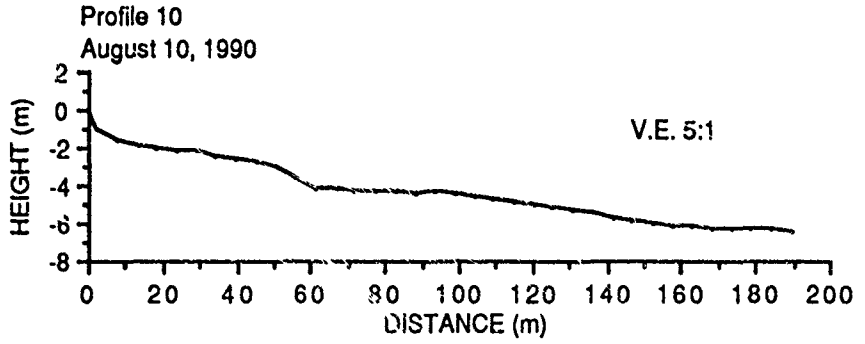
Profile 10
August 10, 1990
V.E. 5:1
HEIGHT (m)
2
0
-2
-4
-6
-8
0
20
40
60
80
100
120
140
160
180
200
DISTANCE (m)

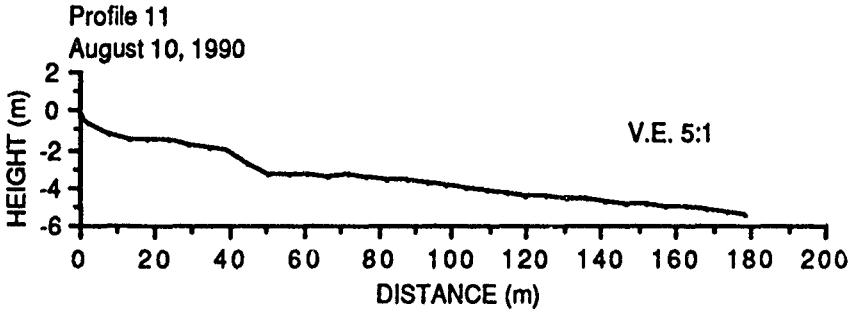
Profile 11
August 10, 1990
V.E. 5:1
HEIGHT (m)
2
0
-2
-4
-6
0
20
40
60
80
100
120
140
160
180
200
DISTANCE (m)

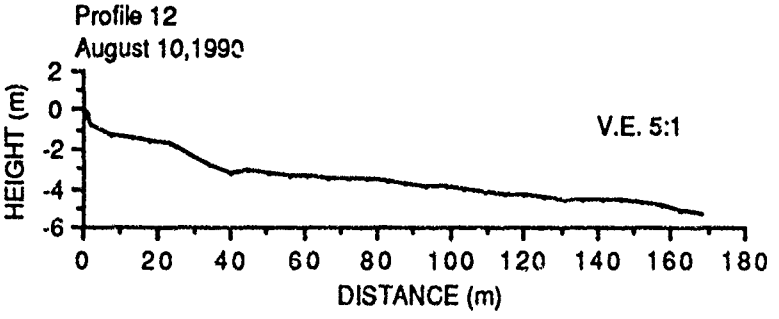
Profile 12
August 10,1990
V.E. 5:1
HEIGHT (m)
2
0
-2
-4
-6
0
20
40
60
80
100
120
140
160
180
DISTANCE (m)

APPENDIX B:

GRAIN SIZE ANALYSIS OF

SEDIMENT GRAB SAMPLES AND CORES

Sample No.	Graphic Mean (ø)	Inclusive Graphic Standard Deviation (ø)	Sample No.	Graphic Mean (ø)	Inclusive Graphic Standard Deviation (ø)
1	2.16	0.28	45	2.08	0.23
2	1.97	0.38	46	2.21	0.34
3	1.85	0.44	47	2.07	0.35
4	1.90	0.39	48	2.39	0.33
5	1.79	0.35	49	2.05	0.26
6	2.02	0.29	50	1.96	0.27
7	1.93	0.25	51	2.05	0.26
8	1.91	0.40	52	2.00	0.24
9	2.01	0.23	53	2.08	0.28
10	1.74	0.37	54	2.09	0.40
11	1.94	0.21	55	2.09	0.30
12	1.65	0.37	56	2.30	0.28
13	1.99	0.40	57	2.25	0.35
14	2.04	0.35	58	2.25	0.35
15	2.18	0.29	59	2.31	0.45
16	2.08	0.36	60	2.49	0.35
17	1.98	0.35	61	2.43	0.36
18	2.17	0.26	62	2.38	0.38
19	2.04	0.33	63	2.05	0.32
20	1.91	0.41	64	2.69	0.30
21	1.95	0.27	65	2.32	0.28
22	2.21	0.35	66	1.87	0.51
23	2.32	0.36	67	2.24	0.38
24	2.06	0.22	68	2.35	0.27
25	2.36	0.24	69	2.02	0.35
26	1.92	0.34	70	1.97	0.31
27	2.25	0.34	71	2.23	0.32
28	2.29	0.27	72	2.32	0.29
29	2.14	0.31	73	2.28	0.34
30	2.12	0.29	74	2.34	0.29
31	2.33	0.31	75	2.35	0.41
32	2.18	0.26	76	2.21	0.36
33	1.99	0.29	77	2.17	0.39
34	2.13	0.27	78	2.18	0.33
35	2.43	0.47	79	2.46	0.33
36	2.13	0.28	80	2.49	0.33
37	2.31	0.33	81	2.44	0.34
38	2.20	0.38	82	2.47	0.31
39	2.28	0.31	83	2.41	0.31
40	2.22	0.33	84	2.38	0.31
41	2.36	0.34	85	2.41	0.32
42	1.83	0.27	86	2.47	0.33
43	2.07	0.25	87	2.29	0.21
44	2.06	0.31	88	2.20	0.35

Sample No.	Graphic Mean (ø)	Inclusive Graphic Standard Deviation (ø)	Sample No.	Graphic Mean (ø)	Inclusive Graphic Standard Deviation (ø)
89	2.36	0.36	133	1.87	0.21
90	2.47	0.32	134	2.01	0.47
91	2.47	0.33	135	1.98	0.29
92	2.43	0.33	136	2.05	0.29
93	2.43	0.37	137	2.10	0.26
94	2.31	0.41	138	2.54	0.21
95	2.25	0.37	139	2.68	0.30
96	2.40	0.32	140	2.94	0.31
97	2.46	0.32	141	2.85	0.30
98	1.80	0.25	142	2.97	0.30
99	1.51	0.67	143	1.88	0.39
100	1.92	0.43	144	1.72	0.30
101	1.88	0.31	145	2.00	0.29
102	1.97	0.26	146	1.66	0.67
103	2.10	0.33	147	2.12	0.40
104	1.73	0.35	148	2.16	0.32
105	1.77	0.55	149	2.14	0.26
106	2.05	0.53	150	2.28	0.42
107	2.31	0.45	151	2.87	0.32
108	2.72	0.37	152	2.89	0.28
109	2.04	0.25	153	2.94	0.33
110	1.55	0.65	154	2.94	0.28
111	2.20	0.40	155	2.02	0.45
112	1.72	0.31	156	2.04	0.41
113	1.93	0.35	157	1.75	0.30
114	1.90	0.25	158	1.98	0.21
115	1.83	0.28	159	1.95	0.25
116	2.21	0.34	160	1.91	0.19
117	2.60	0.47	161	2.04	0.25
118	2.66	0.31	162	2.08	0.25
119	2.86	0.34	163	1.88	0.19
120	1.77	0.48	164	2.03	0.21
121	2.03	0.30	165	1.90	0.33
122	1.80	0.40	166	1.54	0.35
123	2.06	0.38	167	1.89	0.32
124	1.95	0.25	168	2.05	0.29
125	1.98	0.30	169	2.22	0.35
126	2.46	0.12	170	2.40	0.29
127	2.18	0.46	171	2.40	0.24
128	2.42	0.49	172	2.04	0.26
129	2.81	0.32	173	1.35	0.61
130	2.75	0.36	174	1.70	0.29
131	2.82	0.31	175	1.61	0.44
132	1.54	0.30	176	1.87	0.40

Sample No.	Graphic Mean (ø)	Inclusive Graphic Standard Deviation (ø)
177	1.90	0.33
178	1.98	0.32
179	2.28	0.28
180	1.78	0.45
181	2.05	0.24
182	1.68	0.50
183	1.70	0.33
184	1.91	0.25
185	1.93	0.29
186	1.63	0.32
187	1.74	0.37
188	1.71	0.39
189	2.03	0.55
190	1.66	0.29
191	1.96	0.24
192	2.34	0.37
193	2.62	0.36
194	2.89	0.27
195	2.32	0.24
196	2.40	0.28
197	2.37	0.29
198	2.42	0.28
199	2.40	0.29
200	2.02	0.25
201	2.02	0.25
202	2.04	0.27
203	2.04	0.27
204	2.00	0.24
205	2.00	0.20
206	1.95	0.35
207	1.76	0.24
208	1.68	0.39
209	1.80	0.31
210	1.99	0.24
211	2.38	0.24

Sample No.		Depth (m)	Graphic Mean (ø)	Inclusive Graphic Standard Deviation (ø)
Core 1	S-1	0.00	2.28	0.26
	S-2	2.00	2.26	0.31
	S-3	2.10	2.05	0.38
	S-4	3.40	2.18	0.29
Core 2	S-1	0.00	2.29	0.28
	S-2	1.15	2.56	0.41
	S-3	1.50	2.27	0.37
	S-4	2.15	2.05	0.48
Core 3	S-1	0.00	2.00	0.25
	S-2	1.60	1.93	0.38
	S-3	2.10	1.96	0.33
	S-4	2.85	1.68	0.48
Core 4	S-1	0.00	2.20	0.28
	S-2	1.70	2.06	0.33
	S-3	1.86	1.85	0.46
	S-4	2.15	2.98	0.59
Core 5	S-1	3.20	2.13	0.34
Core 6	S-1	0.00	2.29	0.28
	S-2	1.10	2.13	0.29
	S-3	1.62	1.76	0.28
	S-4	2.16	2.43	0.20
Core 7	S-1	0.00	2.16	0.34
	S-2	0.50	2.17	0.26
	S-3	1.20	2.92	0.34
	S-4	1.50	1.93	0.38
	S-5	2.06	2.92	0.34
Core 8	S-1	0.35	2.19	0.32
	S-2	1.00	1.56	0.25
	S-3	1.20	1.89	0.43
	S-4	2.10	1.63	0.71
	S-5	2.48	1.89	0.43
Core 9	S-1	0.10	1.68	0.31
	S-2	0.80	1.88	0.38
	S-3	1.15	1.81	0.34
	S-4	1.48	1.80	0.40
	S-5	1.55	1.81	0.34
Core 10	S-1	0.00	1.92	0.21
	S-2	1.39	1.78	0.31
	S-3	1.62	1.58	0.55
	S-4	1.96	2.44	0.34
Core 11	S-1	0.00	2.05	0.24
	S-2	1.45	2.05	0.25
	S-3	1.82	1.23	0.82
	S-4	2.00	2.05	0.25

Sample No.	Depth (m)	Graphic Mean (ø)	Inclusive Graphic Standard Deviation (ø)	Remarks
Core 11 S-5	2.50	2.15	0.33	
S-6	2.98	1.38	0.90	
Core 12 S-1	0.00	2.00	0.21	
S-2	0.95	1.97	0.19	
S-3	1.24	1.34	0.66	
S-4	1.75	2.14	0.35	
Core 13 S-1	0.00	2.03	0.24	
S-2	1.00	1.86	0.22	
S-3	1.30	1.98	0.36	
S-4	1.90	1.95	0.35	
S-5	2.30	1.98	0.53	
Core 14 S-1	0.00	1.92	0.26	
S-2	1.00	1.69	0.63	
S-3	1.15	2.28	0.44	
S-4	2.70	1.65	0.69	
S-5	2.83	1.57	0.61	
S-6	2.92	2.38	0.42	
S-7	3.65	2.23	0.41	
Core 15 S-1	0.00	1.96	0.29	
S-2	0.83	1.73	0.39	
S-3	1.13	2.43	0.29	
S-4	2.25	2.06	0.81	
S-5	2.80	3.00	0.21	
S-6	2.86	-	-	CARBON
Core 16 S-1	0.00	2.09	0.22	
S-2	1.52	-	-	CARBON
Core 17 S-1	0.15	2.09	0.22	
S-2	1.25	1.02	0.57	
S-3	2.20	2.11	0.35	
Core 18 S-1	0.00	1.80	0.31	
S-2	1.22	2.11	0.24	
S-3	1.44	1.08	0.55	
S-4	1.54	2.06	0.26	
Core 19 S-1	0.00	1.94	0.23	
S-2	1.50	1.82	0.34	
S-3	2.80	1.82	0.50	
S-4	3.00	2.91	0.24	
Core 20 S-1	0.00	3.10	0.30	
S-2	1.50	2.16	0.26	
S-3	2.20	1.37	0.57	
S-4	2.66	1.70	0.48	
Core 21 S-1	0.00	1.92	0.29	
S-2	0.98	1.97	0.42	
S-3	1.50	2.25	0.27	
S-4	1.96	2.08	0.31	

Sample No.	Depth (m)	Graphic Mean (ø)	Inclusive Graphic Standard Deviation (ø)	Remarks
Core 22 S-1	0.00	2.00	0.29	
S-2	0.57	-	-	WOOD MATTER
S-3	1.50	2.15	0.41	
S-4	1.82	1.75	0.14	
Core 23 S-1	0.00	2.03	0.50	
S-2	0.65	1.85	0.39	
S-3	1.00	2.02	0.46	
Core 24 S-1	0.00	2.91	0.30	
S-2	1.50	2.36	0.32	
S-3	2.12	1.56	0.87	
Core 25 S-1	0.20	2.43	0.28	
S-2	1.50	2.15	0.24	
S-3	2.06	1.85	0.31	
S-4	2.30	-	-	CARBON
S-5	2.44	2.25	0.31	
Core 26 S-1	0.00	2.03	0.26	
S-2	1.60	2.12	0.26	
S-3	1.75	2.38	0.42	

APPENDIX C:

CORE DESCRIPTIONS

LEGEND OF CORE DESCRIPTIONS

FINE SAND (2Ø to 3Ø)

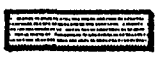
MEDIUM SAND (1Ø to 2Ø)

COARSE AND VERY COARSE SAND (-1Ø to 1Ø)

FINE TO MEDIUM PEBBLE (-4Ø to -1Ø)

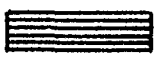
HORIZONTAL CROSS STRATIFICATION

LOW ANGLE CROSS STRATIFICATION

HIGH ANGLE CROSS STRATIFICATION

LOW ANGLE BIDIRECTIONAL CROSS STRATIFICATION

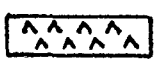
ORGANIC MATTER

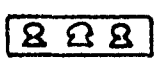
SHELL (COMPLETE)

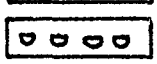
SHELL (FRAGMENT)

CORE 1

ENVIRONMENT: Proximal updrift channel margin linear bar

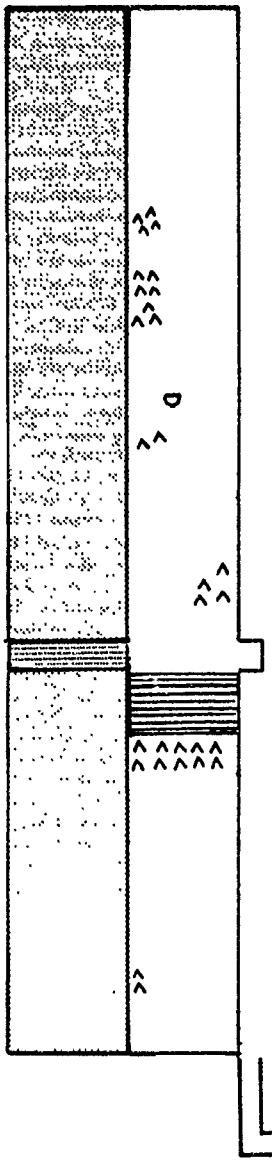

DESCRIPTION

Gray fine sand with intermittant organic matter (wood fragments)

-laminae of black fine sand with organic matter (wood fragments)

-black fine sand with abundant organic matter (wood fragments)

-shell fragment

-black fine sand with organic matter (wood fragments)

-greenish-brown organic matter (wood fragments)

Dark gray medium sand

Gray fine to medium sand with horizontal planar bedding

Gray fine sand

-black fine sand with organic matter (wood fragments)

-organic matter (wood fragments)

Gravel
Coarse Sand
Medium Sand
Fine Sand

50 cm.

CORE 2

ENVIRONMENT: Proximal updrift channel margin linear bar

DESCRIPTION

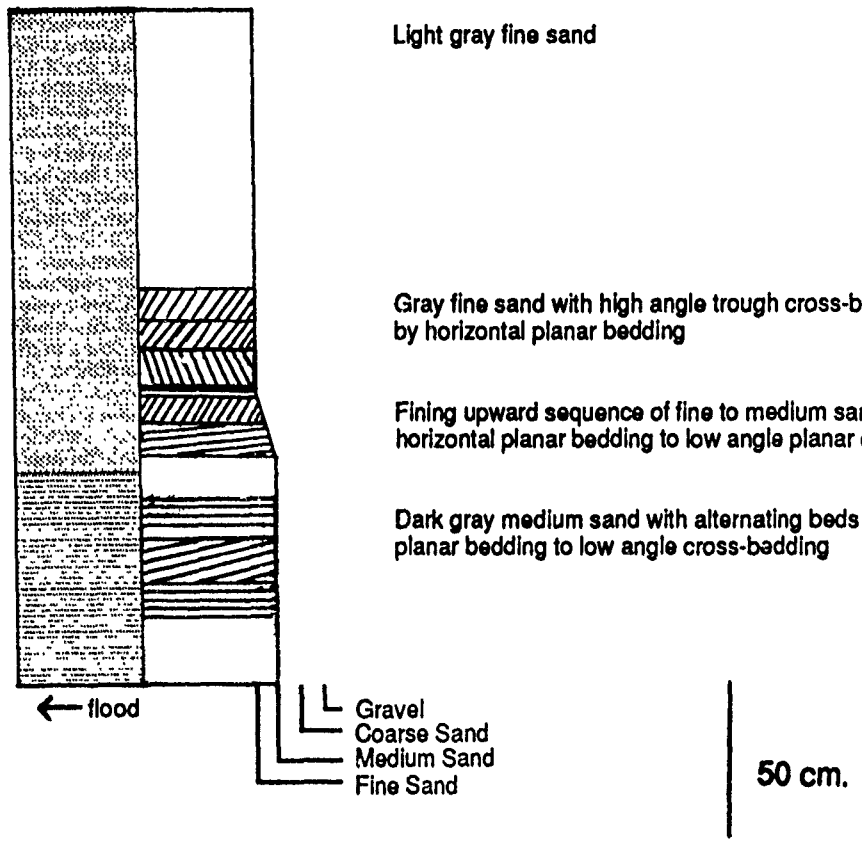

CORE 3
ENVIRONMENT: Updrift Swash bar

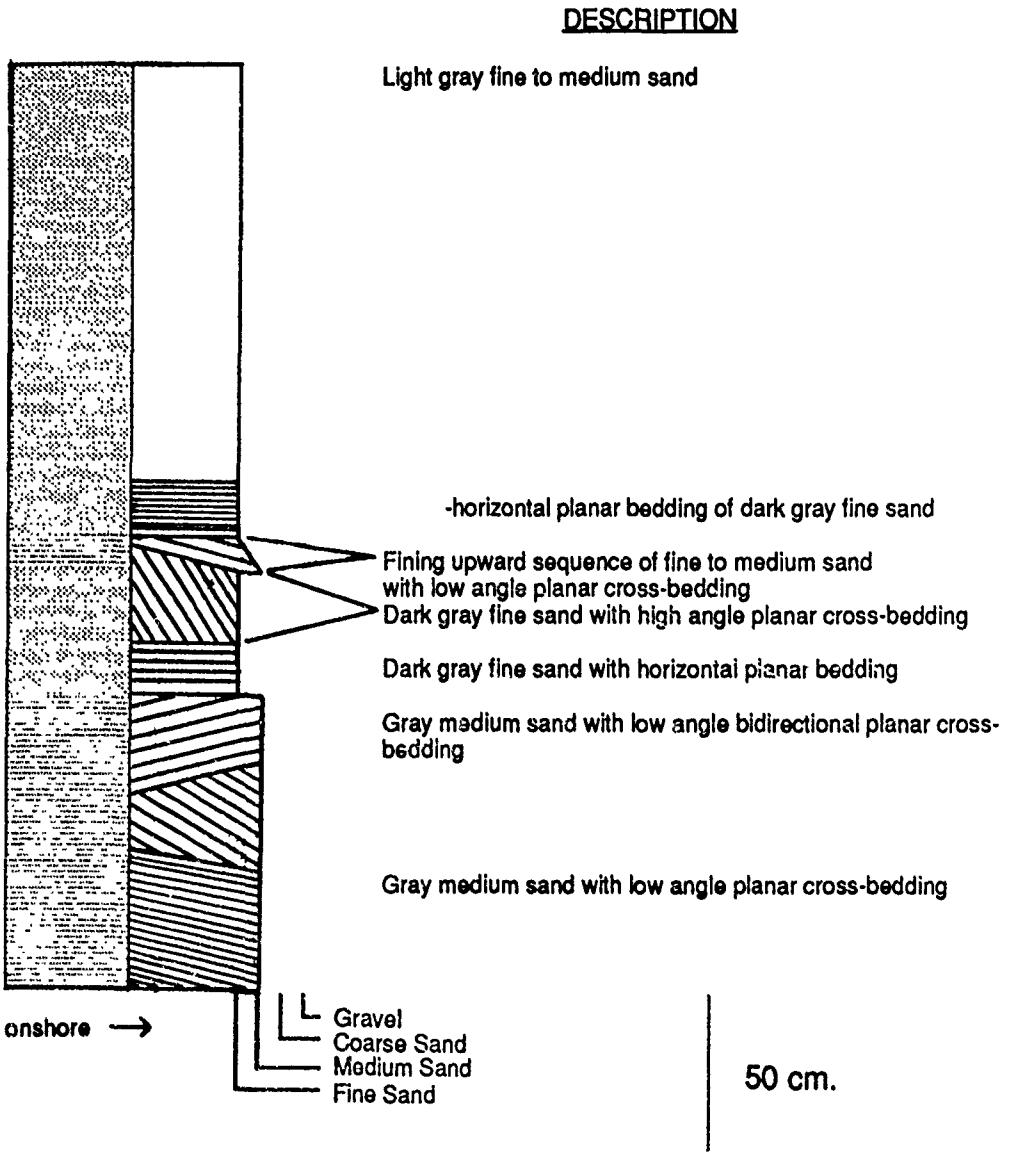

CORE 4
ENVIRONMENT:Updrift swash bar

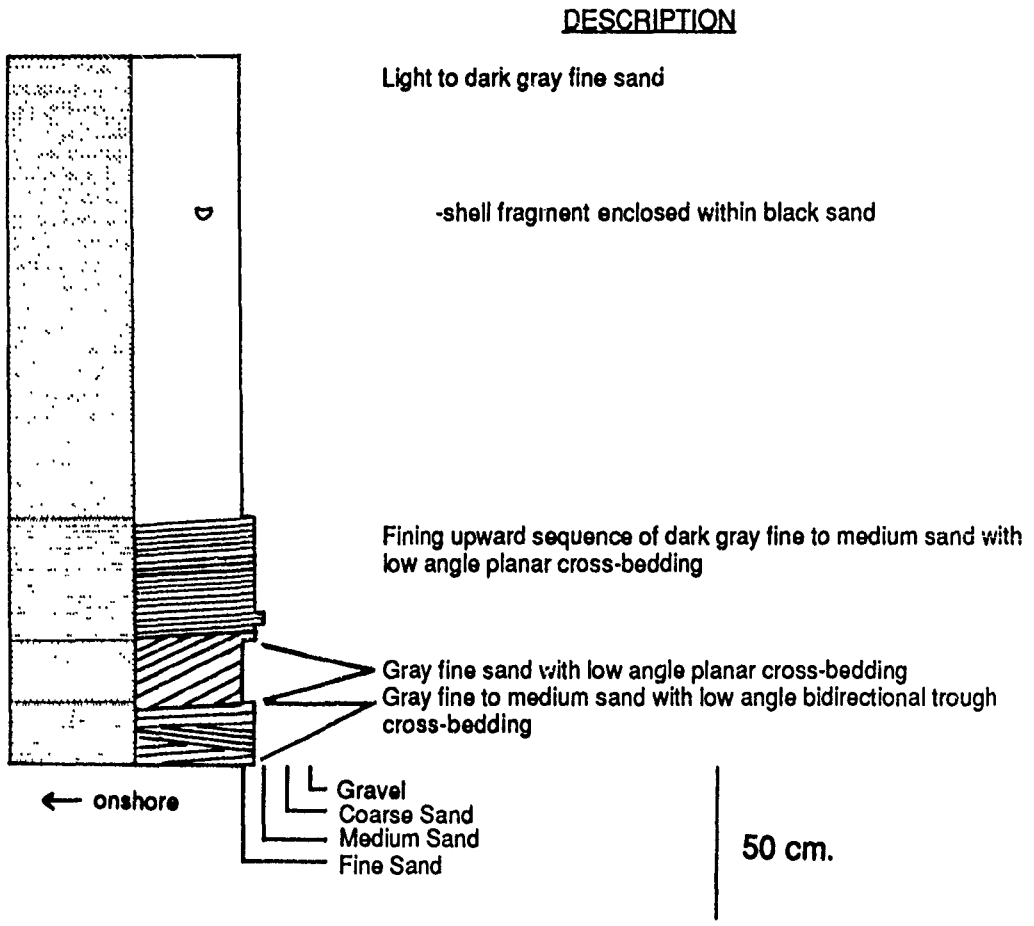

CORE 5
ENVIRONMENT: Updrift channel margin linear bar

DESCRIPTION

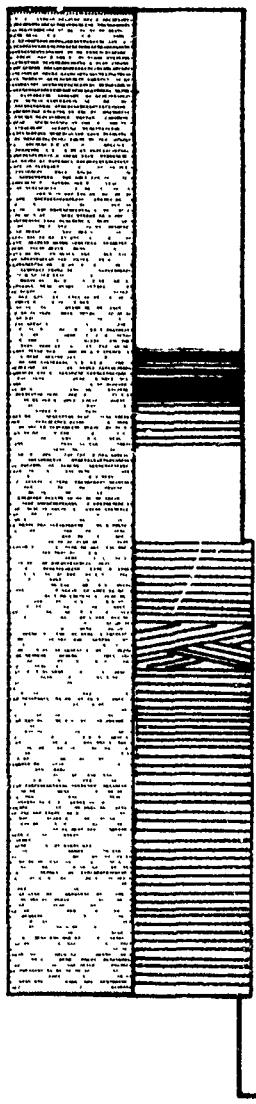

Gray fine sand with occasional horizontal planar laminae and bedding

Dark gray fine to medium sand with horizontal planar bedding

-low angle planar bidirectional cross-bedding

Gravel
Coarse Sand
Medium Sand
Fine Sand

50 cm.

CORE 6

ENVIRONMENT: Updrift channel margin linear bar near main ebb channel

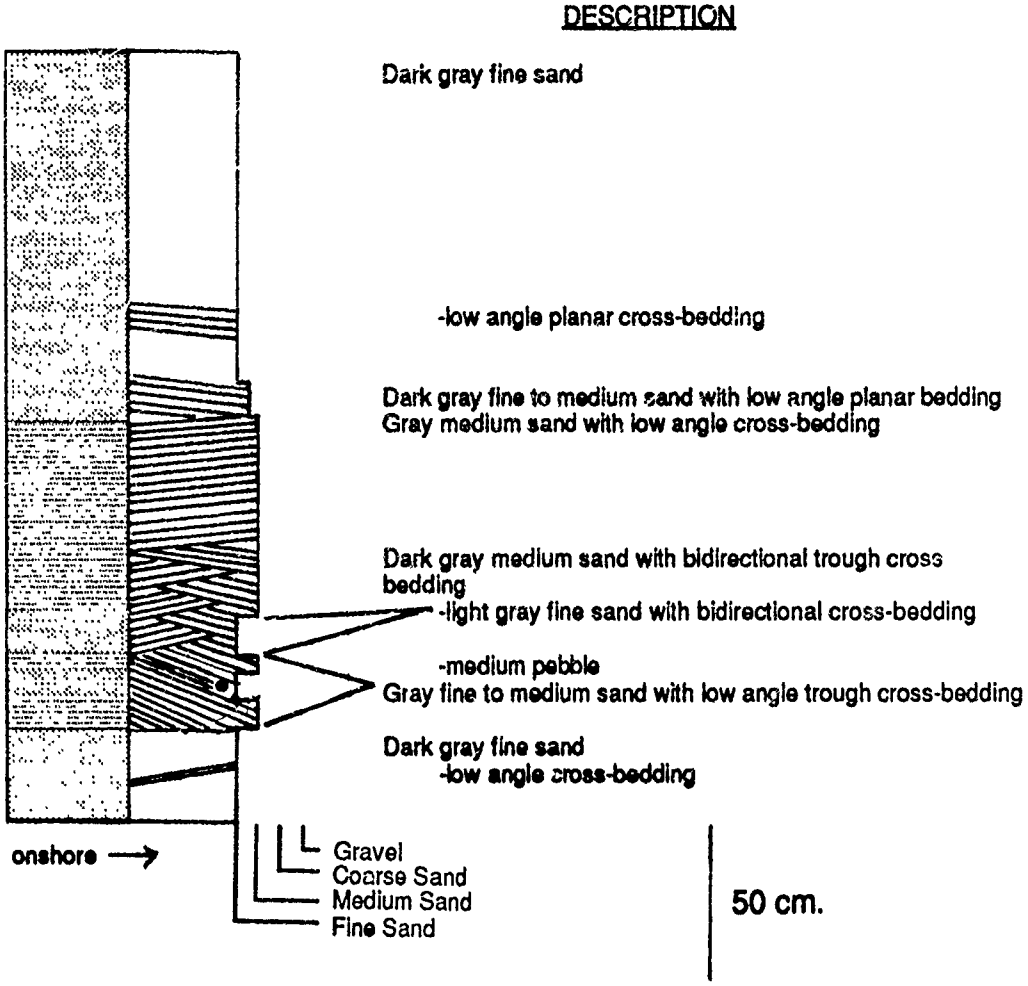

CORE 7

ENVIRONMENT: Updrift marginal flood channel

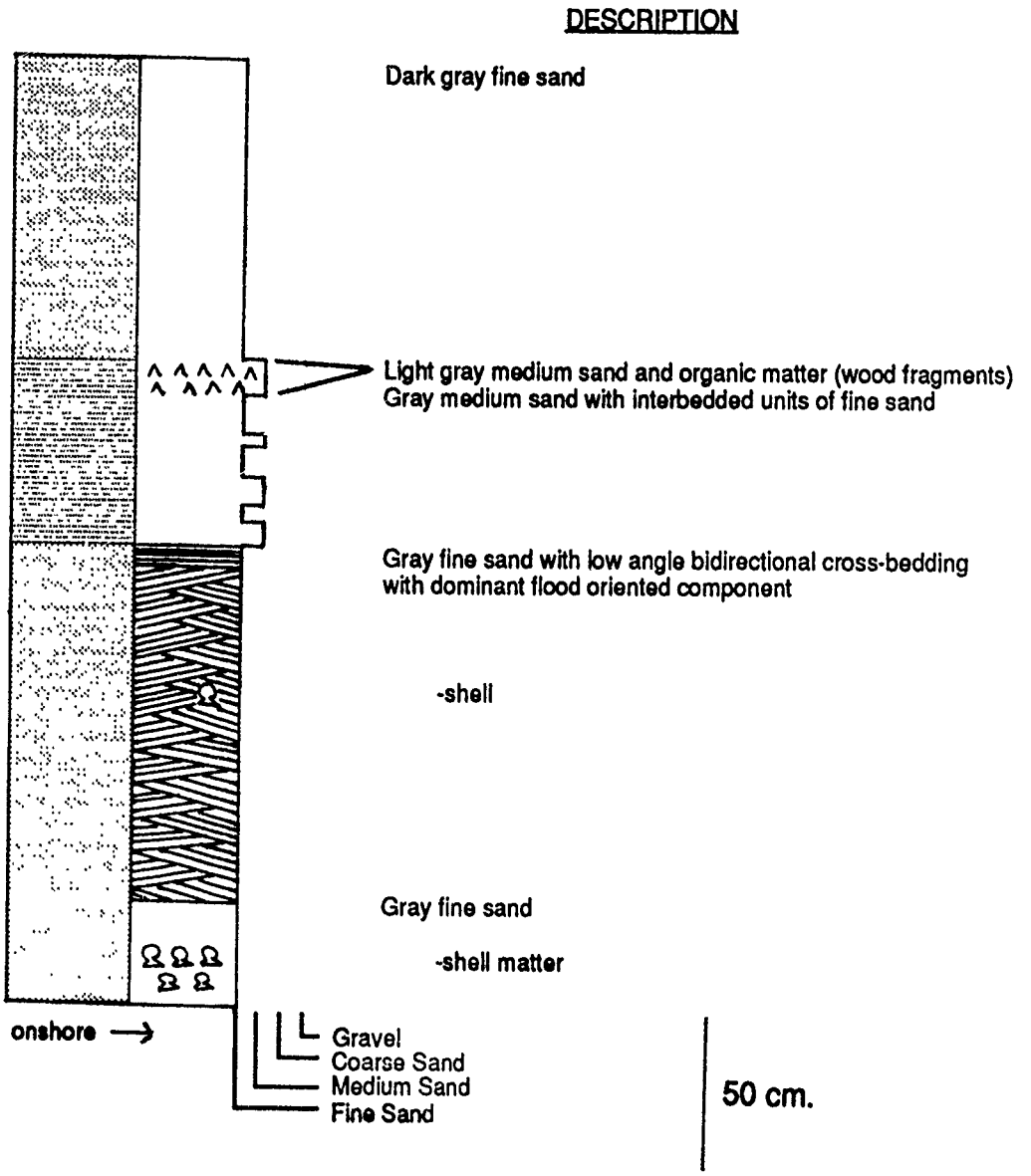

CORE 8
ENVIRONMENT: Updrift marginal flood channel

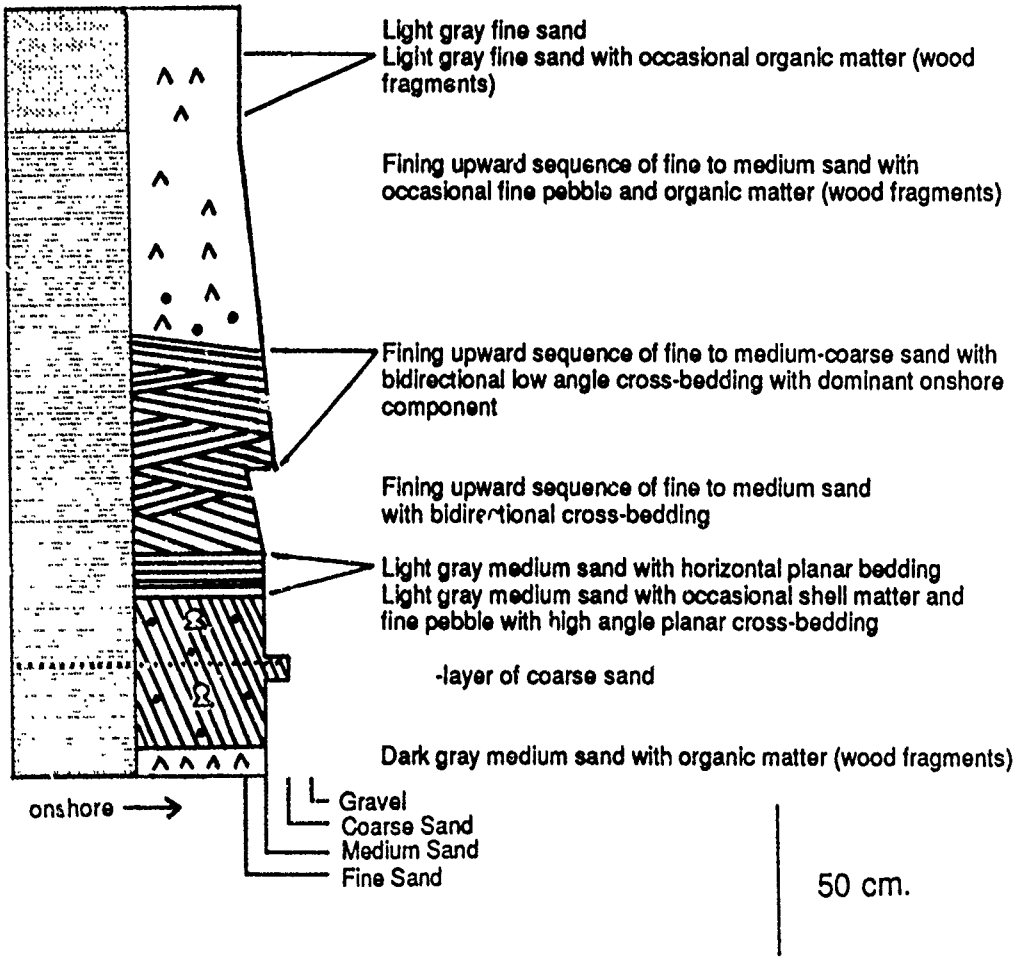

CORE 9

ENVIRONMENT: Downdrift swash bar adjacent to swash platform channel

DESCRIPTION

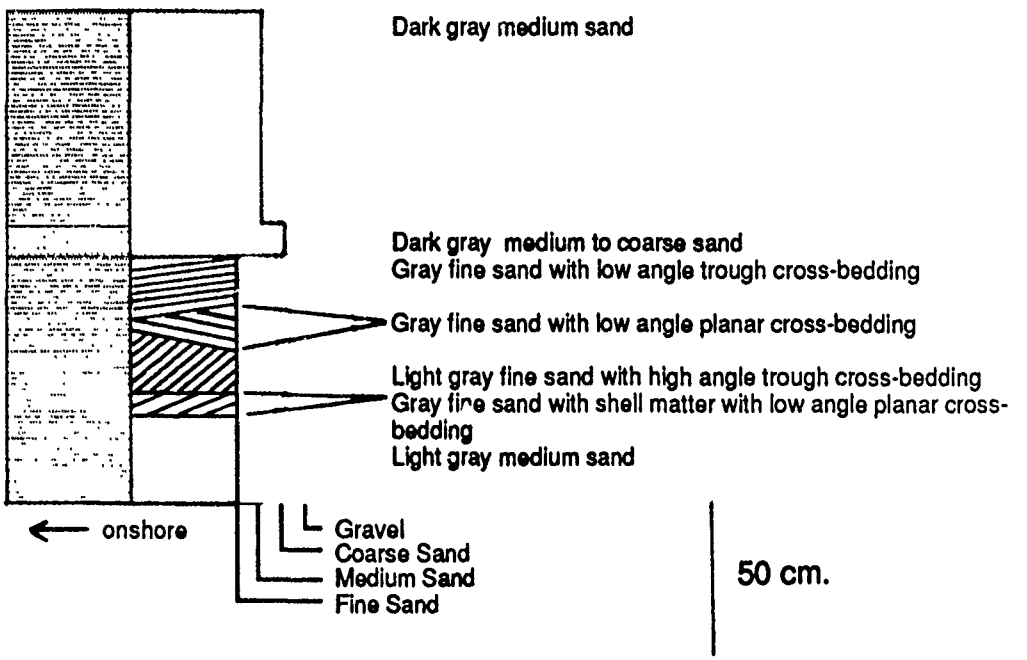

CORE 10
ENVIRONMENT: Downdrift swash bar

DESCRIPTION

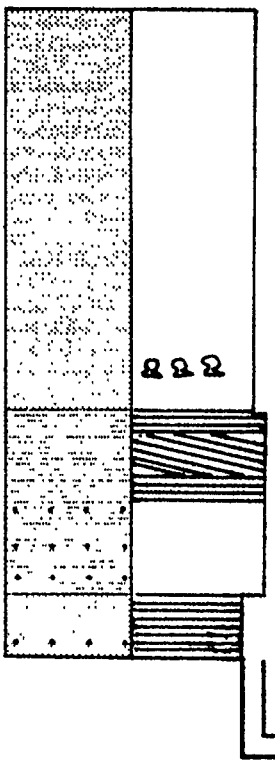

Gray fine to medium sand

-shell matter

Light gray sand with horizontal planar and low angle planar cross-bedding

Dark gray fine to medium sand with occasional layer of medium to coarse sand

Gray fine sand and occasional coarse sand layer with horizontal planar bedding

CORE 11

ENVIRONMENT: Downdrift channel margin linear bar near main ebb channel

DESCRIPTION

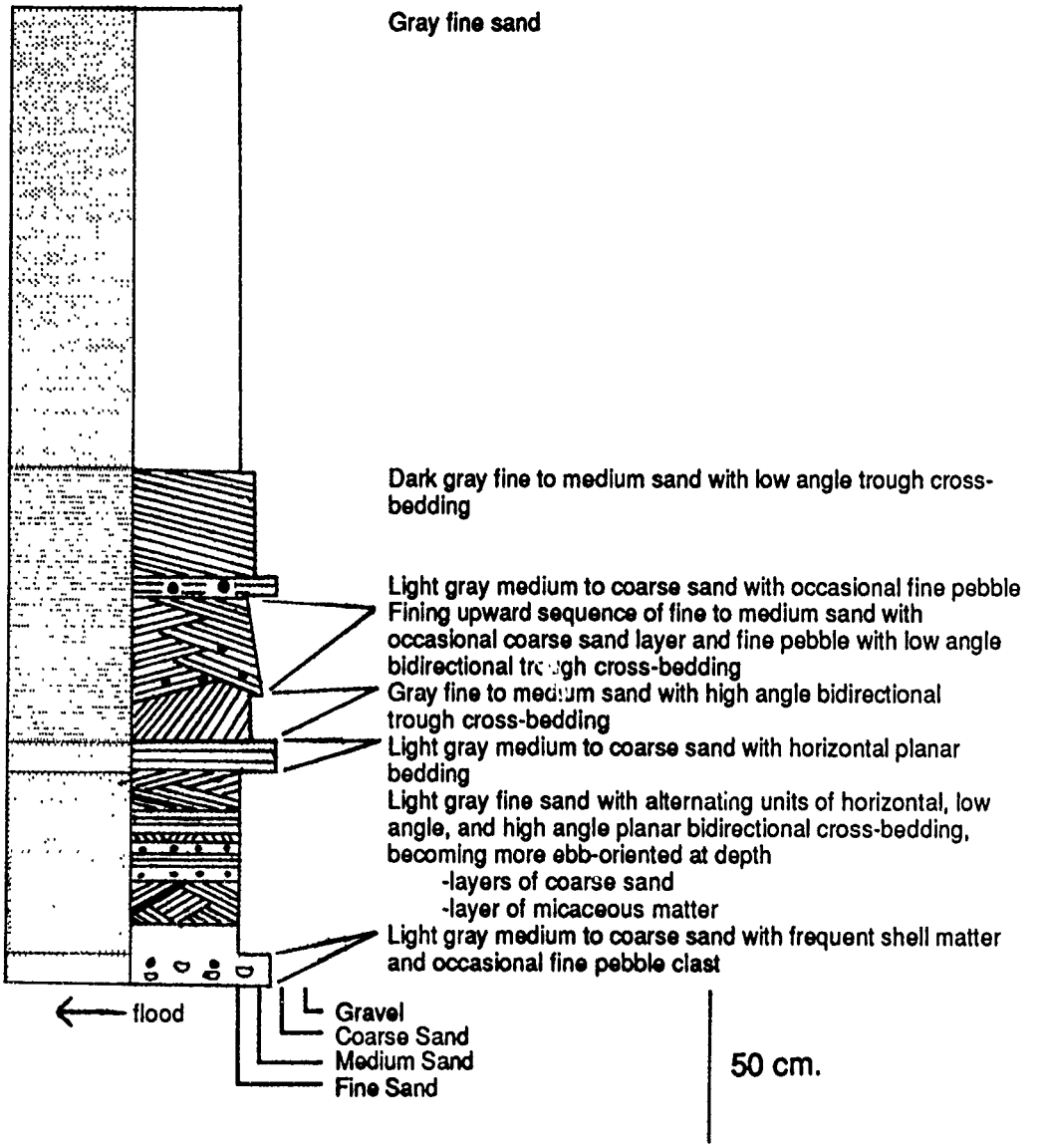

CORE 12

ENVIRONMENT: Downdrift channel margin linear bar near main ebb channel

DESCRIPTION

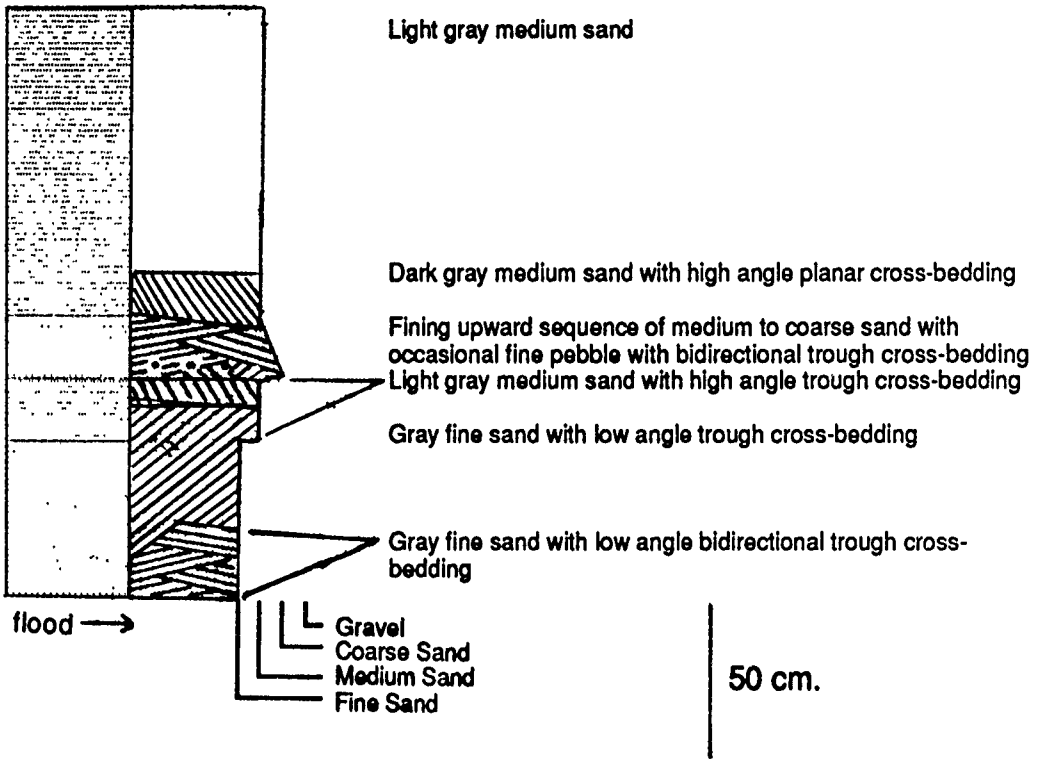

CORE 13
ENVIRONMENT: Downdrift swash bar

DESCRIPTION

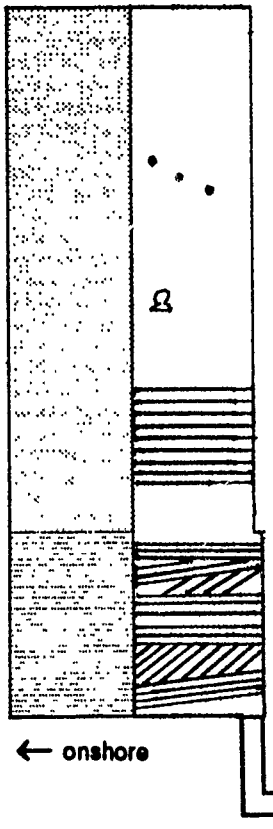

Gray fine to medium sand

-occasional very fine pebble

Gray fine to medium sand with horizontal planar bedding

-shell fragments
-fine pebble clast

Gray medium sand with horizontal planar and low angle planar cross-bedding

CORE14

ENVIRONMENT: Downdrift marginal flood channel

DESCRIPTION

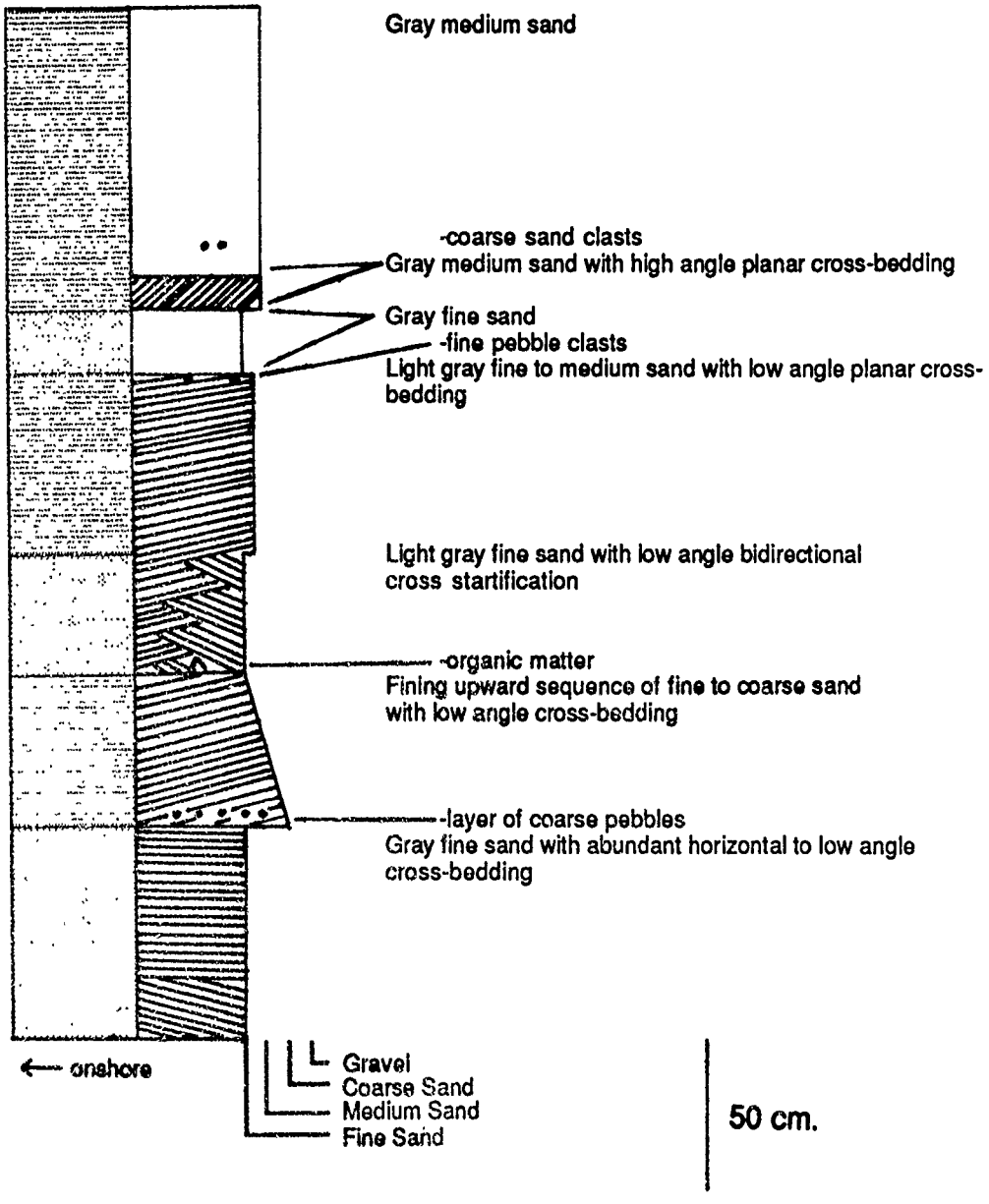

CORE 15

ENVIRONMENT: Downdrift swash platform channel

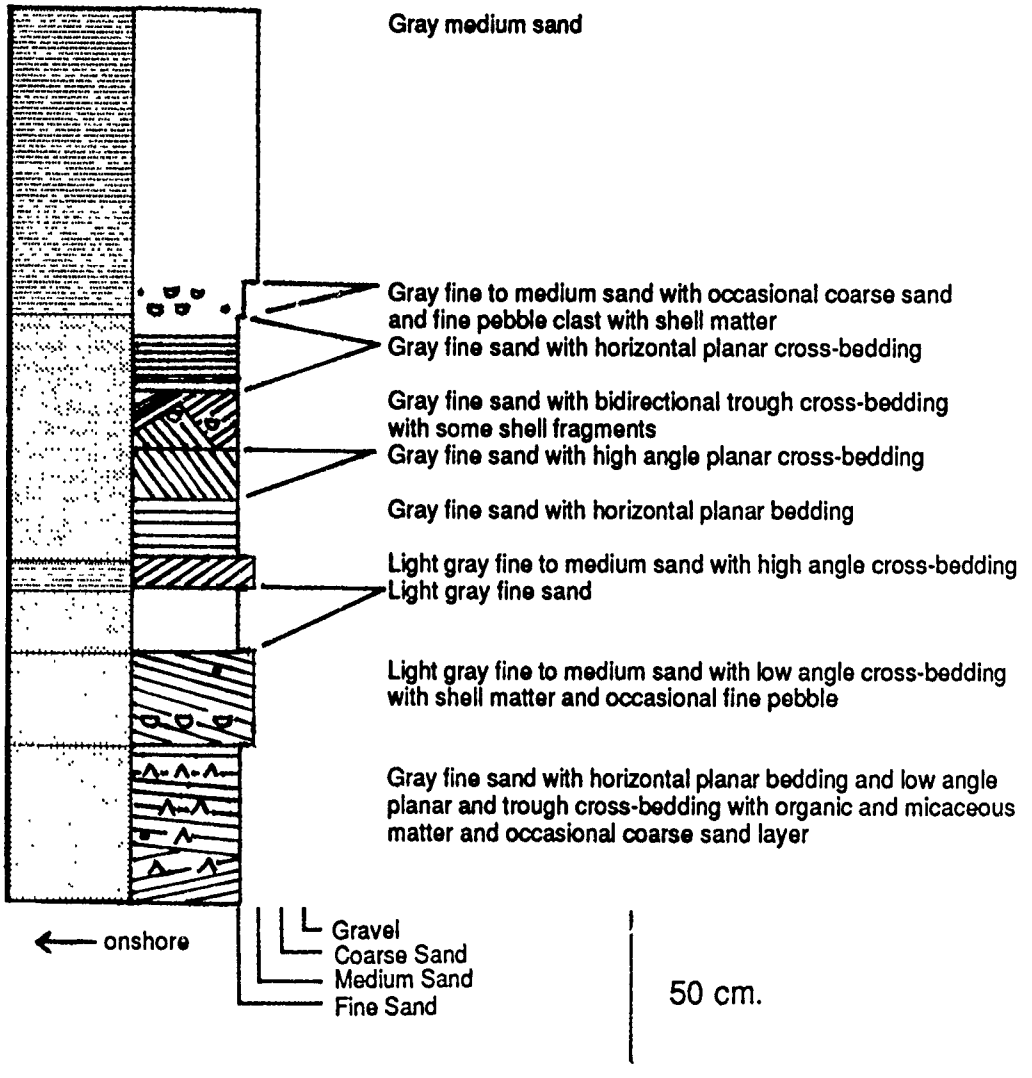

CORE 16

ENVIRONMENT: Downdrift channel margin linear bar near main ebb channel

DESCRIPTION

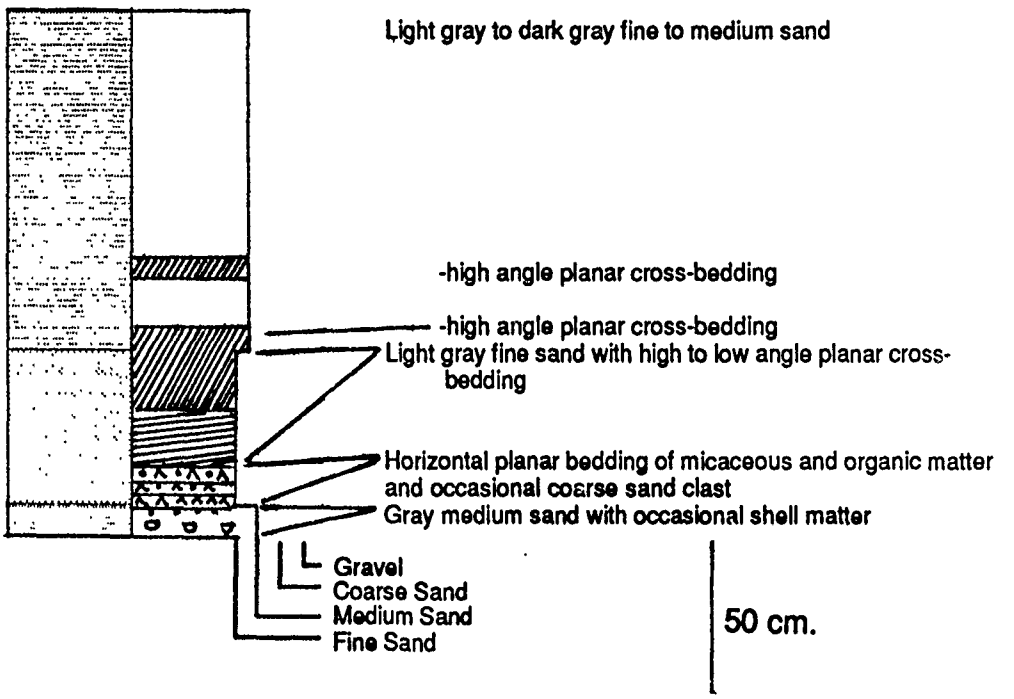

CORE 17

ENVIRONMENT: Swash bar on distal end of downdrift channel margin linear bar

DESCRIPTION

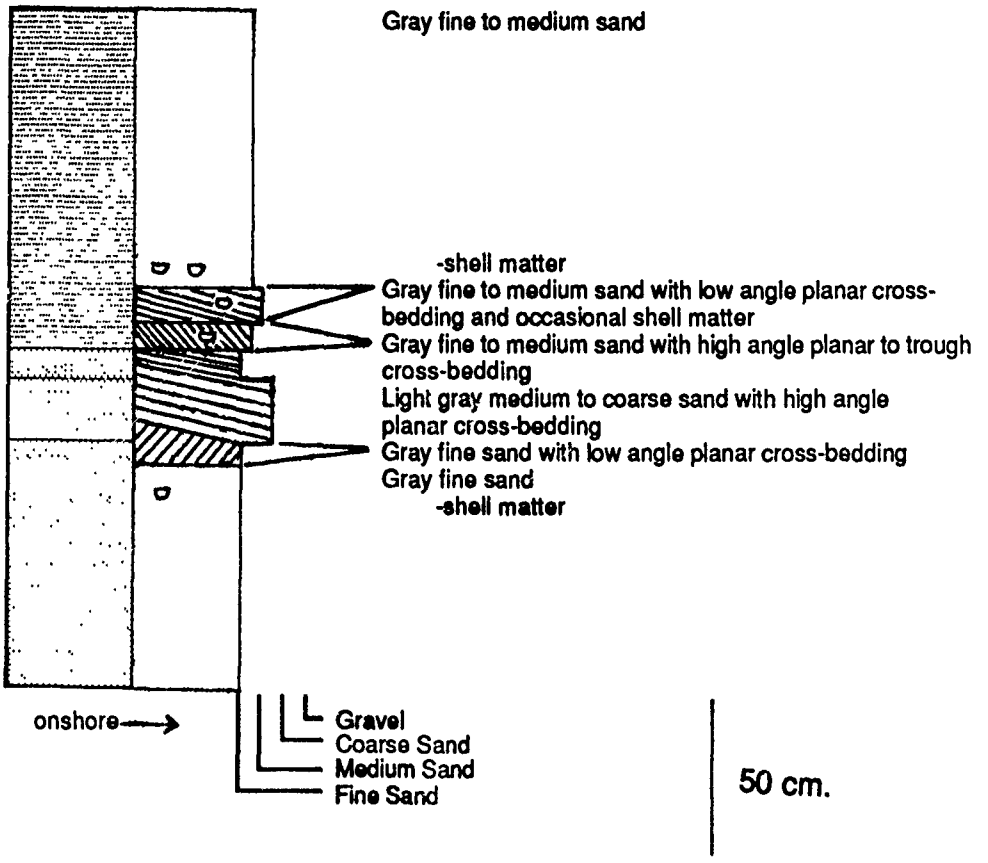

CORE 18
ENVIRONMENT: Downdrift swash bar

DESCRIPTION

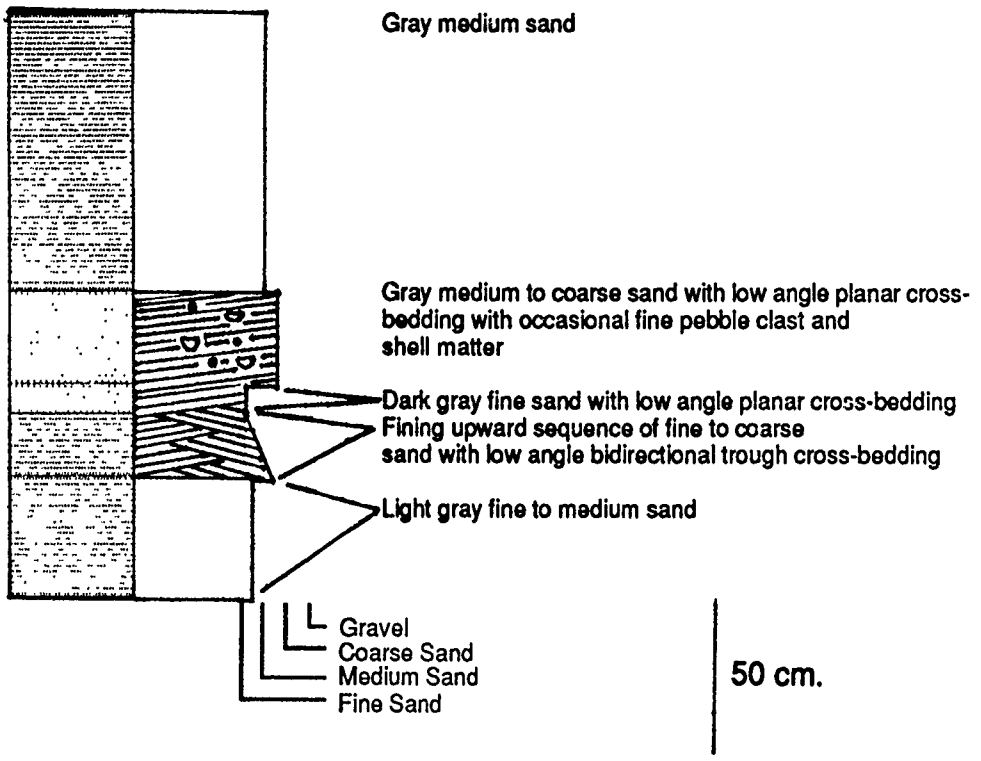

CORE 19
ENVIRONMENT: Downdrift swash bar

DESCRIPTION

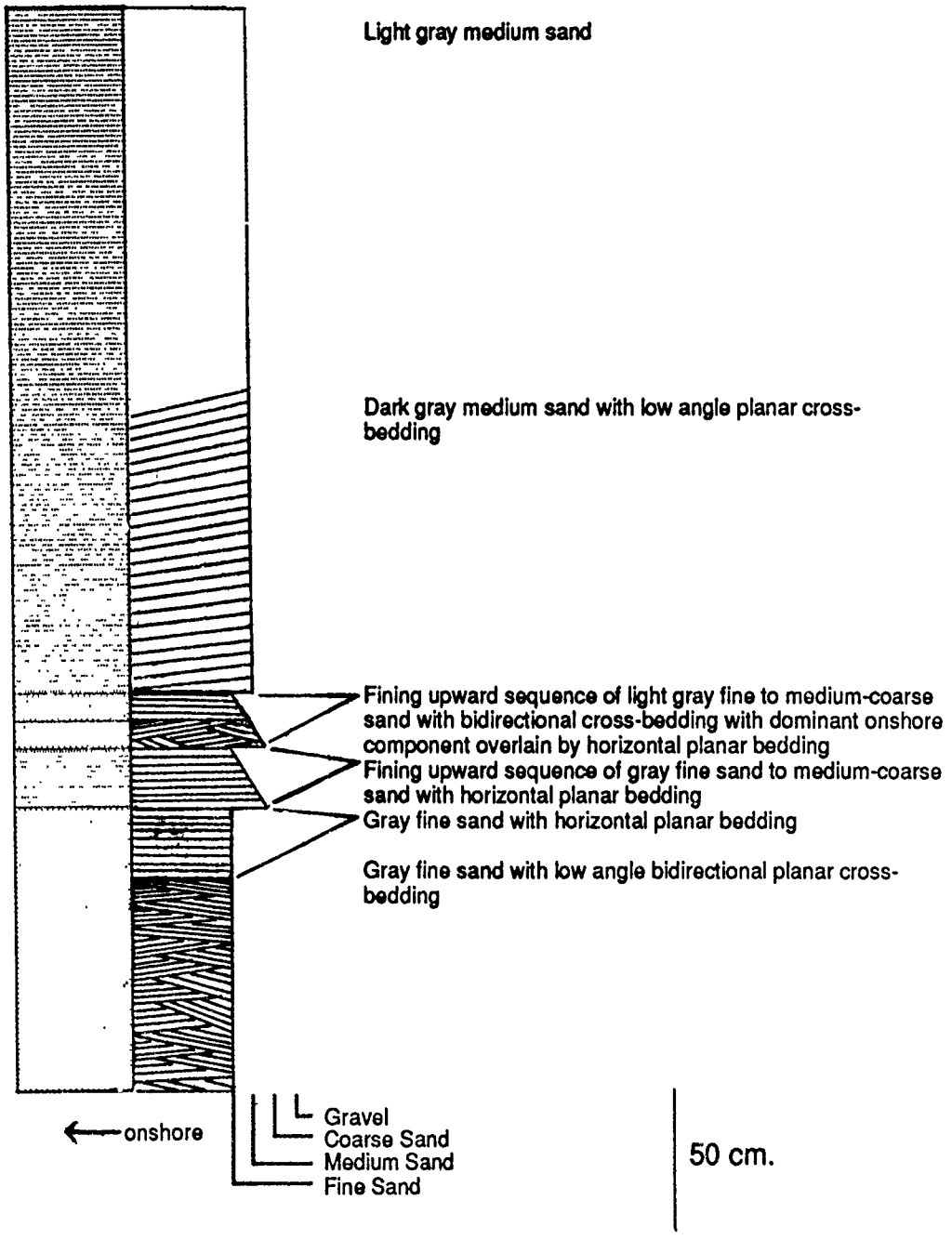

CORE 20

ENVIRONMENT: Swash bar on distal end of updrift channel margin linear bar

DESCRIPTION

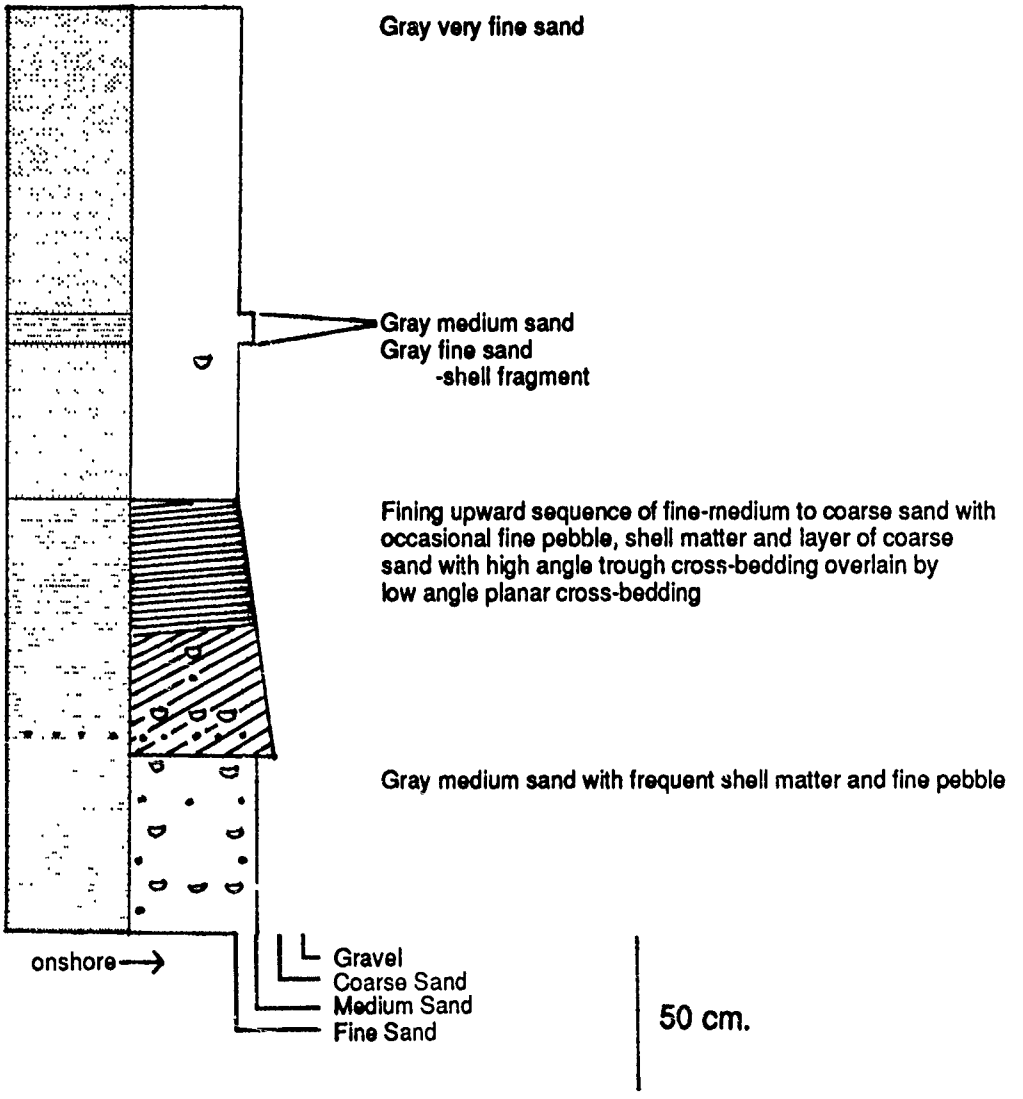

CORE 21

ENVIRONMENT: Swash bar on distal end of updrift channel margin linear bar

DESCRIPTION

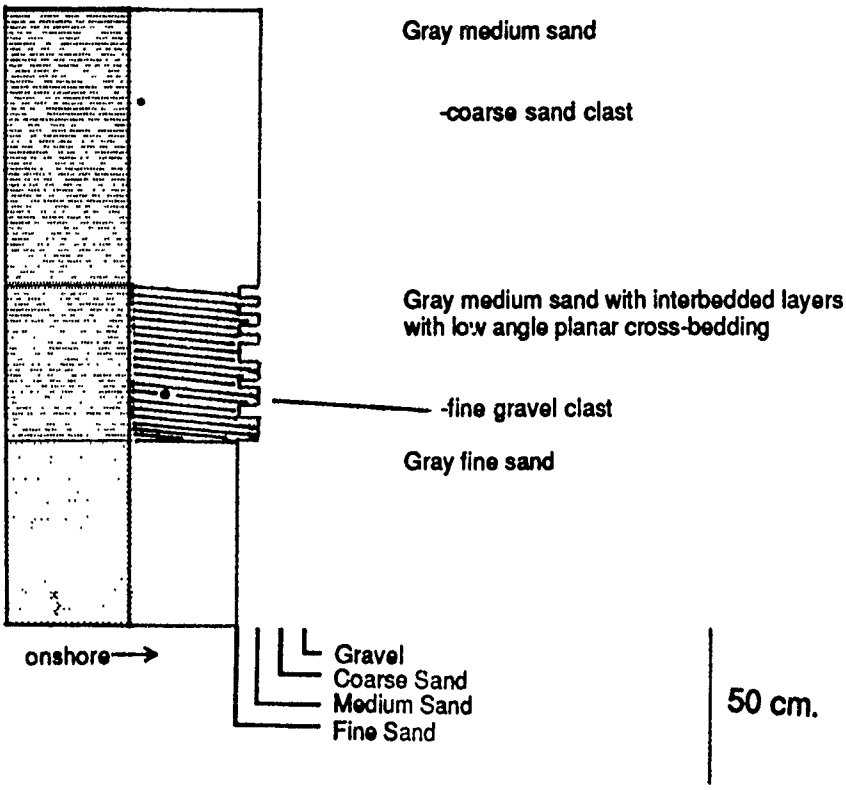

CORE 22

ENVIRONMENT: Swash bar on distal end of updrift channel margin linear bar

DESCRIPTION

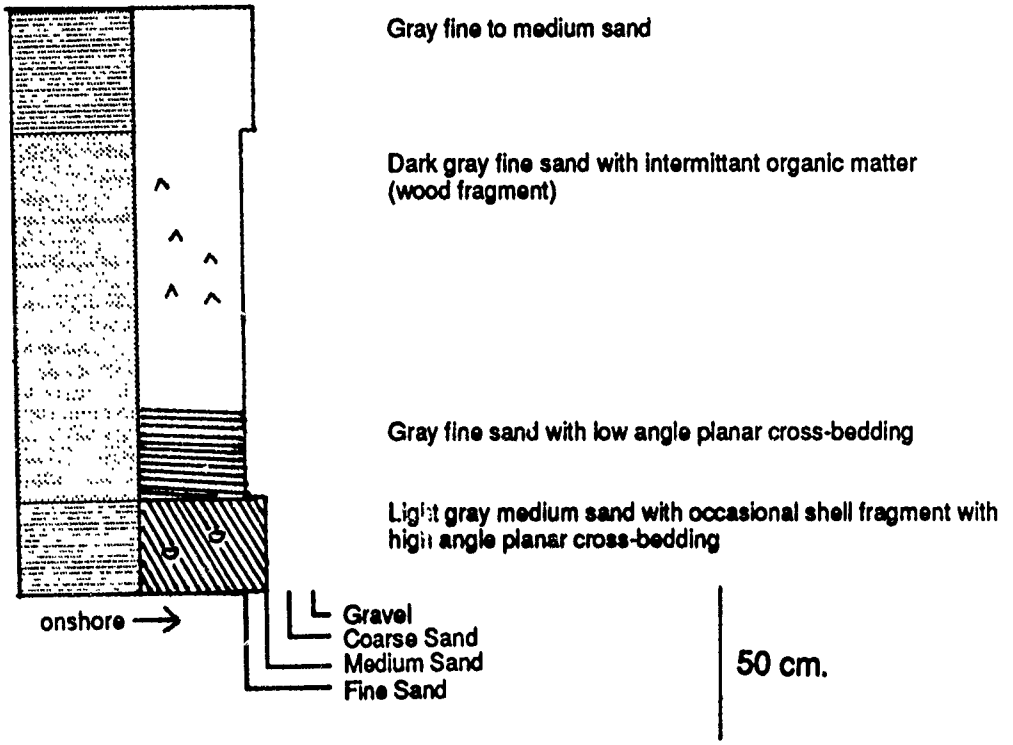

CORE 23

ENVIRONMENT: Updrift marginal flood channel

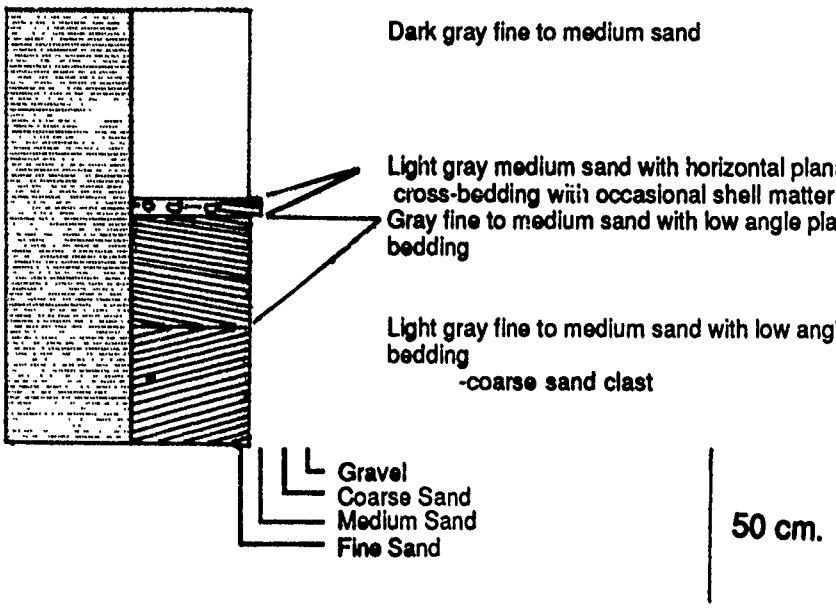

CORE 24

ENVIRONMENT: Updrift channel margin linear bar

DESCRIPTION

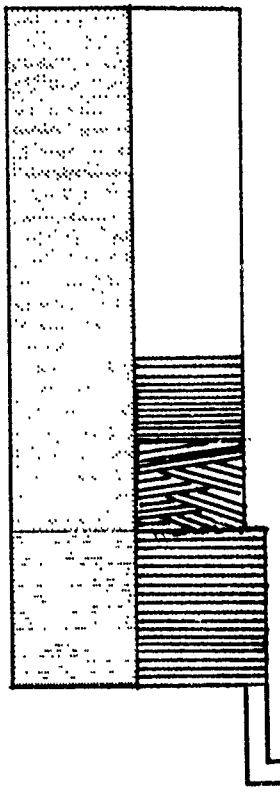

Gray fine sand

Light gray fine sand with horizontal planar bedding

Gray fine sand with low angle bidirectional trough cross-bedding

Gray medium sand with horizontal planar bedding

Gravel
Coarse Sand
Medium Sand
Fine Sand

50 cm.

CORE 25

ENVIRONMENT: Updrift channel margin linear bar near main ebb channel

DESCRIPTION

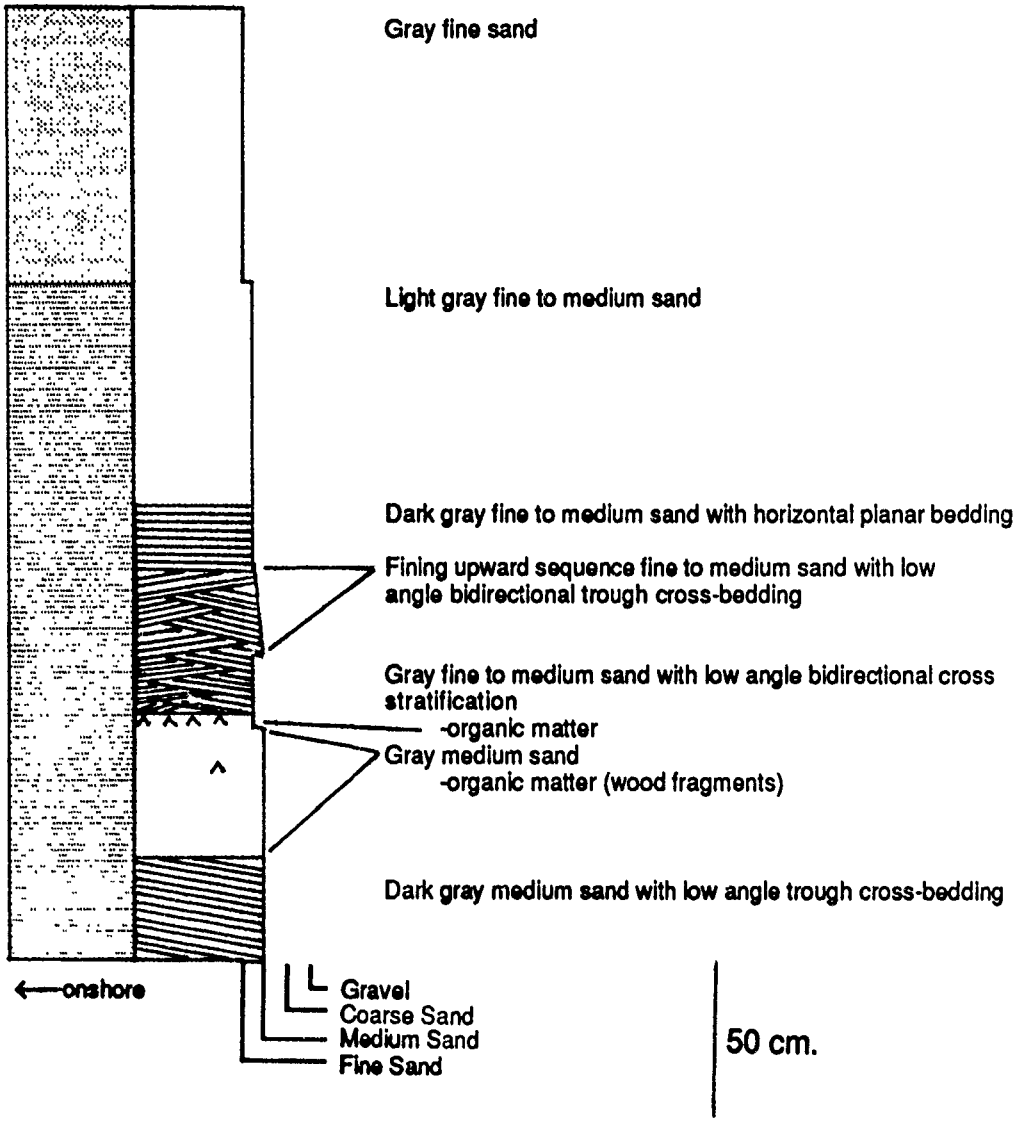

CORE 26

ENVIRONMENT: Downdrift channel margin linear bar near main ebb channel

DESCRIPTION

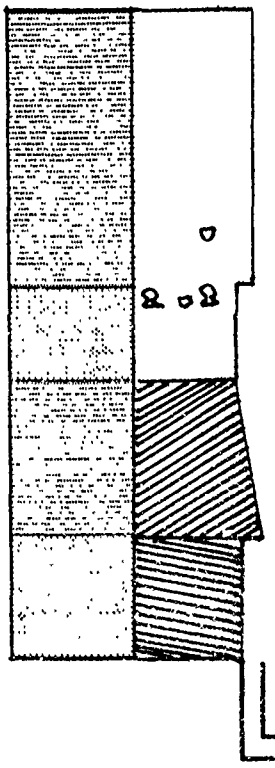

Gray fine to medium sand

-shell matter

Dark gray fine sand with shell matter and horizontal planar bedding

Fining upward sequence of fine to medium sand with high angle trough cross-bedding

Gray fine sand with low angle cross-bedding